Royal Norwegian Council
for Scientific and Industrial Research
(NTNF)

NORSAR

NORSAR Scientific Report No. 2-91/92

Semiannual Technical Summary

1 October 1991 – 31 March 1992

Kjeller, May 1992

APPROVED FOR PUBLIC RELEASE, DISTRIBUTION UNLIMITED

UNCLASSIFIED
SECURITY CLASSIFICATION OF THIS PAGE

REPORT DOCUMENTATION PAGE

1a. REPORT SECURITY CLASSIFICATION **UNCLASSIFIED**	1b. RESTRICTIVE MARKINGS **NOT APPLICABLE**
2a. SECURITY CLASSIFICATION AUTHORITY **NOT APPLICABLE** 2b. DECLASSIFICATION / DOWNGRADING SCHEDULE **NOT APPLICABLE**	3. DISTRIBUTION / AVAILABILITY OF REPORT **APPROVED FOR PUBLIC RELEASE** **DISTRIBUTION UNLIMITED**
4. PERFORMING ORGANIZATION REPORT NUMBER(S) Scientific Report 2-91/92	5. MONITORING ORGANIZATION REPORT NUMBER(S) Scientific Report 2-91/92
6a. NAME OF PERFORMING ORGANIZATION NTNF/NORSAR 6b. OFFICE SYMBOL (If applicable)	7a. NAME OF MONITORING ORGANIZATION HQ/AFTAC/TTS
6c. ADDRESS (City, State, and ZIP Code) Post Box 51 N-2007 Kjeller, Norway	7b. ADDRESS (City, State, and ZIP Code) Patrick AFB, FL 32925-6001
8a. NAME OF FUNDING / SPONSORING ORGANIZATION Defense Advanced Research Proijects Agency 8b. OFFICE SYMBOL (If applicable) NMRO	9. PROCUREMENT INSTRUMENT IDENTIFICATION NUMBER
8c. ADDRESS (City, State, and ZIP Code) 3701 N. Fairfax Dr. #717 Arlington, VA 22203-1714	10. SOURCE OF FUNDING NUMBERS PROGRAM ELEMENT NO. **R&D** / PROJECT NO. **NORSAR Phase 3** / TASK NO. **SOW Task 5.0** / WORK UNIT ACCESSION NO. **Seq.no. 003A2**

11. TITLE (Include Security Classification)

SEMIANNUAL TECHNICAL SUMMARY, 1 OCTOBER 1991 - 31 MARCH 1992 (UNCLASSIFIED)

12. PERSONAL AUTHOR(S)

13a. TYPE OF REPORT	13b. TIME COVERED	14. DATE OF REPORT (Year, Month, Day)	15. PAGE COUNT
Scientific Summary	FROM 1 Oct 91 TO 31 Mar 92	May 1992	152

16. SUPPLEMENTARY NOTATION

NOT APPLICABLE

17. COSATI CODES			18. SUBJECT TERMS (Continue on reverse if necessary and identify by block number)
FIELD	GROUP	SUB-GROUP	
8	11		**NORSAR, Norwegian Seismic Array**

19. ABSTRACT (Continue on reverse if necessary and identify by block number)

This Semiannual Technical Summary describes the operation, maintenance and research activities at the Norwegian Seismic Array (NORSAR), the Norwegian Regional Seismic Array (NORESS) and the Arctic Regional Seismic Array (ARCESS) for the period 1 October 1991 - 31 March 1992. Statistics are also presented for additional seismic stations, which through cooperative agreements with institutions in the host countries provide continuous data to the NORSAR Data Processing Center (NPDC). These stations comprise the Finnish Experimental Seismic Array (FINESA), the German Experimental Seismic Array (GERESS), and two 3-component stations in Poland: Ksiaz and Stary Folwark.

(cont.)

20. DISTRIBUTION / AVAILABILITY OF ABSTRACT ☐ UNCLASSIFIED/UNLIMITED ☐ SAME AS RPT. ☐ DTIC USERS	21. ABSTRACT SECURITY CLASSIFICATION	
22a. NAME OF RESPONSIBLE INDIVIDUAL Mr. Mike Baker	22b. TELEPHONE (Include Area Code) (407) 494-7665	22c. OFFICE SYMBOL AFTAC/TTS

DD FORM 1473, 84 MAR — 83 APR edition may be used until exhausted. All other editions are obsolete.

SECURITY CLASSIFICATION OF THIS PAGE
UNCLASSIFIED

Abstract (cont.)

This Semiannual Report also presents statistics from operation of the Intelligent Monitoring System (IMS). The IMS has been operated in an experimental mode, and the performance has been very satisfactory. Since October 1991, a new version of the IMS that accepts data from an arbitrary number of arrays and single 3-component stations has been operated.

The NORSAR Detection Processing system has been operated throughout the period with an average uptime of 99.6% as compared to 99.3% for the previous reporting period. A total of 1944 seismic events have been reported in the NORSAR monthly seismic bulletin. The performance of the continuous alarm system and the automatic bulletin transfer by telex to AFTAC has been satisfactory. The system for direct retrieval of NORSAR waveform data through an X.25 connection has been tested successfully for acquiring such data by AFTAC. Processing of requests for full NORSAR and regional array data on magnetic tapes has progressed according to established schedules.

On-line detection processing and data recording at the NORSAR Data Processing Center (NDPC) of NORESS, ARCESS, FINESA and GERESS data have been conducted throughout the period. Data from the two stations in Poland have been recorded and processed in an experimental mode. Monthly processing statistics for the arrays as well as results of the IMS analysis for the reporting period are given.

There have been no modifications made to the NORSAR data acquisition system. The process of evaluating and testing technical options for refurbishment of the array is continuing.

Maintenance activities in the period comprise preventive/corrective maintenance in connection with all the NORSAR subarrays, NORESS and ARCESS. In addition, the maintenance center has been involved with occasional maintenance of equipment for FINESA and work in connection with the two stations in Poland. Other activities have involved testing of the NORSAR communications systems, and field studies at sites in Spitsbergen and the Kola Peninsula.

Starting 1 October 1991, an effort has begun to carry out a complete technical refurbishment of the NORSAR array. This project is funded jointly by AFTAC, DARPA and NTNF. During the reporting period, efforts have focused upon continuing our evaluation of technical options for field instrumentation, in particular state-of-the-art A/D converters, data acquisition and synchronization devices. During the next few months, we plan to test several such systems under realistic operating conditions in the field. Initial testing of some systems has already started. When these studies have been completed, a recommendation for a system to be installed will be presented to the funding agencies.

Summaries of nine scientific contributions are presented in Chapter 7 of this report.

Section 7.1 contains an evaluation of global event detection performance during the recently conducted GSETT-2 experiment. The NEIC monthly bulletins have been used as a reference. The global 90% detection threshold is estimated at $m_b = 4.7$, in terms of NEIC

network magnitudes. As expected, the 90% threshold is significantly lower for the northern hemisphere (4.4) than for the southern hemisphere (5.0). A detailed discussion of the largest undetected events in each hemisphere is given. It is pointed out that detection threshold is closely tied to required location accuracy: The more relaxed the location requirements are, the "better" the detection capability will appear to be.

Section 7.2 is a case study of regional detection and location performance during GSETT-2. Using the bulletin of the Seismological Institute, University of Helsinki, as a reference, it is shown that the 90% detection threshold for the GSETT-2 system in Fennoscandia/NW Russia is close to magnitude 2.5 in terms of the duration magnitudes used in that bulletin. A similar study for the western and northern regions of Norway, using the University of Bergen bulletins as a reference, has likewise resulted in an estimated 90% threshold close to magnitude 2.5. The GSETT-2 location accuracy for Fennoscandia/NW Russia has also been evaluated, using known mining sites and other information for a reference. The results show that in a region with dense coverage of high quality arrays such as Fennoscandia, an excellent monitoring capability may be achieved.

Section 7.3 contains a third GSETT-2 detectability study. This study has been conducted for the W. Caucasus region, using as a data base the aftershock sequence from the 29 April 1991 W. Caucasus earthquake. A local bulletin was provided by the Obninsk seismological center for this purpose. We have found that the GSETT-2 detectability is significantly better than that of the NEIC in this particular case (average improvement 0.3 magnitude units). The difference is the largest during the first few hours after the main shock. This indicates that the GSETT-2 system succeeded in alleviating to some extent one of the main monitoring problems for a world-wide network (reduced performance following large earthquakes).

Section 7.4 presents a three-dimensional velocity modelling of the structure beneath the NORSAR array. Six layers down to a depth of 129 km are modeled by both seismic tomography and diffraction tomography. The models are used to construct travel time correction tables for NORSAR P-waves, and the results are compared to real data.

Section 7.5 describes results from a 12-day study of a network of 3 microarrays in Fennoscandia, comprising the center instrument and A-ring of each of the three regional arrays NORESS, ARCESS and FINESA. For each microarray, individual detection processing and f-k analysis are performed, and the generalized beamforming (GBF) technique is used to associate phases automatically to form regional seismic events. By comparison to the full Fennoscandian array network, it is found that successful automatic phase association and regional event location can be achieved using a sparse network of seismic microarrays (interstation distance about 1000 km).

Section 7.6 presents statistics on the number of detections versus apparent slowness for each of the four regional arrays NORESS, ARCESS, GERESS and FINESA. In a series of 3-D plots, all detections reported by each individual array during a 6-month period are displayed. Detections with dominant frequencies above and below 6 Hz are shown separately. The differences between the arrays are discussed, and the reasons for the main peaks in the diagrams are pointed out.

Section 7.7 presents a new array controller (NORAC) developed at NORSAR. The main design idea has been to develop an inexpensive, simple unit that can handle data from a variety of digitizers and that satisfies a number of very specific design requirements not met by currently available systems. The first prototype of NORAC has been tested successfully for a period of 2 months, and will be installed in the planned Apatity high-frequency array.

Section 7.8 presents a summary report on a one-month experiment in continuous threshold monitoring of Novaya Zemlya. Starting 1 February 1992, we began collecting continuous statistics for the Threshold Monitoring performance of NORESS, ARCESS and FINESA with regard to the northern Novaya Zemlya test site. The purpose was to demonstrate, in an experimental mode, the practical application of this monitoring method. Detailed statistics for the month of February have been compiled, and confirm previous reports on the TM capability. Within the confidence limits inherent in the method, we are able to document that no seismic event of $m_b \geq 2.6$ occurred at that test site during the month of February. Only for 0.12% of the time (i.e., 43 minutes during February) did the threshold exceed 2.6, and these occurrences could all be "explained" as resulting from one of the three conditions a) a "large" identified teleseismic event, b) a "large" identified regional event or c) a short outage of the most important array (ARCESS).

Section 7.9 presents a study correlating the number of signal detections and temperature at the two arrays NORESS and ARCESS. In many cases a clear correlation can be seen, for example with increasing number of detections during nighttime. At ARCESS, there is a large increase in detections when the frost occurs in the fall and again in the springtime. At NORESS, there are periods with considerable increase in detection rate not related to temperature, but instead caused by increased water flow in a nearby river.

AFTAC Project Authorization	:	T/9141/B/PKP
ARPA Order No.	:	4138 AMD # 16
Program Code No.	:	0F10
Name of Contractor	:	Royal Norwegian Council for Scientific and Industrial Research (NTNF)
Effective Date of Contract	:	1 Oct 1988
Contract Expiration Date	:	30 Sep 1993
Project Manager	:	Frode Ringdal (06) 81 71 21
Title of Work	:	The Norwegian Seismic Array (NORSAR) Phase 3
Amount of Contract	:	$ 9,954,194
Contract Period Covered by Report	:	1 October 1991 - 31 March 1992

This research was supported by the Advanced Research Projects Agency of the Department of Defense and was monitored by AFTAC, Patrick AFB, FL32925, under contract no. F08606-89-C-0005.

NORSAR Contribution No. 466

Table of Contents

1 Summary

This Semiannual Technical Summary describes the operation, maintenance and research activities at the Norwegian Seismic Array (NORSAR), the Norwegian Regional Seismic Array (NORESS) and the Arctic Regional Seismic Array (ARCESS) for the period 1 October 1991 - 31 March 1992. Statistics are also presented for additional seismic stations, which through cooperative agreements with institutions in the host countries provide continuous data to the NORSAR Data Processing Center (NPDC). These stations comprise the Finnish Experimental Seismic Array (FINESA), the German Experimental Seismic Array (GERESS), and two 3-component stations in Poland: Ksiaz and Stary Folwark.

This Semiannual Report also presents statistics from operation of the Intelligent Monitoring System (IMS). The IMS has been operated in an experimental mode, and the performance has been very satisfactory. Since October 1991, a new version of the IMS that accepts data from an arbitrary number of arrays and single 3-component stations has been operated.

The NORSAR Detection Processing system has been operated throughout the period with an average uptime of 99.6% as compared to 99.3% for the previous reporting period. A total of 1944 seismic events have been reported in the NORSAR monthly seismic bulletin. The performance of the continuous alarm system and the automatic bulletin transfer by telex to AFTAC has been satisfactory. The system for direct retrieval of NORSAR waveform data through an X.25 connection has been tested successfully for acquiring such data by AFTAC. Processing of requests for full NORSAR and regional array data on magnetic tapes has progressed according to established schedules.

On-line detection processing and data recording at the NORSAR Data Processing Center (NDPC) of NORESS, ARCESS, FINESA and GERESS data have been conducted throughout the period. Data from the two stations in Poland have been recorded and processed in an experimental mode. Monthly processing statistics for the arrays as well as results of the IMS analysis for the reporting period are given.

There have been no modifications made to the NORSAR data acquisition system. The process of evaluating and testing technical options for refurbishment of the array is continuing.

Maintenance activities in the period comprise preventive/corrective maintenance in connection with all the NORSAR subarrays, NORESS and ARCESS. In addition, the maintenance center has been involved with occasional maintenance of equipment for FINESA and work in connection with the two stations in Poland. Other activities have involved testing of the NORSAR communications systems, and field studies at sites in Spitsbergen and the Kola Peninsula.

Starting 1 October 1991, an effort has begun to carry out a complete technical refurbishment of the NORSAR array. This project is funded jointly by AFTAC, DARPA and NTNF. During the reporting period, efforts have focused upon continuing our evaluation

of technical options for field instrumentation, in particular state-of-the-art A/D converters, data acquisition and synchronization devices. During the next few months, we plan to test several such systems under realistic operating conditions in the field. Initial testing of some systems has already started. When these studies have been completed, a recommendation for a system to be installed will be presented to the funding agencies.

Summaries of nine scientific contributions are presented in Chapter 7 of this report.

Section 7.1 contains an evaluation of global event detection performance during the recently conducted GSETT-2 experiment. The NEIC monthly bulletins have been used as a reference. The global 90% detection threshold is estimated at $m_b = 4.7$, in terms of NEIC network magnitudes. As expected, the 90% threshold is significantly lower for the northern hemisphere (4.4) than for the southern hemisphere (5.0). A detailed discussion of the largest undetected events in each hemisphere is given. It is pointed out that detection threshold is closely tied to required location accuracy: The more relaxed the location requirements are, the "better" the detection capability will appear to be.

Section 7.2 is a case study of regional detection and location performance during GSETT-2. Using the bulletin of the Seismological Institute, University of Helsinki, as a reference, it is shown that the 90% detection threshold for the GSETT-2 system in Fennoscandia/NW Russia is close to magnitude 2.5 in terms of the duration magnitudes used in that bulletin. A similar study for the western and northern regions of Norway, using the University of Bergen bulletins as a reference, has likewise resulted in an estimated 90% threshold close to magnitude 2.5. The GSETT-2 location accuracy for Fennoscandia/NW Russia has also been evaluated, using known mining sites and other information for a reference. The results show that in a region with dense coverage of high quality arrays such as Fennoscandia, an excellent monitoring capability may be achieved.

Section 7.3 contains a third GSETT-2 detectability study. This study has been conducted for the W. Caucasus region, using as a data base the aftershock sequence from the 29 April 1991 W. Caucasus earthquake. A local bulletin was provided by the Obninsk seismological center for this purpose. We have found that the GSETT-2 detectability is significantly better than that of the NEIC in this particular case (average improvement 0.3 magnitude units). The difference is the largest during the first few hours after the main shock. This indicates that the GSETT-2 system succeeded in alleviating to some extent one of the main monitoring problems for a world-wide network (reduced performance following large earthquakes).

Section 7.4 presents a three-dimensional velocity modelling of the structure beneath the NORSAR array. Six layers down to a depth of 129 km are modeled by both seismic tomography and diffraction tomography. The models are used to construct travel time correction tables for NORSAR P-waves, and the results are compared to real data.

Section 7.5 describes results from a 12-day study of a network of 3 microarrays in Fennoscandia, comprising the center instrument and A-ring of each of the three regional arrays NORESS, ARCESS and FINESA. For each microarray, individual detection processing and f-k analysis are performed, and the generalized beamforming (GBF) technique is used to associate phases automatically to form regional seismic events. By comparison to the full Fennoscandian array network, it is found that successful automatic phase association and regional event location can be achieved using a sparse network of seismic microarrays (interstation distance about 1000 km).

Section 7.6 presents statistics on the number of detections versus apparent slowness for each of the four regional arrays NORESS, ARCESS, GERESS and FINESA. In a series of 3-D plots, all detections reported by each individual array during a 6-month period are displayed. Detections with dominant frequencies above and below 6 Hz are shown separately. The differences between the arrays are discussed, and the reasons for the main peaks in the diagrams are pointed out.

Section 7.7 presents a new array controller (NORAC) developed at NORSAR. The main design idea has been to develop an inexpensive, simple unit that can handle data from a variety of digitizers and that satisfies a number of very specific design requirements not met by currently available systems. The first prototype of NORAC has been tested successfully for a period of 2 months, and will be installed in the planned Apatity high-frequency array.

Section 7.8 presents a summary report on a one-month experiment in continuous threshold monitoring of Novaya Zemlya. Starting 1 February 1992, we began collecting continuous statistics for the Threshold Monitoring performance of NORESS, ARCESS and FINESA with regard to the northern Novaya Zemlya test site. The purpose was to demonstrate, in an experimental mode, the practical application of this monitoring method. Detailed statistics for the month of February have been compiled, and confirm previous reports on the TM capability. Within the confidence limits inherent in the method, we are able to document that no seismic event of $m_b \geq 2.6$ occurred at that test site during the month of February. Only for 0.12% of the time (i.e., 43 minutes during February) did the threshold exceed 2.6, and these occurrences could all be "explained" as resulting from one of the three conditions a) a "large" identified teleseismic event, b) a "large" identified regional event or c) a short outage of the most important array (ARCESS).

Section 7.9 presents a study correlating the number of signal detections and temperature at the two arrays NORESS and ARCESS. In many cases a clear correlation can be seen, for example with increasing number of detections during nighttime. At ARCESS, there is a large increase in detections when the frost occurs in the fall and again in the springtime. At NORESS, there are periods with considerable increase in detection rate not related to temperature, but instead caused by increased water flow in a nearby river.

2 NORSAR Operation

2.1 Detection Processor (DP) operation

There have been 55 breaks in the otherwise continuous operation of the NORSAR online system within the 6-month reporting interval. The uptime percentage for the period is 99.6% as compared to 99.3% for the previous period.

Fig. 2.1.1 and the accompanying Table 2.1.1 both show the daily DP downtime for the days between 1 October 1991 and 31 March 1992. The monthly recording times and percentages are given in Table 2.1.2.

The breaks can be grouped as follows:

a)	Hardware failure	4
b)	Stops related to program work or error	1
c)	Hardware maintenance stops	5
d)	Power jumps and breaks	0
e)	TOD error correction	8
f)	Communication lines	21

The total downtime for the period was 19 hours and 42 minutes. The mean-time-between-failures (MTBF) was 4.6 days, as compared to 5.0 for the previous period.

J. Torstveit

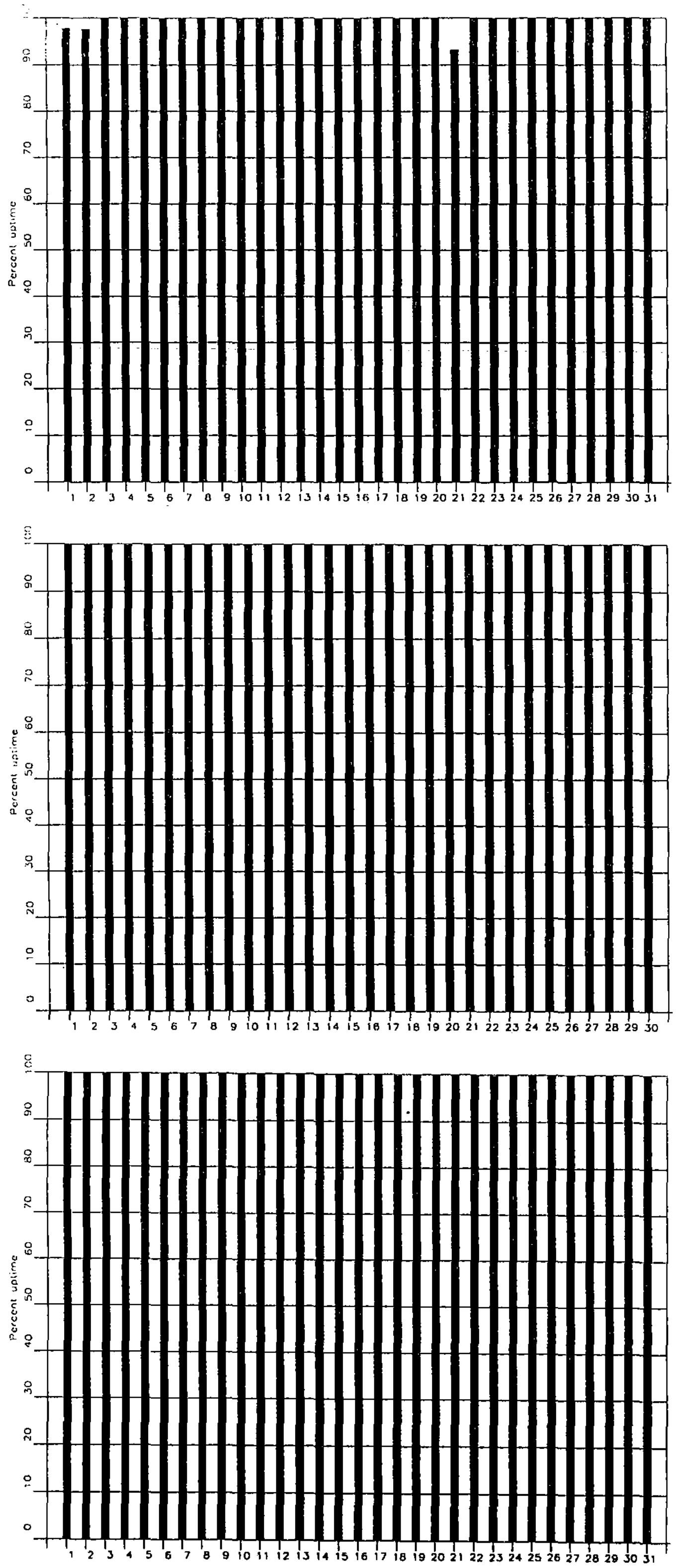

Fig. 2.1.1. Detection Processor uptime for October (top), November (middle) and December (bottom) 1991.

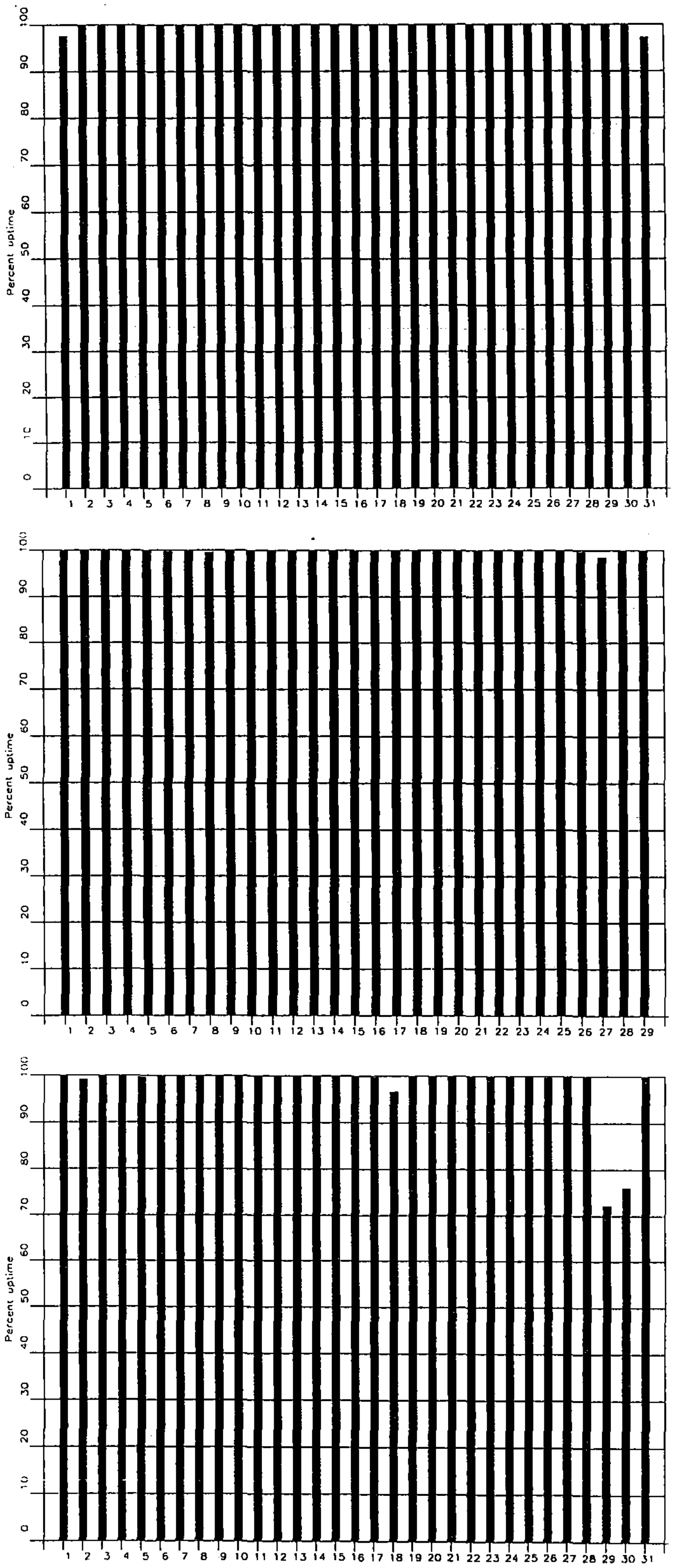

Fig. 2.1.1. Detection Processor uptime for January (top), February (middle) and March (bottom) 1992.

Date	Time	Cause
1 Oct	1226 - 1258	Hardware maintenance
2 Oct	0641 - 0715	Line failure
21 Oct	1000 - 1138	Line failure
1 Jan	1040 - 1114	Software work
31 Jan	0216 - 0256	Hardware failure
8 Feb	1011 - 1017	Hardware failure
27 Feb	0831 - 0854	Hardware maintenance
2 Mar	1033 - 1045	Hardware failure
18 Mar	0252 - 0340	Hardware failure
29 Mar	1720 -	Hardware failure
30 Mar	- 0452	

Table 2.1.1. The major downtimes in the period 1 October 1991 - 31 March 1992.

Month	DP Uptime Hours	DP Uptime %	No. of DP Breaks	No. of Days with Breaks	DP MTBF* (days)
Oct 91	741.07	99.62	7	7	3.9
Nov 91	719.51	99.98	3	3	7.5
Dec 91	695.17	99.96	5	5	5.2
Jan 92	742.27	99.80	8	8	3.4
Feb 92	743.13	99.89	8	6	3.2
Mar 92	730.23	98.17	8	7	3.4
		99.57	39	36	4.6

*Mean-time-between-failures = total uptime/no. of up intervals.

Table 2.1.2. Online system performance, 1 October 1991 - 31 March 1992.

2.2 Array communications

General

Table 2.2.1 reflects the performance of the communications system throughout the reporting period. The most common events which have affected the communications systems have been: Line outage (5), reduced line performance (2), Modcomp stop (2), bad communications cable (1), bad connection (1), SLEM (stuck) (1), and an inoperative Modcomp operator terminal (1).

Detailed Summary

October (weeks 40-44), 30.9-3.11.91

Most reliable performance for all systems weeks 40-42, partly week 44 (-06C). Week 43 01A, 02B and 06C were affected; 01A by a bad communications cable (23-25 Oct), resulting in low line level toward Kjeller (-32.0 dBm). 02B was affected by a bad connection between Lillestrøm and Kjeller (22-23 Oct). 27 Oct 06C changed status (NODATA). A Modcomp restart restored operation 28 October.

November (weeks 45-48), 4.11-1.12.91

Most reliable performance experienced in November 1991, although we had a short outage, approx. 20 mins., on 02C 12 Nov.

December (weeks 49-52), 2-29.12.91

Two communications systems were affected in December 1991: 03C 4-11.12 due to reduced line performance toward the subarray; 06C 5-9.12 probably also caused by reduced line performance. The remaining systems performed most satisfactorily

January (weeks 1-5), 30.12.91-2.2.92

Apart from a Modcomp stop approx. 56 minutes 31 January, all the systems have performed most satisfactorily.

February (weeks 6-9), 3.2-1.3.92

A stuck SLEM affected 06C 25-26 February. The remaining systems performed most satisfactorily.

March (weeks 10-13), 2-29.3.92

02C communications system was down 13-14 March, probably due to a line outage.

06C comunications line went down 29 March at 1720 hrs GMT. Immediately afterwards (17.20.34 GMT), the Modcomp stopped, and we were not able to start it until the next day at 0447 GMT. Service was requested, and between 1246 and 1333 GMT the Modcomp was down. A defective memory cooling fan was replaced. Also the operator terminal was replaced, as the old one failed during the attempts to restart the system.

O.A. Hansen

Sub-Arrays	Oct (5) 30.9-3.10.91	Nov (4) 4.10-1.12.91	Dec (4) 2.12-29.12.91	Jan (5) 30.12.91-2.2.92	Feb (4) 3.2-1.3.92	Mar (4) 2.3-29.3.92	Average 1/2 year
01A	0.021[1)]	0.001	0.001	0.003	0.001	0.002[7)]	0.003
01B	0.001	0.001	0.003	0.003	0.0005	0.0005[8)]	0.001
02B	0.001[2)]	0.0007	0.0006	0.0005	0.0006	0.0006[9)]	0.0006
02C	0.002	0.050	0.001	0.001	0.001	0.0008[10)]	0.009
03C	0.003	0.001	3.574[4)]	0.003	0.004	0.004[11)]	0.597
04C	0.018	0.0007	0.002	0.001	0.002	0.002[12)]	0.004
06C	0.025[3)]	0.0007	1.190[5)]	0.003	0.0008[6)]	0.0006[13)]	0.204
Aver	0.009	0.008	0.68	0.002	0.001	0.001	0.117

Figures representing error rate (in per cent) followed by number 1), 2), etc., are related to legend below.,

Table 2.2.1. Communications performance. The numbers represent error rates in per cent based on total transmitted frames/week (1 October 1991 - 31 March 1992).

1),2)	Average 4 weeks (40-42.44)(40,42,44)
3),4),5),6),7),8),9),11),12),13)	Average 3 weeks (40-42)(50,51,52)(50,51,52)(6,7,8)(10,11,12)(10,11,12)(10,11,12)(10,11,12)(10,11,12)
10)	Average 2 weeks (10,12)

2.3 NORSAR Event Detection operation

In Table 2.3.1 some monthly statistics of the Detection and Event Processor operation are given. The table lists the total number of detections (DPX) triggered by the on-line detector, the total number of detections processed by the automatic event processor (EPX) and the total number of events accepted after analyst review (teleseismic phases, core phases and total).

	Total	Total		Accepted Phases		
	DPX	EPX	P-phases	Core Phases	Sum	Daily
Oct 91	11450	1429	231	83	314	10.1
Nov 91	13225	1454	188	69	257	8.6
Dec 91	13693	1715	446	63	509	16.4
Jan 92	12399	1465	203	53	256	8.3
Feb 92	12225	1249	204	46	250	8.6
Mar 92	11900	1389	289	69	358	11.5
			1561	383	1944	10.6

Table 2.3.1. Detection and Event Processor statistics, 1 October 1991 - 31 March 1992.

NORSAR Detections

The number of detections (phases) reported by the NORSAR detector during day 274 1991, through day 091 1992, was 75,589, giving an average of 413 detections per processed day (183 days processed). Table 2.3.2 shows daily and hourly distribution of detections for NORSAR.

B. Paulsen Gammelby
T. Schøyen

NAO .DPX Hourly distribution of detections

Day	00	01	02	03	04	05	06	07	08	09	10	11	12	13	14	15	16	17	18	19	20	21	22	23	Sum	Date
274	23	18	13	21	15	9	5	5	5	14	17	10	1	15	14	24	22	18	10	25	23	19	19	29	374	Oct 01 Tuesday
275	23	18	26	21	16	32	10	15	12	17	14	10	21	9	24	20	15	26	18	28	16	20	22	23	456	Oct 02 Wednesday
276	17	21	20	23	19	15	6	17	6	10	13	16	14	27	21	25	10	25	13	17	13	11	27	18	404	Oct 03 Thursday
277	22	19	27	22	18	15	11	6	17	12	9	15	27	20	17	13	4	19	28	28	17	31	25	17	439	Oct 04 Friday
278	21	25	21	15	22	29	10	19	12	16	8	18	8	9	12	12	12	14	22	9	14	19	22	19	388	Oct 05 Saturday
279	16	37	14	11	13	23	20	20	18	24	19	10	14	14	9	17	13	21	18	18	20	34	27	21	451	Oct 06 Sunday
280	30	24	25	28	21	19	7	6	5	7	16	16	4	9	9	23	17	8	8	23	19	18	15	24	381	Oct 07 Monday
281	24	27	23	25	27	19	11	1	4	6	1	10	23	14	17	15	5	9	11	9	5	18	13	12	329	Oct 08 Tuesday
282	18	10	15	10	6	5	6	2	2	2	4	1	14	5	16	24	5	15	8	9	7	5	7	9	205	Oct 09 Wednesday
283	19	11	16	11	8	4	5	2	3	5	2	7	8	17	25	2	18	8	10	6	12	6	10	15	230	Oct 10 Thursday
284	11	9	17	21	8	6	1	4	2	5	4	10	9	25	9	12	16	12	13	11	20	12	16	16	269	Oct 11 Friday
285	12	19	15	10	24	21	15	14	8	11	15	11	16	17	11	14	37	15	11	15	13	20	25	21	390	Oct 12 Saturday
286	18	30	18	22	12	15	14	22	13	14	9	14	10	16	12	16	12	16	20	16	14	15	16	25	389	Oct 13 Sunday
287	20	17	13	19	10	10	2	5	6	4	5	2	5	15	14	8	32	9	4	13	16	12	7	11	259	Oct 14 Monday
288	18	11	19	23	14	9	3	11	16	7	7	5	16	21	20	4	19	3	5	9	9	9	6	15	279	Oct 15 Tuesday
289	12	12	15	12	13	16	14	8	25	16	10	7	15	14	12	15	18	18	19	17	17	20	16	11	352	Oct 16 Wednesday
290	16	19	12	8	19	16	12	11	9	16	16	8	15	11	17	13	16	18	18	16	12	6	10	12	326	Oct 17 Thursday
291	9	10	7	10	11	7	4	0	1	1	3	10	5	8	9	2	14	12	3	7	4	2	5	7	151	Oct 18 Friday
292	3	5	6	4	7	22	5	3	8	12	8	11	11	11	8	14	17	28	20	26	21	29	22	21	322	Oct 19 Saturday
293	25	25	24	30	22	27	18	11	12	12	22	11	11	14	17	14	21	19	13	16	19	21	18	15	437	Oct 20 Sunday
294	17	21	15	14	21	13	10	6	9	5	0	8	11	16	12	14	20	22	22	16	15	21	20	31	359	Oct 21 Monday
295	33	22	25	16	26	19	13	10	7	7	14	8	21	14	18	8	10	21	16	24	19	20	18	19	408	Oct 22 Tuesday
296	22	14	15	27	14	9	9	12	4	6	23	4	29	14	24	14	7	17	19	16	20	13	18	17	367	Oct 23 Wednesday
297	21	17	27	22	14	10	9	6	4	21	18	25	14	37	21	12	10	8	15	12	6	10	16	25	380	Oct 24 Thursday
298	18	16	14	17	11	9	3	2	19	19	16	9	12	20	21	5	6	11	14	10	11	23	20	13	319	Oct 25 Friday
299	6	16	27	21	20	14	13	9	5	27	9	7	18	11	14	21	26	20	18	14	28	24	17	25	410	Oct 26 Saturday
300	33	24	27	25	24	30	32	37	27	25	37	16	29	19	24	20	23	29	39	22	24	27	33	29	655	Oct 27 Sunday
301	31	22	38	29	23	17	11	9	12	13	3	8	26	21	25	19	23	21	18	28	16	19	10	18	460	Oct 28 Monday
302	30	30	20	23	21	13	4	4	16	10	10	4	15	14	36	5	14	16	8	10	18	17	15	22	375	Oct 29 Tuesday
303	24	22	33	22	26	22	13	11	7	10	10	3	44	17	19	21	25	15	23	12	19	22	26	25	471	Oct 30 Wednesday
304	23	35	26	21	32	22	9	6	9	31	9	9	5	9	25	14	12	12	24	17	11	19	10	16	406	Oct 31 Thursday
305	16	17	23	13	17	14	11	9	15	13	18	7	33	14	11	19	24	30	25	15	15	24	15	18	416	Nov 01 Friday
306	18	22	18	28	25	27	26	26	18	15	20	19	10	20	22	28	36	23	29	18	18	26	28	24	544	Nov 02 Saturday
307	34	10	19	26	23	31	20	16	22	20	22	14	15	14	19	20	17	12	30	20	25	19	15	21	484	Nov 03 Sunday
308	21	34	13	27	27	26	19	8	13	14	4	5	17	14	15	26	17	14	14	13	20	17	18	20	416	Nov 04 Monday
309	14	19	21	32	15	21	18	27	14	11	10	7	17	9	15	20	26	24	25	22	21	25	20	24	457	Nov 05 Tuesday
310	21	19	26	21	22	21	10	5	8	2	10	10	15	17	14	17	11	17	14	19	16	19	14	27	375	Nov 06 Wednesday
311	14	21	25	16	24	18	13	9	6	23	14	7	16	28	12	17	15	17	21	11	36	18	24	24	429	Nov 07 Thursday
312	15	25	24	20	26	18	11	13	17	19	22	13	23	13	29	25	14	26	15	26	26	26	28	15	489	Nov 08 Friday
313	24	32	26	28	28	37	32	22	32	31	19	25	17	27	35	31	23	24	24	27	27	22	25	15	633	Nov 09 Saturday
314	22	34	28	28	19	32	24	24	27	28	19	14	20	21	20	33	31	19	19	17	19	24	22	18	562	Nov 10 Sunday
315	28	26	18	23	20	12	16	13	15	14	12	23	24	17	11	15	17	15	17	13	19	14	18	20	420	Nov 11 Monday
316	15	20	17	18	15	13	16	10	12	14	12	16	16	13	12	26	15	14	7	10	17	13	19	19	359	Nov 12 Tuesday
317	21	19	15	12	14	9	8	9	4	11	13	16	9	26	15	14	18	20	14	23	20	26	23	16	375	Nov 13 Wednesday
318	24	22	21	16	20	19	22	13	6	9	11	10	9	25	8	17	19	11	10	11	14	16	9	11	353	Nov 14 Thursday
319	8	19	8	9	15	8	4	2	1	0	7	10	7	5	3	11	19	10	8	7	18	17	20	11	227	Nov 15 Friday
320	27	23	25	26	20	12	15	16	14	11	22	17	27	15	10	15	10	15	16	19	13	26	18	11	423	Nov 16 Saturday
321	20	25	24	28	34	31	19	21	18	22	20	24	14	22	26	20	18	45	34	15	31	28	28	26	593	Nov 17 Sunday
322	26	32	22	25	33	13	15	5	16	30	8	13	8	5	11	19	10	9	5	6	10	18	23	20	382	Nov 18 Monday
323	21	20	22	22	28	12	5	4	10	7	12	7	16	18	5	6	15	13	13	14	12	19	30	19	350	Nov 19 Tuesday
324	29	28	31	19	21	11	10	8	10	26	21	6	17	25	10	11	36	12	9	11	9	11	14	24	409	Nov 20 Wednesday
325	24	20	29	23	27	22	14	15	12	6	12	9	23	13	15	10	18	12	20	19	21	16	18	30	428	Nov 21 Thursday
326	20	29	28	16	20	20	19	6	6	17	20	12	14	13	13	16	14	17	18	17	9	16	21	32	413	Nov 22 Friday
327	23	38	20	20	15	18	17	22	12	17	14	16	9	21	13	13	14	17	19	24	20	22	22	27	453	Nov 23 Saturday
328	24	16	20	27	31	31	34	29	19	24	32	27	22	22	25	25	24	22	27	19	26	32	27	30	615	Nov 24 Sunday
329	22	19	27	16	20	19	12	10	6	26	18	7	13	17	34	14	16	23	15	16	16	20	13	16	415	Nov 25 Monday

Table 2.3.2 (Page 1 of 4)

NAO .DPX Hourly distribution of detections

Day	00	01	02	03	04	05	06	07	08	09	10	11	12	13	14	15	16	17	18	19	20	21	22	23	Sum	Date	
330	23	22	13	20	20	16	18	12	10	13	16	13	16	15	22	17	22	15	17	13	4	23	19	17	396	Nov 26 Tuesday	
331	15	15	27	16	15	21	8	5	12	8	8	7	15	15	15	9	19	19	11	14	23	21	20	22	360	Nov 27 Wednesday	
332	22	16	15	25	26	19	5	12	10	12	15	19	26	25	16	17	14	22	16	21	12	22	17	11	415	Nov 28 Thursday	
333	23	18	22	21	26	13	8	5	11	10	5	8	36	17	21	18	9	10	19	19	17	26	21	23	406	Nov 29 Friday	
334	15	27	23	25	26	23	27	22	20	38	23	27	30	26	28	26	28	25	34	23	32	22	22	35	627	Nov 30 Saturday	
335	22	26	27	15	19	13	16	16	18	27	11	11	20	21	15	13	13	16	15	19	14	15	8	14	404	Dec 01 Sunday	
336	16	22	12	17	12	9	16	6	17	5	13	16	18	20	12	11	12	22	14	15	15	19	24	14	357	Dec 02 Monday	
337	14	19	17	14	21	10	9	9	21	8	13	11	21	11	9	11	15	9	15	12	13	16	14	25	337	Dec 03 Tuesday	
338	26	26	15	23	20	29	19	7	9	11	9	14	9	9	24	22	26	10	15	19	20	26	32	26	446	Dec 04 Wednesday	
339	24	19	29	19	20	14	9	15	8	16	7	5	20	10	26	18	26	17	18	14	25	19	21	28	427	Dec 05 Thursday	
340	10	20	20	16	27	18	15	9	7	10	14	20	21	16	13	9	6	14	18	20	15	23	21	16	378	Dec 06 Friday	
341	19	15	16	24	27	28	19	18	17	20	19	23	25	24	26	13	31	31	29	30	30	21	38	26	569	Dec 07 Saturday	
342	40	42	40	43	38	52	42	28	38	18	21	19	26	14	24	8	19	25	21	13	13	16	17	16	633	Dec 08 Sunday	
343	12	20	16	16	18	6	9	2	3	8	6	8	25	10	21	12	9	5	6	18	7	7	19	19	282	Dec 09 Monday	
344	15	20	18	25	21	11	21	14	7	15	11	23	21	14	9	14	19	21	23	22	18	16	18	19	415	Dec 10 Tuesday	
345	19	22	29	28	18	15	25	10	10	17	14	14	10	13	20	12	18	23	29	27	28	20	21	16	458	Dec 11 Wednesday	
346	33	21	28	22	12	18	6	7	11	14	13	16	22	6	30	22	20	19	20	20	24	23	23	29	459	Dec 12 Thursday	
347	29	27	28	65	39	23	14	30	25	9	19	18	26	9	23	26	15	27	24	27	30	29	20	17	599	Dec 13 Friday	
348	17	18	18	22	24	22	14	23	21	20	18	19	24	23	21	26	23	27	26	29	12	22	15	23	507	Dec 14 Saturday	
349	20	26	22	24	19	26	29	25	21	21	21	29	23	17	26	24	21	21	23	29	18	31	29	22	567	Dec 15 Sunday	
350	23	20	21	18	29	15	5	5	13	2	8	20	13	16	11	17	7	7	12	17	7	22	37	32	377	Dec 16 Monday	
351	22	19	43	24	40	11	25	12	15	7	6	22	19	4	27	11	5	20	19	21	26	16	18	35	467	Dec 17 Tuesday	
352	17	33	23	24	12	23	19	10	13	10	15	9	8	23	17	9	22	9	14	6	7	12	9	22	366	Dec 18 Wednesday	
353	12	18	25	22	26	29	15	8	22	9	13	13	26	27	22	16	19	13	13	10	0	8	6	2	374	Dec 19 Thursday	
354	0	4	9	2	1	3	2	0	5	13	3	4	6	13	11	8	6	8	4	8	5	3	9	18	145	Dec 20 Friday	
355	19	16	22	21	25	28	20	24	24	18	15	21	19	22	6	23	22	23	18	21	19	14	18	14	472	Dec 21 Saturday	
356	14	19	18	23	24	18	13	30	21	73	50	32	44	30	20	28	36	31	24	29	21	41	19	8	666	Dec 22 Sunday	
357	10	3	14	8	12	12	15	16	16	11	17	24	22	24	14	27	14	22	11	18	19	10	17	25	381	Dec 23 Monday	
358	23	28	21	29	35	20	23	27	24	24	31	20	34	26	24	16	29	31	20	16	22	13	16	16	568	Dec 24 Tuesday	
359	15	10	16	11	19	16	15	17	21	30	14	35	26	35	26	32	23	32	26	26	22	23	26	27	543	Dec 25 Wednesday	Frste
360	29	35	31	26	29	19	18	21	29	20	32	22	27	28	17	22	21	23	21	22	14	18	22	24	570	Dec 26 Thursday	Andre
361	26	28	30	29	40	27	24	29	22	24	19	14	26	25	23	16	15	20	26	22	22	25	22	20	574	Dec 27 Friday	
362	17	35	25	30	25	32	20	30	25	23	36	35	31	33	18	36	23	23	23	26	27	22	25	21	641	Dec 28 Saturday	
363	26	36	22	34	17	16	22	24	18	8	6	14	6	11	15	10	14	5	21	25	11	12	10	8	391	Dec 29 Sunday	
364	10	10	10	5	7	11	12	7	14	10	7	8	16	17	17	21	17	18	15	21	15	18	28	26	340	Dec 30 Monday	
365	25	26	26	31	33	36	24	31	21	15	16	29	23	16	26	29	22	27	21	24	22	25	28	20	596	Dec 31 Tuesday	
1	12	30	19	13	12	6	1	5	15	0	1	2	2	1	1	1	4	4	8	6	8	16	25	13	205	Jan 01 Wednesday	Frste
2	25	25	30	19	23	25	28	15	12	9	16	15	17	17	22	13	25	22	20	28	15	20	20	12	473	Jan 02 Thursday	
3	20	14	14	17	16	18	24	13	13	10	21	22	31	20	21	18	24	30	18	18	21	21	21	19	464	Jan 03 Friday	
4	22	20	16	18	22	12	32	20	15	21	24	22	13	23	28	25	23	20	17	28	26	22	26	34	529	Jan 04 Saturday	
5	20	23	24	22	15	26	16	24	12	17	22	18	10	15	19	10	19	26	12	24	17	20	14	19	444	Jan 05 Sunday	
6	20	25	25	15	10	13	6	4	12	5	14	12	11	9	16	15	15	16	22	13	24	23	26	16	367	Jan 06 Monday	
7	26	30	30	24	20	21	14	22	9	26	14	18	15	15	14	13	18	26	17	20	12	17	14	21	456	Jan 07 Tuesday	
8	15	14	21	22	20	21	15	7	14	11	19	8	13	13	13	15	17	15	16	14	13	16	16	19	367	Jan 08 Wednesday	
9	18	18	24	28	23	17	19	15	21	24	12	10	14	21	11	13	12	17	15	17	20	17	14	10	410	Jan 09 Thursday	
10	23	21	20	20	16	13	12	13	9	8	3	25	10	14	7	3	10	4	10	14	14	14	28	18	329	Jan 10 Friday	
11	21	19	23	16	15	23	24	20	19	17	15	18	12	15	9	23	6	5	11	8	7	9	6	4	345	Jan 11 Saturday	
12	14	11	15	11	9	6	17	20	17	11	12	26	17	18	22	16	22	27	23	17	23	19	18	20	411	Jan 12 Sunday	
13	22	22	26	21	23	25	9	9	11	12	4	11	37	12	22	12	12	25	22	17	25	18	22	27	446	Jan 13 Monday	
14	24	22	14	22	22	32	20	12	23	18	10	18	24	10	20	22	15	14	16	20	16	29	16	13	452	Jan 14 Tuesday	
15	19	10	19	36	10	23	10	12	23	10	13	10	13	8	13	14	6	16	12	17	14	13	17	20	358	Jan 15 Wednesday	
16	19	32	15	13	17	22	14	10	11	14	21	16	15	19	22	9	12	16	13	9	22	26	20	23	410	Jan 16 Thursday	
17	20	25	20	18	17	15	14	10	12	11	14	19	13	13	15	11	13	18	21	18	19	29	20	16	401	Jan 17 Friday	
18	14	28	24	20	24	30	13	19	21	21	22	16	20	18	24	20	30	33	19	22	22	18	24	29	531	Jan 18 Saturday	
19	25	20	17	22	15	17	12	18	14	10	21	12	28	21	23	27	9	16	18	9	20	28	14	18	434	Jan 19 Sunday	
20	23	17	19	26	13	12	8	7	6	16	9	13	10	22	17	22	11	8	11	15	14	13	12	15	339	Jan 20 Monday	

Table 2.3.2 (Page 2 of 4)

NAO .DPX Hourly distribution of detections

Day	00	01	02	03	04	05	06	07	08	09	10	11	12	13	14	15	16	17	18	19	20	21	22	23	Sum	Date
21	12	18	13	22	13	13	10	10	9	3	21	13	10	15	13	7	19	16	23	21	15	15	22	23	356	Jan 21 Tuesday
22	24	19	25	17	23	14	21	11	24	14	29	19	24	28	23	13	19	20	14	26	15	15	17	11	465	Jan 22 Wednesday
23	9	18	13	18	31	12	17	10	22	20	9	9	14	17	22	17	13	15	12	14	12	21	20	28	393	Jan 23 Thursday
24	23	20	21	19	14	19	8	6	10	9	29	19	16	22	12	14	17	20	18	17	14	18	19	17	401	Jan 24 Friday
25	22	19	28	21	22	21	20	16	19	15	14	20	35	18	15	19	27	20	18	24	33	22	20	25	513	Jan 25 Saturday
26	26	31	30	20	23	14	18	25	16	21	11	19	18	12	23	21	18	18	19	20	18	14	15	15	465	Jan 26 Sunday
27	14	36	21	19	16	18	11	5	10	10	9	18	21	11	15	7	13	4	13	8	17	10	22	12	340	Jan 27 Monday
28	20	18	17	18	15	14	13	8	8	3	15	18	24	11	12	12	5	13	8	10	9	14	11	10	306	Jan 28 Tuesday
29	12	16	17	8	17	9	9	9	10	16	12	13	17	36	10	15	12	13	12	13	16	11	4	20	327	Jan 29 Wednesday
30	15	16	21	12	19	19	16	4	4	16	8	11	20	20	17	6	20	14	14	21	11	16	18	24	362	Jan 30 Thursday
31	35	76	5	19	17	12	8	10	4	10	25	12	24	12	13	11	16	11	16	14	11	18	11	22	412	Jan 31 Friday
32	23	24	20	20	21	33	21	21	17	27	12	18	12	18	19	15	24	22	25	5	0	0	0	0	397	Feb 01 Saturday
33	0	0	33	32	21	21	28	23	34	24	19	19	28	23	19	27	31	25	20	26	19	37	27	18	554	Feb 02 Sunday
34	20	14	20	19	20	18	22	14	13	17	16	11	20	23	13	13	14	16	11	22	13	17	17	24	407	Feb 03 Monday
35	13	18	17	22	17	17	9	15	6	15	13	18	11	28	9	29	26	22	14	16	25	24	15	21	420	Feb 04 Tuesday
36	19	18	20	18	16	16	15	18	9	16	15	20	14	23	11	10	7	15	14	13	7	16	15	22	367	Feb 05 Wednesday
37	14	36	22	32	41	23	24	6	17	17	15	25	25	29	26	21	33	18	22	16	27	21	22	15	547	Feb 06 Thursday
38	22	19	28	26	23	21	17	7	11	21	22	16	17	10	19	20	14	23	14	9	14	10	6	14	403	Feb 07 Friday
39	11	5	13	11	20	15	12	9	14	12	14	15	16	13	23	16	17	16	19	16	22	21	13	19	362	Feb 08 Saturday
40	29	33	21	36	41	30	25	27	25	17	25	19	28	28	18	24	22	22	20	31	28	22	27	21	619	Feb 09 Sunday
41	17	19	16	31	23	10	9	8	12	12	11	15	21	15	15	6	27	15	18	15	24	23	21	17	400	Feb 10 Monday
42	23	22	25	14	23	17	14	22	15	24	20	20	18	13	9	15	17	11	14	12	21	15	19	18	421	Feb 11 Tuesday
43	26	28	22	17	25	24	19	19	17	14	11	11	22	20	9	7	34	11	16	9	8	18	18	18	423	Feb 12 Wednesday
44	18	36	29	13	25	23	11	17	11	6	18	18	16	19	18	21	18	9	11	14	16	16	21	24	428	Feb 13 Thursday
45	18	19	25	25	12	14	10	16	22	12	9	13	21	11	15	20	19	23	14	20	22	20	20	24	424	Feb 14 Friday
46	14	24	18	25	23	12	20	14	19	16	17	8	38	49	13	23	16	16	16	20	23	15	23	16	478	Feb 15 Saturday
47	24	22	20	17	34	27	34	12	31	28	24	18	22	25	25	19	15	14	20	24	22	15	12	20	524	Feb 16 Sunday
48	25	15	22	23	21	19	7	14	5	11	14	12	17	24	17	10	9	15	5	8	12	16	8	11	340	Feb 17 Monday
49	16	16	16	22	16	9	10	4	8	9	28	24	38	22	8	19	13	17	7	13	18	16	21	13	383	Feb 18 Tuesday
50	18	18	12	20	18	15	18	6	6	12	18	31	27	16	22	12	2	9	10	9	12	14	16	12	353	Feb 19 Wednesday
51	18	14	18	13	18	10	7	7	12	14	16	17	18	17	14	27	22	17	15	20	20	12	18	17	381	Feb 20 Thursday
52	12	15	18	19	19	19	15	11	19	15	15	37	11	6	21	18	24	19	15	17	22	7	18	19	411	Feb 21 Friday
53	18	18	13	15	10	9	11	9	6	8	21	7	17	12	19	23	20	24	21	18	24	21	24	25	393	Feb 22 Saturday
54	24	27	19	23	31	28	19	24	19	13	10	16	16	9	9	14	21	24	30	14	26	28	24	15	483	Feb 23 Sunday
55	20	27	22	11	27	18	12	10	10	15	36	17	11	8	26	15	21	10	26	15	14	21	8	10	410	Feb 24 Monday
56	7	11	9	5	4	6	4	4	11	5	9	3	16	7	4	13	11	9	13	5	11	15	21	14	217	Feb 25 Tuesday
57	19	18	13	37	21	26	18	13	13	14	25	17	22	23	17	14	11	15	16	17	26	9	9	24	437	Feb 26 Wednesday
58	11	26	21	21	24	10	7	8	10	15	22	18	29	10	12	18	20	22	22	17	31	24	27	29	454	Feb 27 Thursday
59	19	13	20	17	25	17	10	7	16	8	6	24	14	9	7	7	6	13	18	12	19	15	14	10	326	Feb 28 Friday
60	16	20	26	19	17	24	13	18	13	13	24	7	19	13	21	18	18	22	19	22	22	22	19	24	449	Feb 29 Saturday
61	21	24	29	21	17	31	29	19	20	17	21	13	18	21	24	21	23	24	14	17	20	18	22	16	500	Mar 01 Sunday
62	19	15	14	21	15	9	3	2	2	8	3	14	28	16	17	10	24	11	12	16	17	24	18	13	331	Mar 02 Monday
63	15	36	28	29	35	32	20	15	15	15	8	7	22	16	10	17	23	19	16	20	13	16	19	18	464	Mar 03 Tuesday
64	18	26	18	24	8	10	7	12	12	11	12	32	30	11	9	8	13	15	15	13	15	16	22	15	372	Mar 04 Wednesday
65	22	18	16	22	16	21	12	7	8	12	12	18	34	15	16	21	22	20	15	17	25	10	24	19	422	Mar 05 Thursday
66	27	19	16	27	17	27	12	5	9	8	13	12	29	21	21	16	11	21	13	18	33	11	17	27	430	Mar 06 Friday
67	14	21	23	24	18	27	22	19	24	21	19	19	20	15	25	24	21	18	15	30	24	23	28	20	514	Mar 07 Saturday
68	21	23	19	22	23	16	15	10	21	16	21	16	13	15	12	17	19	16	15	15	16	26	12	20	419	Mar 08 Sunday
69	37	26	27	24	23	15	3	7	9	10	10	3	5	23	8	9	9	15	18	9	17	12	17	15	351	Mar 09 Monday
70	24	16	22	25	21	24	15	6	11	21	9	14	13	13	16	12	16	25	13	18	17	17	17	29	414	Mar 10 Tuesday
71	24	20	35	15	21	20	12	8	11	9	13	9	21	16	19	11	13	19	17	24	17	15	22	22	413	Mar 11 Wednesday
72	17	13	21	18	23	25	26	18	5	15	4	13	16	8	13	15	18	12	12	13	15	23	20	20	383	Mar 12 Thursday
73	23	17	22	22	22	15	14	11	8	9	12	8	15	21	7	12	17	9	17	15	3	3	6	6	314	Mar 13 Friday
74	6	9	10	10	11	12	13	18	12	18	23	14	16	11	14	16	17	15	20	9	13	17	14	11	329	Mar 14 Saturday
75	21	19	18	20	19	13	16	19	27	18	23	29	31	32	24	25	36	35	22	27	26	26	26	28	580	Mar 15 Sunday
76	23	30	34	23	23	15	10	20	10	12	6	6	18	18	14	18	9	17	22	19	19	23	18	22	429	Mar 16 Monday

Table 2.3.2 (Page 3 of 4)

NAO .DPX Hourly distribution of detections

Day	00	01	02	03	04	05	06	07	08	09	10	11	12	13	14	15	16	17	18	19	20	21	22	23	Sum	Date
77	20	17	26	30	24	16	16	7	30	9	18	18	15	11	20	15	31	12	14	13	19	10	21	17	429	Mar 17 Tuesday
78	26	19	15	19	22	14	10	14	15	23	13	11	17	12	17	2	14	20	13	14	21	12	14	17	374	Mar 18 Wednesday
79	13	22	18	4	12	10	20	9	8	13	15	20	34	16	11	10	4	14	8	20	22	7	13	13	336	Mar 19 Thursday
80	10	13	25	21	19	19	16	4	10	12	10	5	13	14	16	13	8	11	15	9	7	14	8	17	309	Mar 20 Friday
81	17	15	12	18	12	7	11	13	11	11	14	15	12	12	11	14	21	9	10	10	13	14	13	23	318	Mar 21 Saturday
82	20	25	27	15	33	15	14	19	23	23	17	18	27	10	11	19	21	14	17	19	14	16	21	19	457	Mar 22 Sunday
83	17	23	30	14	19	12	10	12	7	4	10	5	12	15	10	12	16	14	9	11	12	11	15	18	318	Mar 23 Monday
84	17	22	21	16	20	15	3	2	8	6	7	0	13	12	6	14	6	13	8	14	15	11	8	17	274	Mar 24 Tuesday
85	12	9	14	15	11	6	1	6	13	3	19	4	22	5	9	18	21	21	13	12	9	18	22	10	293	Mar 25 Wednesday
86	10	13	11	11	6	8	2	7	2	2	2	25	7	17	20	10	20	20	11	11	13	8	18	26	280	Mar 26 Thursday
87	21	17	23	18	30	18	5	6	9	9	22	16	22	19	21	21	13	14	26	34	25	24	23	21	457	Mar 27 Friday
88	22	18	25	27	17	26	15	18	20	22	19	16	16	15	16	14	27	16	20	21	14	20	24	16	464	Mar 28 Saturday
89	26	19	17	16	30	19	22	26	22	11	13	15	20	17	12	11	11	3	0	0	0	0	0	0	310	Mar 29 Sunday
90	0	0	0	0	12	10	11	15	5	8	11	21	8	2	15	9	6	6	20	16	21	14	17	11	238	Mar 30 Monday
91	15	22	17	20	11	7	11	5	15	25	6	16	32	18	10	20	19	23	10	9	10	21	20	18	380	Mar 31 Tuesday
NAO	00	01	02	03	04	05	06	07	08	09	10	11	12	13	14	15	16	17	18	19	20	21	22	23		
Sum		3850		3729		3281		2333		2631		2687		3078		2949		3173		3097		3307		3466		
	3554		3791		3696		2612		2483		2686		3393		3056		3179		3040		3161		3366		75598	Total sum
183	19	21	21	20	20	18	14	13	14	14	15	15	19	17	17	16	17	17	17	17	17	18	18	19	413	Total average
128	19	20	20	20	20	16	12	10	11	12	13	13	18	16	16	15	16	16	15	16	16	17	18	19	385	Average workdays
55	20	22	21	21	22	22	19	20	19	20	19	18	20	19	18	20	21	20	20	19	19	21	20	20	479	Average weekends

Table 2.3.2. Daily and hourly distribution of NORSAR detections. For each day is shown number of detections within each hour of the day and number of detections for that day. The end statistics give total number of detections distributed for each hour and the total sum of detections during the period. The averages show number of processed days, hourly distribution and average per processed day.

3 Operation of regional arrays

3.1 Recording of NORESS data at NDPC, Kjeller

Table 3.1.1 lists the main outage times and reasons, and as can be seen the main reasons for the outages are transmission line failures. All outages were of relatively short duration, however.

The average recording time was 99.78% as compared to 89.89% during the previous reporting period.

Date	Time	Cause
04 Oct	1049 - 1059	Transmission line failure
04 Oct	1237 - 1253	Transmission line failure
14 Nov	0945 - 0955	Transmission line failure
14 Nov	2253 -	Transmission line failure
15 Nov	- 0006	
12 Dec	1306 - 1313	Transmission line failure
20 Dec	0021 - 0116	Transmission line failure
03 Jan	1033 - 1225	Testing hardware/software
15 Jan	1121 - 1137	Transmission line failure
24 Jan	1233 - 1256	Hub failure
06 Feb	0210 - 0223	Transmission line failure
21 Feb	0000 - 0026	Transmission line failure
27 Feb	0915 - 1001	Transmission line failure
10 Mar	0916 - 0936	Transmission line failure

Table 3.1.1. Interruptions in recording of NORESS data at NDPC, 1 October 1991 - 31 March 1992.

Monthly uptimes for the NORESS on-line data recording task, taking into account all factors (field installations, transmission line, data center operation) affecting this task were as follows:

October	:	99.86
November	:	99.74
December	:	99.83
January	:	99.53
February	:	99.77
March	:	99.92

Fig. 3.1.1 shows the uptime for the data recording task, or equivalently, the availability of NORESS data in our tape archive, on a day-by-day basis, for the reporting period.

J. Torstveit

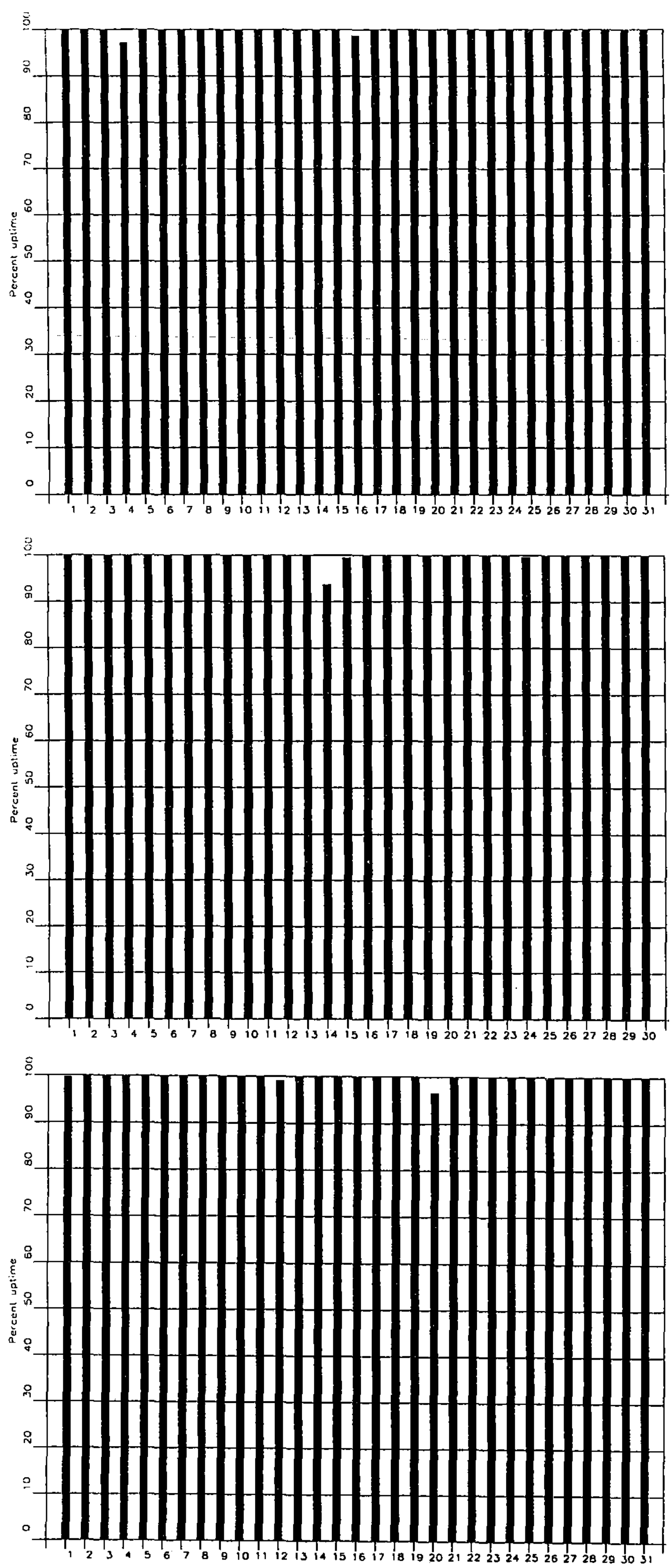

Fig. 3.1.1. NORESS data recording uptime for October (top), November (middle) and December (bottom) 1991.

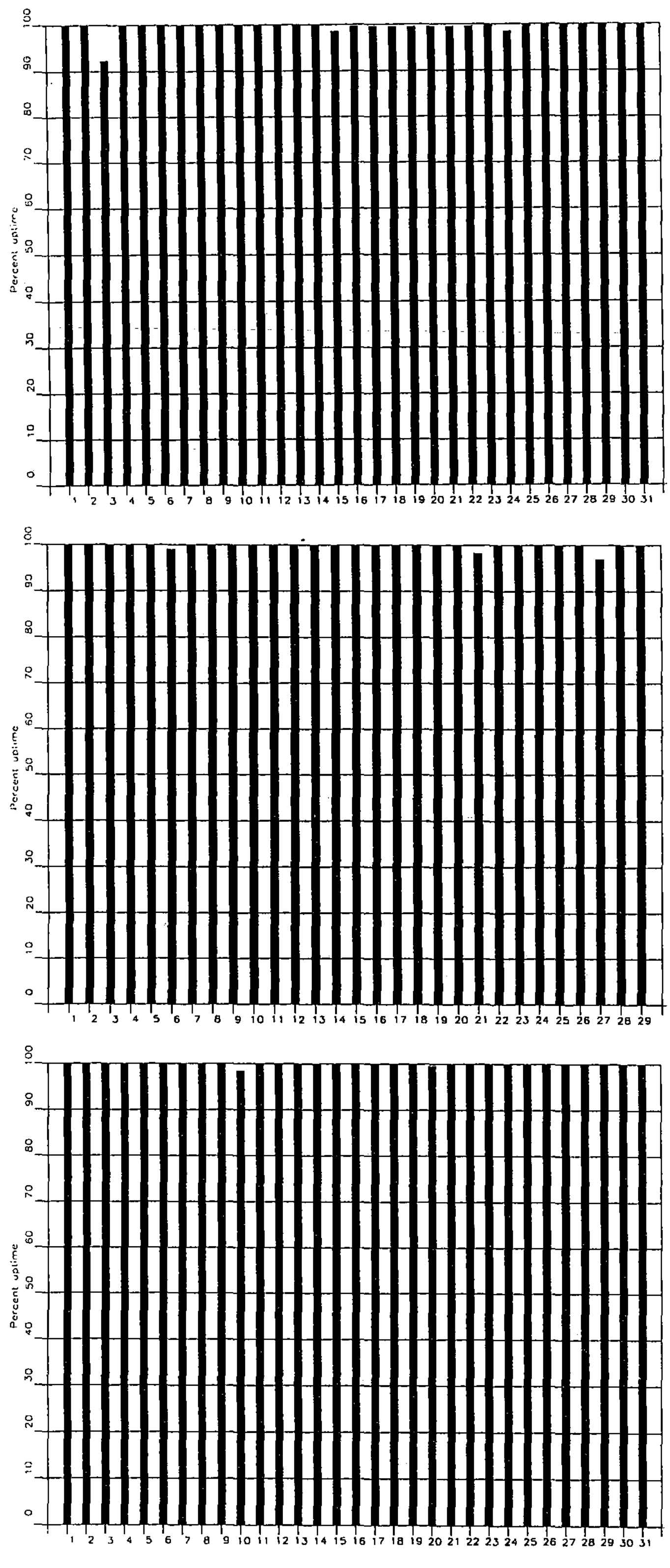

Fig. 3.1.1. (cont.) NORESS data recording uptime for January (top), February (middle) and March (bottom) 1992.

3.2 Recording of ARCESS data at NDPC, Kjeller

Table 3.2.1 lists the main outage times and reasons. The main contributing factor is a power break that resulted from a severe storm on 21 January.

The average recording time was 99.28 % as compared to 97.32% for the previous reporting period..

Date	Time	Cause
07 Dec	1806 - 1940	Hardware failure NDPC
31 Dec	2311 - 0000	Software failure NDPC
21 Jan	1039 -	Power break HUB
22 Jan	- 1200	Powert break HUB

Table 3.2.1. The main interruptions in recording of ARCESS data at NDPC, 1 October 1991 - 31 March 1992.

Monthly uptimes for the ARCESS on-line data recording task, taking into account all factors (field installations, transmissions line, data center operation) affecting this task were as follows:

October	:	99.99%
November	:	99.91%
December	:	99.68%
January	:	96.31%
February	:	99.93%
March	:	99.86%

Fig. 3.2.1. shows the uptime for the data recording task, or equivalently, the availability of ARCESS data in our tape archive, on a day-by-day basis, for the reporting period.

J. Torstveit

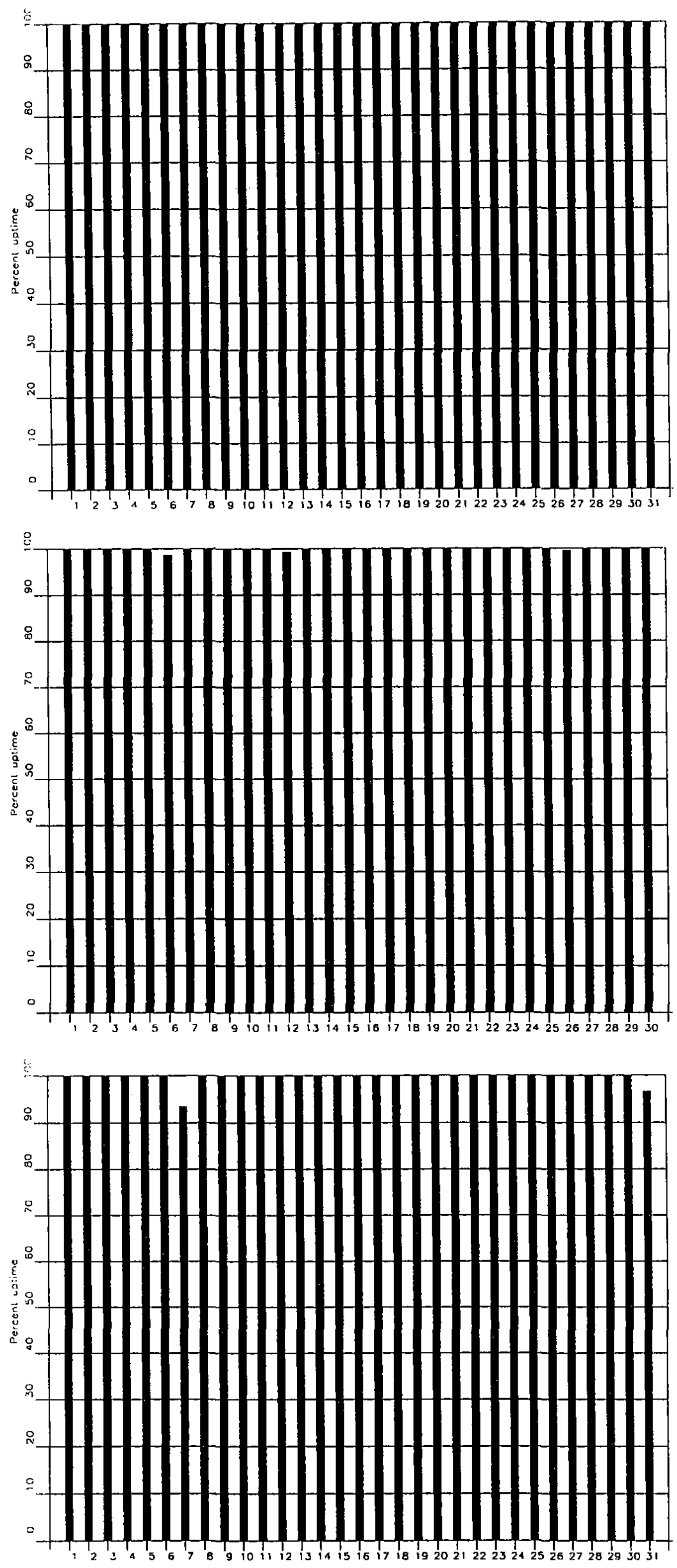

Fig. 3.2.1. ARCESS data recording uptime for October (top), November (middle) and December (bottom) 1991.

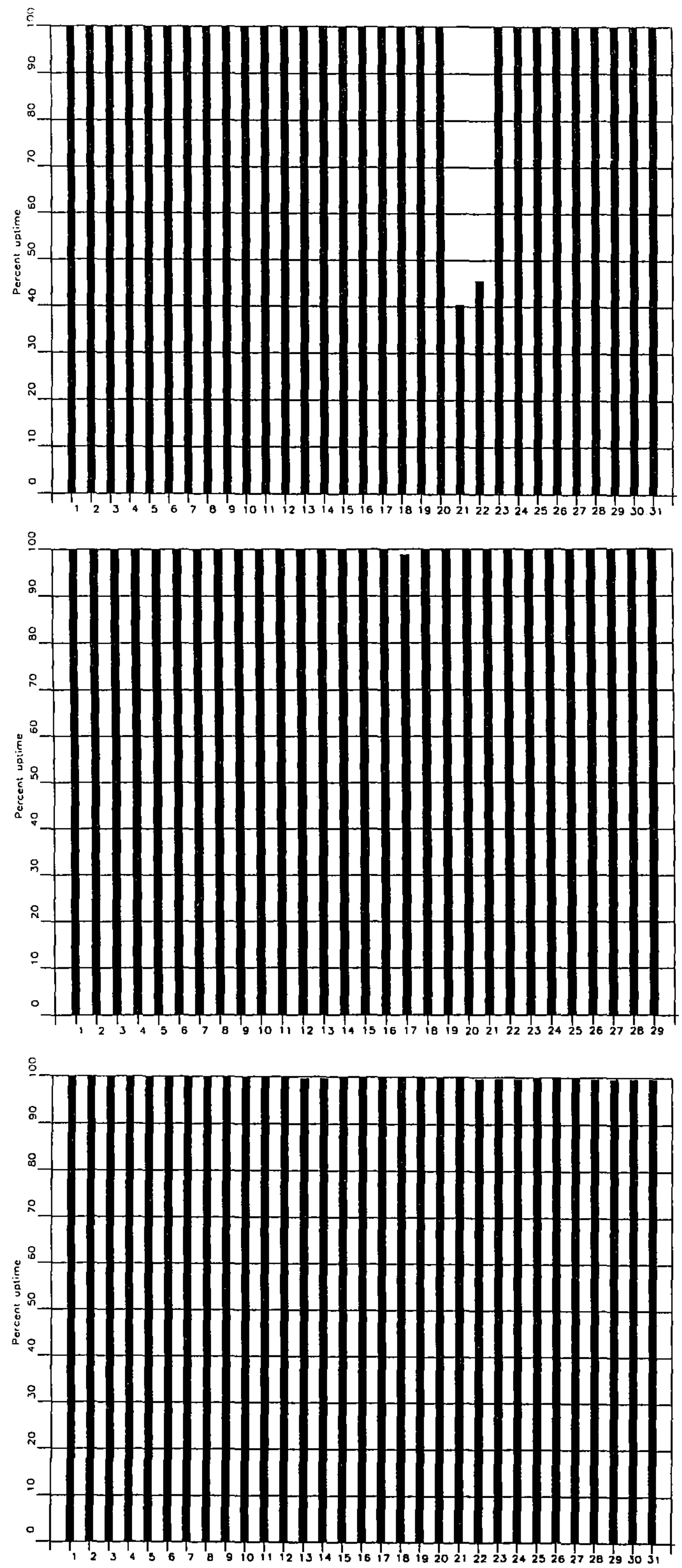

Fig. 3.2.1. ARCESS data recording uptime for January (top), February (middle) and March (bottom) 1992.

3.3 Recording of FINESA data at NDPC, Kjeller

The average recording time was 95.5% as compared to 66.2% for the previous period. As can be seen from Table 3.3.1 below, the only reason for the dowtime is transmission line failure.

Date	Time	Cause
23 Oct	0928 -	Transmission line failure
31 Oct	- 1134	Transmission line failure
05 Jan	1802 - 1834	Transmission line failure
06 Jan	1637 - 1657	Transmission line failure
06 Jan	1712 - 1719	Transmission line failure
06 Jan	1805 - 1811	Transmission line failure
07 Jan	1045 - 1055	Transmission line failure
07 Jan	1240 - 1249	Transmission line failure
07 Jan	1253 - 1259	Transmission line failure
07 Jan	2011 - 2016	Transmission line failure
24 Mar	0449 - 0722	Transmission line failure

Table 3.3.1. The main interruptions in recording of FINESA data at NDPC, 1 October 1991 - 31 March 1992.

Monthly uptimes for the FINESA on-line data recording task, taking into account all factors (field installations, transmission lines, data center operation) affecting this task were as follows:

October	:	74.23%
November	:	99.97%
December	:	99.89%
January	:	99.56%
February	:	99.96%
March	:	99.59%

Fig. 3.3.1 shows the uptime for the data recording task, or equivalently, the availability of FINESA data in our tape archive, on a day-by-day basis, for the reporting period.

J. Torstveit

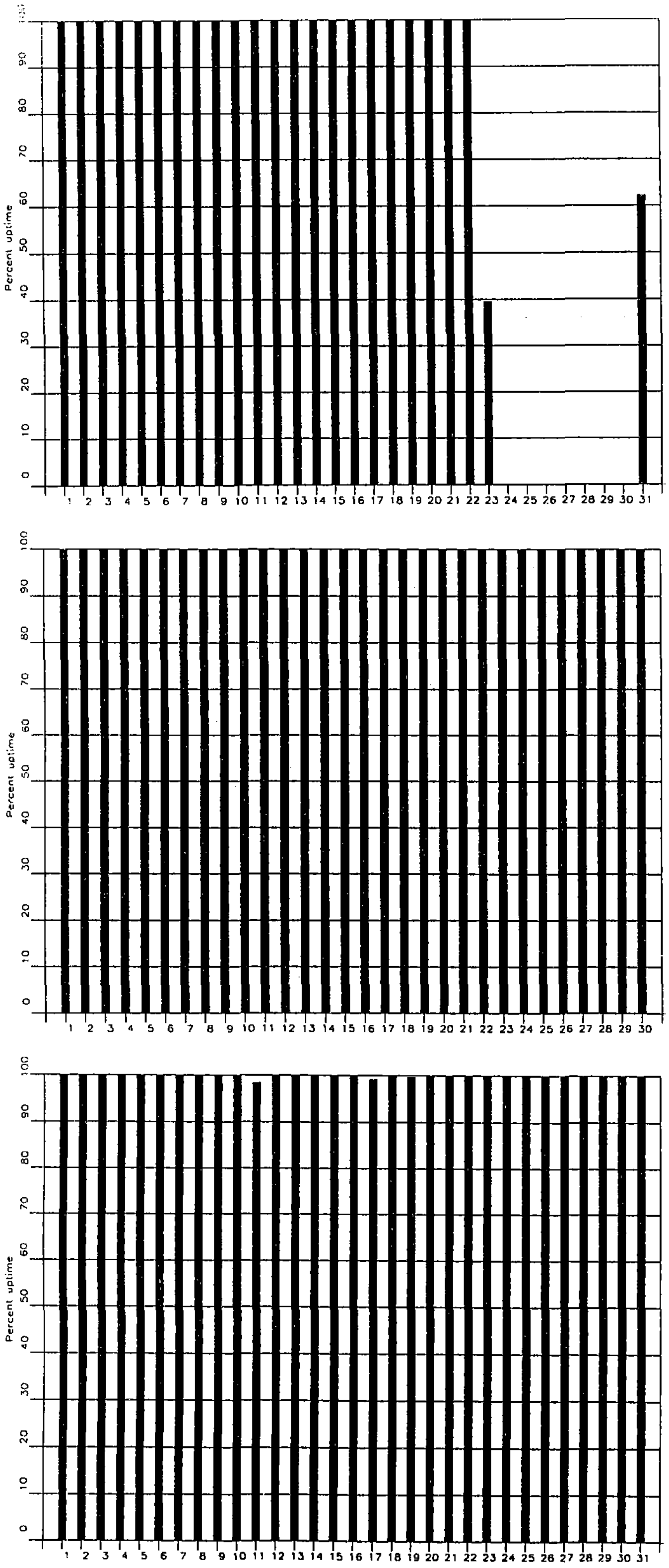

Fig. 3.3.1. FINESA data recording uptime for October (top), November (middle) and December (bottom) 1991.

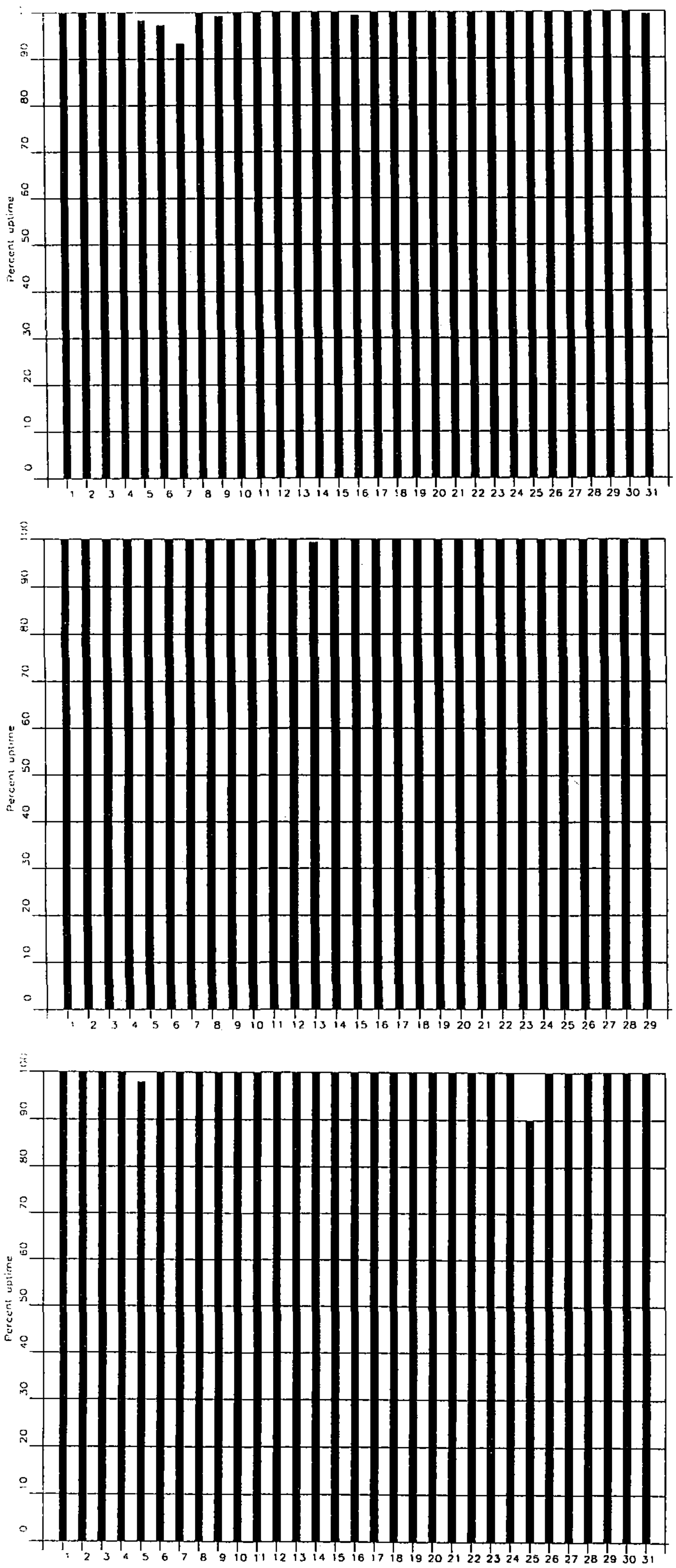

Fig. 3.3.1. FINESA data recording uptime for January (top), February (middle) and March (bottom) 1992.

3.4 Event detection operation

This section reports results from simple one-array automatic processing using signal processing recipes and "ronapp" recipes for the ep program (NORSAR Sci. Rep. No 2-88,89).

Three systems are in parallel operation to associate detected phases and locate events:

1. The ep program with "ronapp" recipes is operated independently on each array to obtain simple one-array automatic solutions.
2. The Generalized Beamforming method (GBF) (see F. Ringdal and T. Kværna (1989), A mulitchannel processing approach to real time network detection, phase association and threshold monitoring, BSSA Vol 79, no 6, 1927-1940) processes the four arrays jointly and presents locations of regional events.
3. The IMS system is operated on the same set of arrivals as ep and GBF and reports also teleseismic events in addition to regional ones.

IMS results are reported in section 3.5 and GBF results in section 3.6.

In addition to these three event association processes, we are running test versions of the so-called Threshold Monitoring (TM) process. This is a process that monitors the seismic amplitude level at the four regional arrays continuously in time to estimate the upper magnitude limit of an event that might go undetected by the network. The current TM process is beamed to several sites of interest, including the Novaya Zemlya test site. Simple displays of so-called threshold curves reveal instants of particular interest; i.e., instants when events above a certain magnitude threshold may have occurred in the target region. Results from the three processes described above are used to help resolve what actually happened during these instances. For more details, see section 7.8.

NORESS detections

The number of detections (phases) reported from day 274 1991, through day 091 1992, was 44,786, giving an average of 245 detections per processed day (183 days processed).

Table 3.4.1 shows daily and hourly distribution of detections for NORESS. See also Section 7.6 for distribution of detections versus apparent velocity and azimuth.

Events automatically located by NORESS

During days 274 1991, through 091 1992, 2716 local and regional events were located by NORESS, based on automatic association of P- and S-type arrivals. This gives an average of 14.8 events per processed day (183 days processed). 63% of these events are within 300 km, and 87% of these events are within 1000 km.

ARCESS detections

The number of detections (phases) reported during day 274 1991, through day 091 1992, was 74,532, giving an average of 407 detections per processed day (183 days processed).

Table 3.4.2 shows daily and hourly distribution of detections for ARCESS.

Events automatically located by ARCESS

During days 274 1991, through 092 1992, 3371 local and regional events were located by ARCESS, based on automatic association of P- and S-type arrivals. This gives an average 18.4 events per processed day (183 days processed). 46% of these events are within 300 km, and 85% of these events are within 1000 km.

FINESA detections

The number of detections (phases) reported during day 274 1991, through day 091 1992, was 50,417, giving an average of 293 detections per processed day (172 days processed).

Table 3.4.3 shows daily and hourly distribution of detections for FINESA.

Events automatically located by FINESA

During days 274 1991, through 091 1992, 3055 local and regional events were located by FINESA, based on automatic association of P- and S-type arrivals. This gives an average of 17.8 events per processed day (172 days processed). 67% of these events are within 300 km, and 88% of these events are within 1000 km.

GERESS detections

The number of detections (phases) reported from day 274 1991, through day 091 1992, was 30,407, giving an average of 182 detections per processed day (167 days processed).

Table 3.4.4 shows daily and hourly distribution of detections for GERESS.

Events automatically located by GERESS

During days 274 1991, through 091 1992, 2224 local and regional events were located by GERESS, based on automatic association of P- and S-type arrivals. This gives an average of 13.3 events per processed day (167 days processed). 68% of these events are within 300 km, and 88% of these events are within 1000 km.

Poland detections

The number of detections (phases) reported by the station KSP from day 274 1991, through day 351 1991, was 27,448, giving an average of 352 detections per processed day (78 days processed).

Table 3.4.5 shows daily and hourly distribution of detections for the KSP station in Poland.

The data transmitted from the station SFP were very unreliable and were not process during the reporting period. It was found that the signal processing results for KSP data generated too many false events for IMS; consequently this processing was stopped during December 1991.

J. Fyen

NRS .FKX Hourly distribution of detections

Day	00	01	02	03	04	05	06	07	08	09	10	11	12	13	14	15	16	17	18	19	20	21	22	23	Sum	Date
274	2	3	4	9	5	6	2	1	7	16	10	2	9	22	17	19	16	12	4	4	10	5	6	14	205	Oct 01 Tuesday
275	20	0	2	4	4	3	2	5	16	14	11	3	14	7	18	14	6	17	7	5	17	3	3	1	196	Oct 02 Wednesday
276	0	3	5	4	7	3	2	5	7	11	10	18	7	8	6	10	8	12	12	8	16	3	8	2	175	Oct 03 Thursday
277	3	4	1	2	5	4	8	3	10	5	2	3	3	15	14	8	4	8	7	7	9	2	1	4	132	Oct 04 Friday
278	8	7	5	2	3	4	2	7	6	7	2	0	7	8	2	4	5	6	8	9	3	5	8	4	122	Oct 05 Saturday
279	1	10	0	4	3	13	2	3	7	8	14	5	9	10	0	4	1	5	1	5	5	5	1	3	119	Oct 06 Sunday
280	4	4	3	5	9	3	2	2	0	4	6	6	10	12	9	18	12	13	19	3	15	4	5	1	169	Oct 07 Monday
281	1	8	5	3	10	4	6	2	2	3	1	6	25	15	10	13	7	10	3	5	11	7	6	1	164	Oct 08 Tuesday
282	7	1	6	3	7	3	2	8	6	6	8	4	9	21	16	20	11	17	3	5	16	2	2	3	186	Oct 09 Wednesday
283	7	5	3	3	18	5	1	4	1	5	5	8	5	22	22	13	25	8	17	8	27	8	3	7	230	Oct 10 Thursday
284	3	1	6	10	5	8	4	6	8	3	6	6	10	17	14	7	8	14	10	5	17	0	0	0	168	Oct 11 Friday
285	9	1	2	1	2	6	4	0	3	2	1	15	7	2	4	8	26	5	4	1	6	0	4	0	113	Oct 12 Saturday
286	6	9	1	8	3	5	3	9	1	3	7	25	2	2	3	5	0	1	7	4	1	1	6	1	113	Oct 13 Sunday
287	2	1	4	6	17	5	4	6	4	6	6	2	19	21	10	14	22	9	14	11	19	5	2	5	214	Oct 14 Monday
288	1	2	0	8	5	14	4	6	3	7	15	10	18	32	23	9	17	2	1	5	24	0	0	9	215	Oct 15 Tuesday
289	4	2	3	3	7	3	5	9	4	9	10	3	10	16	17	18	14	6	4	3	8	11	0	4	173	Oct 16 Wednesday
290	3	4	2	3	8	10	2	2	8	10	5	2	12	17	13	11	18	19	10	6	11	5	0	3	184	Oct 17 Thursday
291	3	2	1	4	2	2	1	6	2	5	2	9	10	14	9	1	6	10	5	3	10	2	2	2	113	Oct 18 Friday
292	1	4	5	0	6	16	3	1	14	17	5	3	19	15	7	16	2	7	1	0	3	10	10	0	165	Oct 19 Saturday
293	5	12	6	4	6	9	10	4	5	5	4	8	0	8	12	1	3	3	1	0	0	1	2	1	110	Oct 20 Sunday
294	1	0	10	0	8	3	1	5	5	4	5	9	7	19	14	8	6	20	8	8	10	4	1	8	164	Oct 21 Monday
295	6	1	2	5	5	2	2	4	2	9	15	24	13	28	22	17	8	32	0	4	8	9	2	0	220	Oct 22 Tuesday
296	3	2	1	0	6	4	2	2	5	1	8	6	21	20	15	3	26	4	13	9	17	4	5	5	182	Oct 23 Wednesday
297	6	4	4	2	9	22	1	10	15	11	18	14	15	44	31	16	33	11	8	0	21	0	1	5	301	Oct 24 Thursday
298	6	17	1	5	13	6	3	3	14	18	20	13	21	19	15	10	4	20	22	0	20	8	4	0	262	Oct 25 Friday
299	0	0	9	2	5	5	8	3	7	7	5	8	11	27	17	13	5	5	5	3	7	6	8	5	171	Oct 26 Saturday
300	6	3	2	5	2	7	9	3	5	9	7	8	46	37	11	26	31	0	5	7	3	5	11	6	254	Oct 27 Sunday
301	5	10	3	4	11	3	2	31	9	7	13	4	20	23	20	13	41	17	10	6	13	5	6	1	277	Oct 28 Monday
302	1	4	5	3	12	7	4	3	10	24	8	7	12	29	36	6	11	3	4	6	8	3	4	6	216	Oct 29 Tuesday
303	4	5	1	5	11	7	0	11	16	4	10	5	38	12	12	8	20	25	8	4	19	2	7	5	239	Oct 30 Wednesday
304	0	9	9	6	9	3	3	5	5	8	2	21	16	8	10	21	5	14	2	13	16	5	5	2	197	Oct 31 Thursday
305	2	3	2	3	8	7	3	4	5	4	17	9	13	10	8	5	9	17	15	5	18	5	4	4	180	Nov 01 Friday
306	2	8	6	5	2	12	5	6	2	3	9	4	10	5	9	5	8	5	8	1	1	3	2	4	125	Nov 02 Saturday
307	5	3	3	2	4	7	12	8	10	19	42	25	33	28	11	23	18	10	24	2	7	4	2	5	307	Nov 03 Sunday
308	4	7	4	8	6	7	6	1	1	28	2	4	10	8	12	18	26	11	15	2	10	5	3	4	202	Nov 04 Monday
309	2	1	6	4	4	3	4	11	5	4	10	2	10	11	6	10	3	2	5	4	8	5	2	3	125	Nov 05 Tuesday
310	2	1	2	3	5	8	24	5	13	20	10	27	12	19	14	13	2	17	23	14	5	1	3	3	246	Nov 06 Wednesday
311	2	2	2	1	7	1	6	8	4	0	6	1	2	22	14	27	12	7	8	1	10	5	0	3	151	Nov 07 Thursday
312	2	8	1	2	2	7	2	5	2	9	6	7	11	13	17	18	1	16	15	5	2	0	7	1	159	Nov 08 Friday
313	2	1	2	1	3	10	6	14	9	4	7	9	4	5	21	7	3	5	5	5	2	1	4	4	134	Nov 09 Saturday
314	7	3	6	4	0	6	8	5	18	22	36	34	36	21	34	10	11	6	4	3	4	5	5	4	292	Nov 10 Sunday
315	6	4	6	4	2	8	6	2	2	4	4	6	11	8	8	12	12	18	24	4	3	5	13	2	174	Nov 11 Monday
316	1	2	3	2	4	4	5	31	7	9	13	19	20	23	22	22	4	1	8	4	4	7	0	4	219	Nov 12 Tuesday
317	11	5	8	2	2	7	5	2	4	7	8	16	17	20	31	15	3	1	8	10	4	18	2	4	210	Nov 13 Wednesday
318	0	2	1	2	9	6	4	3	1	0	10	8	9	16	17	15	9	2	7	8	10	4	5	0	148	Nov 14 Thursday
319	1	1	0	4	2	1	11	10	1	6	7	8	6	13	4	5	3	10	17	0	8	7	6	8	139	Nov 15 Friday
320	14	9	8	8	10	12	15	8	9	4	9	3	24	13	21	30	25	22	27	25	25	21	29	7	378	Nov 16 Saturday
321	9	23	30	25	77	57	52	50	23	6	11	11	11	15	6	27	22	11	4	5	13	15	36	97	636	Nov 17 Sunday
322	76	70	28	3	4	5	5	15	17	29	2	32	10	24	52	52	40	33	42	40	51	53	60	52	795	Nov 18 Monday
323	67	88	84	64	44	30	31	7	12	3	7	17	16	22	18	14	11	22	43	57	59	69	77	84	946	Nov 19 Tuesday
324	71	76	76	77	79	88	57	43	21	21	15	7	20	40	23	38	9	13	2	2	7	5	41	75	906	Nov 20 Wednesday
325	77	49	44	9	6	15	9	2	5	7	9	10	18	19	0	8	14	1	11	5	6	6	5	8	343	Nov 21 Thursday
326	3	4	1	3	6	15	19	5	4	1	4	12	5	9	6	7	5	2	18	0	2	2	4	8	145	Nov 22 Friday
327	3	4	5	6	1	0	6	11	9	3	7	9	4	8	5	11	13	20	26	43	34	4	16	19	267	Nov 23 Saturday
328	4	5	3	5	6	5	7	16	5	2	5	8	0	1	8	3	20	22	6	2	2	7	7	2	151	Nov 24 Sunday
329	5	4	3	4	4	7	6	18	11	22	9	4	22	19	30	7	5	26	8	3	24	5	3	32	281	Nov 25 Monday

Table 3.4.1 (Page 1 of 4)

NRS .FKX Hourly distribution of detections

Day	00	01	02	03	04	05	06	07	08	09	10	11	12	13	14	15	16	17	18	19	20	21	22	23	Sum	Date		
330	5	2	36	16	9	6	5	8	17	22	13	20	41	22	19	5	31	13	4	9	27	15	5	28	378	Nov 26	Tuesday	
331	20	1	3	2	1	8	2	14	15	11	19	11	21	8	28	10	8	2	25	5	11	6	4	29	264	Nov 27	Wednesday	
332	16	1	2	8	2	6	4	19	10	3	7	17	26	28	26	9	3	8	16	4	4	3	2	3	227	Nov 28	Thursday	
333	27	14	2	5	10	1	2	14	16	18	17	6	25	33	21	7	1	9	21	12	11	9	4	7	292	Nov 29	Friday	
334	3	5	1	3	6	1	2	7	2	15	6	3	14	16	6	53	30	13	7	1	1	2	7	4	208	Nov 30	Saturday	
335	4	3	2	4	4	3	5	9	5	7	5	7	7	6	15	30	18	0	1	1	5	5	5	6	157	Dec 01	Sunday	
336	3	7	7	8	10	2	10	8	11	2	7	11	17	18	27	1	2	17	18	20	6	12	24	6	254	Dec 02	Monday	
337	15	3	6	5	7	1	10	11	20	10	12	7	13	22	13	8	3	8	8	3	7	2	5	7	206	Dec 03	Tuesday	
338	36	40	0	6	8	1	2	3	12	9	13	5	13	13	21	18	18	3	9	8	7	24	26	4	299	Dec 04	Wednesday	
339	12	13	16	6	5	2	1	4	6	18	8	1	8	16	34	15	11	0	3	2	5	7	2	3	198	Dec 05	Thursday	
340	1	4	2	0	12	2	5	10	6	6	8	20	16	22	24	13	15	7	18	19	25	26	14	20	295	Dec 06	Friday	
341	32	27	27	26	32	11	5	7	6	5	7	18	13	9	28	25	55	57	67	44	52	57	57	59	726	Dec 07	Saturday	
342	60	57	59	62	61	61	47	56	26	7	10	14	21	14	12	5	10	26	10	17	55	51	53	23	817	Dec 08	Sunday	
343	6	11	1	16	15	6	0	3	1	12	3	4	21	9	35	56	36	26	36	29	37	5	7	7	382	Dec 09	Monday	
344	11	8	1	2	4	2	4	4	5	12	6	13	15	11	9	11	4	6	4	1	12	4	6	17	172	Dec 10	Tuesday	
345	36	11	0	0	3	15	21	11	9	10	8	15	20	12	14	10	20	28	30	7	16	20	18	23	357	Dec 11	Wednesday	
346	22	25	37	36	30	12	9	5	4	6	6	21	14	6	18	5	8	6	1	3	7	3	6	2	292	Dec 12	Thursday	
347	9	1	9	20	18	9	9	5	8	6	4	14	20	14	13	11	5	9	15	11	33	5	5	3	256	Dec 13	Friday	
348	7	5	16	9	9	15	19	10	16	11	5	19	14	22	12	9	25	38	27	38	17	14	7	8	372	Dec 14	Saturday	
349	9	5	3	5	5	13	16	23	10	13	10	20	12	15	10	13	5	4	4	6	4	15	4	32	256	Dec 15	Sunday	
350	12	20	31	33	39	19	10	11	12	14	7	7	9	23	14	15	4	6	10	2	8	3	8	4	321	Dec 16	Monday	
351	6	3	7	6	8	5	9	8	6	8	6	11	18	18	19	6	2	2	1	5	6	4	8	5	177	Dec 17	Tuesday	
352	2	2	2	4	5	3	0	4	9	4	20	9	15	33	12	8	13	5	8	7	9	20	10	5	209	Dec 18	Wednesday	
353	4	10	10	13	21	7	9	3	10	14	13	8	30	22	22	8	4	3	2	9	4	8	4	0	238	Dec 19	Thursday	
354	1	0	4	1	2	5	2	1	10	4	8	7	15	15	3	4	5	8	3	0	2	3	5	0	108	Dec 20	Friday	
355	3	0	2	6	9	13	8	12	2	7	2	5	6	15	6	28	5	4	4	9	4	10	10	20	190	Dec 21	Saturday	
356	22	27	32	27	45	47	31	38	29	61	54	28	22	17	17	16	25	11	15	5	3	19	9	4	604	Dec 22	Sunday	
357	4	0	6	4	10	10	1	5	9	3	9	9	22	14	8	8	7	2	4	6	11	3	6	3	164	Dec 23	Monday	
358	3	4	4	16	16	4	5	11	12	4	14	11	21	31	32	16	19	29	22	21	24	21	24	10	374	Dec 24	Tuesday	
359	2	5	9	12	7	19	14	17	11	9	9	12	15	19	9	6	8	3	1	10	2	1	9	4	213	Dec 25	Wednesday	Frste
360	11	6	4	12	3	7	6	4	7	1	10	12	9	9	5	6	2	2	1	6	3	2	2	10	140	Dec 26	Thursday	Andre
361	10	8	4	3	16	2	3	3	8	6	14	9	14	15	4	2	1	4	8	6	14	10	2	1	167	Dec 27	Friday	
362	0	7	5	10	11	5	4	6	10	25	27	16	36	15	3	7	2	1	5	5	3	5	7	0	215	Dec 28	Saturday	
363	2	4	0	0	2	7	2	6	3	4	1	2	4	5	7	2	0	1	9	16	2	4	0	3	86	Dec 29	Sunday	
364	4	4	0	1	3	1	8	5	3	2	7	5	10	4	6	2	4	5	4	2	10	1	9	2	102	Dec 30	Monday	
365	4	5	7	5	16	16	6	7	4	2	4	2	15	27	2	2	9	4	6	8	4	5	2	0	162	Dec 31	Tuesday	
1	0	4	0	0	0	2	1	2	14	0	3	2	1	3	0	5	2	1	2	2	3	3	12	2	64	Jan 01	Wednesday	Frste
2	6	5	8	3	3	7	1	4	2	2	3	8	6	6	4	1	8	2	4	5	6	5	1	3	103	Jan 02	Thursday	
3	1	1	4	5	3	3	5	6	3	3	3	1	6	2	4	4	3	6	13	8	6	5	2	1	98	Jan 03	Friday	
4	4	12	3	9	14	3	17	12	2	11	1	5	10	21	26	12	7	10	14	22	12	11	11	13	262	Jan 04	Saturday	
5	20	23	19	27	27	41	27	19	18	11	20	20	28	20	12	10	13	20	12	18	13	19	35	31	503	Jan 05	Sunday	
6	14	9	10	3	7	2	0	1	3	7	6	2	13	6	11	2	5	2	4	13	7	10	7	2	146	Jan 06	Monday	
7	1	12	6	17	2	2	7	2	2	9	6	8	7	10	15	8	4	7	4	3	11	3	0	7	153	Jan 07	Tuesday	
8	4	2	6	3	5	2	2	4	4	3	7	4	15	11	10	4	6	3	7	5	15	8	4	9	143	Jan 08	Wednesday	
9	12	14	21	11	6	1	2	2	7	13	15	7	16	14	16	15	12	11	5	3	7	16	14	21	261	Jan 09	Thursday	
10	25	37	28	43	37	13	5	7	3	5	7	17	15	17	10	5	4	5	7	5	2	2	13	4	316	Jan 10	Friday	
11	1	2	2	3	2	2	6	1	3	7	6	2	2	5	5	6	1	4	8	0	4	3	1	4	80	Jan 11	Saturday	
12	5	4	10	10	3	6	2	5	5	1	2	13	7	10	6	11	5	3	2	4	4	6	2	2	128	Jan 12	Sunday	
13	3	6	5	7	5	2	2	1	7	21	10	22	38	7	25	6	8	6	6	13	8	10	5	9	232	Jan 13	Monday	
14	26	14	10	17	4	1	1	3	0	5	12	16	17	20	21	12	6	9	9	7	6	10	4	16	246	Jan 14	Tuesday	
15	4	8	3	9	0	3	3	14	10	6	18	3	9	16	12	17	13	8	3	0	10	2	2	17	190	Jan 15	Wednesday	
16	7	14	5	7	11	5	3	4	2	9	17	10	10	11	16	6	7	4	17	17	9	18	8	6	223	Jan 16	Thursday	
17	7	22	8	9	9	6	11	18	14	15	20	26	9	16	30	11	6	8	10	22	9	7	2	4	299	Jan 17	Friday	
18	5	6	7	9	6	7	3	7	3	7	8	11	11	9	4	6	5	16	4	2	2	3	3	8	152	Jan 18	Saturday	
19	8	3	5	6	2	6	4	10	8	5	5	1	9	4	2	6	6	7	5	3	4	1	3	8	121	Jan 19	Sunday	
20	6	2	6	6	3	1	1	5	4	12	15	13	13	23	20	10	7	4	5	3	3	5	3	9	179	Jan 20	Monday	

Table 3.4.1 (Page 2 of 4)

NRS .FKX Hourly distribution of detections

Day	00	01	02	03	04	05	06	07	08	09	10	11	12	13	14	15	16	17	18	19	20	21	22	23	Sum	Date
21	6	8	1	10	8	10	10	7	8	3	12	7	11	14	19	7	3	12	10	3	7	9	9	7	201	Jan 21 Tuesday
22	7	24	10	12	20	4	8	12	30	6	36	32	64	28	34	28	8	5	6	14	4	5	7	3	407	Jan 22 Wednesday
23	3	7	1	4	12	4	9	4	15	8	3	5	19	10	13	15	10	8	15	4	15	8	11	11	214	Jan 23 Thursday
24	10	10	3	3	3	9	1	4	7	5	11	16	7	17	9	3	15	2	7	8	6	1	7	12	176	Jan 24 Friday
25	8	7	5	10	17	18	15	21	9	8	12	18	14	5	7	8	8	5	16	5	5	3	6	7	237	Jan 25 Saturday
26	13	21	24	23	10	34	34	30	15	29	11	9	8	5	1	1	5	10	7	2	6	7	1	2	308	Jan 26 Sunday
27	1	9	4	1	2	3	3	1	7	4	2	12	14	9	9	11	4	2	6	10	5	2	19	15	155	Jan 27 Monday
28	11	3	4	3	3	3	3	4	5	6	8	12	15	17	13	11	8	6	2	9	13	5	13	6	183	Jan 28 Tuesday
29	5	0	4	3	4	2	3	3	6	4	5	8	18	29	12	7	4	8	8	25	13	1	20	5	197	Jan 29 Wednesday
30	15	31	18	16	21	16	9	3	7	8	4	7	21	25	21	7	13	14	27	23	10	17	17	51	401	Jan 30 Thursday
31	29	33	23	40	27	18	12	15	5	12	12	11	26	13	10	3	5	6	15	3	6	1	2	8	335	Jan 31 Friday
32	5	0	2	2	5	4	17	7	8	21	2	14	3	4	22	11	16	12	9	11	5	1	13	19	213	Feb 01 Saturday
33	47	67	59	36	23	22	15	13	13	7	16	13	13	0	4	6	2	13	11	13	6	6	3	0	408	Feb 02 Sunday
34	5	2	3	5	1	3	5	3	0	13	2	5	19	21	11	6	6	3	2	11	11	8	8	4	157	Feb 03 Monday
35	20	32	34	25	10	13	8	4	12	7	12	9	9	29	15	16	22	14	16	7	25	42	45	32	458	Feb 04 Tuesday
36	19	30	15	28	31	38	11	9	5	7	9	20	10	10	4	8	0	5	2	7	21	18	17	22	346	Feb 05 Wednesday
37	9	22	4	10	12	8	1	0	10	12	2	13	25	19	13	7	20	2	20	2	17	26	4	1	259	Feb 06 Thursday
38	9	8	9	7	5	5	5	2	6	10	15	17	16	16	13	3	7	4	10	6	24	9	1	5	212	Feb 07 Friday
39	3	1	4	1	5	2	8	6	11	3	13	10	6	8	19	1	54	16	7	7	6	21	32	18	262	Feb 08 Saturday
40	13	6	1	1	12	3	7	5	11	3	6	1	5	1	5	4	2	4	5	6	16	34	5	1	157	Feb 09 Sunday
41	1	3	3	9	5	1	1	4	9	12	8	17	10	15	10	5	8	5	6	12	7	8	16	4	179	Feb 10 Monday
42	9	17	22	18	15	6	9	6	3	13	15	12	8	15	22	12	23	12	15	17	12	11	16	17	325	Feb 11 Tuesday
43	23	28	22	22	23	5	5	0	11	6	1	9	15	23	11	7	20	5	4	1	8	5	4	22	280	Feb 12 Wednesday
44	14	9	9	2	3	3	11	2	6	2	10	14	20	19	16	22	8	6	4	6	14	3	9	5	217	Feb 13 Thursday
45	18	5	3	11	3	3	1	12	9	8	8	16	21	11	5	12	4	3	2	35	13	18	1	38	260	Feb 14 Friday
46	2	4	2	2	5	7	4	2	17	8	4	7	48	9	2	3	6	5	5	11	4	4	6	10	177	Feb 15 Saturday
47	10	10	7	12	10	13	20	14	12	9	9	3	3	9	10	8	9	18	14	12	5	17	13	23	270	Feb 16 Sunday
48	25	19	14	15	5	12	7	9	2	10	8	6	12	21	27	10	14	5	3	5	13	15	7	18	282	Feb 17 Monday
49	19	13	19	20	16	12	15	10	3	5	16	17	29	18	11	16	9	14	4	8	2	7	2	2	287	Feb 18 Tuesday
50	4	13	42	43	35	14	9	3	6	11	7	21	15	19	19	17	6	4	7	7	15	4	6	3	330	Feb 19 Wednesday
51	7	4	3	1	2	2	3	1	6	7	20	9	14	9	17	8	21	8	5	17	14	7	9	2	196	Feb 20 Thursday
52	2	3	5	5	4	4	1	3	1	10	10	31	9	7	14	14	16	16	10	11	17	8	7	1	209	Feb 21 Friday
53	4	3	2	2	2	2	2	0	3	3	4	8	9	6	0	8	3	6	1	2	0	0	2	1	73	Feb 22 Saturday
54	7	3	6	4	2	6	7	5	1	0	1	4	2	5	1	3	9	17	21	11	22	15	16	18	186	Feb 23 Sunday
55	19	22	11	1	1	4	3	2	1	5	23	5	10	5	17	2	8	3	23	19	24	11	15	3	237	Feb 24 Monday
56	15	14	11	5	11	8	7	0	5	6	4	9	17	15	15	9	10	14	13	26	16	22	19	15	286	Feb 25 Tuesday
57	8	19	21	32	27	10	9	9	5	8	14	9	16	17	10	15	2	4	16	11	4	35	12	1	314	Feb 26 Wednesday
58	4	28	25	19	38	7	3	0	3	3	13	16	22	3	9	8	6	8	14	11	10	26	2	5	283	Feb 27 Thursday
59	43	1	1	0	6	0	2	1	7	9	11	19	15	9	13	5	5	7	9	7	1	2	1	1	175	Feb 28 Friday
60	1	1	7	1	2	6	3	2	2	1	5	8	6	8	12	6	4	8	0	1	7	5	1	7	104	Feb 29 Saturday
61	2	2	4	23	4	27	19	1	2	5	1	3	5	15	8	7	4	8	11	3	8	7	2	2	173	Mar 01 Sunday
62	1	1	5	11	7	3	1	2	4	2	5	6	20	5	11	11	11	9	4	12	3	6	2	9	151	Mar 02 Monday
63	1	12	3	8	15	7	5	3	4	9	5	11	16	11	13	13	12	6	17	17	10	8	27	22	255	Mar 03 Tuesday
64	8	7	31	32	24	7	2	2	10	7	9	13	23	21	16	6	5	2	2	3	4	5	5	1	245	Mar 04 Wednesday
65	10	0	9	9	9	2	3	2	7	4	10	5	25	15	10	20	15	9	8	11	13	10	7	7	220	Mar 05 Thursday
66	4	4	22	33	35	21	20	12	12	21	20	14	25	18	16	11	2	21	16	5	19	3	4	7	365	Mar 06 Friday
67	1	5	11	1	4	0	12	3	4	10	4	47	9	33	24	4	23	4	2	5	7	5	9	9	236	Mar 07 Saturday
68	5	4	2	9	6	4	4	3	6	1	4	6	7	3	1	3	7	3	8	6	8	9	8	5	122	Mar 08 Sunday
69	3	3	2	4	15	4	14	35	46	4	43	33	42	18	47	51	51	27	8	9	9	17	5	0	490	Mar 09 Monday
70	3	0	2	2	6	5	14	39	38	11	53	38	44	8	49	65	55	10	4	8	11	4	1	0	470	Mar 10 Tuesday
71	9	2	7	0	1	2	2	46	44	12	37	39	30	33	51	36	49	2	5	4	16	5	10	6	448	Mar 11 Wednesday
72	6	4	1	3	3	1	14	22	8	5	15	14	14	7	17	17	23	11	12	5	10	1	11	10	234	Mar 12 Thursday
73	6	2	4	3	2	3	11	12	10	4	20	9	15	21	13	9	14	13	11	5	1	1	3	2	194	Mar 13 Friday
74	0	0	2	1	6	29	7	5	1	37	14	27	29	11	1	1	0	3	3	1	2	4	4	4	192	Mar 14 Saturday
75	5	13	27	24	10	7	35	30	15	3	5	10	10	12	7	4	13	6	8	2	22	1	3	8	280	Mar 15 Sunday
76	4	6	24	17	13	7	1	16	10	11	17	6	16	18	12	13	5	10	17	5	5	6	4	8	251	Mar 16 Monday

Table 3.4.1 (Page 3 of 4)

NRS .FKX Hourly distribution of detections

Day	00	01	02	03	04	05	06	07	08	09	10	11	12	13	14	15	16	17	18	19	20	21	22	23	Sum	Date
77	2	2	2	1	1	3	2	6	23	2	8	9	12	6	8	17	18	3	5	5	8	13	7	11	174	Mar 17 Tuesday
78	6	4	0	3	6	1	3	1	2	10	12	7	10	11	13	6	13	13	2	3	19	1	1	2	149	Mar 18 Wednesday
79	0	1	2	6	7	1	9	6	3	5	15	14	24	15	16	13	10	11	10	14	14	1	1	3	201	Mar 19 Thursday
80	1	0	3	4	3	8	5	1	8	8	11	9	9	21	4	12	8	9	17	4	18	4	2	2	171	Mar 20 Friday
81	4	4	4	5	1	6	3	5	5	12	7	12	4	9	4	4	10	8	9	5	9	8	4	13	155	Mar 21 Saturday
82	6	6	0	3	12	0	5	4	3	1	7	6	5	1	3	7	4	0	2	5	2	2	2	3	89	Mar 22 Sunday
83	5	2	4	4	8	4	30	16	16	7	16	12	15	25	26	11	9	11	17	3	11	1	1	2	256	Mar 23 Monday
84	2	6	3	8	6	3	44	35	21	20	15	2	11	21	6	14	4	18	2	7	24	7	2	4	285	Mar 24 Tuesday
85	0	1	2	1	3	1	3	1	9	7	7	1	12	7	15	16	20	14	4	7	24	6	7	4	172	Mar 25 Wednesday
86	1	3	3	2	6	0	1	3	4	5	11	25	13	15	20	12	18	12	5	8	5	13	3	1	189	Mar 26 Thursday
87	10	7	2	2	15	7	6	4	4	3	10	13	17	17	12	5	3	9	23	7	8	7	2	4	197	Mar 27 Friday
88	5	9	12	6	6	7	7	6	5	5	9	7	3	2	2	3	3	18	12	14	12	29	27	29	238	Mar 28 Saturday
89	30	41	63	53	56	43	37	20	12	5	4	14	14	13	9	3	1	12	12	11	20	15	13	25	526	Mar 29 Sunday
90	21	24	27	14	9	9	9	13	1	7	12	23	8	22	7	5	17	12	9	10	19	7	2	0	287	Mar 30 Monday
91	1	8	6	18	2	2	4	3	9	13	2	9	21	24	8	16	19	14	22	7	8	3	7	4	230	Mar 31 Tuesday
NRS	00	01	02	03	04	05	06	07	08	09	10	11	12	13	14	15	16	17	18	19	20	21	22	23		
Sum	1724	1792	1720	1744	1880	1553	1455	1553	1519	1576	1861	2062	2745	2752	2573	2131	2084	1768	1828	1536	2059	1599	1557	1715	44786	Total sum
183	9	10	9	10	10	8	8	8	8	9	10	11	15	15	14	12	11	10	10	8	11	9	9	9	245	Total average
128	10	10	9	9	10	7	6	8	8	8	11	11	16	17	16	12	12	10	10	8	12	8	8	9	247	Average workdays
55	8	9	10	10	11	12	11	11	9	9	9	11	12	11	9	10	11	10	9	8	9	9	10	11	239	Average weekends

Table 3.4.1. Daily and hourly distribution of NORESS detections. For each day is shown number of detections within each hour of the day and number of detections for that day. The end statistics give total number of detections distributed for each hour and the total sum of detections during the period. The averages show number of processed days, hourly distribution and average per processed day.

ARC .FKX Hourly distribution of detections

Day	00	01	02	03	04	05	06	07	08	09	10	11	12	13	14	15	16	17	18	19	20	21	22	23	Sum	Date
274	2	7	0	7	7	5	28	14	14	17	22	37	16	28	33	14	23	4	12	11	11	5	13	16	346	Oct 01 Tuesday
275	21	30	4	6	11	5	39	11	22	25	31	35	26	30	34	15	14	14	10	7	12	5	17	17	441	Oct 02 Wednesday
276	3	13	20	8	4	20	24	14	27	23	31	13	32	23	38	22	20	13	28	17	7	19	11	26	456	Oct 03 Thursday
277	28	7	4	4	7	15	23	23	8	23	8	10	27	34	29	26	13	10	11	14	15	17	11	23	390	Oct 04 Friday
278	16	10	40	2	10	13	15	16	14	14	18	14	13	8	25	21	5	7	6	13	8	1	7	17	313	Oct 05 Saturday
279	1	9	10	6	13	15	6	13	7	9	11	6	5	22	17	13	4	12	26	16	13	28	2	9	273	Oct 06 Sunday
280	7	11	10	12	7	14	20	17	17	32	45	26	37	40	17	11	20	15	4	8	15	5	13	18	421	Oct 07 Monday
281	8	3	5	16	12	7	11	8	23	16	18	22	31	20	34	9	14	4	2	18	15	20	13	15	344	Oct 08 Tuesday
282	8	9	5	5	5	6	24	27	18	20	37	13	27	31	19	18	9	10	15	6	7	4	4	11	338	Oct 09 Wednesday
283	5	4	5	4	7	9	16	16	15	26	37	14	13	30	27	14	31	8	12	19	13	7	23	29	384	Oct 10 Thursday
284	5	5	6	14	18	5	13	16	13	33	18	16	13	53	25	7	16	18	12	11	16	15	13	23	384	Oct 11 Friday
285	1	2	5	4	3	6	12	7	14	4	21	11	19	21	13	6	15	3	7	8	6	12	12	21	233	Oct 12 Saturday
286	13	21	5	10	6	10	8	11	7	7	6	10	11	6	19	23	4	15	31	16	17	16	11	20	303	Oct 13 Sunday
287	16	21	8	12	3	16	8	19	33	39	38	32	20	21	28	9	22	26	19	18	17	19	8	24	476	Oct 14 Monday
288	8	1	2	17	4	10	21	8	9	16	9	18	5	35	30	0	0	0	0	3	10	29	20	18	273	Oct 15 Tuesday
289	11	3	3	12	9	15	28	26	15	29	29	16	21	12	26	1	12	18	19	14	3	11	11	30	374	Oct 16 Wednesday
290	4	5	2	13	11	22	17	13	10	29	6	10	12	27	25	36	10	28	6	12	2	9	0	11	320	Oct 17 Thursday
291	15	13	5	4	5	6	7	10	6	11	8	7	10	21	11	10	4	13	4	5	4	3	8	5	195	Oct 18 Friday
292	3	2	4	2	19	16	16	13	11	15	17	6	25	29	29	26	17	39	45	13	23	50	71	71	562	Oct 19 Saturday
293	53	78	93	82	91	98	87	17	22	18	28	42	72	164	99	68	74	18	31	50	34	31	41	27	1418	Oct 20 Sunday
294	36	3	4	3	14	8	12	1	9	16	14	26	38	111	28	11	12	12	15	11	33	61	88	57	623	Oct 21 Monday
295	98	124	104	107	82	79	30	11	8	20	19	10	24	23	27	12	12	9	9	3	5	6	5	12	839	Oct 22 Tuesday
296	4	6	12	9	63	153	181	28	6	17	26	15	29	77	181	156	131	172	141	67	63	43	96	84	1760	Oct 23 Wednesday
297	51	13	9	6	10	6	20	17	16	32	34	36	24	29	40	8	9	7	4	4	6	3	12	12	408	Oct 24 Thursday
298	1	3	5	7	21	6	9	5	11	5	17	16	18	19	28	12	10	6	7	18	17	12	14	23	290	Oct 25 Friday
299	9	7	23	66	22	11	10	7	8	5	13	11	20	30	13	9	7	12	6	8	8	8	14	6	333	Oct 26 Saturday
300	5	11	11	7	6	13	5	15	27	50	128	121	131	34	108	173	65	91	222	218	199	208	162	114	2124	Oct 27 Sunday
301	91	58	25	35	35	63	71	63	31	24	28	26	37	37	23	28	17	51	58	27	11	19	7	19	884	Oct 28 Monday
302	10	5	12	6	7	7	18	16	24	23	23	32	28	25	25	29	16	35	15	7	7	7	14	22	413	Oct 29 Tuesday
303	8	3	4	9	6	8	19	28	28	27	11	28	30	42	29	23	14	19	54	30	46	128	58	65	717	Oct 30 Wednesday
304	62	139	85	206	172	43	24	17	16	32	19	32	43	40	68	20	50	7	11	42	54	65	108	175	1530	Oct 31 Thursday
305	181	190	104	14	9	8	37	23	72	27	44	32	43	39	101	106	170	27	14	21	7	37	43	37	1386	Nov 01 Friday
306	13	15	8	4	7	12	12	5	13	25	57	30	38	45	39	19	7	8	3	52	34	9	15	12	482	Nov 02 Saturday
307	6	5	8	5	5	10	10	13	4	17	8	9	4	9	14	8	10	23	9	13	8	7	13	8	226	Nov 03 Sunday
308	3	10	5	8	10	11	23	39	26	44	27	39	40	36	34	7	13	20	10	14	30	7	6	20	482	Nov 04 Monday
309	14	3	2	15	4	13	16	15	52	19	42	23	34	9	22	23	10	11	27	55	40	45	15	31	540	Nov 05 Tuesday
310	44	10	18	10	7	18	34	49	19	27	26	20	40	37	8	4	8	8	14	24	14	11	10	24	484	Nov 06 Wednesday
311	7	7	4	3	11	4	34	18	20	33	23	23	46	48	22	19	20	8	30	40	41	19	11	20	511	Nov 07 Thursday
312	14	5	20	22	6	23	21	17	56	26	34	47	40	64	19	18	7	16	3	26	11	9	30	18	552	Nov 08 Friday
313	13	3	15	6	7	19	48	19	9	16	14	20	13	16	25	8	4	22	7	16	6	1	5	21	333	Nov 09 Saturday
314	2	7	7	3	3	6	8	6	5	7	2	13	10	10	12	15	3	18	15	39	15	5	13	8	232	Nov 10 Sunday
315	7	30	11	8	5	10	17	21	11	17	27	18	27	27	8	8	17	9	13	10	16	9	16	27	369	Nov 11 Monday
316	5	9	5	9	10	7	26	6	20	13	10	7	12	66	26	38	19	15	14	14	6	22	28	20	407	Nov 12 Tuesday
317	14	7	12	9	5	6	20	11	11	12	34	24	39	38	15	12	17	2	7	18	8	12	16	30	379	Nov 13 Wednesday
318	4	9	15	25	18	10	36	19	13	57	84	57	56	31	29	20	0	22	19	11	0	20	8	16	579	Nov 14 Thursday
319	9	6	3	11	6	21	24	18	33	20	20	30	44	42	17	5	15	24	17	7	10	15	16	20	433	Nov 15 Friday
320	17	9	6	9	18	7	12	20	8	7	21	31	42	32	39	26	9	30	45	47	17	11	13	9	485	Nov 16 Saturday
321	6	2	6	7	10	13	9	15	4	0	9	8	2	0	9	3	10	6	4	7	22	7	20	12	191	Nov 17 Sunday
322	6	3	1	2	9	5	17	10	23	26	11	39	34	13	19	13	13	7	12	12	9	6	13	23	326	Nov 18 Monday
323	10	13	14	9	13	10	14	11	9	15	15	22	21	29	9	4	8	12	5	7	15	10	21	19	315	Nov 19 Tuesday
324	9	24	18	11	12	21	22	11	7	26	27	26	28	30	22	18	10	18	5	15	3	16	10	16	405	Nov 20 Wednesday
325	4	6	18	2	5	10	13	3	6	13	13	17	21	21	22	2	25	14	2	5	8	12	19	21	282	Nov 21 Thursday
326	11	13	6	4	15	8	19	6	17	20	15	20	24	39	22	21	11	13	9	7	14	9	24	12	359	Nov 22 Friday
327	6	3	7	10	15	28	28	13	8	13	15	11	27	20	39	26	29	21	13	15	9	5	24	33	418	Nov 23 Saturday
328	22	14	11	6	14	7	10	3	13	2	18	4	9	12	16	6	2	17	4	4	16	9	14	10	243	Nov 24 Sunday
329	5	5	3	3	7	18	13	6	7	24	15	23	32	21	19	4	11	10	14	12	8	3	6	15	284	Nov 25 Monday

Table 3.4.2 (Page 1 of 4)

ARC .FKX Hourly distribution of detections

Day	00	01	02	03	04	05	06	07	08	09	10	11	12	13	14	15	16	17	18	19	20	21	22	23	Sum	Date	
330	7	6	9	2	12	5	11	16	21	28	28	23	24	22	24	14	4	7	10	25	11	10	17	19	355	Nov 26 Tuesday	
331	12	6	6	8	12	15	6	2	5	17	22	17	40	20	31	20	7	32	12	12	8	13	11	18	352	Nov 27 Wednesday	
332	12	8	17	6	18	12	15	2	10	8	31	13	16	22	10	19	16	17	8	10	21	10	6	19	326	Nov 28 Thursday	
333	13	3	4	7	22	5	17	6	35	43	36	20	34	23	22	11	11	21	17	5	7	16	8	13	399	Nov 29 Friday	
334	5	3	9	8	2	10	12	9	4	18	14	15	11	25	27	8	14	9	16	9	1	6	7	14	256	Nov 30 Saturday	
335	4	3	2	3	1	3	5	9	1	9	6	3	8	8	12	8	7	6	8	14	3	3	6	13	145	Dec 01 Sunday	
336	1	6	5	1	7	7	6	9	10	6	12	15	18	22	17	12	8	18	17	12	1	6	13	21	250	Dec 02 Monday	
337	10	8	3	1	8	4	14	6	14	15	37	62	28	32	6	7	7	6	6	23	7	15	15	14	348	Dec 03 Tuesday	
338	12	2	0	10	5	4	22	7	8	7	19	27	35	29	14	16	11	18	6	20	13	18	8	6	317	Dec 04 Wednesday	
339	4	7	6	10	10	3	12	9	10	21	27	9	20	11	16	18	4	6	15	11	17	7	13	14	280	Dec 05 Thursday	
340	7	10	15	6	5	6	11	12	16	22	44	22	23	18	33	21	13	41	4	12	7	8	11	18	385	Dec 06 Friday	
341	14	11	7	5	14	5	7	2	5	15	10	20	14	18	20	8	20	11	1	1	25	3	4	13	253	Dec 07 Saturday	
342	6	12	4	12	7	12	11	7	28	78	61	15	18	8	10	15	5	28	4	13	15	7	7	13	396	Dec 08 Sunday	
343	8	10	7	3	5	14	24	15	7	23	14	10	10	14	9	11	10	3	14	7	9	9	16	26	278	Dec 09 Monday	
344	15	10	8	8	6	8	13	7	14	10	16	33	19	8	24	4	16	15	5	9	16	6	19	16	305	Dec 10 Tuesday	
345	2	6	6	1	7	10	9	4	25	9	8	14	13	16	9	11	9	7	6	7	7	4	5	1	196	Dec 11 Wednesday	
346	7	3	4	3	8	5	15	10	11	8	11	21	24	15	18	11	13	12	4	8	3	8	9	22	253	Dec 12 Thursday	
347	18	16	25	48	38	27	34	30	39	28	68	64	51	70	69	63	36	22	33	32	36	10	19	39	915	Dec 13 Friday	
348	20	6	6	12	11	8	16	25	17	20	13	33	33	35	30	14	7	6	4	11	7	11	13	24	382	Dec 14 Saturday	
349	9	5	9	7	7	14	12	7	5	20	9	10	15	12	5	17	6	8	18	23	9	20	2	16	265	Dec 15 Sunday	
350	4	7	1	3	5	5	3	2	5	6	5	9	1	7	3	13	5	5	2	2	5	5	12	15	130	Dec 16 Monday	
351	9	2	8	10	20	29	33	15	24	14	27	20	28	25	21	6	13	11	10	14	9	7	15	26	396	Dec 17 Tuesday	
352	4	17	4	9	5	10	11	13	10	7	18	34	38	39	9	9	20	11	13	13	7	20	6	53	380	Dec 18 Wednesday	
353	66	21	9	12	14	25	11	12	8	17	15	20	23	23	16	17	3	9	17	22	18	17	11	22	428	Dec 19 Thursday	
354	19	6	9	7	10	13	17	8	14	10	16	29	21	17	23	8	6	2	14	5	17	4	6	18	299	Dec 20 Friday	
355	4	1	4	11	16	9	4	6	6	10	27	12	12	22	14	2	5	4	2	6	8	3	11	17	216	Dec 21 Saturday	
356	3	3	5	3	15	7	2	14	11	39	28	36	31	34	11	16	14	11	7	11	17	22	8	13	361	Dec 22 Sunday	
357	10	9	15	40	15	29	29	11	26	29	14	17	22	20	15	20	22	6	11	11	7	6	13	15	412	Dec 23 Monday	
358	6	10	18	21	25	13	15	18	13	17	17	18	12	8	10	8	10	11	2	11	6	2	5	11	287	Dec 24 Tuesday	
359	1	8	27	10	22	28	14	12	9	5	14	14	19	12	8	1	6	8	1	16	13	12	24	15	299	Dec 25 Wednesday	Frste
360	22	26	22	16	14	17	21	10	20	12	17	23	13	8	13	11	2	8	11	15	12	13	18	24	368	Dec 26 Thursday	Andre
361	7	14	10	8	25	14	7	4	13	21	16	30	23	43	14	8	2	7	10	15	5	16	9	14	335	Dec 27 Friday	
362	4	18	12	10	11	8	12	10	14	14	23	22	21	22	15	26	6	13	8	14	3	3	1	12	302	Dec 28 Saturday	
363	0	1	3	4	4	2	4	3	6	6	9	3	0	5	20	19	2	7	11	6	8	2	6	7	138	Dec 29 Sunday	
364	2	1	1	1	3	3	2	4	5	0	3	1	11	6	8	9	11	4	4	15	11	6	12	31	154	Dec 30 Monday	
365	33	18	12	7	14	12	9	3	15	10	7	5	2	6	16	11	10	13	5	12	5	6	4	0	235	Dec 31 Tuesday	
1	3	9	2	6	8	4	5	4	32	6	13	3	4	2	9	2	3	3	4	6	4	6	12	1	151	Jan 01 Wednesday	Frste
2	8	4	6	4	11	13	14	9	15	9	14	14	15	12	3	6	11	8	12	19	6	12	26	10	261	Jan 02 Thursday	
3	4	5	7	25	26	10	15	15	16	21	45	51	52	55	45	56	79	70	47	45	41	40	43	41	854	Jan 03 Friday	
4	43	82	73	64	52	28	34	21	29	21	14	28	33	34	37	18	19	38	40	43	43	52	48	32	926	Jan 04 Saturday	
5	15	13	14	6	4	11	2	14	6	5	19	7	22	6	10	1	0	6	8	16	22	12	18	14	251	Jan 05 Sunday	
6	6	6	5	5	2	10	13	16	18	9	12	25	10	16	16	6	13	5	9	17	8	17	17	14	275	Jan 06 Monday	
7	11	9	11	15	19	21	30	36	26	17	19	16	36	26	19	9	7	17	3	5	6	7	18	24	407	Jan 07 Tuesday	
8	5	8	11	4	0	18	20	20	38	30	27	30	37	23	24	28	24	29	33	26	26	8	9	21	499	Jan 08 Wednesday	
9	8	2	0	3	13	17	24	25	26	29	24	22	35	21	26	43	38	40	37	35	34	33	47	43	625	Jan 09 Thursday	
10	40	37	46	33	28	20	36	42	46	35	44	36	28	40	44	12	11	8	10	10	13	12	28	22	681	Jan 10 Friday	
11	11	25	2	11	12	3	9	4	3	6	10	14	5	4	7	15	8	13	23	30	29	43	53	34	374	Jan 11 Saturday	
12	19	6	3	3	5	4	5	2	4	5	3	3	7	3	6	7	3	7	11	7	8	15	10	20	166	Jan 12 Sunday	
13	18	17	15	14	12	11	25	32	36	43	42	49	42	56	57	63	49	48	60	62	39	23	14	16	843	Jan 13 Monday	
14	7	11	10	8	7	12	32	29	22	29	34	33	36	18	35	25	33	24	12	9	9	3	5	13	456	Jan 14 Tuesday	
15	3	7	6	5	5	5	8	12	5	3	11	17	5	13	8	7	4	8	5	2	2	2	1	7	151	Jan 15 Wednesday	
16	4	2	2	6	3	6	8	7	4	8	20	10	15	8	9	8	2	6	8	5	6	5	0	6	158	Jan 16 Thursday	
17	3	2	2	4	4	8	18	23	24	18	11	16	8	24	11	5	11	7	3	6	4	4	2	20	238	Jan 17 Friday	
18	8	2	4	0	7	8	7	13	18	14	18	14	20	23	23	9	20	15	13	15	9	12	12	32	316	Jan 18 Saturday	
19	13	14	13	6	6	1	12	14	3	6	7	10	12	7	10	48	18	12	11	20	10	3	5	18	279	Jan 19 Sunday	
20	13	13	7	15	26	11	23	44	39	31	23	19	10	17	0	5	7	4	6	7	5	5	4	10	344	Jan 20 Monday	

Table 3.4.2 (Page 2 of 4)

ARC .FKX Hourly distribution of detections

Day	00	01	02	03	04	05	06	07	08	09	10	11	12	13	14	15	16	17	18	19	20	21	22	23	Sum	Date
21	3	2	1	15	29	48	22	15	3	7	5	0	0	0	0	0	0	0	0	0	0	0	0	0	150	Jan 21 Tuesday
22	0	0	0	0	0	0	0	0	0	0	0	0	0	0	80	68	52	57	38	31	23	37	34	24	444	Jan 22 Wednesday
23	19	13	6	9	22	13	18	16	21	20	27	63	64	72	73	53	51	74	76	106	82	44	79	119	1140	Jan 23 Thursday
24	120	72	69	81	47	0	0	0	0	0	0	0	0	0	0	0	13	4	6	2	1	7	6	15	443	Jan 24 Friday
25	4	3	5	17	5	9	6	1	17	10	16	32	28	4	9	8	7	4	4	11	2	4	12	49	267	Jan 25 Saturday
26	22	29	5	10	6	28	68	77	54	28	9	10	47	53	80	53	67	71	67	63	73	56	36	26	1038	Jan 26 Sunday
27	18	9	12	12	11	11	22	29	30	37	26	20	26	10	30	14	29	19	19	12	21	29	30	32	508	Jan 27 Monday
28	14	1	1	6	6	13	18	35	24	28	11	12	35	15	20	19	17	12	16	15	9	14	14	4	359	Jan 28 Tuesday
29	2	1	7	3	2	5	5	4	2	4	16	15	17	15	10	13	11	4	12	10	9	9	19	22	217	Jan 29 Wednesday
30	3	4	7	10	12	12	20	17	13	12	8	13	20	13	6	12	6	8	5	6	5	6	13	28	259	Jan 30 Thursday
31	5	6	8	5	7	4	8	9	17	18	20	20	37	9	12	5	0	5	3	3	1	5	4	19	230	Jan 31 Friday
32	24	5	3	15	52	21	15	14	14	29	9	27	34	23	25	9	6	17	2	13	9	9	9	61	445	Feb 01 Saturday
33	16	3	5	9	15	31	5	31	56	81	26	51	24	14	33	28	8	17	51	53	88	92	90	108	935	Feb 02 Sunday
34	134	134	95	100	36	59	44	25	9	19	20	27	22	24	8	14	12	13	7	14	14	15	5	18	868	Feb 03 Monday
35	7	5	5	1	6	9	10	4	4	11	26	25	16	24	11	15	11	12	4	9	9	9	17	22	272	Feb 04 Tuesday
36	6	11	10	13	16	12	11	6	3	13	23	13	23	21	16	12	7	8	5	9	4	4	15	27	288	Feb 05 Wednesday
37	21	30	23	28	26	25	15	36	38	45	50	61	57	51	49	53	43	61	51	42	48	27	25	13	918	Feb 06 Thursday
38	11	15	17	12	26	17	29	9	26	30	13	20	36	20	31	19	14	21	18	19	9	12	24	20	468	Feb 07 Friday
39	6	2	2	3	4	2	3	1	5	5	5	24	3	4	8	5	10	17	9	4	4	7	9	7	149	Feb 08 Saturday
40	2	2	4	6	14	7	14	22	7	6	11	1	11	8	16	5	14	6	6	20	12	15	5	10	224	Feb 09 Sunday
41	4	8	4	6	0	15	9	12	12	8	18	15	21	11	17	18	7	11	3	8	7	7	17	17	255	Feb 10 Monday
42	13	17	5	9	6	2	14	16	11	15	21	23	17	11	19	11	5	3	14	7	13	3	21	23	299	Feb 11 Tuesday
43	1	6	4	2	11	9	5	5	8	9	6	17	22	6	15	8	18	17	12	17	22	4	16	13	253	Feb 12 Wednesday
44	9	16	13	9	10	7	14	11	18	13	11	14	16	9	16	4	13	5	8	7	8	8	11	13	263	Feb 13 Thursday
45	4	10	8	12	8	10	15	5	23	9	12	20	21	24	27	5	17	11	11	10	17	13	10	28	330	Feb 14 Friday
46	9	12	5	6	15	7	8	7	13	5	15	23	24	24	11	9	12	6	15	7	7	3	11	9	263	Feb 15 Saturday
47	3	4	10	9	8	6	6	2	9	12	7	7	13	14	17	6	20	11	7	6	30	14	13	9	243	Feb 16 Sunday
48	14	5	4	6	9	20	9	8	11	24	20	16	26	18	24	14	12	14	14	8	18	11	6	20	331	Feb 17 Monday
49	5	6	9	1	7	11	5	4	8	11	33	13	28	23	20	6	17	16	9	19	15	22	36	34	358	Feb 18 Tuesday
50	19	31	24	16	21	5	23	12	14	17	18	25	29	27	16	14	5	7	11	13	12	12	17	17	405	Feb 19 Wednesday
51	7	15	10	6	6	12	25	10	18	19	18	21	28	31	24	17	14	9	14	15	11	22	14	12	378	Feb 20 Thursday
52	4	7	8	15	6	12	18	8	18	22	27	37	30	35	14	12	23	9	11	13	9	6	34	20	398	Feb 21 Friday
53	2	5	11	5	13	5	5	5	4	7	14	25	25	10	12	5	17	15	4	10	6	15	11	14	245	Feb 22 Saturday
54	7	3	4	11	6	18	10	8	4	2	3	7	6	4	11	4	7	6	5	7	19	8	4	15	179	Feb 23 Sunday
55	7	5	4	8	6	7	3	7	0	9	5	9	10	7	13	4	11	9	17	16	1	13	12	16	199	Feb 24 Monday
56	13	6	4	8	3	7	9	13	13	8	15	27	21	14	12	5	16	5	14	5	8	11	19	13	269	Feb 25 Tuesday
57	9	8	8	13	8	7	13	13	12	12	13	25	29	24	20	10	7	12	16	11	8	12	5	9	304	Feb 26 Wednesday
58	4	3	8	3	7	9	12	7	6	25	20	18	54	11	18	11	4	10	21	5	12	11	6	16	301	Feb 27 Thursday
59	12	5	13	6	3	6	8	6	20	19	17	32	40	24	26	3	15	11	7	7	2	9	8	12	311	Feb 28 Friday
60	5	4	2	9	12	5	7	19	1	13	16	13	15	4	7	8	5	7	4	9	23	16	6	14	224	Feb 29 Saturday
61	2	7	9	1	6	8	5	15	4	1	10	7	16	5	11	9	4	3	9	19	10	4	26	9	200	Mar 01 Sunday
62	2	3	5	6	14	27	12	9	10	21	4	27	29	33	27	14	18	18	4	23	15	1	11	22	355	Mar 02 Monday
63	5	20	10	11	14	10	16	20	15	22	19	22	17	26	12	16	4	8	14	17	7	5	17	27	354	Mar 03 Tuesday
64	3	6	4	10	3	7	11	21	19	15	9	32	29	21	16	17	2	5	2	16	6	4	9	18	285	Mar 04 Wednesday
65	4	13	9	24	7	12	11	23	10	17	17	15	25	24	27	12	11	10	8	6	10	8	9	20	332	Mar 05 Thursday
66	9	6	5	13	8	7	16	20	19	7	20	25	35	23	11	24	11	15	15	3	13	9	16	13	343	Mar 06 Friday
67	3	5	13	1	14	6	8	4	8	11	10	18	7	6	10	7	6	9	9	8	9	5	14	18	209	Mar 07 Saturday
68	4	4	1	4	5	8	8	3	10	4	7	9	5	17	12	17	10	22	8	19	9	10	4	10	210	Mar 08 Sunday
69	3	3	3	5	7	9	14	8	11	17	11	11	13	18	12	12	9	12	4	3	6	3	8	22	224	Mar 09 Monday
70	1	1	5	6	5	8	9	9	12	32	21	16	20	10	16	7	4	10	5	7	6	6	7	19	242	Mar 10 Tuesday
71	7	7	10	9	2	5	13	14	18	14	16	18	30	15	12	16	4	13	5	17	5	9	12	12	283	Mar 11 Wednesday
72	6	3	3	4	13	14	8	8	21	27	17	21	34	21	13	20	27	10	7	13	11	12	6	22	341	Mar 12 Thursday
73	20	9	6	10	7	6	13	14	20	14	36	22	28	23	21	12	22	39	10	16	8	12	24	15	407	Mar 13 Friday
74	7	9	6	13	11	10	13	9	8	16	16	17	21	7	13	14	12	12	2	12	9	9	15	20	281	Mar 14 Saturday
75	4	6	7	3	8	2	5	16	13	4	15	9	11	12	15	14	28	10	21	14	12	22	2	11	264	Mar 15 Sunday
76	6	4	10	13	2	10	12	11	22	19	17	12	14	30	16	15	16	10	4	14	8	12	9	37	323	Mar 16 Monday

Table 3.4.2 (Page 3 of 4)

ARC .FKX Hourly distribution of detections

Day	00	01	02	03	04	05	06	07	08	09	10	11	12	13	14	15	16	17	18	19	20	21	22	23	Sum	Date
77	16	8	22	13	26	21	27	22	36	17	19	31	17	15	19	11	20	5	17	15	17	13	13	16	436	Mar 17 Tuesday
78	9	1	13	6	9	10	9	13	24	17	19	31	34	18	18	9	7	12	2	6	9	10	13	17	316	Mar 18 Wednesday
79	0	11	12	16	9	10	17	9	23	27	28	25	53	15	24	47	12	16	11	20	16	7	10	19	437	Mar 19 Thursday
80	3	5	12	27	11	9	19	16	29	18	40	24	41	36	14	7	9	18	12	18	11	6	16	18	419	Mar 20 Friday
81	10	15	5	11	11	9	13	10	10	9	23	36	14	3	16	14	13	10	8	10	12	10	8	14	294	Mar 21 Saturday
82	6	10	15	11	18	8	11	7	15	10	10	21	5	8	12	15	11	10	17	15	17	17	20	15	304	Mar 22 Sunday
83	14	1	4	8	9	8	12	8	22	24	22	22	16	4	11	9	14	6	5	9	9	6	13	29	285	Mar 23 Monday
84	11	29	15	30	23	16	18	13	28	13	24	12	36	17	25	9	12	25	4	16	18	9	18	22	443	Mar 24 Tuesday
85	11	13	15	17	19	31	20	37	41	48	25	38	37	24	39	27	13	13	10	15	14	20	24	26	577	Mar 25 Wednesday
86	22	28	13	25	19	16	29	20	14	18	18	27	27	24	28	14	24	19	12	12	9	11	20	20	469	Mar 26 Thursday
87	12	18	2	6	8	6	15	8	18	33	29	26	36	28	29	23	16	9	4	14	15	13	19	12	399	Mar 27 Friday
88	7	4	11	11	7	10	20	6	13	15	16	21	15	10	10	6	8	10	4	7	7	11	5	19	253	Mar 28 Saturday
89	10	9	7	1	15	9	7	13	9	18	5	8	15	32	12	13	19	8	10	12	15	21	13	4	285	Mar 29 Sunday
90	13	4	6	8	9	23	17	18	7	24	18	21	29	9	10	18	8	16	8	20	12	28	30	4	360	Mar 30 Monday
91	5	15	8	8	4	9	13	24	19	37	13	31	31	25	5	23	18	21	26	13	17	22	13	10	410	Mar 31 Tuesday

ARC	00	01	02	03	04	05	06	07	08	09	10	11	12	13	14	15	16	17	18	19	20	21	22	23		
Sum	2489	2421	2126	2342	2434	2495	3131	2570	2951	3370	3727	3947	4476	4274	4162	3190	2865	2906	2751	3101	2786	2795	3194	4029	74532	Total sum
183	14	13	12	13	13	14	17	14	16	18	20	22	24	23	23	17	16	16	15	17	15	15	17	22	407	Total average
128	15	14	12	14	13	14	19	15	18	20	22	23	26	25	23	17	17	16	14	15	13	14	17	22	420	Average workdays
55	10	11	11	11	13	12	13	12	12	15	17	18	20	18	21	17	13	15	17	21	19	18	18	21	373	Average weekends

Table 3.4.2. Daily and hourly distribution of ARCESS detections. For each day is shown number of detections within each hour of the day and number of detections for that day. The end statistics give total number of detections distributed for each hour and the total sum of detections during the period. The averages show number of processed days, hourly distribution and average per processed day.

FIN .FKX Hourly distribution of detections

Day	00	01	02	03	04	05	06	07	08	09	10	11	12	13	14	15	16	17	18	19	20	21	22	23	Sum	Date
274	4	2	6	14	1	9	9	4	8	11	27	11	19	35	25	10	20	29	8	15	40	4	12	14	337	Oct 01 Tuesday
275	29	8	68	94	56	12	12	11	15	13	11	13	15	23	24	15	18	5	12	32	6	16	30	32	570	Oct 02 Wednesday
276	44	39	13	55	7	5	9	18	7	18	7	12	30	53	7	6	2	1	6	6	6	9	4	6	370	Oct 03 Thursday
277	8	6	5	6	10	8	3	4	12	10	15	14	18	17	18	17	21	5	12	13	9	24	8	7	270	Oct 04 Friday
278	17	15	9	11	14	7	19	8	14	9	26	14	19	23	20	8	10	5	26	4	7	5	5	6	301	Oct 05 Saturday
279	6	13	12	2	3	8	32	11	23	7	9	4	7	6	4	5	2	5	6	3	6	6	3	8	191	Oct 06 Sunday
280	9	21	12	9	8	6	12	8	14	15	19	14	21	16	8	20	21	6	11	8	6	11	5	11	291	Oct 07 Monday
281	4	5	10	8	7	14	14	11	6	11	14	14	23	26	10	5	17	13	10	2	5	1	7	5	242	Oct 08 Tuesday
282	5	6	9	10	7	3	0	6	8	11	14	18	14	14	10	23	4	8	4	5	3	4	13	13	212	Oct 09 Wednesday
283	4	4	10	7	8	6	0	3	1	14	10	20	16	16	20	11	3	4	6	5	8	10	9	9	204	Oct 10 Thursday
284	11	12	8	18	9	4	5	8	9	16	6	14	11	27	10	5	3	0	5	5	8	6	3	5	208	Oct 11 Friday
285	5	2	3	3	7	13	10	3	0	9	2	6	3	6	11	4	12	2	2	6	7	6	8	3	133	Oct 12 Saturday
286	10	10	5	37	6	3	7	7	42	25	18	37	8	36	33	14	53	31	24	16	16	12	8	20	478	Oct 13 Sunday
287	10	17	8	5	12	9	1	9	14	15	35	19	25	24	21	19	22	34	20	27	22	14	19	30	431	Oct 14 Monday
288	40	40	20	42	23	13	18	9	6	23	17	21	36	30	18	4	18	5	24	15	11	7	8	12	460	Oct 15 Tuesday
289	9	7	9	7	7	5	9	5	11	7	28	42	30	37	8	6	8	6	7	5	8	4	7	7	279	Oct 16 Wednesday
290	14	22	20	15	11	14	11	3	3	20	34	25	21	31	27	13	10	24	5	17	11	9	16	4	380	Oct 17 Thursday
291	14	13	20	3	11	3	10	18	11	12	15	18	24	30	23	15	4	8	6	7	11	5	7	3	291	Oct 18 Friday
292	3	6	8	4	5	13	4	5	7	10	8	4	6	3	5	7	6	7	1	2	1	12	7	5	139	Oct 19 Saturday
293	11	18	12	14	14	12	14	9	12	14	12	10	5	0	8	0	9	4	9	6	3	10	2	9	217	Oct 20 Sunday
294	3	3	7	11	6	0	2	3	3	6	9	13	21	24	10	10	1	1	8	7	2	2	9	7	168	Oct 21 Monday
295	3	6	1	2	5	3	2	1	5	3	15	14	14	14	4	4	3	1	0	5	1	2	3	1	112	Oct 22 Tuesday
296	4	2	4	9	10	5	4	6	13	3	0	0	0	0	0	0	0	0	0	0	0	0	0	0	60	Oct 23 Wednesday
297	0	0	0	0	0	0	0	0	0	0	0	0	0	0	0	0	0	0	0	0	0	0	0	0	0	Oct 24 Thursday
298	0	0	0	0	0	0	0	0	0	0	0	0	0	0	0	0	0	0	0	0	0	0	0	0	0	Oct 25 Friday
299	0	0	0	0	0	0	0	0	0	0	0	0	0	0	0	0	0	0	0	0	0	0	0	0	0	Oct 26 Saturday
300	0	0	0	0	0	0	0	0	0	0	0	0	0	0	0	0	0	0	0	0	0	0	0	0	0	Oct 27 Sunday
301	0	0	0	0	0	0	0	0	0	0	0	0	0	0	0	0	0	0	0	0	0	0	0	0	0	Oct 28 Monday
302	0	0	0	0	0	0	0	0	0	0	0	0	0	0	0	0	0	0	0	0	0	0	0	0	0	Oct 29 Tuesday
303	0	0	0	0	0	0	0	0	0	0	0	0	0	0	0	0	0	0	0	0	0	0	0	0	0	Oct 30 Wednesday
304	0	0	0	0	0	0	0	0	0	0	0	6	19	22	10	1	3	3	3	7	6	6	6	11	103	Oct 31 Thursday
305	1	4	1	10	1	4	5	2	1	11	14	15	18	11	5	8	15	20	23	16	10	8	7	14	224	Nov 01 Friday
306	15	8	16	14	15	20	16	28	20	23	23	30	35	39	51	35	44	29	30	27	19	11	16	12	576	Nov 02 Saturday
307	15	14	18	14	8	7	11	20	25	17	31	25	15	7	7	6	9	12	17	25	11	12	18	16	360	Nov 03 Sunday
308	13	13	11	28	21	17	14	21	12	9	9	16	21	11	12	6	5	4	5	12	7	15	16	19	317	Nov 04 Monday
309	17	12	15	22	8	7	16	14	7	13	12	11	19	11	7	11	8	8	15	3	3	8	8	2	257	Nov 05 Tuesday
310	9	6	5	10	5	5	4	8	10	11	15	16	20	14	2	11	5	14	5	5	2	8	9	8	207	Nov 06 Wednesday
311	4	6	7	5	5	7	9	5	6	16	11	18	16	17	10	8	7	10	7	10	8	5	7	8	212	Nov 07 Thursday
312	8	8	9	13	6	10	8	10	7	9	12	5	9	11	10	8	6	10	6	10	6	4	6	4	195	Nov 08 Friday
313	3	6	2	2	0	4	21	11	2	3	8	9	11	4	6	4	3	3	6	1	1	3	2	9	124	Nov 09 Saturday
314	5	3	2	16	1	1	2	2	14	13	3	2	6	8	7	3	1	8	3	7	7	8	6	3	131	Nov 10 Sunday
315	7	6	4	11	9	3	3	2	5	7	7	10	15	19	12	8	11	9	6	7	8	1	14	7	191	Nov 11 Monday
316	16	14	12	13	13	4	3	2	4	13	10	16	17	19	15	4	5	17	13	3	8	7	5	10	243	Nov 12 Tuesday
317	11	2	5	3	7	2	1	2	7	14	16	24	40	42	40	27	27	22	18	12	10	14	11	6	363	Nov 13 Wednesday
318	10	2	18	28	9	2	4	1	5	15	6	8	17	22	2	4	6	3	4	2	5	5	6	10	194	Nov 14 Thursday
319	4	2	6	7	2	1	3	3	2	9	12	19	26	14	6	1	4	5	6	6	4	2	1	16	161	Nov 15 Friday
320	23	26	16	19	7	4	4	2	4	2	8	10	7	12	2	6	3	4	3	5	0	1	8	7	183	Nov 16 Saturday
321	7	1	2	7	7	9	9	12	2	3	8	9	11	19	6	3	10	9	10	11	12	7	1	6	181	Nov 17 Sunday
322	3	8	3	16	2	6	5	2	10	11	11	12	13	15	12	6	11	17	21	19	20	17	16	17	273	Nov 18 Monday
323	18	17	17	15	15	6	3	2	4	9	7	10	10	22	13	5	4	4	1	1	2	8	15	4	212	Nov 19 Tuesday
324	4	10	8	13	8	2	0	2	4	13	15	24	13	17	4	3	3	1	4	4	3	4	7	8	174	Nov 20 Wednesday
325	7	6	4	9	6	5	0	0	5	6	14	7	18	20	14	3	3	1	0	5	6	10	33	46	228	Nov 21 Thursday
326	40	46	49	33	13	8	6	11	12	18	22	25	13	13	7	11	16	9	7	8	11	3	3	5	389	Nov 22 Friday
327	3	6	18	5	6	7	4	7	0	4	12	9	6	5	1	1	5	10	24	21	25	17	8	12	216	Nov 23 Saturday
328	0	5	1	6	3	1	1	0	0	2	2	6	2	3	10	5	4	2	23	10	8	19	17	20	150	Nov 24 Sunday
329	15	14	20	17	14	7	4	3	4	7	16	19	14	13	10	6	6	7	5	10	3	3	6	9	232	Nov 25 Monday

Table 3.4.3 (Page 1 of 4)

FIN .FKX Hourly distribution of detections

Day	00	01	02	03	04	05	06	07	08	09	10	11	12	13	14	15	16	17	18	19	20	21	22	23	Sum	Date	
330	6	9	2	10	11	4	3	3	4	7	2	6	5	9	3	14	4	8	14	8	5	2	6	5	150	Nov 26 Tuesday	
331	12	14	14	19	9	7	6	12	2	7	6	9	23	17	12	2	0	1	3	2	5	2	7	9	200	Nov 27 Wednesday	
332	9	8	6	12	1	3	3	0	16	11	14	21	29	19	6	3	5	9	1	5	9	5	11	7	213	Nov 28 Thursday	
333	12	19	15	9	11	9	7	3	4	14	20	20	23	22	10	4	6	7	10	4	13	10	11	7	270	Nov 29 Friday	
334	7	3	1	11	14	3	3	5	3	12	9	7	16	9	3	7	4	0	3	3	0	2	1	0	126	Nov 30 Saturday	
335	0	1	0	2	3	1	4	4	3	5	6	0	0	4	8	8	7	16	23	18	20	11	21	22	187	Dec 01 Sunday	
336	23	24	17	31	17	12	3	5	10	14	16	19	29	17	9	16	8	12	3	5	2	8	4	3	307	Dec 02 Monday	
337	7	15	7	5	5	4	3	11	10	8	19	17	19	14	4	6	11	5	14	3	9	3	4	6	209	Dec 03 Tuesday	
338	10	10	12	16	9	1	0	1	5	12	11	12	26	19	9	11	15	21	18	7	20	25	24	23	317	Dec 04 Wednesday	
339	25	26	16	12	22	12	7	7	7	18	13	13	22	23	6	6	1	1	12	10	14	2	0	5	280	Dec 05 Thursday	
340	4	8	4	13	6	6	1	3	8	6	26	17	20	21	5	4	1	7	5	6	8	7	2	11	199	Dec 06 Friday	
341	11	16	12	16	15	17	8	8	11	5	3	14	28	30	16	1	8	8	4	3	4	5	3	2	248	Dec 07 Saturday	
342	1	12	15	15	2	8	6	5	15	6	9	3	12	4	3	2	3	8	8	10	5	10	9	9	180	Dec 08 Sunday	
343	3	14	4	12	17	6	4	1	3	19	20	17	24	23	24	7	13	12	15	21	13	11	26	35	344	Dec 09 Monday	
344	20	33	26	17	10	3	10	2	8	12	15	19	24	12	5	4	4	6	5	4	9	8	6	10	272	Dec 10 Tuesday	
345	3	4	5	4	7	1	1	1	7	10	13	17	21	13	5	3	6	7	8	12	17	6	6	90	267	Dec 11 Wednesday	
346	77	71	187	159	112	111	80	68	27	29	47	42	45	0	0	0	0	0	0	0	0	0	0	0	1055	Dec 12 Thursday	
347	0	0	0	0	0	0	0	0	0	0	0	0	0	0	0	0	0	0	0	0	0	0	0	0	0	Dec 13 Friday	
348	0	0	0	0	0	0	0	0	0	0	0	0	0	0	0	0	0	0	0	0	0	0	0	0	0	Dec 14 Saturday	
349	0	0	0	0	0	0	0	0	0	0	0	0	0	0	0	0	0	0	0	0	0	0	0	0	0	Dec 15 Sunday	
350	0	0	0	0	0	0	0	0	0	0	0	0	0	0	0	0	0	0	0	0	0	0	0	0	0	Dec 16 Monday	
351	0	0	0	0	0	0	0	0	0	0	0	0	0	1	8	6	5	2	1	2	2	3	6	11	47	Dec 17 Tuesday	
352	10	10	21	49	70	47	22	30	30	80	42	20	26	8	11	20	12	6	5	5	7	6	9	8	554	Dec 18 Wednesday	
353	9	11	9	9	9	4	29	46	15	75	36	30	30	24	16	5	4	1	2	8	3	17	3	7	402	Dec 19 Thursday	
354	16	18	22	55	41	18	13	13	9	18	28	24	24	28	9	19	8	14	31	27	35	47	47	18	582	Dec 20 Friday	
355	10	14	20	23	31	32	42	27	22	32	42	44	30	29	27	14	7	10	18	23	14	4	5	3	523	Dec 21 Saturday	
356	3	6	6	12	4	3	3	5	9	37	26	17	43	32	41	44	52	37	50	52	52	34	38	41	647	Dec 22 Sunday	
357	20	18	19	25	12	6	12	6	7	18	18	14	16	18	5	9	9	7	4	3	8	3	9	2	268	Dec 23 Monday	
358	0	1	5	10	10	5	4	4	6	15	23	11	25	27	24	27	26	27	8	3	7	15	18	18	319	Dec 24 Tuesday	
359	25	40	25	22	33	5	2	2	2	4	7	6	23	11	8	1	5	10	19	32	38	37	47	31	435	Dec 25 Wednesday	Frste
360	37	27	7	6	5	4	2	5	6	1	15	13	19	10	9	3	6	1	2	8	8	5	24	12	235	Dec 26 Thursday	Andre
361	4	11	8	3	12	4	5	1	10	11	25	10	29	20	6	2	3	4	3	1	9	6	2	1	190	Dec 27 Friday	
362	3	8	4	11	1	5	5	1	13	17	21	19	13	15	4	9	4	3	4	4	3	3	2	0	172	Dec 28 Saturday	
363	2	3	4	2	4	5	1	2	0	10	9	10	8	10	22	15	12	23	42	40	31	56	42	48	401	Dec 29 Sunday	
364	55	38	23	32	39	28	13	10	22	21	24	22	29	37	34	48	36	49	37	54	43	55	58	53	860	Dec 30 Monday	
365	35	11	12	5	12	17	11	10	17	8	15	13	16	15	11	13	11	7	8	9	10	11	12	6	295	Dec 31 Tuesday	
1	6	9	10	17	14	10	5	7	14	6	18	2	4	9	10	6	13	20	42	30	32	46	62	56	448	Jan 01 Wednesday	Frste
2	58	51	61	61	50	48	43	52	33	48	29	36	21	19	9	14	13	23	18	24	4	6	7	6	734	Jan 02 Thursday	
3	4	10	6	3	3	19	26	11	5	11	22	17	25	10	6	6	4	5	2	8	17	26	30	12	288	Jan 03 Friday	
4	8	4	3	13	10	9	10	2	1	14	9	8	6	12	10	5	3	8	4	10	49	42	49	39	328	Jan 04 Saturday	
5	52	49	60	46	41	43	41	10	15	22	36	46	50	11	6	20	16	15	6	9	3	8	3	2	610	Jan 05 Sunday	
6	6	7	4	2	0	9	3	2	6	8	12	8	12	3	11	11	13	11	8	17	30	34	33	28	278	Jan 06 Monday	
7	14	15	23	14	8	5	12	9	11	11	14	11	11	14	7	3	5	9	6	3	0	2	6	4	217	Jan 07 Tuesday	
8	16	13	3	6	3	5	2	4	2	9	6	14	24	16	11	8	2	6	4	6	2	2	3	2	169	Jan 08 Wednesday	
9	9	2	1	9	2	5	3	1	2	10	22	27	16	23	15	3	5	8	7	12	5	8	5	5	205	Jan 09 Thursday	
10	4	6	12	7	42	31	2	8	11	15	22	27	25	21	14	34	32	13	9	1	4	87	12	21	460	Jan 10 Friday	
11	21	10	6	8	5	4	6	6	4	2	6	3	7	4	6	7	5	1	1	21	18	31	32	34	248	Jan 11 Saturday	
12	21	14	17	8	19	13	17	29	18	26	18	45	52	44	56	49	47	44	46	31	32	27	17	18	708	Jan 12 Sunday	
13	19	20	16	10	9	8	9	6	7	16	12	15	39	19	42	20	23	24	32	25	38	38	34	16	497	Jan 13 Monday	
14	13	6	5	11	6	7	5	7	33	35	12	16	26	13	10	5	5	3	3	20	14	8	7	12	282	Jan 14 Tuesday	
15	6	6	4	10	13	29	8	15	16	13	10	23	25	25	20	7	4	20	2	47	42	36	16	35	432	Jan 15 Wednesday	
16	34	48	37	12	2	7	4	2	2	11	12	24	33	14	11	4	7	11	13	11	14	7	9	13	342	Jan 16 Thursday	
17	6	9	6	7	4	6	13	5	4	17	17	41	25	25	20	17	9	10	13	16	10	15	12	12	319	Jan 17 Friday	
18	12	8	7	10	5	19	6	8	7	4	6	6	14	5	2	6	5	7	3	3	12	4	3	6	168	Jan 18 Saturday	
19	30	39	22	23	39	37	42	36	32	24	23	21	17	17	12	27	32	33	35	26	35	32	27	29	690	Jan 19 Sunday	
20	22	15	7	14	13	5	4	7	4	8	11	19	32	12	14	7	18	8	4	6	6	2	3	6	247	Jan 20 Monday	

Table 3.4.3 (Page 2 of 4)

FIN .FKX Hourly distribution of detections

Day	00	01	02	03	04	05	06	07	08	09	10	11	12	13	14	15	16	17	18	19	20	21	22	23	Sum	Date
21	8	5	5	11	5	4	2	1	4	12	13	10	16	16	16	8	5	5	7	4	4	4	3	1	169	Jan 21 Tuesday
22	6	20	16	10	2	2	6	6	12	12	36	36	50	32	26	12	6	6	8	14	4	8	6	5	341	Jan 22 Wednesday
23	5	0	1	2	5	1	9	4	11	12	11	24	24	17	5	10	4	9	11	7	0	17	5	4	198	Jan 23 Thursday
24	7	7	11	6	13	14	5	5	10	15	21	34	23	23	7	2	19	9	4	14	10	5	9	9	282	Jan 24 Friday
25	3	5	5	10	9	4	13	11	5	10	10	10	9	14	1	3	5	5	18	10	4	21	36	65	286	Jan 25 Saturday
26	54	94	68	18	59	25	6	1	7	5	5	3	4	3	1	5	9	4	8	9	7	12	12	11	430	Jan 26 Sunday
27	6	10	10	8	9	6	4	2	7	12	8	24	20	11	10	2	9	5	5	9	7	3	6	5	198	Jan 27 Monday
28	5	6	7	5	9	7	4	10	18	19	23	41	29	46	33	39	28	33	39	45	34	28	25	28	561	Jan 28 Tuesday
29	17	26	20	23	12	12	10	14	22	30	23	36	44	39	15	16	29	17	15	14	14	18	22	18	506	Jan 29 Wednesday
30	22	33	30	36	42	30	6	6	9	13	17	14	26	28	12	2	13	24	18	21	36	18	30	14	500	Jan 30 Thursday
31	5	9	21	24	24	29	25	15	13	27	28	20	32	14	6	2	10	21	7	1	5	1	3	2	344	Jan 31 Friday
32	4	3	2	4	4	6	4	0	6	12	4	5	5	1	2	3	4	2	3	9	7	2	1	6	99	Feb 01 Saturday
33	10	31	11	22	11	15	16	23	25	13	13	16	18	18	30	13	13	11	6	11	14	10	30	31	411	Feb 02 Sunday
34	7	8	8	7	4	9	10	20	14	32	51	52	28	36	28	27	36	18	7	9	10	9	5	4	439	Feb 03 Monday
35	4	7	9	3	3	4	7	5	9	17	12	34	33	32	14	4	4	4	1	4	3	4	8	1	226	Feb 04 Tuesday
36	5	8	6	9	2	8	13	6	10	22	18	24	26	23	16	6	4	24	79	59	29	36	8	18	459	Feb 05 Wednesday
37	11	7	9	14	9	12	2	4	8	13	13	12	23	20	10	2	6	6	5	5	11	4	2	3	211	Feb 06 Thursday
38	5	7	19	11	3	2	5	5	8	13	22	9	36	7	16	2	5	2	1	6	21	9	6	8	228	Feb 07 Friday
39	6	17	10	13	19	10	14	13	27	18	16	24	14	13	20	9	4	22	15	13	11	15	23	17	363	Feb 08 Saturday
40	35	23	40	36	50	50	59	53	42	40	30	13	9	17	18	37	37	23	14	14	8	9	14	5	676	Feb 09 Sunday
41	6	4	3	9	2	2	1	1	7	12	11	21	13	16	11	6	5	1	1	5	1	5	5	4	152	Feb 10 Monday
42	3	4	13	6	18	11	6	2	10	17	25	25	17	21	12	11	2	3	2	5	5	5	3	2	228	Feb 11 Tuesday
43	3	7	6	8	3	4	3	5	16	9	10	24	30	23	10	7	14	7	5	1	3	6	8	27	239	Feb 12 Wednesday
44	7	7	6	3	6	5	4	5	11	10	15	23	20	24	11	14	8	3	5	9	1	3	3	2	205	Feb 13 Thursday
45	6	2	4	5	4	0	1	2	12	20	44	28	24	23	12	6	3	4	0	2	0	2	3	3	210	Feb 14 Friday
46	3	16	2	3	10	10	11	16	5	14	12	10	7	12	1	9	5	7	6	8	19	12	19	17	234	Feb 15 Saturday
47	12	2	3	7	8	5	4	4	8	10	5	3	7	6	27	2	4	9	15	2	12	5	8	7	175	Feb 16 Sunday
48	7	17	41	16	5	6	2	2	3	10	9	20	15	13	15	10	5	3	5	11	8	6	4	34	267	Feb 17 Monday
49	12	3	0	8	2	1	0	2	10	8	28	15	29	21	16	5	1	9	1	29	11	8	11	6	236	Feb 18 Tuesday
50	16	32	18	24	31	19	17	20	12	27	16	25	55	18	7	13	5	2	7	7	10	2	10	6	399	Feb 19 Wednesday
51	6	16	12	17	19	5	1	2	12	20	18	14	14	12	13	8	11	8	3	12	17	22	37	30	329	Feb 20 Thursday
52	34	38	36	35	34	20	13	11	16	20	22	36	31	6	5	4	4	5	7	7	6	4	9	4	407	Feb 21 Friday
53	3	6	5	9	6	9	2	3	4	8	4	10	6	4	2	8	3	16	4	4	0	2	0	2	120	Feb 22 Saturday
54	6	3	2	3	4	4	2	2	2	1	4	10	6	0	3	4	2	3	9	8	15	7	12	4	116	Feb 23 Sunday
55	10	10	9	12	7	4	2	0	1	13	16	12	15	13	15	6	2	6	6	9	9	9	4	7	197	Feb 24 Monday
56	14	9	9	3	1	3	0	0	5	13	13	9	10	22	9	12	14	6	3	8	6	6	17	21	213	Feb 25 Tuesday
57	30	12	14	17	4	2	3	5	5	9	10	20	22	15	10	8	14	4	6	8	12	7	7	13	257	Feb 26 Wednesday
58	6	8	11	2	8	6	4	1	8	30	15	24	31	17	10	1	9	6	6	8	10	8	9	7	245	Feb 27 Thursday
59	12	11	2	7	7	12	3	3	12	24	17	28	39	24	14	2	5	3	6	3	3	2	1	0	240	Feb 28 Friday
60	1	2	2	6	3	5	4	5	3	7	4	17	8	11	6	4	9	7	1	5	10	1	6	6	133	Feb 29 Saturday
61	8	7	8	13	7	5	5	5	1	4	5	5	1	1	5	2	0	5	4	8	9	8	6	5	127	Mar 01 Sunday
62	4	11	7	6	9	1	2	0	0	17	13	26	29	9	8	7	5	7	0	4	6	8	6	7	192	Mar 02 Monday
63	10	19	4	5	14	8	7	8	4	17	18	21	17	23	15	7	7	12	9	9	8	10	11	13	276	Mar 03 Tuesday
64	5	15	8	10	4	7	5	8	6	9	19	27	33	19	11	12	7	9	4	6	7	9	9	14	263	Mar 04 Wednesday
65	13	7	7	14	4	1	1	6	6	17	12	15	23	25	10	15	32	23	14	15	22	9	4	5	300	Mar 05 Thursday
66	11	4	4	16	3	7	0	4	10	15	12	23	32	23	4	4	6	9	7	4	10	16	15	13	252	Mar 06 Friday
67	16	13	12	14	1	5	8	5	4	4	5	6	0	4	9	17	8	11	16	30	28	14	27	18	275	Mar 07 Saturday
68	15	11	8	12	6	2	2	2	2	2	9	5	6	3	4	4	4	1	6	13	49	125	101	71	463	Mar 08 Sunday
69	48	34	15	12	8	4	5	4	7	6	9	8	28	6	13	9	6	10	10	8	2	7	16	51	326	Mar 09 Monday
70	46	30	16	14	21	3	2	2	10	15	12	13	11	6	16	12	1	4	5	6	8	9	6	6	274	Mar 10 Tuesday
71	6	9	6	7	3	3	3	4	9	12	18	18	25	10	9	13	11	4	10	11	9	21	18	27	266	Mar 11 Wednesday
72	18	27	28	21	2	5	2	4	7	14	10	18	27	26	21	16	23	23	28	36	44	44	38	29	511	Mar 12 Thursday
73	29	19	24	22	17	7	9	7	8	16	18	9	29	13	17	7	8	10	9	11	8	13	13	5	328	Mar 13 Friday
74	13	5	6	12	12	22	20	5	12	20	25	22	14	22	1	1	3	4	3	3	3	4	6	1	239	Mar 14 Saturday
75	1	8	3	8	4	2	3	5	3	5	4	2	3	5	12	7	21	4	15	4	13	11	3	11	157	Mar 15 Sunday
76	8	9	5	5	3	6	1	4	9	6	10	12	16	16	12	8	6	4	5	6	17	6	8	6	190	Mar 16 Monday

Table 3.4.3 (Page 3 of 4)

FIN .FKX Hourly distribution of detections

Day	00	01	02	03	04	05	06	07	08	09	10	11	12	13	14	15	16	17	18	19	20	21	22	23	Sum	Date
77	4	7	10	4	2	5	2	7	21	12	17	12	19	19	10	5	12	13	12	6	6	8	3	2	218	Mar 17 Tuesday
78	6	7	3	7	7	4	2	8	5	17	14	7	19	14	9	6	15	10	7	7	5	6	1	11	197	Mar 18 Wednesday
79	3	4	6	7	2	4	7	5	5	16	8	14	22	11	11	5	3	5	5	9	13	7	3	11	186	Mar 19 Thursday
80	11	11	10	8	5	4	9	4	12	25	14	18	21	19	11	15	8	4	7	9	9	3	2	4	243	Mar 20 Friday
81	5	3	3	12	3	6	7	2	5	9	8	8	7	4	2	3	7	5	1	6	7	2	3	11	129	Mar 21 Saturday
82	5	7	4	3	6	1	3	2	7	4	5	2	1	5	4	3	5	6	11	6	8	11	8	7	124	Mar 22 Sunday
83	12	6	11	13	5	4	5	8	4	9	11	16	18	20	10	9	9	1	8	4	8	14	12	12	229	Mar 23 Monday
84	10	17	17	5	10	3	4	3	8	16	19	12	16	22	15	8	11	7	2	11	6	10	6	12	250	Mar 24 Tuesday
85	7	6	6	9	7	0	0	7	11	14	15	17	35	9	8	2	4	7	7	11	8	24	12	15	241	Mar 25 Wednesday
86	16	9	7	17	12	5	1	7	2	23	20	24	24	27	16	7	15	15	5	4	9	2	6	3	276	Mar 26 Thursday
87	15	5	4	8	8	4	5	9	7	26	18	23	33	31	11	9	9	3	3	8	7	5	7	2	260	Mar 27 Friday
88	4	4	5	12	5	16	5	2	13	11	10	17	5	7	3	7	4	3	6	2	6	2	1	1	151	Mar 28 Saturday
89	6	7	6	7	8	3	6	9	10	12	1	10	16	18	9	7	8	20	4	9	10	16	5	19	226	Mar 29 Sunday
90	12	9	9	6	5	2	9	6	7	10	17	15	24	7	14	8	8	4	8	8	11	5	2	8	214	Mar 30 Monday
91	6	11	13	7	2	3	3	11	10	12	17	14	29	28	8	7	7	2	4	9	5	4	6	17	235	Mar 31 Tuesday
FIN	00	01	02	03	04	05	06	07	08	09	10	11	12	13	14	15	16	17	18	19	20	21	22	23		
Sum	2154	2255	2179	2441	1974	1583	1400	1342	1624	2436	2637	2909	3433	2944	2086	1610	1712	1676	1734	1905	1965	2068	2089	2261	50417	Total sum
172	13	13	13	14	11	9	8	8	9	14	15	17	20	17	12	9	10	10	10	11	11	12	12	13	293	Total average
121	13	13	13	15	11	9	7	7	9	15	17	19	23	19	12	9	9	9	9	10	10	11	10	12	292	Average workdays
51	11	13	11	12	11	10	11	9	10	11	12	12	12	12	11	9	11	11	13	13	14	15	16	16	288	Average weekends

Table 3.4.3. Daily and hourly distribution of FINESA detections. For each day is shown number of detections within each hour of the day and number of detections for that day. The end statistics give total number of detections distributed for each hour and the total sum of detections during the period. The averages show number of processed days, hourly distribution and average per processed day.

GER .FKX Hourly distribution of detections

Day	00	01	02	03	04	05	06	07	08	09	10	11	12	13	14	15	16	17	18	19	20	21	22	23	Sum	Date
274	8	14	4	10	7	3	4	2	8	9	9	8	23	3	16	24	8	6	2	1	8	4	11	16	208	Oct 01 Tuesday
275	12	9	9	13	6	2	15	23	2	22	32	30	31	26	13	18	15	7	14	10	18	9	0	2	338	Oct 02 Wednesday
276	5	0	4	3	1	0	4	4	11	5	4	5	43	2	8	7	5	4	4	2	7	8	0	3	139	Oct 03 Thursday
277	8	7	2	1	4	2	0	4	5	10	18	22	32	15	5	6	6	2	5	3	12	7	3	3	182	Oct 04 Friday
278	6	7	6	2	11	14	11	8	0	4	4	5	7	7	6	6	6	5	10	6	4	2	4	6	147	Oct 05 Saturday
279	1	8	5	2	2	3	2	0	0	7	4	9	2	10	7	3	4	5	1	5	2	1	7	4	94	Oct 06 Sunday
280	3	6	4	2	7	5	3	6	17	2	17	23	22	7	8	15	16	2	3	4	2	9	2	2	187	Oct 07 Monday
281	6	8	3	5	4	8	2	3	21	8	14	0	14	12	16	14	7	7	12	9	18	11	18	1	221	Oct 08 Tuesday
282	6	2	5	3	7	2	18	10	26	34	19	19	17	7	14	15	8	13	9	17	1	3	0	5	260	Oct 09 Wednesday
283	9	9	4	7	4	8	1	11	18	9	25	20	28	13	17	20	9	7	12	3	9	4	5	0	252	Oct 10 Thursday
284	6	5	8	10	0	7	3	2	6	14	21	5	32	3	15	9	10	2	5	9	9	3	3	4	191	Oct 11 Friday
285	2	5	4	0	0	10	3	7	10	3	7	13	25	1	5	1	11	1	1	0	4	0	4	0	117	Oct 12 Saturday
286	1	8	1	2	0	0	0	0	0	0	0	0	0	0	0	0	0	0	0	0	0	0	0	0	12	Oct 13 Sunday
287	0	0	0	0	0	0	0	0	0	0	11	19	26	14	26	8	22	17	12	7	15	4	10	9	200	Oct 14 Monday
288	1	3	0	9	4	6	2	5	10	21	24	32	16	23	11	17	20	4	9	9	2	6	1	9	244	Oct 15 Tuesday
289	2	4	1	12	0	2	6	8	8	8	8	14	17	17	4	9	21	5	5	7	9	4	3	17	191	Oct 16 Wednesday
290	8	7	8	7	14	14	19	16	21	22	26	36	34	20	33	29	19	13	11	14	12	20	14	21	438	Oct 17 Thursday
291	9	17	6	7	8	10	9	11	14	27	26	27	18	17	23	10	20	14	6	13	11	2	8	7	320	Oct 18 Friday
292	4	8	13	9	11	12	6	5	5	9	1	8	16	7	5	9	5	9	2	2	1	14	2	1	164	Oct 19 Saturday
293	3	4	4	5	5	6	4	2	0	0	0	0	0	0	0	0	0	0	3	3	6	11	12	3	71	Oct 20 Sunday
294	2	5	10	2	3	1	2	2	10	13	12	15	20	13	11	8	9	2	15	11	30	16	4	8	224	Oct 21 Monday
295	2	2	3	2	3	4	7	11	20	5	19	7	29	10	11	6	24	5	16	16	10	1	1	9	223	Oct 22 Tuesday
296	10	10	10	10	7	11	5	5	13	9	18	21	23	7	18	3	6	9	7	3	14	3	4	5	231	Oct 23 Wednesday
297	8	3	3	5	3	3	2	5	17	11	21	13	29	14	11	13	6	4	2	1	3	3	2	6	188	Oct 24 Thursday
298	5	5	1	4	2	5	5	2	14	9	10	11	19	11	12	5	11	2	3	2	3	12	6	1	160	Oct 25 Friday
299	2	3	13	3	1	8	2	2	2	8	1	1	8	19	18	0	1	2	3	0	0	1	1	0	99	Oct 26 Saturday
300	5	0	1	0	1	4	2	3	0	12	4	2	12	3	8	7	5	2	2	1	4	10	8	9	105	Oct 27 Sunday
301	6	7	7	1	1	7	3	4	10	3	20	19	6	12	7	3	8	10	3	10	5	7	1	3	163	Oct 28 Monday
302	1	9	0	2	5	8	0	8	4	6	11	11	17	12	5	8	4	6	2	4	7	13	7	5	155	Oct 29 Tuesday
303	8	17	10	9	10	3	0	3	7	11	8	17	21	3	6	17	8	2	5	6	5	2	8	6	192	Oct 30 Wednesday
304	3	3	7	4	1	4	0	0	2	21	5	15	12	5	10	10	3	1	13	4	7	2	6	5	143	Oct 31 Thursday
305	4	0	3	13	1	8	8	5	6	13	17	23	22	20	14	1	9	7	17	13	26	6	10	8	254	Nov 01 Friday
306	9	6	1	2	0	8	3	2	6	6	13	12	13	9	5	9	11	22	9	1	9	2	17	4	179	Nov 02 Saturday
307	12	2	0	0	3	4	6	1	5	5	9	10	12	4	0	7	5	11	3	5	7	13	0	6	130	Nov 03 Sunday
308	4	13	8	8	8	4	8	14	9	4	8	26	9	4	2	4	1	7	4	4	8	1	4	5	167	Nov 04 Monday
309	1	7	8	6	9	14	15	14	16	29	28	9	24	14	16	15	8	7	11	13	4	10	3	4	285	Nov 05 Tuesday
310	2	5	6	4	4	0	1	0	15	5	10	17	15	7	11	5	1	1	11	3	2	4	12	7	148	Nov 06 Wednesday
311	16	13	3	14	14	13	21	14	16	8	15	36	36	18	28	40	16	23	8	3	11	10	7	18	401	Nov 07 Thursday
312	6	10	11	19	27	19	14	21	33	20	13	47	39	19	18	11	8	8	9	11	3	11	7	5	389	Nov 08 Friday
313	7	2	5	4	7	6	7	3	5	3	6	9	4	8	18	11	13	6	7	5	4	8	4	3	155	Nov 09 Saturday
314	6	4	4	2	2	2	2	2	6	3	1	3	13	4	5	7	0	4	10	6	4	2	4	1	97	Nov 10 Sunday
315	15	9	7	12	10	5	1	3	9	14	16	16	16	11	13	8	14	9	12	1	9	3	8	7	228	Nov 11 Monday
316	10	4	3	3	12	5	5	2	9	19	28	16	13	3	7	14	5	2	5	6	9	9	2	3	194	Nov 12 Tuesday
317	3	1	4	2	5	3	6	8	16	12	15	27	18	4	9	9	6	7	11	13	6	9	7	3	204	Nov 13 Wednesday
318	0	5	6	3	7	3	1	9	5	7	11	33	27	4	10	6	16	15	1	15	16	13	17	20	250	Nov 14 Thursday
319	20	12	5	14	0	8	2	3	8	6	3	13	15	17	12	0	5	16	10	15	6	13	0	5	208	Nov 15 Friday
320	3	2	1	0	2	1	0	1	11	19	15	15	16	11	10	14	5	5	12	11	19	8	11	1	193	Nov 16 Saturday
321	12	0	0	0	0	0	0	0	0	0	0	0	0	0	0	0	0	0	0	0	0	0	0	0	12	Nov 17 Sunday
322	0	0	0	0	0	0	0	0	0	0	0	21	20	15	24	4	2	7	7	5	12	6	10	7	140	Nov 18 Monday
323	5	7	4	4	5	2	4	7	18	18	26	23	11	15	24	14	11	15	34	19	16	15	20	18	335	Nov 19 Tuesday
324	12	13	12	4	15	1	3	6	25	18	17	29	31	26	14	11	0	12	16	11	13	24	4	14	331	Nov 20 Wednesday
325	11	6	8	0	4	2	5	4	10	12	23	23	21	17	1	12	1	0	4	3	0	9	5	5	186	Nov 21 Thursday
326	9	2	3	1	7	1	3	11	22	9	35	30	27	6	12	3	5	12	11	8	9	24	1	4	255	Nov 22 Friday
327	6	11	1	2	4	6	7	7	2	14	18	29	11	18	13	8	8	11	5	5	6	3	9	7	211	Nov 23 Saturday
328	3	1	7	3	3	1	0	2	8	5	10	4	4	4	11	1	10	6	12	6	13	4	3	3	124	Nov 24 Sunday
329	1	8	4	6	8	1	3	2	10	20	13	13	19	3	0	0	5	10	2	3	5	16	3	4	159	Nov 25 Monday

Table 3.4.4 (Page 1 of 4)

GER .FKX Hourly distribution of detections

Day	00	01	02	03	04	05	06	07	08	09	10	11	12	13	14	15	16	17	18	19	20	21	22	23	Sum	Date	
330	1	2	8	4	3	0	5	10	6	12	24	21	13	19	14	5	10	2	2	9	1	2	1	0	174	Nov 26 Tuesday	
331	6	6	2	3	10	0	1	5	14	11	27	31	19	19	14	4	8	3	1	0	5	1	4	2	196	Nov 27 Wednesday	
332	2	4	0	4	1	1	5	5	13	7	20	30	24	15	13	12	8	9	6	3	3	1	3	1	190	Nov 28 Thursday	
333	0	5	5	3	11	1	2	10	15	16	7	20	11	10	12	3	4	11	5	5	0	4	3	2	165	Nov 29 Friday	
334	8	3	5	7	6	7	6	5	7	4	16	11	5	7	12	1	7	2	2	5	4	6	1	1	138	Nov 30 Saturday	
335	7	2	9	5	3	6	2	4	1	10	10	4	11	5	3	3	6	2	9	2	9	2	8	6	129	Dec 01 Sunday	
336	4	5	7	4	3	5	10	3	15	26	18	13	26	20	13	23	4	15	6	6	2	8	3	5	244	Dec 02 Monday	
337	2	3	5	11	3	4	1	6	19	13	24	28	17	15	10	17	8	4	3	1	3	1	5	0	203	Dec 03 Tuesday	
338	11	3	5	9	3	2	5	7	14	15	35	26	18	27	6	8	3	0	0	5	0	4	6	2	214	Dec 04 Wednesday	
339	5	3	3	2	2	0	2	5	1	2	16	26	20	7	16	0	0	0	0	0	0	0	0	0	110	Dec 05 Thursday	
340	0	0	0	0	0	0	0	0	0	0	0	0	0	0	0	0	0	0	0	0	0	0	0	0	0	Dec 06 Friday	
341	0	0	0	0	0	0	0	0	0	0	0	0	0	0	0	0	0	0	0	0	0	0	0	0	0	Dec 07 Saturday	
342	0	0	0	0	0	0	0	0	0	0	0	0	0	0	0	0	0	0	0	0	0	0	0	0	0	Dec 08 Sunday	
343	0	0	0	0	0	0	0	0	0	0	0	0	0	0	0	0	0	0	0	0	0	0	0	0	0	Dec 09 Monday	
344	0	0	0	0	0	0	0	0	0	0	0	0	0	0	0	0	0	0	0	0	0	0	0	0	0	Dec 10 Tuesday	
345	0	0	0	0	0	0	0	0	0	0	0	0	0	0	0	0	0	0	0	0	0	0	0	0	0	Dec 11 Wednesday	
346	0	0	0	0	0	0	0	0	0	0	0	0	0	0	0	0	0	0	0	0	0	0	0	0	0	Dec 12 Thursday	
347	0	0	0	0	0	0	0	0	0	0	0	0	0	0	0	0	0	0	0	0	0	0	0	0	0	Dec 13 Friday	
348	0	0	0	0	0	0	0	0	0	0	0	0	0	0	0	0	0	0	0	0	0	0	0	0	0	Dec 14 Saturday	
349	0	0	0	0	0	0	0	0	0	0	3	4	10	2	0	3	3	5	3	5	8	7	7	6	66	Dec 15 Sunday	
350	2	7	3	0	2	1	1	4	5	11	13	10	26	16	4	14	1	6	8	1	1	3	2	4	145	Dec 16 Monday	
351	4	0	2	5	9	1	2	8	14	10	8	20	25	8	4	9	2	3	4	0	6	0	5	11	160	Dec 17 Tuesday	
352	6	8	7	4	9	6	12	14	16	24	9	15	11	17	4	0	7	6	6	3	3	5	4	5	201	Dec 18 Wednesday	
353	1	7	10	13	8	2	1	6	7	4	6	12	18	21	23	7	11	4	13	24	40	25	15	11	289	Dec 19 Thursday	
354	17	21	28	36	28	35	12	9	29	19	20	6	21	17	16	16	8	20	20	15	12	8	11	7	431	Dec 20 Friday	
355	4	11	6	7	14	7	6	8	8	15	9	10	13	9	8	9	8	7	12	11	13	22	14	7	238	Dec 21 Saturday	
356	4	6	9	4	14	11	7	10	17	34	14	23	12	3	8	10	5	3	1	4	6	12	13	4	234	Dec 22 Sunday	
357	6	9	15	15	14	19	21	27	27	20	26	24	21	27	12	19	17	25	22	14	20	16	28	13	457	Dec 23 Monday	
358	21	22	8	13	16	17	4	4	2	8	11	10	18	5	13	5	5	5	2	4	3	6	5	2	209	Dec 24 Tuesday	
359	4	3	1	2	3	3	1	3	3	3	1	1	8	6	1	3	2	3	2	3	0	0	6	3	65	Dec 25 Wednesday	Frste
360	5	2	3	3	7	11	10	24	19	21	21	24	20	18	17	13	14	14	9	15	19	17	13	14	333	Dec 26 Thursday	Andre
361	9	9	8	7	24	10	3	4	2	7	1	11	7	5	9	13	3	5	5	8	9	6	1	5	171	Dec 27 Friday	
362	0	12	3	9	4	7	3	6	7	3	16	5	5	5	0	2	7	5	1	8	1	3	1	9	122	Dec 28 Saturday	
363	5	6	5	2	5	9	3	1	2	5	4	0	2	1	4	1	2	6	5	4	4	5	1	2	84	Dec 29 Sunday	
364	9	5	2	3	4	4	4	7	5	1	10	7	9	3	6	4	6	8	4	3	1	3	6	3	117	Dec 30 Monday	
365	2	2	2	1	7	2	2	1	2	4	1	4	2	3	3	5	7	4	5	6	0	5	3	1	74	Dec 31 Tuesday	
1	3	3	4	1	8	0	3	5	4	6	9	5	7	6	5	12	8	7	12	9	10	15	9	9	160	Jan 01 Wednesday	Frste
2	11	14	10	6	4	13	8	11	22	12	13	22	12	16	6	2	8	5	3	13	9	17	4	6	247	Jan 02 Thursday	
3	15	13	1	9	2	6	8	1	6	9	1	2	8	7	6	2	7	4	2	6	2	2	9	4	132	Jan 03 Friday	
4	3	5	13	21	24	18	18	9	17	14	16	27	16	5	14	3	13	4	24	18	13	17	15	12	339	Jan 04 Saturday	
5	5	5	5	1	1	6	4	1	3	1	12	7	7	6	6	9	17	30	35	30	37	30	25	26	309	Jan 05 Sunday	
6	24	13	16	29	16	23	6	10	18	25	24	20	19	29	16	13	8	9	5	5	6	6	3	3	346	Jan 06 Monday	
7	3	6	3	6	3	2	0	2	5	11	16	8	16	6	11	2	2	5	1	0	4	3	0	0	115	Jan 07 Tuesday	
8	2	1	1	5	2	3	0	2	7	6	7	10	21	4	6	7	7	4	8	3	4	3	3	2	118	Jan 08 Wednesday	
9	0	2	1	1	6	3	0	10	8	14	15	7	14	9	3	4	1	1	6	4	3	2	4	2	120	Jan 09 Thursday	
10	3	8	5	2	1	0	3	1	11	20	9	16	18	9	9	5	3	7	6	3	7	2	1	9	158	Jan 10 Friday	
11	0	6	0	9	0	0	4	1	2	5	5	9	9	17	6	10	6	7	3	5	8	6	0	2	120	Jan 11 Saturday	
12	10	3	11	13	9	19	13	11	9	18	4	9	2	0	3	3	4	1	5	6	1	4	4	4	166	Jan 12 Sunday	
13	1	3	6	2	4	0	4	2	8	10	3	12	28	5	8	3	1	2	10	6	4	5	6	2	135	Jan 13 Monday	
14	5	2	4	7	1	2	2	1	4	3	9	7	28	8	6	3	8	3	5	0	5	3	4	3	123	Jan 14 Tuesday	
15	1	3	5	1	0	2	0	2	6	5	9	7	11	12	8	1	8	3	5	5	7	5	0	10	116	Jan 15 Wednesday	
16	4	5	3	1	6	8	1	8	5	7	33	6	18	5	4	2	5	4	9	11	9	12	13	13	192	Jan 16 Thursday	
17	9	10	7	0	3	2	3	3	6	10	7	12	11	7	2	4	4	6	12	1	11	2	1	11	144	Jan 17 Friday	
18	1	2	7	0	7	5	3	1	2	1	6	10	1	9	21	2	0	8	6	7	6	2	5	3	115	Jan 18 Saturday	
19	6	8	1	1	2	2	0	3	1	1	4	12	10	9	8	1	3	7	5	2	3	2	1	4	96	Jan 19 Sunday	
20	4	10	10	4	1	3	4	0	10	15	10	10	4	11	12	6	10	3	5	1	3	1	2	4	143	Jan 20 Monday	

Table 3.4.4 (Page 2 of 4)

GER .FKX Hourly distribution of detections

Day	00	01	02	03	04	05	06	07	08	09	10	11	12	13	14	15	16	17	18	19	20	21	22	23	Sum	Date
21	2	6	2	0	7	5	0	0	0	0	0	0	0	0	6	7	3	2	7	7	9	5	5	6	79	Jan 21 Tuesday
22	4	22	22	18	16	4	12	6	14	12	18	12	32	6	10	30	8	1	4	7	4	6	4	4	276	Jan 22 Wednesday
23	1	1	1	0	8	2	6	3	8	9	13	10	17	17	9	8	5	6	10	8	22	10	13	5	192	Jan 23 Thursday
24	7	1	1	0	1	5	0	4	12	4	9	17	18	6	4	5	9	2	5	8	10	1	4	1	134	Jan 24 Friday
25	0	4	1	0	2	0	3	0	2	10	3	6	13	2	14	15	15	27	29	29	16	28	39	11	269	Jan 25 Saturday
26	2	2	8	1	2	2	2	7	2	26	3	7	5	21	5	2	6	1	4	0	7	3	0	5	123	Jan 26 Sunday
27	0	4	5	0	0	0	0	3	8	5	15	10	25	2	14	1	2	1	0	4	5	3	9	1	117	Jan 27 Monday
28	4	2	3	6	3	2	0	2	6	12	6	13	17	11	7	7	9	5	5	2	4	5	3	1	135	Jan 28 Tuesday
29	0	1	5	3	4	0	1	0	11	11	9	5	25	8	8	2	6	2	14	14	13	15	19	0	176	Jan 29 Wednesday
30	0	5	4	2	21	6	4	2	8	10	21	0	19	21	27	7	13	15	12	27	21	54	9	6	314	Jan 30 Thursday
31	6	1	0	6	4	2	0	3	3	0	0	0	0	11	11	3	3	1	0	9	13	0	4	1	81	Jan 31 Friday
32	3	1	2	3	5	8	0	2	1	8	4	10	14	6	15	13	3	7	5	15	12	11	4	7	159	Feb 01 Saturday
33	9	0	3	3	0	1	1	2	15	2	3	6	1	7	12	12	11	2	4	4	4	7	6	6	121	Feb 02 Sunday
34	5	1	1	3	2	8	8	5	9	7	19	11	4	0	0	0	0	0	0	0	0	0	0	0	83	Feb 03 Monday
35	0	0	0	0	0	0	0	0	0	0	0	0	0	0	0	0	0	0	0	0	0	0	0	0	0	Feb 04 Tuesday
36	0	0	0	0	0	0	0	0	16	12	7	11	23	7	2	7	2	0	2	3	29	8	4	9	142	Feb 05 Wednesday
37	3	6	15	11	10	1	0	3	11	12	0	0	0	0	0	0	0	0	0	0	0	0	0	0	72	Feb 06 Thursday
38	0	0	0	0	0	0	0	0	0	0	0	0	0	0	0	0	0	0	0	0	0	0	0	0	0	Feb 07 Friday
39	0	0	0	0	0	0	0	0	0	0	0	0	0	0	0	0	0	0	0	0	0	0	0	0	0	Feb 08 Saturday
40	0	0	0	0	0	0	0	0	0	0	0	0	0	0	0	0	0	0	0	0	0	0	0	0	0	Feb 09 Sunday
41	0	0	0	0	0	0	0	0	0	1	20	18	18	10	11	5	15	3	5	4	6	4	5	3	128	Feb 10 Monday
42	6	0	4	2	0	0	2	1	6	12	4	4	0	3	4	9	3	6	5	4	1	8	3	1	88	Feb 11 Tuesday
43	5	6	1	1	0	0	7	5	13	13	21	13	14	6	9	4	8	4	1	4	4	10	2	3	154	Feb 12 Wednesday
44	10	11	4	2	3	2	4	5	12	3	9	17	19	11	22	11	4	3	0	9	2	7	8	3	181	Feb 13 Thursday
45	1	2	2	0	1	1	0	0	3	4	8	22	26	4	14	3	3	2	5	10	11	1	0	1	124	Feb 14 Friday
46	1	8	1	0	3	9	12	9	15	11	2	2	0	0	2	0	0	0	0	0	0	0	0	0	75	Feb 15 Saturday
47	0	0	0	0	0	0	0	0	0	0	2	0	5	0	0	0	0	0	0	0	0	0	0	2	9	Feb 16 Sunday
48	0	0	0	0	0	0	0	0	0	0	0	0	0	0	0	0	0	0	0	0	0	0	0	0	0	Feb 17 Monday
49	0	0	0	0	0	0	0	0	0	0	2	2	0	0	3	0	0	0	0	0	0	2	0	0	9	Feb 18 Tuesday
50	0	0	0	0	0	1	0	3	2	11	1	13	13	6	9	1	5	5	2	4	0	0	2	2	80	Feb 19 Wednesday
51	4	0	1	2	1	0	1	4	0	9	2	16	17	13	18	5	8	9	15	13	7	12	3	1	161	Feb 20 Thursday
52	3	3	0	0	2	0	1	4	17	10	5	1	8	8	12	7	2	9	4	2	1	2	5	0	106	Feb 21 Friday
53	2	1	1	1	3	5	2	0	5	10	11	10	5	1	9	0	3	9	4	4	3	4	3	2	98	Feb 22 Saturday
54	5	4	8	7	3	4	11	17	15	14	28	29	23	19	19	22	11	10	4	4	7	5	3	3	275	Feb 23 Sunday
55	5	8	6	4	4	4	3	4	13	17	10	9	9	6	15	4	0	2	6	15	8	10	1	4	167	Feb 24 Monday
56	4	2	3	0	14	2	0	10	19	7	16	13	23	14	3	9	8	2	14	2	3	6	3	4	181	Feb 25 Tuesday
57	0	1	2	4	0	4	1	6	5	8	25	4	26	16	4	3	9	7	6	19	3	8	2	4	167	Feb 26 Wednesday
58	6	5	4	1	4	3	2	0	14	6	12	19	27	9	2	2	8	1	8	8	9	9	0	0	159	Feb 27 Thursday
59	5	6	3	7	4	3	2	3	11	14	14	6	2	29	2	5	0	2	2	6	10	4	1	2	143	Feb 28 Friday
60	7	3	4	3	9	5	12	4	3	10	7	12	12	3	5	7	10	8	3	1	2	6	0	3	139	Feb 29 Saturday
61	1	1	5	1	3	2	4	3	2	0	0	3	12	2	6	8	4	5	0	3	2	1	1	2	71	Mar 01 Sunday
62	4	1	2	2	11	0	2	6	2	17	12	5	19	17	4	18	15	9	2	4	11	2	6	7	178	Mar 02 Monday
63	2	12	11	11	10	12	9	18	28	6	0	5	46	23	26	14	11	10	6	11	4	14	13	15	317	Mar 03 Tuesday
64	17	18	18	4	11	16	6	2	8	8	11	17	21	13	12	5	3	1	4	2	4	2	1	3	207	Mar 04 Wednesday
65	8	7	9	4	9	1	2	0	6	29	34	19	14	17	15	7	5	2	1	0	8	3	1	4	205	Mar 05 Thursday
66	5	1	2	2	6	3	2	1	14	28	13	12	21	8	2	3	3	6	4	2	4	1	2	11	156	Mar 06 Friday
67	2	3	2	1	0	5	3	2	7	8	2	6	1	1	0	4	6	2	5	0	1	2	7	0	70	Mar 07 Saturday
68	1	2	1	10	1	4	0	1	3	2	0	5	8	0	1	2	1	6	3	2	5	6	2	4	70	Mar 08 Sunday
69	9	12	6	6	9	6	2	1	13	11	11	18	15	10	15	8	1	10	3	4	3	2	3	2	180	Mar 09 Monday
70	7	8	1	6	0	0	0	0	0	0	14	12	16	26	12	19	8	8	2	1	2	14	5	2	163	Mar 10 Tuesday
71	3	4	3	9	4	7	3	7	14	15	24	3	11	3	9	16	4	7	5	8	3	7	8	7	184	Mar 11 Wednesday
72	6	5	9	7	5	3	2	6	18	10	35	27	30	25	34	26	17	6	4	6	20	14	13	18	346	Mar 12 Thursday
73	16	22	29	27	26	27	25	35	45	24	35	43	34	23	29	37	32	23	44	32	28	24	25	17	702	Mar 13 Friday
74	11	5	0	11	14	18	7	10	11	11	14	4	9	6	8	4	3	1	2	4	5	1	7	11	177	Mar 14 Saturday
75	6	6	4	3	8	5	8	8	7	8	18	10	6	0	5	1	9	10	6	5	4	2	0	5	144	Mar 15 Sunday
76	1	4	5	2	3	7	0	3	49	11	28	14	20	6	3	4	10	1	1	6	0	3	4	6	191	Mar 16 Monday

Table 3.4.4 (Page 3 of 4)

GER .FKX Hourly distribution of detections

Day	00	01	02	03	04	05	06	07	08	09	10	11	12	13	14	15	16	17	18	19	20	21	22	23	Sum	Date
77	6	2	3	2	2	7	1	3	25	9	19	11	10	17	10	15	8	3	2	6	2	0	4	8	175	Mar 17 Tuesday
78	2	5	4	7	4	3	2	17	25	11	27	24	11	6	13	5	10	2	8	2	12	4	1	4	209	Mar 18 Wednesday
79	4	4	1	1	1	4	7	11	13	5	23	18	27	12	11	16	12	4	16	5	8	17	4	11	235	Mar 19 Thursday
80	8	4	5	7	3	12	2	5	28	15	20	26	21	8	12	10	11	11	4	19	9	4	9	4	257	Mar 20 Friday
81	6	4	0	3	7	7	9	1	4	1	11	10	7	7	9	1	2	4	17	0	0	0	0	0	110	Mar 21 Saturday
82	0	0	0	0	0	0	0	0	0	0	0	0	0	0	0	0	0	0	0	0	0	0	0	0	0	Mar 22 Sunday
83	0	0	0	0	0	0	0	0	0	0	0	0	0	0	0	0	0	0	0	0	0	0	0	0	0	Mar 23 Monday
84	0	0	0	0	0	0	0	0	0	0	0	0	0	0	0	0	0	0	3	8	7	5	0	9	32	Mar 24 Tuesday
85	9	2	5	4	4	0	0	5	23	12	20	12	21	11	9	15	5	9	7	2	6	3	3	4	191	Mar 25 Wednesday
86	2	9	5	3	0	2	1	3	10	11	13	21	9	11	7	7	17	5	6	3	4	4	2	2	157	Mar 26 Thursday
87	5	0	3	0	1	5	2	12	14	8	16	25	21	10	2	6	8	3	2	9	7	1	0	0	160	Mar 27 Friday
88	10	7	3	2	2	11	11	1	2	3	11	9	8	11	2	6	3	2	7	12	11	9	8	3	154	Mar 28 Saturday
89	4	6	2	2	3	1	3	3	8	2	5	3	7	18	3	3	11	3	3	1	3	9	7	12	122	Mar 29 Sunday
90	6	4	3	0	4	6	13	11	10	20	18	22	16	12	8	7	2	5	11	10	7	1	7	5	208	Mar 30 Monday
91	6	2	2	13	3	3	6	8	11	15	23	13	14	9	9	14	3	1	7	1	1	5	8	4	181	Mar 31 Tuesday

GER	00	01	02	03	04	05	06	07	08	09	10	11	12	13	14	15	16	17	18	19	20	21	22	23		
Sum	874	916	817	826	903	852	717	901	1663	1703	2132	2267	2622	1676	1626	1323	1177	1011	1131	1091	1218	1152	928	881	30407	Total sum
167	5	5	5	5	5	5	4	5	10	10	13	14	16	10	10	8	7	6	7	7	7	7	6	5	182	Total average
118	5	6	5	5	6	5	4	6	12	11	15	16	19	11	11	9	7	6	7	7	8	7	5	5	198	Average workdays
49	4	4	4	4	5	6	5	4	5	7	7	8	9	6	7	5	6	6	6	6	6	7	6	5	139	Average weekends

Table 3.4.4. Daily and hourly distribution of GERESS detections. For each day is shown number of detections within each hour of the day and number of detections for that day. The end statistics give total number of detections distributed for each hour and the total sum of detections during the period. The averages show number of processed days, hourly distribution and average per processed day.

KSP .FKX Hourly distribution of detections

Day	00	01	02	03	04	05	06	07	08	09	10	11	12	13	14	15	16	17	18	19	20	21	22	23	Sum	Date
274	14	11	13	23	25	9	18	4	7	10	6	3	13	6	2	16	4	0	6	9	19	24	13	27	282	Oct 01 Tuesday
275	9	16	13	24	22	9	2	8	7	8	9	7	9	8	11	5	5	4	9	4	22	13	22	15	261	Oct 02 Wednesday
276	1	6	6	15	17	4	1	1	7	4	11	8	12	13	11	16	10	14	10	15	24	27	15	29	277	Oct 03 Thursday
277	23	14	7	11	27	8	2	10	4	12	7	8	16	22	26	14	16	15	18	27	19	28	19	32	385	Oct 04 Friday
278	21	4	14	23	26	19	14	5	19	18	12	14	17	21	26	12	23	18	19	8	11	6	12	13	375	Oct 05 Saturday
279	14	13	12	9	22	12	12	8	20	16	9	18	15	11	22	20	21	25	18	22	12	48	19	9	407	Oct 06 Sunday
280	24	19	8	16	17	6	5	2	5	9	5	2	9	20	22	14	13	6	2	11	21	29	32	17	314	Oct 07 Monday
281	17	15	11	11	16	7	4	3	3	13	16	12	22	10	7	7	9	7	4	6	18	21	24	10	273	Oct 08 Tuesday
282	4	12	17	15	22	10	3	6	6	14	15	8	19	11	22	27	14	15	5	6	21	15	20	17	324	Oct 09 Wednesday
283	4	15	14	19	34	8	7	2	6	4	12	8	22	20	10	10	6	18	8	9	17	27	22	17	319	Oct 10 Thursday
284	28	7	17	14	28	7	10	8	4	14	7	9	16	18	13	14	15	14	1	15	17	24	18	13	331	Oct 11 Friday
285	16	14	22	8	29	11	4	9	11	8	7	10	11	14	15	9	20	7	9	4	28	19	21	16	322	Oct 12 Saturday
286	11	15	21	30	29	16	27	24	15	12	12	17	19	8	14	15	18	35	21	11	14	12	14	27	437	Oct 13 Sunday
287	10	12	32	22	18	7	5	5	5	7	6	13	27	8	6	7	16	9	4	4	17	14	12	33	299	Oct 14 Monday
288	11	5	9	13	16	9	2	5	10	2	14	13	12	14	11	9	2	8	1	5	20	19	16	9	235	Oct 15 Tuesday
289	10	21	8	4	19	17	6	0	5	5	3	16	16	10	7	6	5	9	8	10	18	15	20	29	267	Oct 16 Wednesday
290	12	38	13	14	19	2	3	5	4	11	4	13	10	6	4	8	12	14	7	2	8	22	19	9	259	Oct 17 Thursday
291	20	9	7	5	16	4	17	11	1	6	8	3	6	10	8	7	16	11	23	25	29	25	14	12	293	Oct 18 Friday
292	3	14	10	12	13	20	12	18	12	18	13	30	17	10	29	10	13	31	20	27	21	28	28	20	429	Oct 19 Saturday
293	16	26	13	7	29	19	20	26	30	21	13	17	31	11	15	17	22	13	13	14	18	17	16	19	443	Oct 20 Sunday
294	9	4	17	15	15	4	8	3	6	4	10	11	9	10	7	9	14	13	10	4	9	18	7	16	232	Oct 21 Monday
295	12	8	13	21	22	5	1	5	13	12	5	7	21	7	10	9	13	8	6	30	13	21	7	14	283	Oct 22 Tuesday
296	7	3	8	12	23	5	1	3	8	18	15	19	19	1	18	16	1	10	5	12	13	19	16	13	265	Oct 23 Wednesday
297	16	12	10	14	15	10	2	12	15	9	4	14	20	15	8	14	18	6	4	2	13	20	6	16	275	Oct 24 Thursday
298	22	5	7	17	26	14	17	17	19	11	16	24	9	11	5	7	4	5	15	13	31	18	24	20	357	Oct 25 Friday
299	12	23	23	23	26	35	14	10	15	14	19	14	17	19	20	16	29	27	20	13	15	17	27	21	469	Oct 26 Saturday
300	31	19	18	27	12	22	28	21	19	37	17	17	19	11	15	10	11	39	29	5	18	29	18	6	478	Oct 27 Sunday
301	10	11	9	24	15	4	14	8	13	6	6	7	16	12	5	4	9	14	3	7	15	29	11	9	261	Oct 28 Monday
302	5	13	14	11	34	5	5	23	5	9	13	10	16	9	2	5	2	6	3	1	14	26	11	15	257	Oct 29 Tuesday
303	7	12	14	19	21	13	5	6	5	18	26	20	19	14	6	13	20	3	13	9	14	32	21	16	346	Oct 30 Wednesday
304	6	13	16	20	22	9	12	5	8	11	9	13	23	9	12	11	9	11	10	11	23	21	21	15	320	Oct 31 Thursday
305	25	10	21	16	21	20	13	20	5	5	13	27	27	31	24	15	25	15	10	4	6	12	9	8	382	Nov 01 Friday
306	9	13	18	12	8	0	10	16	9	5	7	8	13	10	7	9	8	13	18	9	21	25	10	13	271	Nov 02 Saturday
307	8	2	26	13	25	13	17	27	7	25	15	38	21	9	13	15	9	28	22	9	21	15	20	26	424	Nov 03 Sunday
308	8	9	20	14	10	7	6	2	4	10	11	23	27	11	1	5	10	1	12	0	10	17	40	46	304	Nov 04 Monday
309	27	56	64	16	27	20	11	7	1	11	2	5	10	9	14	11	5	13	8	16	14	33	66	69	515	Nov 05 Tuesday
310	38	69	65	31	19	3	7	41	21	14	6	7	25	9	12	6	13	14	11	10	16	30	53	47	567	Nov 06 Wednesday
311	48	67	33	15	16	5	9	4	3	13	6	11	12	5	3	15	6	9	6	11	21	9	19	14	360	Nov 07 Thursday
312	37	4	13	9	13	9	4	4	21	8	5	11	28	12	6	7	5	23	7	12	6	18	6	12	280	Nov 08 Friday
313	3	7	14	12	16	2	9	8	8	9	15	22	9	13	21	16	20	26	16	12	14	20	14	24	330	Nov 09 Saturday
314	9	9	22	29	28	7	22	21	21	16	12	9	23	18	18	14	13	35	18	9	23	21	12	20	429	Nov 10 Sunday
315	9	10	19	25	16	2	15	8	6	6	2	6	14	11	8	8	3	3	7	13	16	15	17	15	254	Nov 11 Monday
316	15	6	57	16	31	17	4	2	3	18	12	7	16	13	28	7	2	6	6	4	13	15	6	12	316	Nov 12 Tuesday
317	8	5	7	32	19	1	0	4	3	9	10	18	20	5	11	11	6	5	12	18	14	39	46	29	332	Nov 13 Wednesday
318	37	12	31	33	21	7	2	13	2	6	1	13	13	16	14	4	9	21	8	7	17	36	22	9	354	Nov 14 Thursday
319	21	26	14	4	46	14	13	9	4	6	19	7	29	10	4	4	3	12	5	6	18	27	56	71	428	Nov 15 Friday
320	16	55	35	7	20	6	2	3	9	3	3	12	8	17	7	8	19	18	14	21	32	32	41	73	461	Nov 16 Saturday
321	13	27	21	17	23	9	11	14	7	19	12	14	16	12	33	28	16	25	30	12	23	20	34	14	450	Nov 17 Sunday
322	15	14	25	33	35	13	19	4	7	13	12	18	19	10	11	5	15	10	18	0	15	22	20	15	368	Nov 18 Monday
323	9	9	15	14	20	8	12	9	10	15	3	11	21	14	10	28	21	8	14	13	18	34	51	61	428	Nov 19 Tuesday
324	14	63	19	15	25	13	18	1	14	8	7	13	21	12	6	8	12	5	10	10	15	28	23	7	367	Nov 20 Wednesday
325	6	6	24	27	16	8	6	13	6	8	9	16	13	15	16	5	3	18	10	11	16	32	27	43	354	Nov 21 Thursday
326	36	30	26	22	28	3	5	7	6	6	20	10	23	13	6	8	9	18	14	11	18	30	21	20	390	Nov 22 Friday
327	32	25	34	22	23	8	11	10	11	9	7	8	17	11	7	9	22	16	21	15	25	23	21	26	413	Nov 23 Saturday
328	5	14	16	30	21	19	19	22	6	30	6	14	23	34	22	24	12	26	13	12	23	15	16	19	441	Nov 24 Sunday
329	18	21	21	17	42	9	4	5	6	9	7	12	15	17	12	10	17	8	13	7	11	23	35	35	374	Nov 25 Monday

Table 3.4.5 (Page 1 of 2)

KSP .FKX Hourly distribution of detections

Day	00	01	02	03	04	05	06	07	08	09	10	11	12	13	14	15	16	17	18	19	20	21	22	23	Sum	Date
330	35	5	16	14	25	8	6	1	3	8	9	9	23	17	10	6	8	4	7	6	14	17	16	8	275	Nov 26 Tuesday
331	17	10	16	12	14	7	7	16	4	3	14	11	9	18	11	11	10	5	8	7	19	19	13	16	277	Nov 27 Wednesday
332	8	21	22	17	18	11	4	6	8	4	22	16	29	8	6	6	7	9	14	7	15	28	9	19	314	Nov 28 Thursday
333	17	21	23	16	24	9	2	16	0	0	0	20	14	5	4	7	9	13	11	8	19	24	16	17	295	Nov 29 Friday
334	3	6	11	23	23	9	13	4	17	17	16	11	25	12	12	23	32	28	10	27	32	29	29	17	429	Nov 30 Saturday
335	11	15	18	33	37	13	22	18	30	30	18	17	24	19	20	20	24	25	25	21	26	25	15	23	529	Dec 01 Sunday
336	19	33	28	8	19	10	16	9	9	14	21	14	35	7	7	10	6	8	7	5	10	31	12	8	346	Dec 02 Monday
337	3	9	11	12	21	4	3	6	5	3	10	24	14	10	4	4	10	1	2	10	16	17	10	29	238	Dec 03 Tuesday
338	29	7	16	30	19	3	5	0	4	7	5	5	13	3	3	7	5	8	9	18	15	32	12	12	267	Dec 04 Wednesday
339	41	17	19	15	11	8	4	3	0	10	13	19	16	6	10	8	5	27	5	7	35	15	19	5	318	Dec 05 Thursday
340	12	12	11	35	26	4	6	9	2	11	5	9	14	8	8	2	8	6	11	17	15	15	17	15	278	Dec 06 Friday
341	14	28	20	13	18	2	18	10	11	12	5	11	19	17	20	12	42	33	22	27	24	10	16	11	415	Dec 07 Saturday
342	13	1	22	13	12	27	23	37	35	44	24	17	34	12	19	14	15	37	24	16	20	31	31	17	538	Dec 08 Sunday
343	21	15	18	14	23	10	3	6	10	7	10	9	20	19	5	10	5	6	4	8	8	19	8	9	267	Dec 09 Monday
344	5	14	7	11	15	7	5	6	11	10	6	9	13	8	13	9	9	3	8	4	17	24	40	57	311	Dec 10 Tuesday
345	51	61	78	5	18	6	10	7	8	10	17	13	19	5	6	9	4	12	13	8	18	22	20	13	433	Dec 11 Wednesday
346	15	30	30	19	25	7	3	9	6	9	7	16	23	18	11	11	17	8	8	11	16	39	16	13	367	Dec 12 Thursday
347	18	12	25	26	20	17	9	12	8	12	15	15	21	8	5	14	7	10	13	8	27	24	20	11	357	Dec 13 Friday
348	10	9	14	10	12	14	7	11	25	18	30	39	86	35	33	11	0	0	0	0	6	14	15	25	424	Dec 14 Saturday
349	10	83	33	18	27	14	39	16	34	24	20	31	25	9	19	10	19	31	13	37	31	22	23	20	608	Dec 15 Sunday
350	17	46	16	8	16	7	8	6	5	11	8	6	21	8	11	11	6	9	13	12	17	13	14	13	302	Dec 16 Monday
351	7	15	16	9	18	10	5	7	9	9	4	14	16	7	11	12	6	18	0	0	0	0	0	0	193	Dec 17 Tuesday

KSP	00	01	02	03	04	05	06	07	08	09	10	11	12	13	14	15	16	17	18	19	20	21	22	23		
Sum	1247	1448	1546	1340	1685	760	748	762	751	915	830	1060	1483	965	951	864	927	1092	874	857	1378	1744	1601	1620	27448	Total sum
78	16	19	20	17	22	10	10	10	10	12	11	14	19	12	12	11	12	14	11	11	18	22	21	21	352	Total average
56	17	18	20	17	22	8	7	8	7	9	10	12	18	11	10	10	9	10	9	9	16	23	21	21	320	Average workdays
22	13	19	20	18	22	14	16	15	17	18	13	18	22	15	19	15	19	24	18	15	21	22	21	21	433	Average weekends

Table 3.4.5. Daily and hourly distribution of KSP detections. For each day is shown number of detections within each hour of the day and number of detections for that day. The end statistics give total number of detections distributed for each hour and the total sum of detections during the period. The averages show number of processed days, hourly distribution and average per processed day.

3.5 IMS operation

The Intelligent Monitoring System (IMS) was installed at NORSAR in December 1989 and was operated at NORSAR from 1 January 1990 for automatic processing of data from ARCESS and NORESS. A new version of IMS that accepts data from an arbitrary number of arrays and single 3-component stations was installed at NORSAR in October 1991, and regular operation of the system comprising analysis of data from the 4 arrays ARCESS, NORESS, FINESA and GERESS started on 15 October 1991. As opposed to the first version of IMS, the one in current operation also locates events at teleseismic distance.

The operational stability of IMS has been very good during the reporting period. In fact the IMS event processor (pipeline) has had no downtime of its own; i.e., all data available to IMS have been processed by IMS.

Events automatically located by IMS

During days 288 1991, through 091 1992, 14,817 events (local, regional, teleseismic) were automatically located by IMS. This gives an average of 88.7 events per processed day (167 days processed). 40% of these events are within 300 km of nearest station, and 65% of these events are within 1000 km of nearest station.

46.3% of these events were defined by 2 regional phases and 13.8% were defined by 2 teleseismic phases. 87.4% of all events had 3 defining phases or less. 20.2% of the available detections (phases) were automatically associated to events.

Events located by analyst review of IMS results

During days 288, 1991, through 091, 1992, 8,087 events (local, regional and teleseismic) were defined following analyst review of IMS results. This gives an average of 51.8 events per processed day (167 days processed). 59% of these events are within 300 km of nearest station, and 73% of these events are within 1000 km of nearest station.

46.1% of these events were defined by 2 regional phases and 3.6% were defined by 2 teleseismic phases. 64.4% of all events had 3 defining phases or less. 11.3% of the available detections (phases) were associated to events. See section 7.6 for comments on the percentage of associated phases.

76.9% of the events had regional phases only. 21.4% of the events had teleseismic phases only.

Phase and event statistics

Table 3.5.1 gives a sumary of phase detections and events declared by IMS. From top to bottom the table gives the total number of detections by the IMS, the number of detections that are associated with events automatically declared by the IMS, the number of detections that are not associated with any events, the number of events automatically declared by the IMS, the total number of events defined by the analyst, and finally the number of events accepted by the analyst without any changes (i.e., from the set of events automatically declared by the IMS).

	Oct 91	**Nov 91**	**Dec 91**	**Jan 92**	**Feb 92**	**Mar 92**	**Total**
Phase detections	53275	45501	38258	35905	28252	30921	232112
-Associated phases	9778	8668	8496	5892	5626	8431	46891
-Unassociated phases	43497	36833	29762	30013	22626	22490	185221
Events automatically declared by IMS	3232	2772	2575	1846	1738	2654	14817
No. of events defined by the analyst	916	1350	1242	1025	1364	2190	8087
No. of events accepted without modifications	241	301	259	290	354	880	2325

Table 3.5.1. IMS phase detections and event summary.

U. Baadshaug
B. Ferstad
B. Paulsen Gammelby
B.Kr. Hokland
L.B. Loughran

3.6 GBF operation

Events automatically located by GBF

During days 274 1991, through 091 1992, 10,120 local and regional events were located by GBF. This gives an average of 55.3 events per processed day (183 days processed). 68% of these events are within 300 km of nearest station, and 89% of these events are within 1000 km of the nearest station.

76.9% of these events were defined by 2 regional phases. Teleseismic phases are currently not used by GBF. 86.7% of all events had 3 defining phases or less.

13.4% of the available detections (phases,including teleseismic) were associated to regional events.

T. Kværna

4 Improvements and Modifications

4.1 NORSAR

NORSAR data acquisition

No modification has been made to the NORSAR data acquisition system.

The data are recorded on a 30-hour circular disk buffer on the IBM system, and archived onto 1/2 inch magnetic tapes. In addition to this, the data are now regularly transmitted to a SUN system for recording on a 48-hour circular disk buffer.

NORSAR detection processing

The NORSAR detection processor has been running satisfactorily on the IBM 4381 computer during this reporting period.

Detection statistics are given in section 2. In addition to the detection processing done on IBM, the dp program is doing regular detection processing on a SUN system, using the unix-based circular disk buffer (see below). A detection SNR threshold of 20.0 triggers automatic saving of waveforms into CSS 3.0 data files.

NORSAR event processing

There have been no changes in the routine processing of NORSAR events, using the IBM system.

The new circular buffer on a SUN system will be used to convert old software and develop new event processor software for NORSAR data. The main difference between regional array processing as performed on the high-frequency arrays and NORSAR teleseismic array processing is that body waves do not have a plane wavefront across NORSAR. The consequence is that plane-wave fk-analysis does not work properly, and time delay corrections have to be used for beamforming. A new data base for time delay corrections needs to be built. With these new corrections and a higher sampling rate after the refurbishment, the large array will have excellent resolution in slowness space, and will provide very useful automatic locations for teleseismic signals. However, as an intermediate process, the old data files and programs for subarray time delay corrections have been converted for the SUN version of NORSAR event processing.

NORSAR refurbishment

Testing of new digitizers and data archiving systems have continued. The buried cables in the NORSAR array limit the amount of DC voltage that can be supplied at the remote sites. This necessitates testing at the actual remote sites, and we have been able to run the Nanometrics 16 bit gain-ranged converter (16 bit resolution, 24 bit dynamic range) with available DC power.

Another important issue is whether the 7 existing telephone lines to the subarray vaults may be upgraded from 2400 baud to 9600 baud. This has been discussed with the local telephone company, and some limited tests have been carried out. Within the subarrays there seems to be no problem in using existing cables for higher speed. An in-house project is underway to develop an acquisition system that meets the needs for both the NORSAR array and the other planned data acquisition projects (Apatity and Spitsbergen). The NORAC unit - NORSAR Array Controller - is described in section 7.7.

Using the NORAC, we have successfully collected synchronized data simultaneously from Nanometrics RD3 and Teledyne Geotech PDAS-100 (experimental version) digitizers.

At the NORSAR data center we are also evaluating the different acquisition systems at the NORESS/ARCESS, FINESA, NORSAR, and GERESS arrays, and the Poland and Apatity three-component stations. This experience allows us to concentrate our testing on how easily the digitizers may be synchronized and timed. For a detailed analysis of digitizer noise and resolution, we will also refer to manufacturers' specifications and experience at other installations. In our testing we will benefit from the simultaneous recording of NORESS and NORSAR data. It will be possible to arrange a setup with three independent recordings from the same instrument.

The problem with power at the remote sensors limits the number of systems that can be used in the refurbishment. The 24 bit resolution digitizers that are on the market have options for signal detection and data recording. This makes the systems needlessly sophisticated and expensive as compared to what is needed for the NORSAR refurbishment. These systems also generally comsume too much power for installation at the NORSAR seismometer vaults.

The plan for the NORSAR refurbishment is to test digitizers during the spring and summer of 1992, and depending on whether tecnical requirements are met, we may start refurbishing one subarray during this autumn. A parallel recording of data for a longer period needs to be performed to ensure that we can correctly convert back and forth to the NORSAR data recorded over the past 20 years, to ensure continuity in the NORSAR data archive.

4.2 NORESS/ARCESS/FINESA/GERESS/Poland

Detection processing

The routine detection processing of the arrays is running satisfactorily on each of the array's SUN-3/280 acquisition systems. The same program is used for NORSAR, NORESS, ARCESS, FINESA, GERESS, KSP, SFP, but with different "recipes". The beam table for NORESS and ARCESS is found in NORSAR Sci. Rep. No. 1-89/90. The beam table for FINESA and GERESS is found in NORSAR Sci. Rep. No. 1-90/91.

Detection statistics are given in section 3.

Event processing. Phase estimation.

This process performs f-k and polarization analysis for each detection to determine phase velocity, azimuth and type of phase, and the results are put into the ORACLE detection data base for use by the IMS. Detection data for the three-component Polish stations were made available for IMS for a period, but created too many false events. These data are therefore currently not used in IMS processing.

Plot and epicenter determination

A description of single-array event processing is found in NORSAR Sci. Rep. No. 2-88/89, and NORSAR Sci. Rep. No. 2-89/90.

J. Fyen

5 Maintenance Activities

5.1 Activities in the field and at the Maintenance Center

This section summarizes the activities at the Maintenance Center (NMC) Hamar, and NDPC activities related to monitoring and control of NORSAR, including monitoring of NORESS and ARCESS. Activities at other field installations are also listed.

Activities involve preventive and corrective maintenance, modification of equipment, etc.

NORSAR

NORSAR subarrays were visited in October, November and December 1991 and January and February 1992. The different jobs involved adjustment of gain SP/LP channels and Mass Position (MP) and Free Period (FP) LP seismometers. Other activities have been replacement of relay card LP equipment, replacement of MP/FP motor EW seismometer LP, and RA-5 amplifiers SP channels. Cable splicing and location of cables have also been done. Activities related to NORSAR upgrading have continued throughout the period.

NORESS

This array was visited in October 1991 and January 1992. The Comsat satellite earth station was demounted including the 5 m antenna. Sites A1, C7 and D6 were repaired. The GPS clock was replaced with an LF-DC clock. Hub 13 interface card was replaced and Hub transmission speed changed from 32 to the original 64 Kbits.

ARCESS

In January the array was visited by NTA representatives. After a power failure they restarted the UPS (Uninterruptable Power Supply). Also the air-conditioner failed, but the local NORSAR representative started a ventilator fan.

Subarray/ Area	Task	Date
NORSAR		
01A	Adjusted channel gain all SP/LP instruments	4 Oct 91
	Also adjusted FP/MP LP instruments	
	Replaced 4y relay card	
01A	Cable splicing SP04	25,28,29 30 Oct
01B	Cable splicing SP05	16,22 Oct
	Replaced RA-5 SP04	22 Oct
02B	Adjusted channel gain all SP/LP instruments	1 Oct
	Adjusted FP/MP LP seismometers	
02B	Adjusted FP/MP. LP instruments which afterwards could be adjusted from NORSAR, Kjeller	31 Oct
06C	Replaced RA-5 SP02	2 Oct
02B (tel)	Power unit receiver station replaced	31 Oct
NORESS	Demounted Comsat satellite earth station, incl. 5 m antenna	14,17 Oct
	Repaired A1, C7 and D6	18 Oct
NDPC	Daily check of all arrays, i.e., NORSAR, NORESS, ARCESS, FINESA, GERESS and Poland (KSP,SFP). NORSAR SP/LP instruments calibrated every week. Free Period (FP) and Mass Position (MP) have been measured and adjusted when outside tolerances, when feasible from NORSAR, Kjeller.	Oct
NORSAR		
01B	Replaced RA-5 amplifier SP04. Also cable was spliced	6,7,8 Nov
04C	Adjusted channel gain SP01,06	
	Adjusted channel gain all LP instruments	4 Nov
	Adjusted FP/MP	
06C	Replaced RA-5 amplifier SP00	4 Nov
NDPC	Daily check of all arrays, i.e., NORSAR, NORESS, ARCESS, FINESA, GERESS and Poland (KSP,SFP). NORSAR SP/LP instruments calibrated every week (- week 48). Free Period (FP) and Mass Position (MP) have been measured and adjusted when outside tolerances.	Nov

Table 5.1. Activities in the field and the NORSAR Maintenance Center, including NDPC activities related to the NORSAR, NORESS, ARCESS, FINESA and GERESS arrays and the two 3-component stations in Poland (KSP, SFP), 1 October 1991 - 31 March 1992.

Subarray/ Area	Task	Date
NORSAR		
01B (area)	Visited in connection with location of cables (in trenches) for Ringsaker Power Company	2 Dec
NMC	NORSAR upgrading tasks	Dec
NDPC	Daily check of all arrays, i.e., NORSAR, NORESS, ARCESS, FINESA, GERESS and Poland (KSP, partly SFP). NORSAR SP/LP instruments calibrated every week. Free Period (FP) and Mass Position (MP) have been measured and adjusted when outside tolerances, when possible from NORSAR, Kjeller.	Dec
		1992
NORSAR		
01A	Adjusted gain all SP/LP channels	29 Jan
01B	Adjusted MP/FP all LP instruments	23 Jan
02B	Adjusted gain all SP/LP channels	21 Jan
03C	Adjusted gain all SL/LP channels	27 Jan
	Adjusted MP/FP all LP insruments	
04C	Adjusted gain all SP/LP channels	28 Jan
	Adjusted MP/FP all LP insruments	
06C	Adjusted gain all SP/LP channels	15 Jan
	Adjusted MP/FP all LP insruments	
	Replaced MP/FP motor EW seismometer	
06C	Adjusted gain channel 06	24 Jan
NORESS	GPS clock was replaced with an LF-DC clock	15 Jan
	Replaced Hub 13 interface card	16 Jan
	Hub transmission speed changed from 32 to 64 Kbits	23 Jan
ARCESS	Power failure	21 Jan
	NTA representative started the UPS	21 Jan
	Air-conditioner failed. Temperature rose to 40°C. NORSAR local representative started a ventilator fan	23 Jan

Table 5.1 (cont.)

Subarray/ Area	Task	Date
NDPC	Daily check of all arrays, i.e., NORSAR, NORESS, ARCESS, FINESA, GERESS and Poland (KSP). NORSAR SP/LP instruments calibrated every week. Free Period (FP) and Mass Position (MP) have been measured and adjusted when outside tolerances, when possible from NORSAR, Kjeller.	Jan
NORSAR		
02B	Adjusted MP/FP all LP instruments	19 Feb
	Adjusted channel gain all LP channels	
	Adjusted channel gain SP01, 04 and 05	
06C	Adjusted MP/FP all LP instruments	18 Feb
	Adjusted channel gain all LP instruments	
	SLEM reset	26 Feb
NDPC	Daily check of all arrays, i.e., NORSAR, NORESS, ARCESS, FINESA, GERESS and Poland (KSP). NORSAR SP/LP instruments calibrated every week. Free Period (FP) and Mass Position (MP) have been measured and adjusted when outside tolerances, when possible from NORSAR, Kjeller.	Feb
NMC	NORSAR upgrading continued	Mar
NDPC	Daily check of all arrays, i.e., NORSAR, NORESS, ARCESS, FINESA, GERESS and Poland (KSP, SFP since 18.3.92). NORSAR SP/LP instruments calibrated every week. Free Period (FP) and Mass Position (MP) have been measured and adjusted when outside tolerances, when possible from NORSAR, Kjeller.	Mar

Table 5.1 (cont.)

5.2 Array status

As of 31 March 1992 the following NORSAR channels deviated from tolerances:

01A 01	8 Hz filter
02	8 Hz filter
04	30 dB attenuation

O.A. Hansen

6 Documentation Developed

Bungum, H., A. Dahle, G. Toro, R. McGuire and O.T. Gudmestad (1992): Ground motions from intraplate earthquakes, Proc. 10th World Conf. on Earthq. Eng., Madrid, August 92.

Dahle, A., H. Bungum, J. Havskov and B. Aspen (1992): Seismic surveillance of the Blåsjø Reservoir, Proc. 10th World Conf. on Earthq. Eng., Madrid, August 92.

Hestholm, S.R, B.O. Ruud and E.S. Husebye (1992): Synthesizing 2D wave propagation in a heterogeneous lithosphere using finite difference techniques, manuscript submitted for publication.

Kværna, T. (1992): Continuous seismic threshold monitoring of the northern Novaya Zemlya test site; long-term operational characteristics, AFGL Scientific Rep. No. 12, 28 February 1992.

Mykkeltveit, S. (ed.) (1991): NORSAR Basic Seismological Research, Annual Technical Report, AFGL Scientific Rep. No. 11, 29 November 1991.

Ringdal, F. and T. Kværna (1992): Continuous seismic Threshold Monitoring, submitted to Geophy. J. Int.

Ruud, B.O., E.S. Husebye and .S.R. Hestholm (1992): On crustal, short-period Rg propagation using array records from 4 continents, manuscript submitted for publication.

Ruud, B.O., E.S. Husebye and C.D. Lindholm (1992): An exercise in automating seismic record analysis and network bulletin production, manuscript submitted for publication.

Semiannual Tech. Summary, 1 Apr - 30 Sep 91, NORSAR Sci. Rep. 1-91/92, Kjeller, Norway.

7 Summary of Technical Reports/Papers Published

7.1 Global event detection performance during GSETT-2

Introduction

During the period 22 April to 9 June 1991, the Conference on Disarmament's Group of Scientific Experts carried out the main phase of its Second Technical Test (GSETT-2) (Reference: CD/1144). A total of 34 countries participated in this test, providing seismic data for 42 consecutive data days from 60 stations distributed around the globe (Fig. 7.1.1). Data were recorded and processed at National Data Centers, and parameters as well as waveform segments were transmitted to four experimental International Data Centers (EIDCs) for further analysis. Results of these analyses were summarized in event bulletins, which were transmitted back to participants from the EIDCs.

An important aspect of the performance evaluation of GSETT-2 is the completeness and quality of the final event bulletin (FEB). This seismological output is closely linked to the actual spatial distribution of seismic stations. For GSETT-2, a very heterogeneous global coverage yielded large regional variations in detection threshold. About one half of the participating stations were situated in and around Europe, consequently a large number of small events were detected, mainly quarry blasts and rock bursts of magnitude 1 to 4. On the other hand, in many areas of the globe where the station distribution was very sparse, only larger earthquakes were detected.

In this paper a preliminary assessment is made of the global event detection capability during GSETT-2. By comparing the FEBs to the bulletins of the National Earthquake Information Center (NEIC), we obtain detection statistics separately for the northern and southern hemisphere. We make no assessment in this paper of the location precision of the GSETT-2 network solutions. In sections 7.2 and 7.3, a more detailed discussion of the GSETT-2 performance in some selected regions is presented.

Method

The method used for detectability estimation has been described by Ringdal (1975), and is briefly summarized as follows:

1. A reference system, independent of the system to be evaluated, is used. Event lists and magnitudes from this reference system are compiled.
2. For each reference event, a comparison is made to see if the system to be evaluated has detected the event.
3. Based on the number of detections/no detections at each magnitude, a maximum likelihood approach is made to estimate a "detection curve" of the form

$$G(m;\mu,\sigma) = \int_{-\infty}^{m} \frac{1}{\sqrt{2\pi}\sigma} e^{\frac{(x-\mu)^2}{2\sigma^2}} dx \quad (1)$$

Here $G(m;\mu,\sigma)$ denotes the incremental probability of detection, given event magnitude m. The detection curve is completely characterized by the parameters μ and σ. The 50 and 90 per cent incremental detection thresholds (μ_{50} and μ_{90}) become:

$$\mu_{50} = \mu \quad (2)$$

$$\mu_{90} = \mu + 1.29 \cdot \sigma \quad (3)$$

It should be noted that while the method assumes that the reference network provides independent event estimates, it is not necessary to have a complete event catalogue in any given magnitude range. Thus the reference events actually selected are assumed to be randomly sampled from the total number of events available, much in the same way as opinion survey polls attempt to address randomly selected subsets of the population. The resulting detectability estimates will be representative for the region considered only to the extent that the reference event set is representative.

When applying the method in practice, it is often desirable to restrict the range of values of σ when maximizing the likelihood function. This is done to reduce the influence of outliers in the data set. In this paper we have restricted σ to the interval 0.10-0.80 m_b units.

Reference network

The reference data base for this study has been the monthly bulletin from the U.S. National Earthquake Information Center (NEIC).

For the main phase of GSETT-2, upon which this analysis is based, the reference NEIC catalogue contained 829 seismic events with an assigned m_b value. The magnitude range was 2.6-6.4.

The criteria used to determine if a given reference event had been detected by the GSETT-2 network was as follows:

- Epicenter difference at most 3.0 degrees
- Origin time difference at most 60 seconds.

These criteria are the same as those used when merging FEB bulletins.

Results

The initial results from the detectability study are presented in Figs. 7.1.2-7.1.4. Each figure is based upon analyst comparison of the reference events with bulletin reports according to the criteria defined above.

Fig. 7.1.2 shows detectability statistics for the entire globe taken together. The 50% and 90% thresholds are estimated at m_b 3.7 and 4.7, respectively. In view of expected regional differences, we will look at the northern and southern hemisphere separately.

Fig. 7.1.3 shows results for the northern hemisphere. The estimated 50% and 90% thresholds are m_b 3.4 and 4.4, respectively. We observe that there is a relatively large range in detectability; thus there are detected events below $m_b = 3.0$, and non-detections as high as $m_b = 5.0$. This is of course due to the large regional variations in GSETT-2 network capability.

It is of interest to discuss in some details a few of the *non-detected* events of relatively large magnitude: Table 7.1.1 lists all NEIC-reported events of $m_b \geq 4.5$ in the northern hemisphere that were not detected according to the criterion given above. The following comments apply:

- Events 2, 4, 8, 9, 14 and 15 were not reported by any EIDC during GSETT-2.
- Events 5, 6, 7 occurred during the W. Caucasus aftershock sequence, and were not reported originally during GSETT-2 due to heavy workload. They were properly reported after reprocessing.
- Events 1, 3, 10, 11, 12, 13 and 16 were reported during GSETT-2, but the FEB location differed too much from the NEIC location to satisfy the "event matching" criterion.

Note that in some cases (1, 3, 13) one EIDC had a solution that was significantly closer to the NEIC solution than the one selected for the FEB.

In at least one case (event 12) it appears that the FEB solution was significantly better than the NEIC solution.

Fig. 7.1.4 shows results for the southern hemisphere. The estimated capabilities are considerably less than for the northern hemisphere, with 50% and 90% thresholds of $m_b = 4.1$ and 5.1, respectively.

Again, it is of interest to discuss some of the largest non-detected events: Table 7.1.2 lists the NEIC-reported events of $m_b \geq 5.0$ in the southern hemisphere that were not detected. The following comments apply:

- Events 1 and 2 were not reported by any EIDC during GSETT-2.
- Events 3, 4, 5, 6, and 7 were reported during GSETT-2, but the FEB location differed too much from the NEIC location to satisfy the "event matching" criterion.

Note that for events 3 and 5, there were EIDCs that had solutions very close to the NEIC solution, but they were not selected for the FEB.

In assessing these results, it must be remembered that "detection threshold" is closely tied to "location accuracy". The more relaxed our location requirements are, the "better" the detection capability will appear to be. Our results here represent what we think is a reasonable compromise for a global network of the type employed in GSETT-2. It would be of great interest to compare these results to theoretical network capability studies under the different assumptions and conditions in the models.

In this study, all magnitudes refer to reported NEIC network m_b values. The question of a possible bias in network m_b estimates has not been addressed here, but would need to be taken into account when comparing the results to theoretical capability studies.

F. Ringdal
S. Mykkeltveit
U. Baadshaug

References

CD/1144 (1992): Report on the Group of Scientific Experts' second technical test (GSETT-2), Conference on Disarmament, Geneva.

Ringdal, F. (1975): On the estimation of seismic detection thresholds, Bull. Seism. Soc. Am., 65, 1631-1642.

No.	FEB	IDC	ORIGIN TIME	LAT	LON	DPT	NOB	MB
1	CSS	USGS	1991-113:08.58.47.700	9.97	-83.26	10	9	4.6
1	STO	STO	1991-113:08.58.48.100	13.14	-86.81	2	9	3.4
2	CSS	USGS	1991-114:19.11.45.700	31.81	104.54	33	10	4.7
3	CSS	USGS	1991-117:14.48.42.400	17.18	-100.30	53	38	4.6
3	STO	STO	1991-117:14.48.41.500	16.76	-103.80	1	11	4.0
4	CSS	USGS	1991-119:00.51.44.800	13.88	-92.59	62	7	4.6
5	CSS	USGS	1991-119:09.59.24.000	42.62	43.40	10	64	4.6
6	CSS	USGS	1991-119:10.19.41.300	42.22	43.59	10	24	4.5
7	CSS	USGS	1991-119:11.10.11.900	42.58	43.90	10	67	4.7
8	CSS	USGS	1991-119:18.28.17.500	51.00	-178.38	33	12	4.7
9	CSS	USGS	1991-122:06.54.14.300	34.80	26.48	20	32	4.6
10	CSS	USGS	1991-130:05.31.04.400	10.04	124.16	84	5	4.6
10	MOS	STO	1991-130:05.31.08.100	10.48	128.52	88	6	3.4
11	CSS	USGS	1991-136:20.31.05.200	17.04	-102.31	33	35	4.6
11	CNB	WAS	1991-136:20.32.10.400	21.23	-102.99	367	13	3.4
12	CSS	USGS	1991-145:18.59.23.200	42.96	147.59	33	6	4.8
12	STO	CNB	1991-145:18.59.47.700	44.33	137.97	11	18	4.1
13	CSS	USGS	1991-146:17.28.01.300	27.05	99.75	33	9	5.0
13	MOS	MOS	1991-146:17.29.22.600	15.91	103.93	16	8	3.7
14	CSS	USGS	1991-147:12.02.25.700	32.92	56.33	33	5	4.6
15	CSS	USGS	1991-148:20.04.50.000	24.65	94.36	142	9	4.7
16	CSS	USGS	1991-152:06.01.48.700	1.65	123.25	10	7	4.7
16	CNB	WAS	1991-152:06.00.21.700	10.58	119.27	0	8	4.1

Table 7.1.1. NEIC-reported events of $m_b \geq 4.5$ in the northern hemisphere not reported in the FEB (using the event matching criteria given in the text). Whenever an FEB event is close to matching one of the NEIC events, it is listed below it.

o.	FEB	IDC	ORIGIN TIME	LAT	LON	DPT	NOB	MB
1	CSS	USGS	1991-112:19.18.43.500	-11.48	166.19	63	13	5.1
2	CSS	USGS	1991-116:05.25.24.800	-5.43	129.73	227	11	5.0
3	CSS	USGS	1991-128:08.51.40.300	-22.04	68.32	10	37	5.1
3	CNB	WAS	1991-128:08.52.43.900	-20.42	69.73	582	16	3.7
4	CSS	USGS	1991-130:23.30.44.500	-37.00	-98.93	10	10	5.1
4	MOS	STO	1991-130:23.31.03.000	-34.47	-96.46	1	6	4.1
5	CSS	SGS	1991-134:19.17.53.800	-57.72	-25.37	52	16	5.1
5	MOS	CNB	1991-134:19.18.26.800	-34.13	-28.39	1	11	4.3
6	CSS	USGS	1991-141:12.43.35.800	-7.25	129.43	58	14	5.0
6	STO	WAS	1991-141:12.43.02.100	-6.52	126.14	0	8	4.2
7	CSS	USGS	1991-153:11.08.11.200	-18.81	-173.17	33	22	5.2
7	STO	STO	1991-153:11.09.17.800	-19.97	-178.43	285	27	4.7

Table 7.1.2. NEIC-reported events of $m_b \geq 5.0$ in the southern hemisphere not reported in the FEB (using the event matching criteria given in the text). Whenever an FEB event is close to matching one of the NEIC events, it is listed below it.

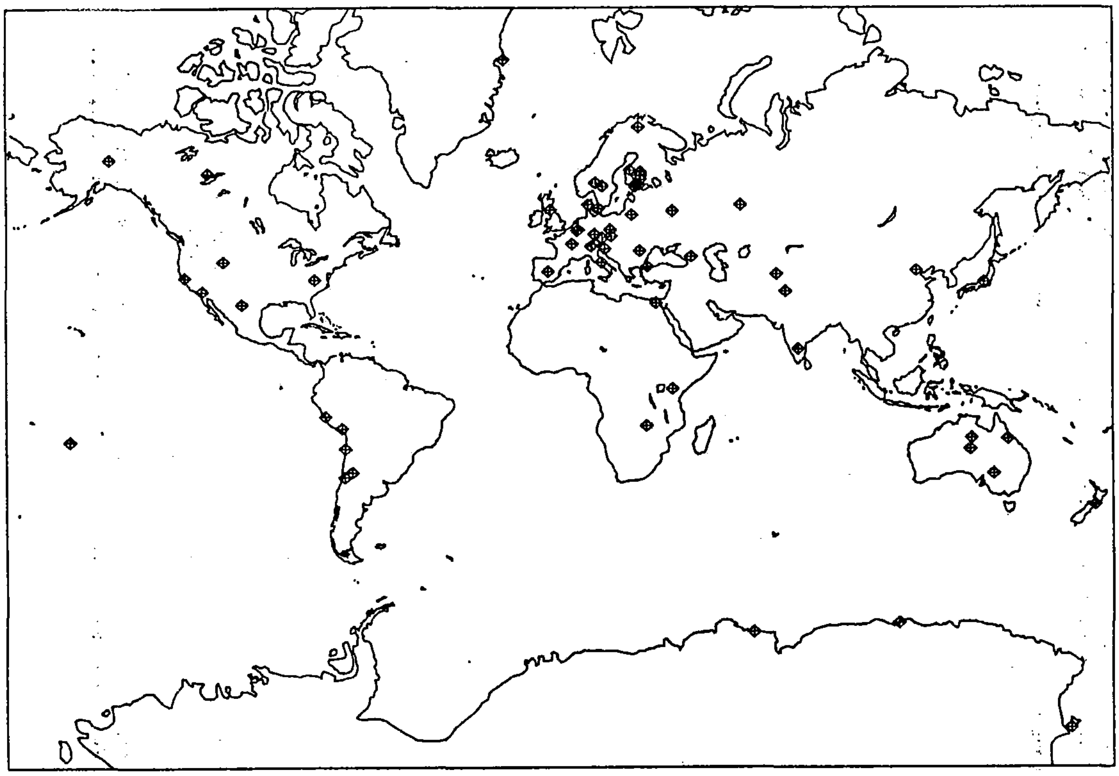

Fig. 7.1.1. Stations participating in the main phase of GSETT-2, April-June 1991 (after CD/1144). Detailed descriptions of station characteristics can be found in Group of Scientific Experts' Sourcebook for International Seismic Data Exchange, CRP/167.

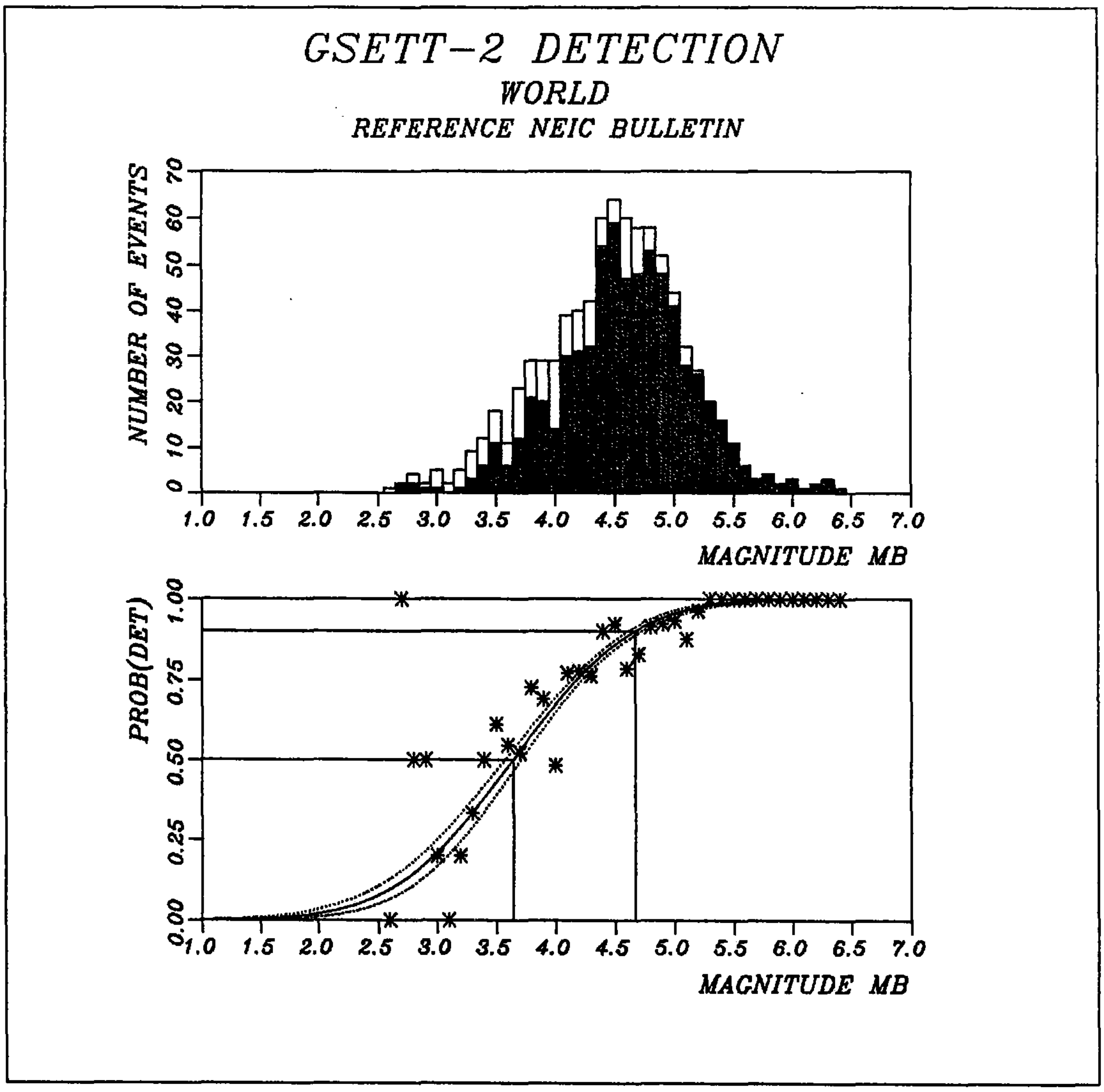

Fig. 7.1.2. Maximum likelihood detectability estimation for the GSETT-2 network, using the NEIC monthly bulletin as a reference. This figure shows statistics for the **entire world.** The upper half shows the reference event set and the number of events actually detected for each magnitude. The lower half shows the maximum likelihood detectability curve and its confidence limits. The actual percentage of detected events at each magnitude is also shown. The criteria for associating FEB events to NEIC events are given in the text.

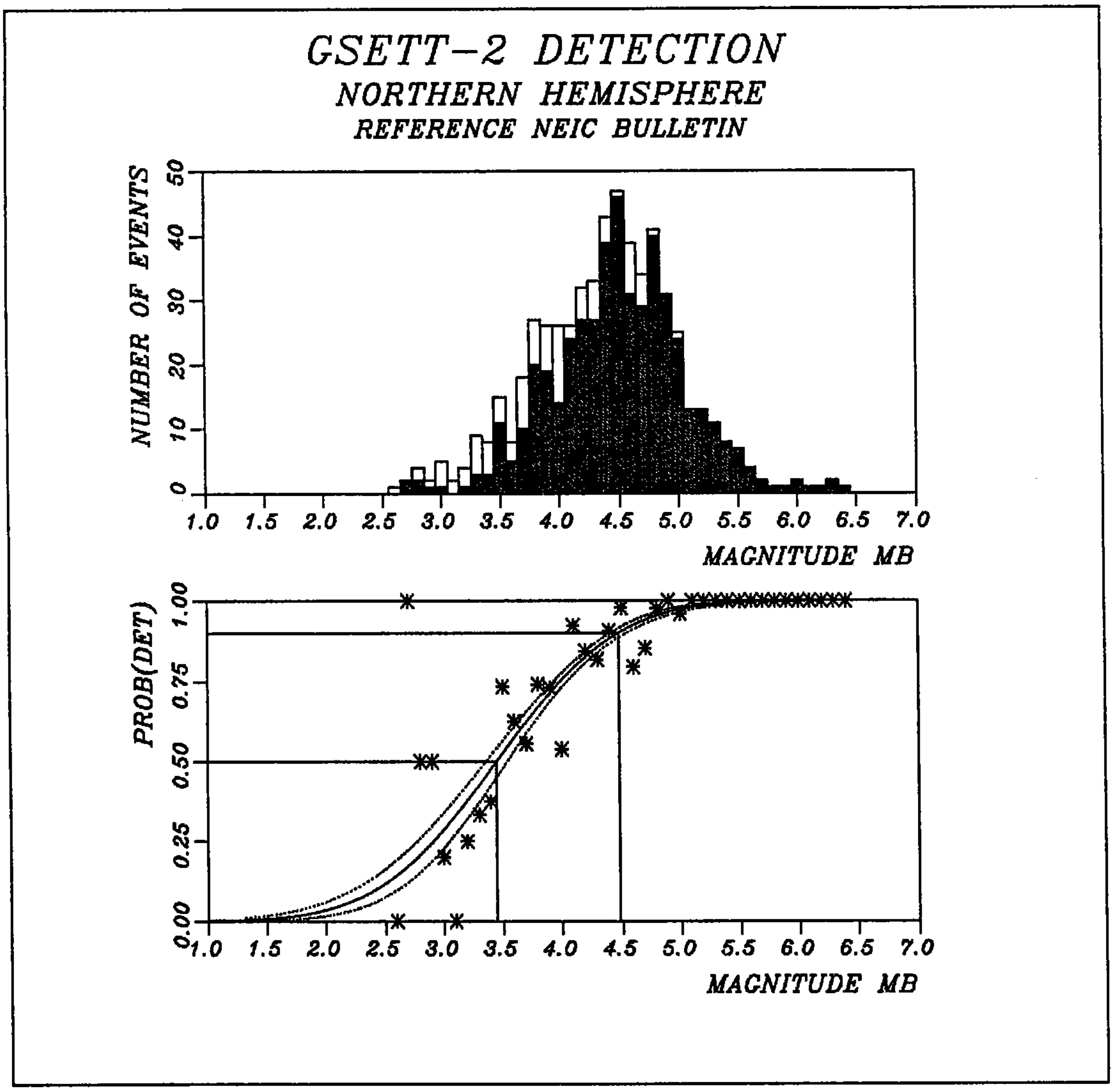

Fig. 7.1.3. Maximum likelihood detectability estimation for the GSETT-2 network, using the NEIC monthly bulletin as a reference. This figure shows statistics for the **northern hemisphere**. The upper half shows the reference event set and the number of events actually detected for each magnitude. The lower half shows the maximum likelihood detectability curve and its confidence limits. The actual percentage of detected events at each magnitude is also shown. The criteria for associating FEB events to NEIC events are given in the text.

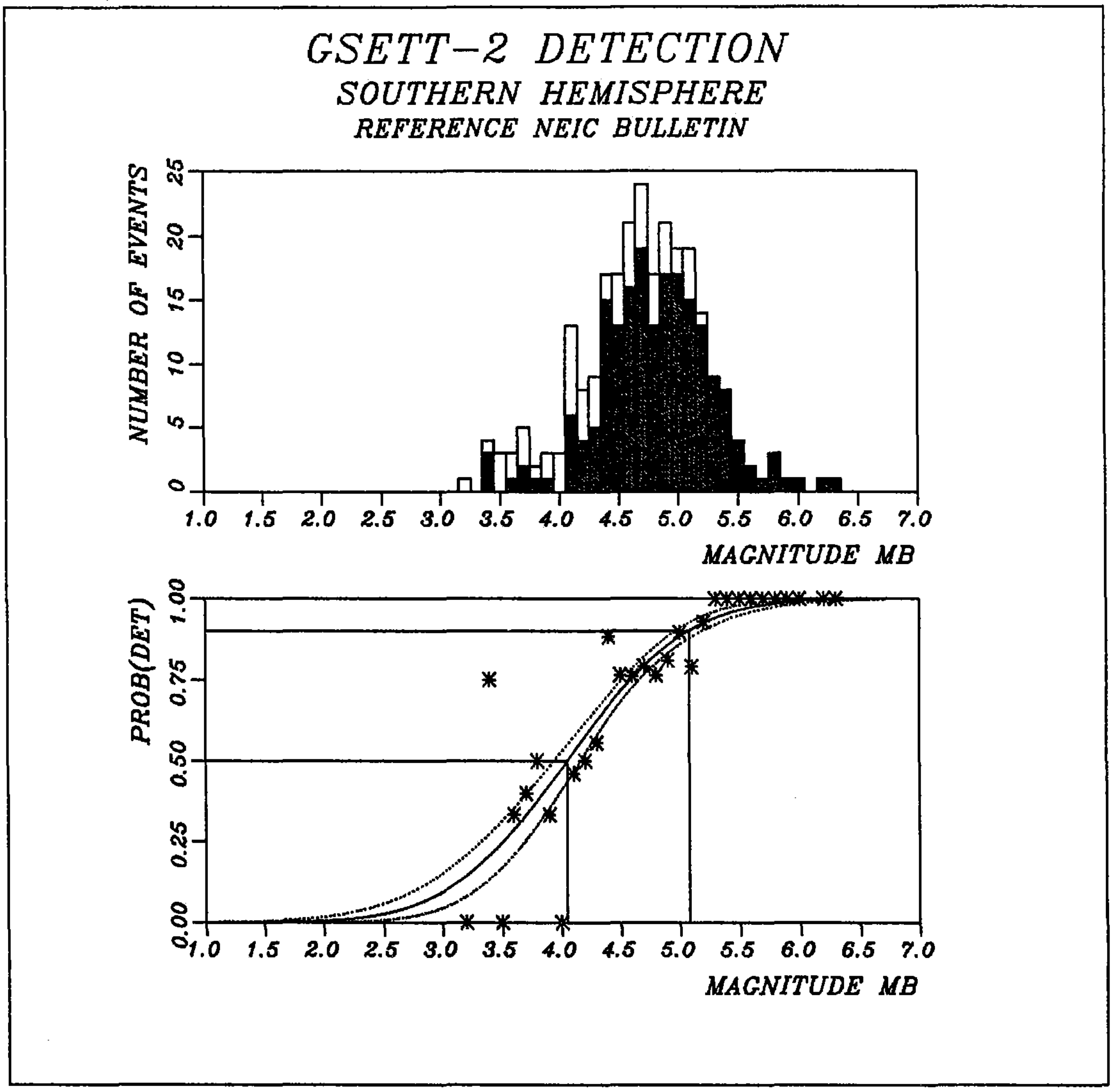

Fig. 7.1.4. Maximum likelihood detectability estimation for the GSETT-2 network, using the NEIC monthly bulletin as a reference. This figure shows statistics for the **southern hemisphere.** The upper half shows the reference event set and the number of events actually detected for each magnitude. The lower half shows the maximum likelihood detectability curve and its confidence limits. The actual percentage of detected events at each magnitude is also shown. The criteria for associating FEB events to NEIC events are given in the text.

7.2 Regional detection and location performance during GSETT-2: Initial results for the Fennoscandian array network

Introduction

In this paper a preliminary assessment is made of the event detection and location capability during GSETT-2 for Fennoscandia and NW Russia. This is the region that had maybe the best instrumental coverage during the experiment. In particular the regional arrays deployed in this area made significant contributions.

Our results for this region represent in a sense the "best" regional performance during GSETT-2. It is in no way representative for the performance on a global or more extended regional scale. However, it does serve to illustrate the potential capabilities of a monitoring network, assuming that an adequate density and number of high quality, sensitive array stations are deployed.

This investigation is composed of three separate studies. Firstly, we describe the results of a detectability study, where the reference data base is the seismic bulletin published by the University of Helsinki, Finland. The second study is also on detectability, and here the reference data base is the bulletin published by the University of Bergen, Norway. The third part of the investigation is a study on event location performance, where event locations in the FEBs are compared with locations published in the Helsinki bulletin.

Detectability study: Comparisons with the bulletin of the University of Helsinki

Method

The method used for detectability estimation has been described by Ringdal (1975):

- A reference system, independent of the system to be evaluated, is used. Event lists and magnitudes from this reference system are compiled.
- For each reference event, a comparison is made to see if the system to be evaluated has detected the event.
- Based on the number of detections/no detections at each magnitude, a maximum likelihood "detection curve" is estimated.

Reference network

The reference data base for this study has been the catalogue of seismic events in northern Europe regularly compiled by the Seismological Institute, University of Helsinki.

The stations used in compiling this catalogue are in almost all cases comprised on the Finnish seismic network single stations. For all practical purposes, the compilation is independent of the regional arrays in Fennoscandia (NORESS, ARCESS, FINESA). The magnitudes quoted in the bulletin are likewise derived independently of the regional arrays, and comprise either duration magnitudes (in most cases) or local magnitudes.

These magnitudes are fairly consistent with magnitudes calculated by the Intelligent Monitoring System, while their relationship to teleseismic m_b estimates is at present not well established.

For the month of May 1991, upon which this analysis is based, the reference catalogue contained 321 seismic events in the region bounded by 58°-70°N, 20°-40°E, of which 108 had an assigned magnitude in the range 1.7-2.9.

Results

The initial results from the detectability study are summarized in Figs. 7.2.1-7.2.2 (see also Ringdal, 1991). The figures are based upon analyst comparison of the reference events with bulletin reports according to the criteria:

a) **NDC-reported event:**

In Fig. 7.2.1, an event is considered detected if it was reported with 2 phases (P and S; or P and Lg) by at least one of the three regional arrays (NORESS, ARCESS, FINESA). In terms of GSETT-2 final event bulletins, this means that the event was either located as a multi-station event, or listed as an NDC-reported event. We note that the 50% threshold is close to 1.7, and the 90% threshold is 2.3 in this case.

b) **FEB-reported events**:

In Fig. 7.2.2, the FEB-reported events, located by at least one IDC, are shown. (We have not counted as detected events those events whose definition depended upon reportings from the Finnish network stations KAF and VAF, since these two stations were part of the reference network.) This added requirement has the effect of increasing the 50% threshold to 2.1, and the 90% threshold to 2.4.

Detectability study: Comparisons with the bulletin of the University of Bergen

Reference network

The seismic bulletin published by the Institute of Solid Earth Physics of the University of Bergen, Norway, has been the reference data base for this study.

The stations used by the University of Bergen in compiling their bulletin are shown in Fig. 7.2.3. The events reported in this bulletin are basically confined to southwestern and northern Norway, the North Sea and the continental margin to the west of Norway. This bulletin thus very suitably supplements the Helsinki bulletin with respect to coverage of Fennoscandian seismic events.

Detections from NORESS and ARCESS are to a certain extent used in compilation of the University of Bergen bulletin. However, only events that were reported without use of NORESS/ARCESS readings, or that would have been reported even if NORESS/ARCESS data were not used (i.e., events for which the University of Bergen network alone had a sufficient number of phases), were used as reference events. The magnitudes given in the University of Bergen bulletin are duration magnitudes. These magnitude values are generally higher than those calculated by the Intelligent Monitoring System (typically by 0.5 magnitude units).

For the GSETT-2 period, 22 April - 2 June 1991, the University of Bergen bulletin contains 83 events satisfying the criteria mentioned above (a couple of small events very close to the JMI network are excluded from consideration). The coda magnitudes are in the range 0.3-4.0.

Results

For each of the 83 events in the reference data base, we checked whether or not the event was reported during GSETT-2 by the Norwegian NDC. Such reports of local/regional events always included a FOCUS line, and the event origin time and geographical coordinates were based on at least one P- and one S-phase from either NORESS or ARCESS. The results from this study are presented in Fig. 7.2.4, where the detectability curve has been computed in accordance with the method outlined above.

We can see from Fig. 7.2.4 that the 50% threshold is close to 1.5, and that the 90% threshold is a little less than 2.5. These results should be compared to those in Fig. 7.2.1, which were obtained for the same reporting criterion (two phases on at least one array). Taking into account that the University of Bergen magnitudes are slightly higher than those reported by IMS and the University of Helsinki, it appears that 90% event detection probability of the Fennoscandian regional array network is at magnitude 2.5 or lower across the entire Fennoscandia from the Norwegian continental shelf to northwestern Russia.

It should be noted that for three events counted as detected events in Fig. 7.2.4, only a single P phase was reported by the Norwegian NDC during GSETT-2. For one of these events, an Sn phase was also automatically detected, but by mistake not reported during GSETT-2. For the other two events, there were no automatic S-phase detections, but inspection of the associated waveforms reveals the presence of a regional event that could and would have been reported as such given more time and resources during the NDC analysis stage.

Event location performance: Comparison between the FEBs and the University of Helsinki bulletin

Data base

To evaluate the regional event location performance for Fennoscandia and northwestern Russia, we again selected as a reference data base the bulletin published by the Institute of Seismology of the University of Helsinki. For the GSETT-2 test period 22 April - 2 June 1991, altogether 430 local and regional events were reported in the Helsinki bulletins, and 257 of these events were also found in the "IDC section" of the corresponding FEBs. (Two different solutions were given for two of these events, thus resulting in a total of 259 events in the FEB data base.)

It must be noted that the two data bases are not entirely independent relative to each other: The FEB events located in Finland were generally composed of reported or added readings from the stations KAF, VAF (part of the reference network) and the FINESA array. However, this interdependence does not represent a problem in the study on event location performance reported on here.

The 257 reference events comprised six earthquakes, one in central Finland, one in the Svalbard region, and four in the North Sea/Norwegian Sea, while the remaining events were presumed regional explosions of low magnitude. Fig. 7.2.5 shows the epicenters of the events, together with the stations of the Finnish Seismograph Network.

Due to the relatively high mining activity in the region, a normal practice in producing the Helsinki bulletin is to apply a brief reporting, i.e., manually determined source information with no phase readings, to events from the known sites. However, epicenters for the events reported by the Finnish NDC during GSETT-2 were determined using an iterative location procedure.

According to the estimated location accuracy, the reference events were divided into five groups:

Group I

Nineteen quarry blasts from seven Finnish mines or quarries. The blasts were confirmed by the responsible authorities, and the location was reported with an accuracy of better than $\pm$ 500 m. In the Helsinki bulletin, the complete location procedure was applied for 14 of these events, and a true location accuracy of 4.2 $\pm$ 3 km was calculated for this group.

Group II

Events located in the area where the coverage of the reference network is good (approximately 60^o-66^oN and 22^o-29^oE). The average station-to-epicenter distance is 150 km. As the events in group I also belong to this group, a reasonable estimate for the location accuracy is $\pm$ 5 km.

Group III

Events located at the edges of the Finnish network, including the coast of Estonia. The average epicentral distance is 250 km. Events from the known mines in northern Sweden and northwestern Russia -- reported with manually determined epicenters in the Helsinki bulletin -- are also included in this group. The accuracy of the Helsinki bulletin location is estimated to be $\pm$ 10 km.

Group IV

Events in northern Fennoscandia, northwestern Russia and the Baltic Sea, the average epicentral distance being 450 km. Estimated accuracy of the location in the Helsinki bulletin is $\pm$ 15 km.

Group V

Five earthquakes off continental Fennoscandia, in the Norwegian Sea and the North Sea. The events are far from the reference network, the average distance being 1000 km. However, as these event reports contain also readings from other seismological institutes in the region (13-30 stations were used in the epicenter determination), a reasonable estimate for the location accuracy is ± 20 km.

Results from the FEB analysis

Table 7.2.1 shows the number of FEB events in each of the five groups versus the EIDC responsible for the representative solution. In Table 7.2.1 it is noteworthy that 61 per cent of the representative solutions for Fennoscandian events originated from the WAS EIDC. The median value plus 25% and 75% quadratiles (Q) for differences between the FEB solution and the true location (group I) or the reference location (groups II-V) are also given in Table 7.2.1.

Group	**CNB**	**MOS**	**STO**	**WAS**	**Total**	**Median**	**25% Q**	**75% Q**
						(km)	**(km)**	**(km)**
I	6	-	-	13	19	10.2	6.2	22.6
II	10	-	3	40	53	13.6	8.1	24.3
III	45	6	23	91	165	29.0	15.1	49.3
IV	-	-	4	13	17	36.6	17.7	53.7
V	1	-	2	2	5	42.5	27.5	87.7
Total	62	6	32	159	259			

Table 7.2.1. Location statistics for the regional events.

From Table 7.2.1 we make the following observations:

Group I events:

The median FEB location error (relative to true location) is 10.2 km. This can be compared to a true location error of 4.2 km obtained by using Finnish network data.

Group II events:

Here, the reference locations are estimated to be accurate to ± 5 km. The median FEB location "error" relative to these estimates is 13.6 km. Thus the FEB performance is similar to Group I events. (Estimate of "absolute" error is $\sqrt{13.6^2 - 5^2}$ km = 12.6 km.)

Group III events:

Here, the reference locations are estimated to be accurate to ± 10 km. The median FEB location "error" is 29.0 km. An estimate of "absolute" error is $\sqrt{29^2 - 10^2}$ km = 27.2 km. Thus Group III events have clearly inferior location accuracy compared to Groups I and II.

Group IV events:

Here, the reference locations are estimated to be accurate to ± 15 km. The median FEB location "error" relative to these estimates is 36.6 km. An estimate of the "absolute" error is $\sqrt{36.6^2 - 15^2}$ km = 33.4 km. This is slightly higher than for Group III.

Group V events:

Here, the number of events is too low to compute any meaningful statistics, but the FEB performance seems to be not very different from Group IV events.

A closer inspection of the FEBs shows that the location accuracy varied considerably between different EIDCs. The scatter can partly be explained by the different degree of experience with the analysis of data from this region. For example, some EIDCs did not place any constraints on the event depth in the location procedure for many of the events dealt with here.

Part of the location differences are due to the different velocity models used in the Helsinki bulletin and at the EIDCs. To illustrate this, we have plotted in Fig. 7.2.6 the difference in epicentral distance derived from the WAS EIDC standard travel-time tables and the Helsinki velocity model used in the Helsinki bulletin. As can be seen from the figure, differences up to 11 km exist at the regional distance range. The differences may be even greater in case other velocity models are applied.

Conclusions

The regional evaluation of detection results from GSETT-2 presented here shows that in a region with dense coverage of high-quality array stations as in Fennoscandia, it is possible to detect seismic events at very low magnitudes.

The 90 per cent threshold of around magnitude 2.5 found in this study for different parts of Fennoscandia must of course be considered with the appropriate caution: Thus it refers to regional magnitude scales that currently are not well calibrated in terms of global magnitude. Also, in other geological environments, the wave propagation and array noise suppression characteristics may be different. Therefore, it is not known to which extent such results would be possible to duplicate in other parts of the world.

Evaluation of the regional event location performance in Fennoscandia showed that in an area where the coverage of the GSETT-2 network is good, the location accuracy approaches that obtained by national networks.

There are indications that the location errors may be reduced by using regional velocity models. In addition, knowledge on the characteristics of seismicity in the region would further improve the results.

S. Mykkeltveit
M. Uski, Univ. of Helsinki, Finland

References

Ringdal, F. (1975): On the estimation of seismic detection thresholds, *Bull. Seism. Soc. Am.*, 65, 1631-1642.

Ringdal, F. (1991): Regional detection performance during GSETT-2: Initial results for the Fennoscandian array network. Semiann. Tech. Summ., 1Mar - 30 Sep 1991, NORSAR Sci. Rep. 1-91/92, Nov 91, NORSAR, Kjeller, Norway.

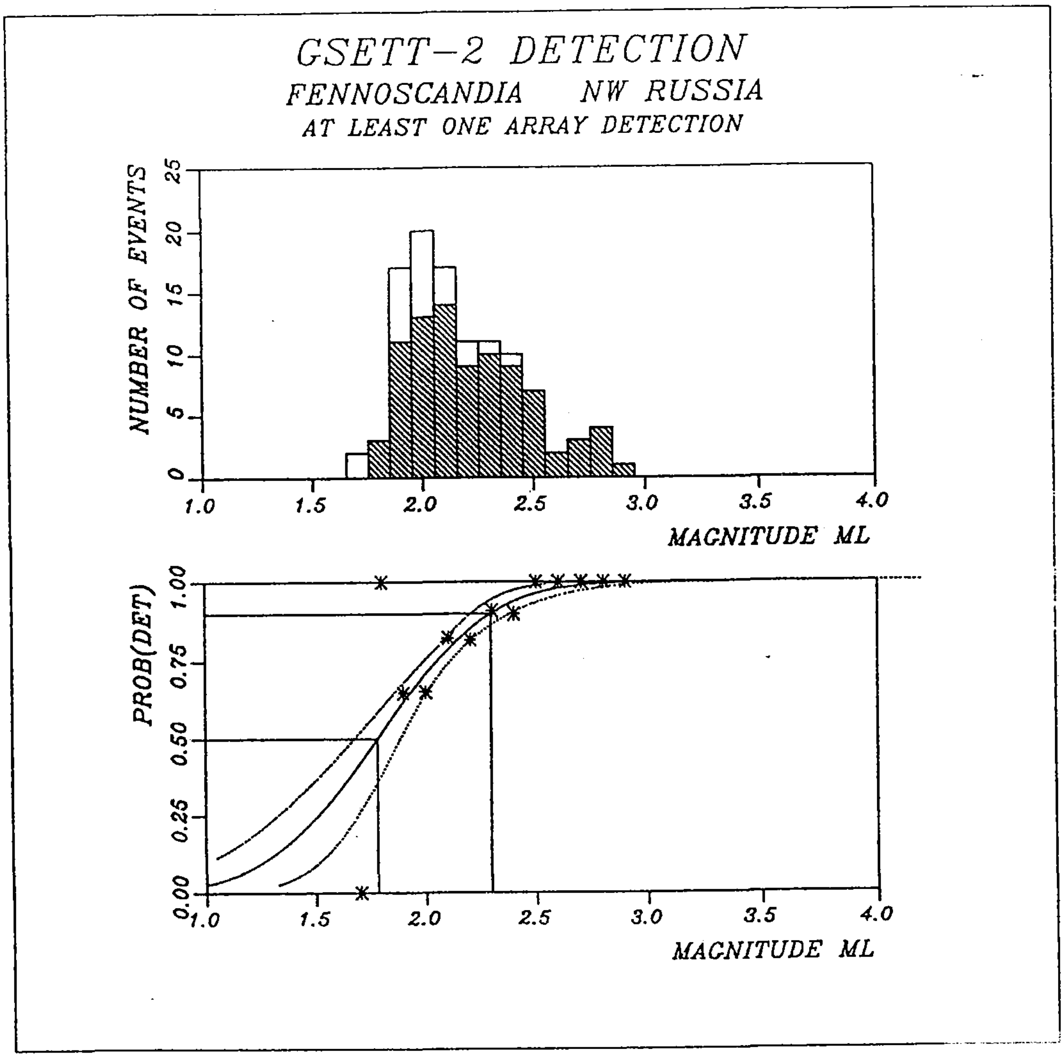

Fig. 7.2.1. Maximum likelihood detectability estimation for Fennoscandia-NW Russia using the Univ. of Helsinki bulletin as a reference. The upper half shows the reference event set and the number of events actually detected for each magnitude. The lower half shows the maximum likelihood detectability curve and its confidence limits. The actual percentage of detected events at each magnitude is also shown. This figure is based upon a one-array detection requirement.

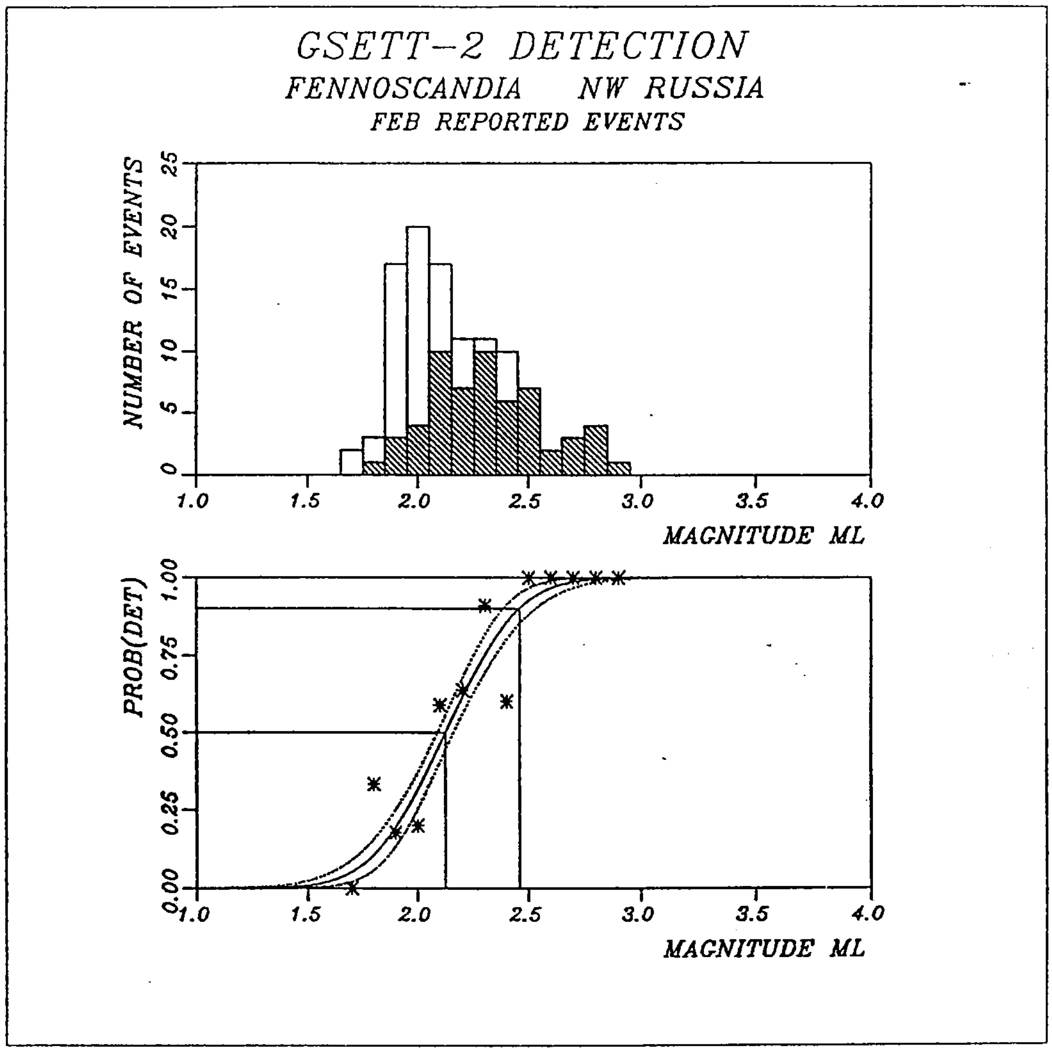

Fig. 7.2.2. Maximum likelihood detectability estimation for Fennoscandia-NW Russia using the Univ. of Helsinki bulletin as a reference. The upper half shows the reference event set and the number of events actually detected for each magnitude. The lower half shows the maximum likelihood detectability curve and its confidence limits. The actual percentage of detected events at each magnitude is also shown. This figure is based upon FEB reported events as discussed in the text.

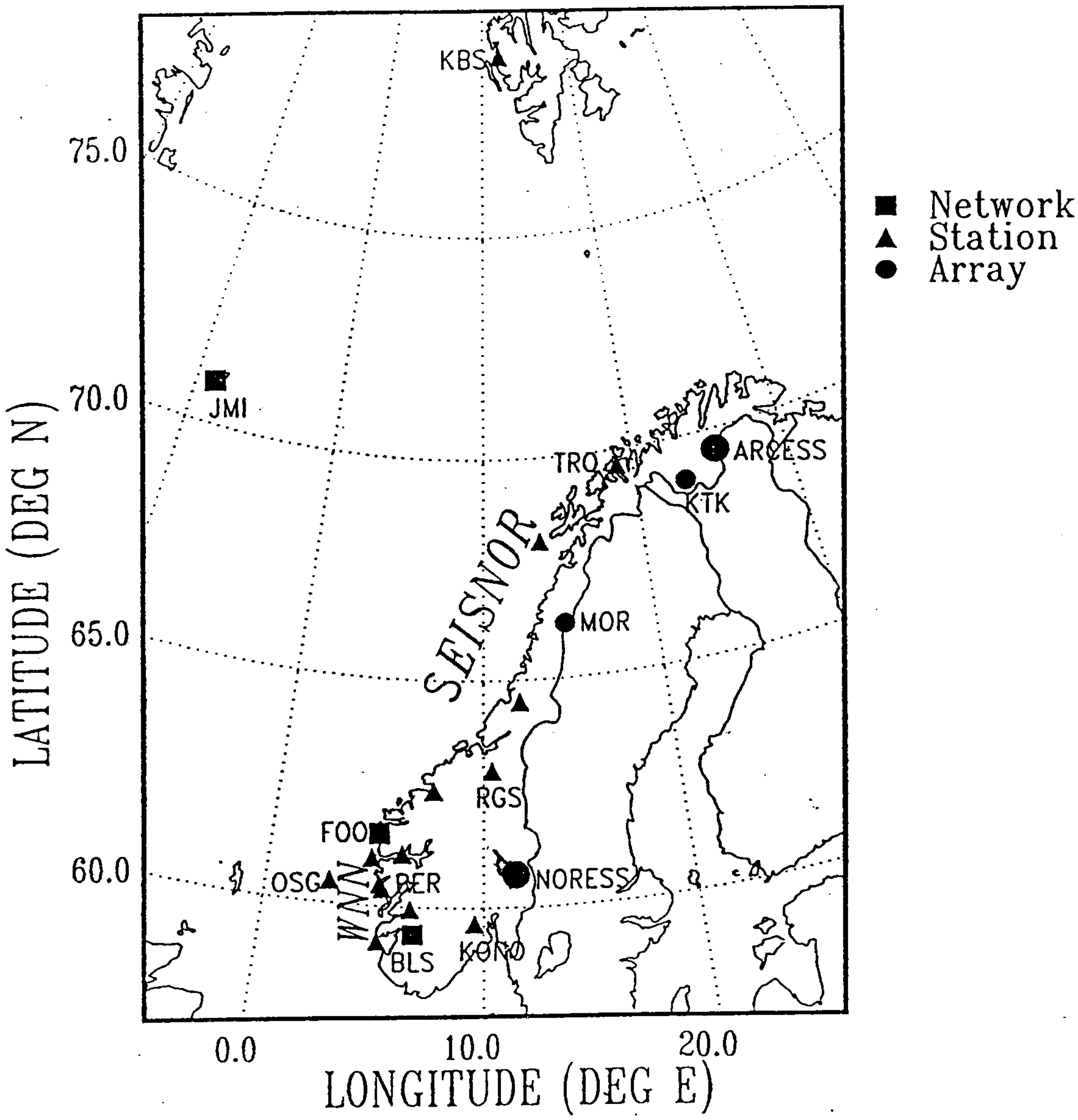

Fig. 7.2.3. The map shows the stations of the WWN and SEISNOR networks operated by the University of Bergen and used in their bulletin work. Note that BLS, FOO and JMI are small networks comprising 4, 3 and 2 stations, respectively, and that MOR and KTK are small-aperture (0.5 km) 6-element arrays. The locations of NORESS and ARCESS are also shown.

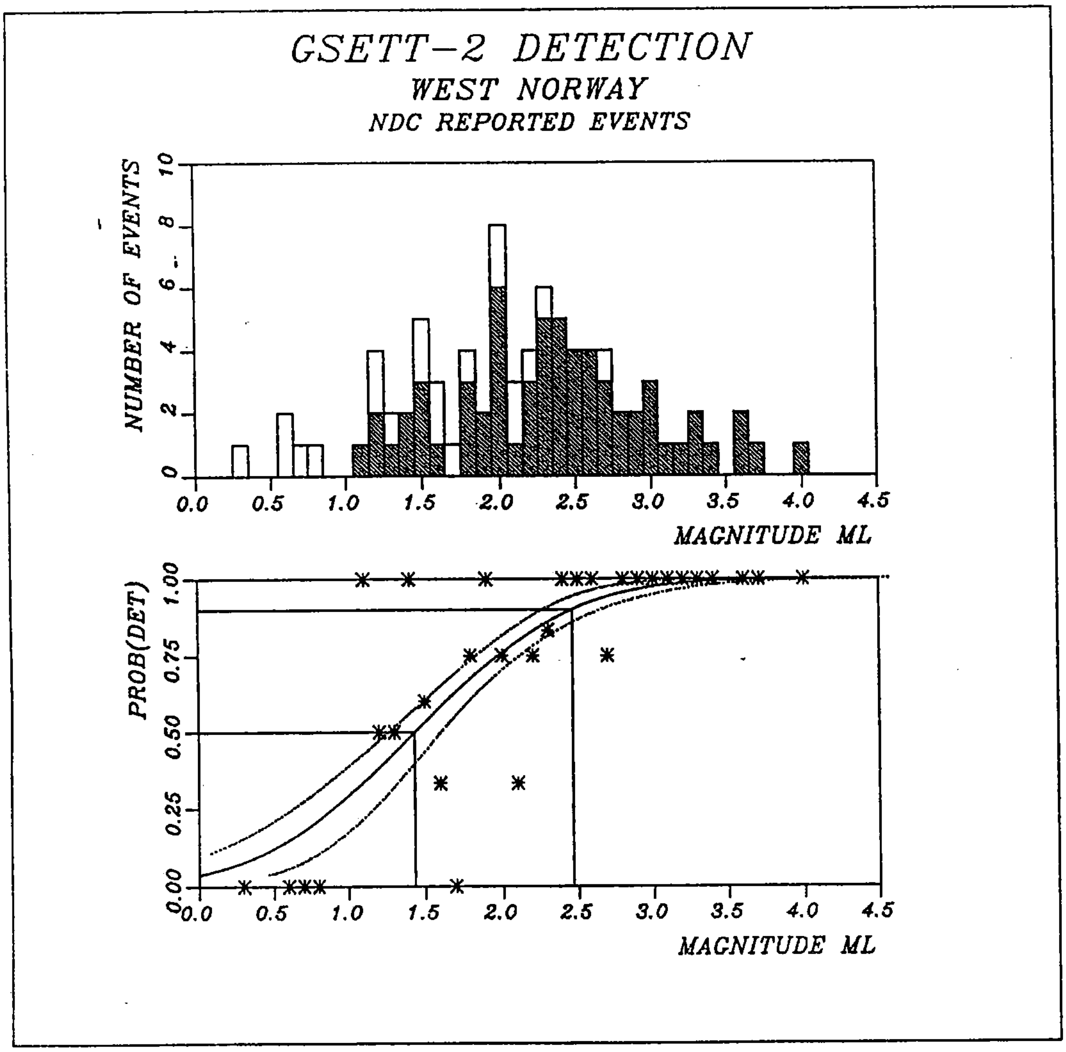

Fig. 7.2.4. Maximum likelihood detectability estimation for western Norway using the Univ. of Bergen bulletin as a reference. The upper half shows the reference event set and the number of events actually detected for each magnitude. The lower half shows the maximum likelihood detectability curve and its confidence limits. The actual percentage of detected events at each magnitude is also shown. This figure is based upon a one-array detection requirement.

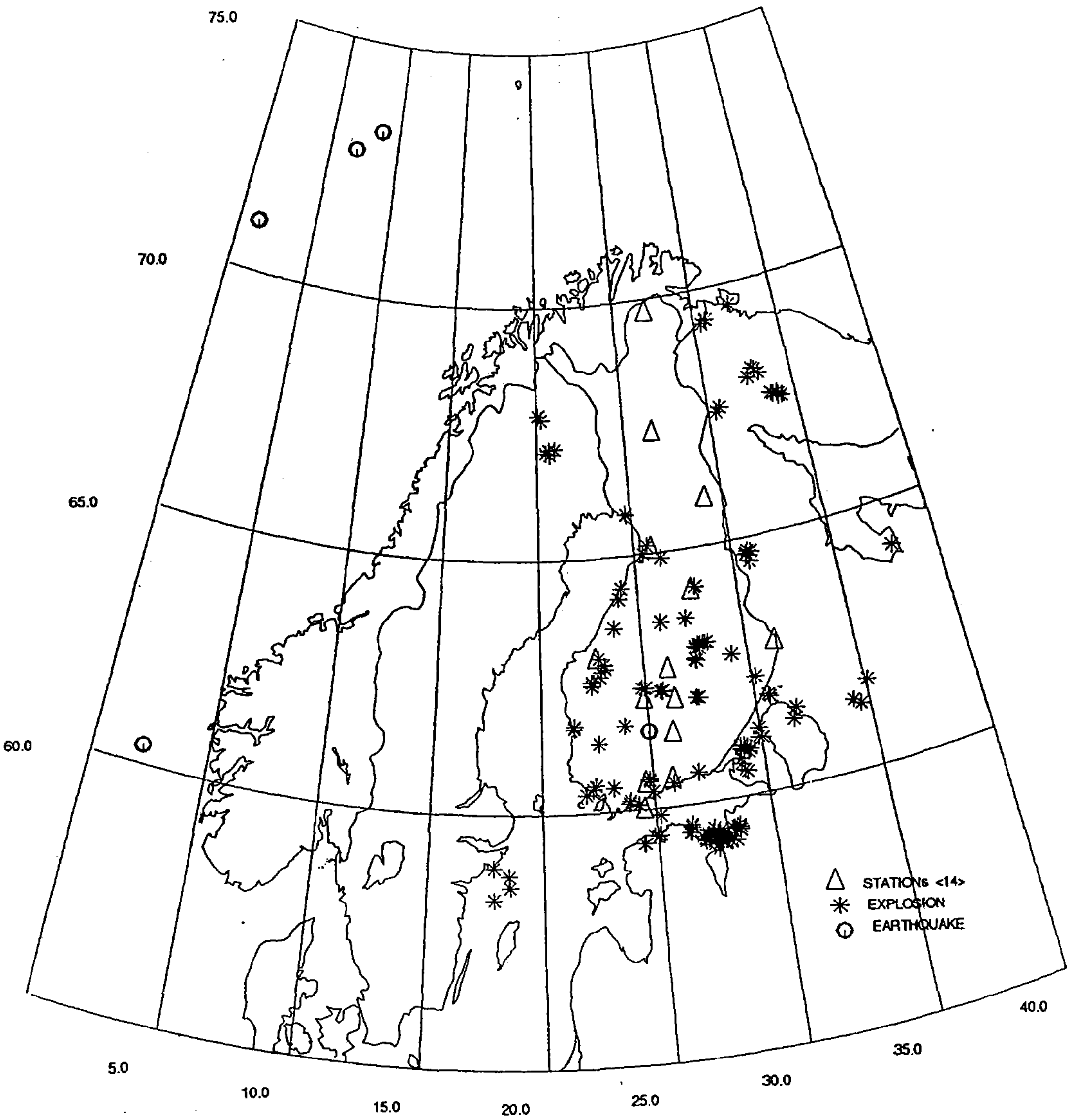

Fig. 7.2.5. Epicenters of the 257 reference events common to the Helsinki bulletin and the FEBs, and stations of the Finnish Seismograph Network. One earthquake (79.89°N, 24.23°E) lies outside the range of the map.

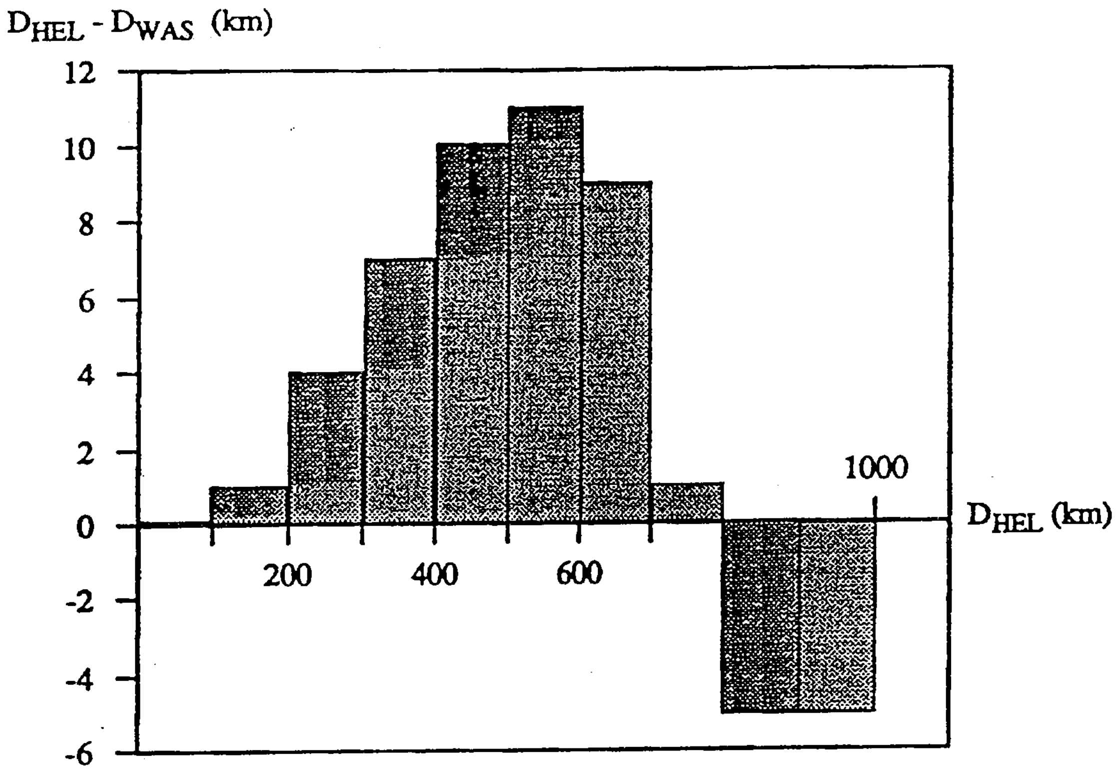

Fig. 7.2.6. The difference between the epicentral distances D_{HEL} and D_{WAS} plotted versus D_{HEL}. D_{HEL} is a distance calculated from the Helsinki velocity model using the travel-time difference of the first arriving P- and S-pair. D_{WAS} is the corresponding distance obtained from the WAS EIDC velocity model.

7.3 GSETT-2 Evaluation: Detection of aftershocks from the W. Caucasus earthquake of 29 April 1991

Introduction

On 29 April 1991 a large earthquake (M_S = 7.3) occurred in western Caucasus, with coordinates 42.453N, 43.673E, h = 17 km (NEIC).

The earthquake was followed by a large number of aftershocks. According to the catalogue of Starovoit et al (1992), 114 aftershocks were recorded on the day of the main shock (29 April) and 360 aftershocks had been recorded by the end of May.

The earthquake occurred early during GSETT-2 (main phase), and caused a considerable load at the NDCs as well as EIDCs. The day 29 April has been selected as one of the days for which reprocessing will be made at EIDCs. Consequently, this day is useful for studying the performance of the experimental global system during a day of particularly high seismic activity.

Method

In this paper we address the detection capability of the system in place during GSETT-2, and compare with NEIC bulletins. We use the method of Ringdal (1975), whereby the system to be evaluated is compared with an independent reference system. The reference is in this case provided by the catalogue of Starovoit et al (1992). The event sizes in that catalogue are quoted in terms of the K-value of each event. The K-value is related to M_S by the formula

$$K = M_s \cdot 1.8 + 4.0 \qquad (1)$$

We have converted all K-values to M_S using (1) prior to applying the maximum-likelihood estimation technique.

Data

Table 7.3.1 summarizes the number of detected events by the various systems. We note that the two EIDCs for which we had data (reprocessed CELs from Stockholm and Washington) had a very similar performance, and reported about half of the events in the reference catalogue. NEIC reported only one third of the reference events in their monthly bulletin. The rapid QED service (Quick Epicenter Determination) reported very few of the events.

Note that the QED follows approximately the same time schedule as the CELs and FEB. Therefore, a comparison between the QED and the final CEL is of interest. We note, however, that the revised CELs were compiled with a delay of many months.

Detectability

The results of the detectability study are summarized in Figs. 7.3.1-6.3.4 and Table 7.3.2.

Figs. 7.3.1-7.3.2 show the detectability estimates for the GSETT-2 revised CEL (STOIDC) and NEIC. The data cover aftershocks during the day 29 April. The detectability of GSETT-2 is better than NEIC by at least one half magnitude unit. However, it is noteworthy that almost all of the "larger" events missed by either system were earthquakes within 3 hours of the main shock.

In light of this observation, we also computed detectability statistics for the time interval 12-24 GMT on 29 April, i.e., excluding the first 3 hours after the main shock. The results are shown in Figs. 7.3.3-7.3.4, and show improvements for both systems. In particular, the improvement is significant for NEIC.

Conclusion

The detectability of the GSETT-2 system for the W. Caucasus earthquake sequence is better than that of NEIC. The difference is particularly significant during the first 3 hours after the main shock.

It appears that a main reason for this good GSETT-2 performance is the reporting by sensitive regional arrays. It was also helpful to have a local station (KIV) at only 2 degrees distance, but it appears that almost all of the events would have been reported even without KIV data. However, the KIV data undoubtedly contributed to improving the location accuracy of the GSETT-2 reportings.

F. Ringdal

References

Ringdal, F. (1975): On the estimation of seismic detection thresholds, *Bull. Seism. Soc. Am.*, 65, 1631-1642.

Starovoit et al (1992): Catalog of aftershocks of the West Caucasus earthquake of 29 April 1991.

	Number of Events
Starovoit et al catalogue	115
Stockholm CEL (revised)	63
Washington CEL (revised)	57
NEIC monthly list	35
QED list	6

Table 7.3.1. Earthquakes reported for 29 April 1991, Caucasus sequence. For the two CELs in the table, only events confirmed by the Starovoit et al catalogue have been counted.

	μ	σ	μ_{90}
All events on 29 April:			
GSETT-2 revised CEL	3.62	0.28	3.98
NEIC	4.07	0.37	4.55
Events during 1200-2400 on 29 April:			
GSETT-2 revised CEL	3.58	0.22	3.86
NEIC	3.86	0.10	3.99

Table 7.3.2. Detectability estimates for Caucasus sequence, in terms of M_s computed from Starovoit et al (1992). Note that μ is the 50% incremental detection threshold, and μ_{90} is the 90% threshold

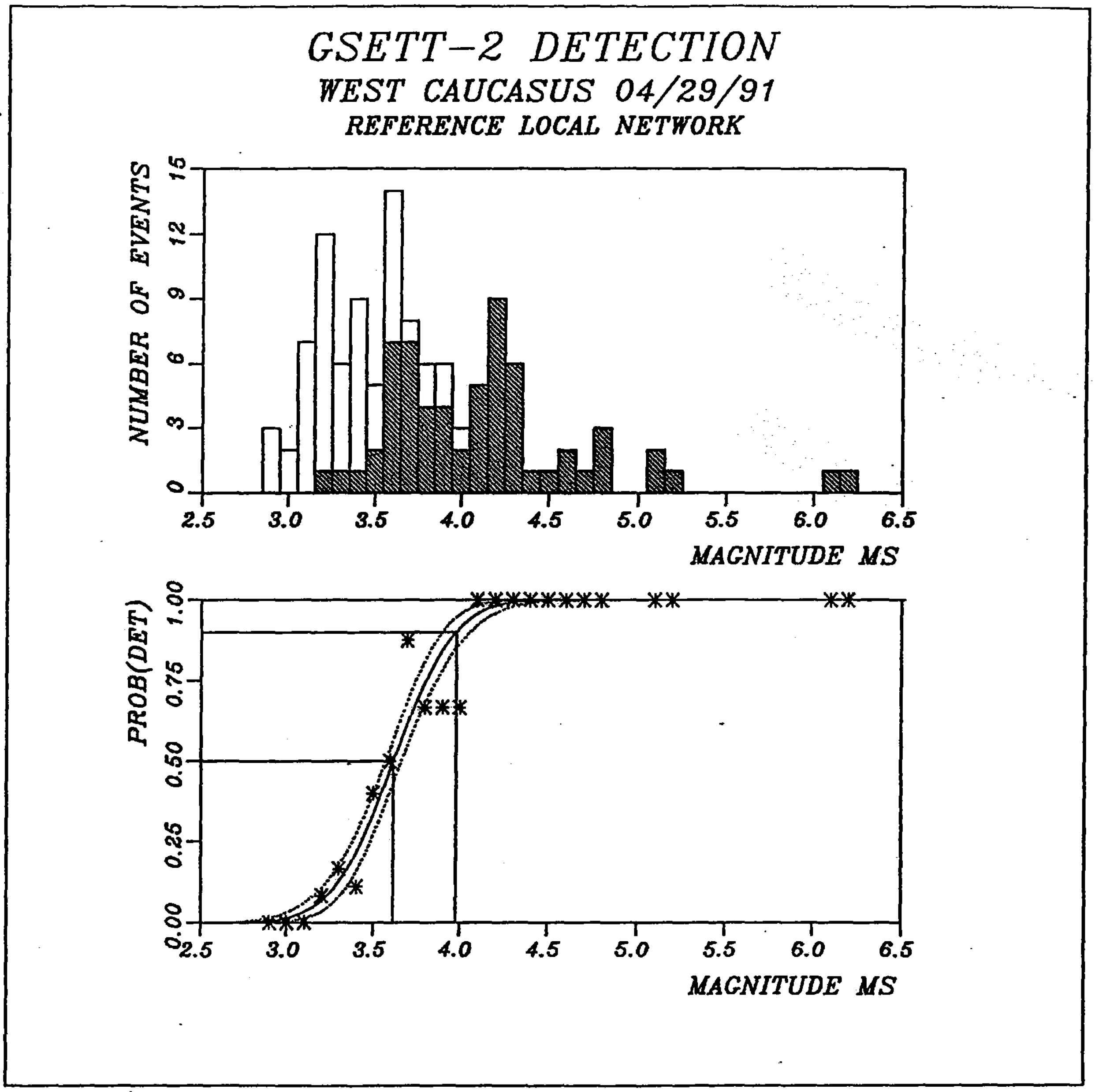

Fig. 7.3.1. *Detectability results for GSETT-2 revised CEL; 29 April:* Detectability estimate for W. Caucasus aftershocks using the catalogue of Starovoit et al (1992) as reference. The upper part shows the number of reference events at each magnitude, with the hatched columns indicating the number of detections. The lower part is a maximum likelihood detection curve.

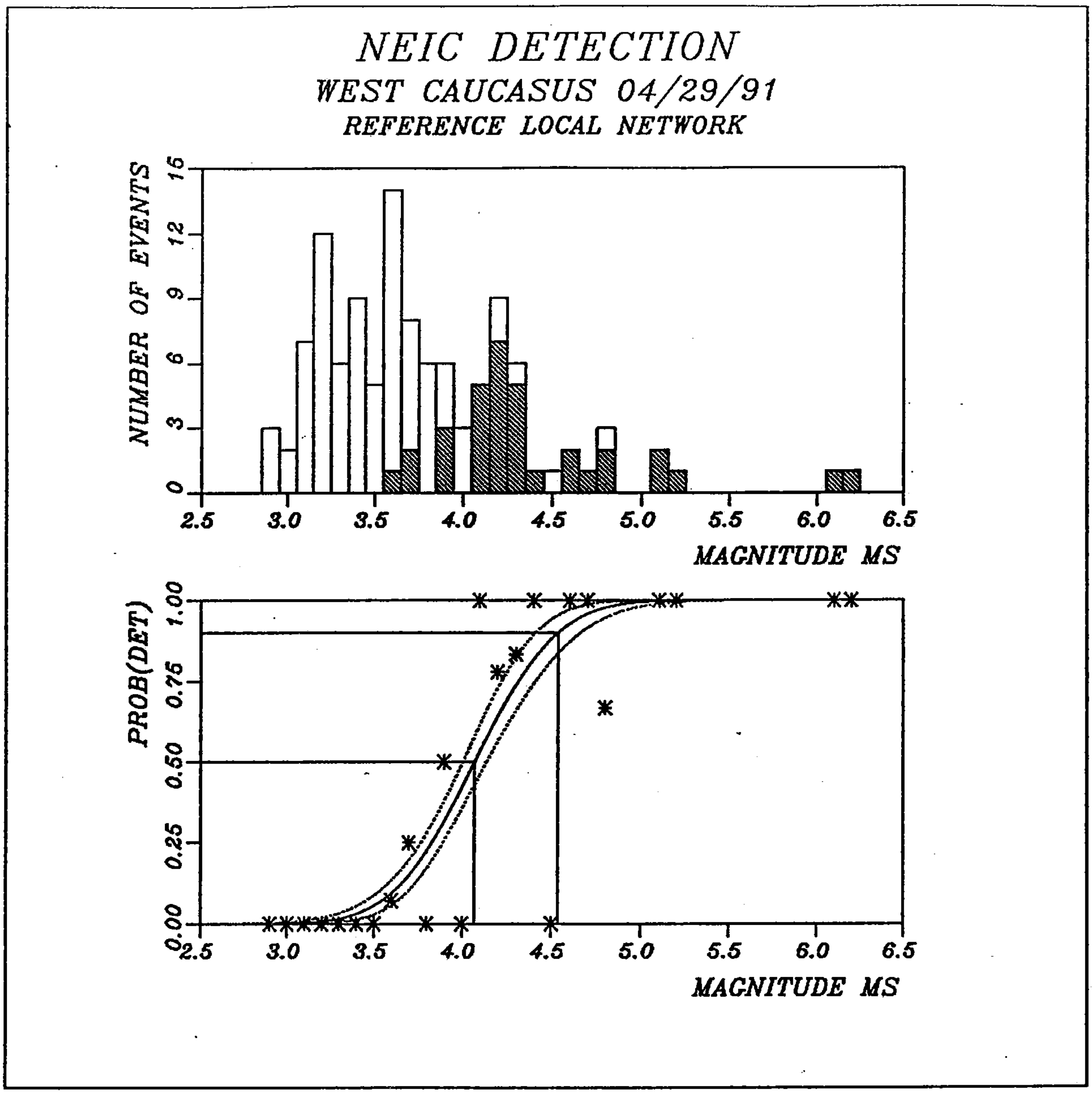

Fig. 7.3.2. *Detectabililty results for NEIC bulletin; 29 April:* Detectability estimate for W. Caucasus aftershocks using the catalogue of Starovoit et al (1992) as reference. The upper part shows the number of reference events at each magnitude, with the hatched columns indicating the number of detections. The lower part is a maximum likelihood detection curve.

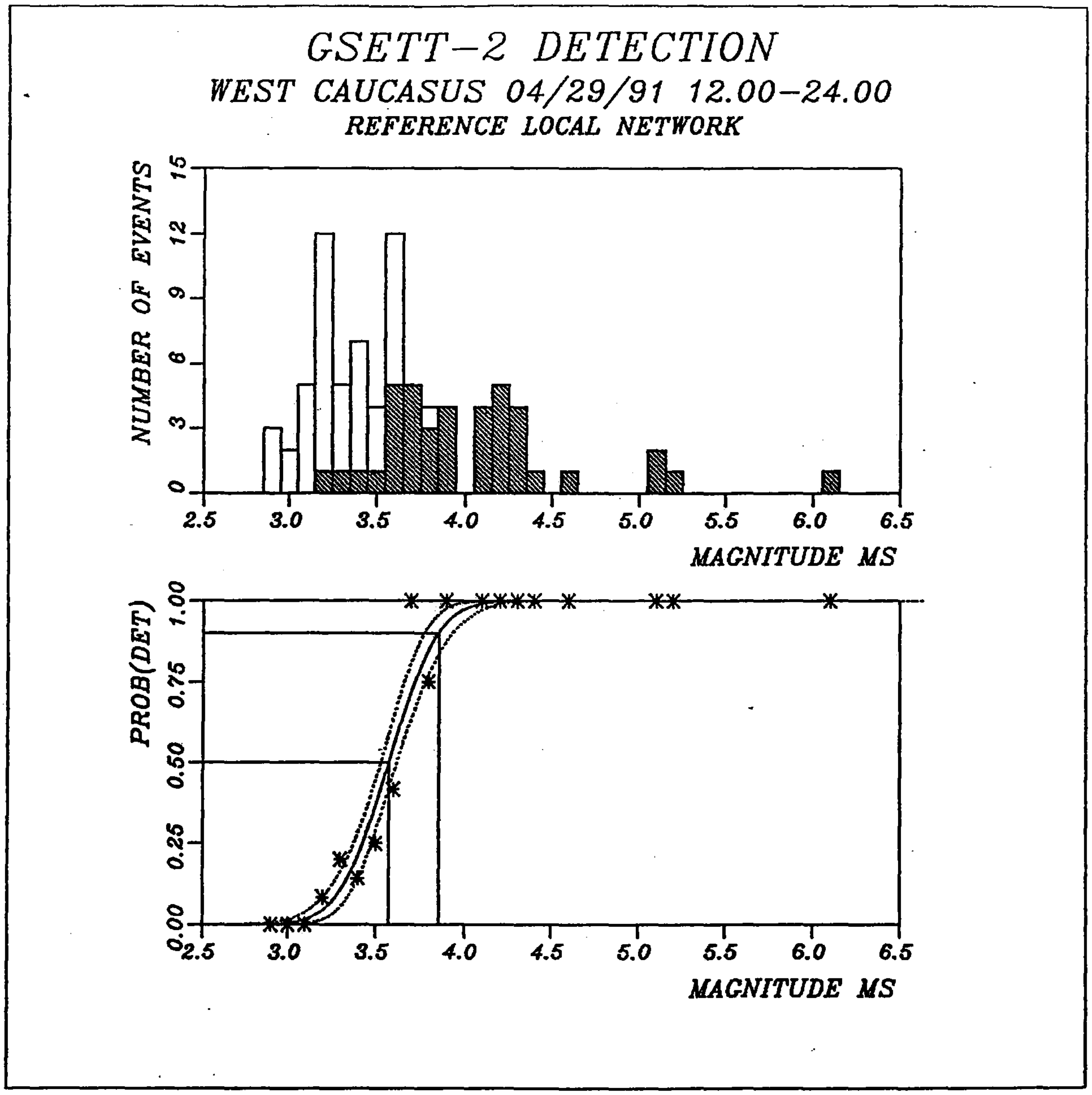

Fig. 7.3.3. *Detectability results for GSETT-2 revised CEL; 29 April 1200-2400*: Detectability estimate for W. Caucasus aftershocks using the catalogue of Starovoit et al (1992) as reference. The upper part shows the number of reference events at each magnitude, with the hatched columns indicating the number of detections. The lower part is a maximum likelihood detection curve.

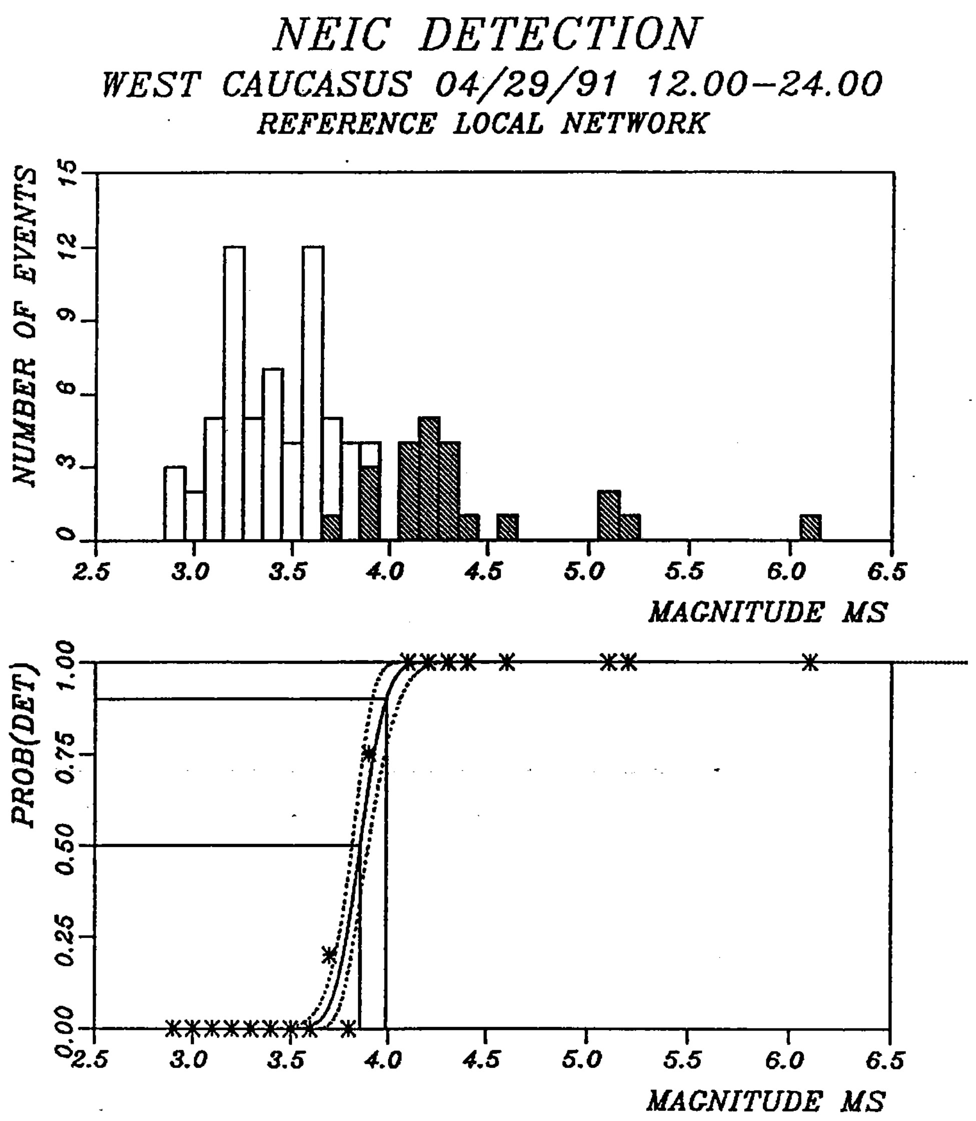

Fig. 7.3.4. *Detectability results for NEIC bulletin; 29 April 1200-2400*: Detectability estimate for W. Caucasus aftershocks using the catalogue of Starovoit et al (1992) as reference. The upper part shows the number of reference events at each magnitude, with the hatched columns indicating the number of detections. The lower part is a maximum likelihood detection curve.

7.4 Travel time corrections for a 3-D velocity model beneath the NORSAR array

Introduction

For the purpose of improving the event location capability of the NORSAR array, Berteussen (1974) constructed a time correction table from average arrival time residuals for 94 different incident P-wave directions, and Berteussen (1976) concluded that almost all of the observed time residuals across the array can be corrected for by using this table, and therefore the residuals have their origin in the upper mantle and crust beneath the array. Time corrections are computed from this table by linear interpolation between nodes in incident slowness space, and this table is the one most frequently used for time corrections at NORSAR. Due to the very nonuniform distribution of earthquakes, interpolation is unavoidable in this kind of correction procedure. However, if the observed residuals could be explained in terms of subsurface structures, another type of correction table could be made by forward modeling the effects of such structures.

In one of the first applications of travel time tomography in seismology, Aki et al (1977) inverted the time residuals of the NORSAR time correction table for P-wave velocity perturbations beneath the array, and a similar experiment has been done with a slightly different and larger data set. Systematic analysis of this data set revealed the significant influence of diffraction effects like focusing and defocusing from low and high velocity zones, and diffraction effects have been taken into account, in a first-order approximation, using a reformulation of diffraction tomography (Ødegaard and Doornbos, 1992). Synthetic data have been computed for the velocity models produced by ordinary seismic tomography and by diffraction tomography, and from these data correction tables have been constructed. There is no further need for interpolation when using these correction tables. Some results concerning these tables are presented.

Tomography

The basis of ordinary seismic tomography (ST) is the simple relation:

$$\delta\tau = \int_{ray} \delta s \cdot d\sigma \qquad (1)$$

This equation states that a change in travel time is due to a slowness perturbation $\delta s = -v^{-2}\delta v$ along the ray, and it predicts a time shift of a reference pulse u_0:

$$\mathbf{u}(\mathbf{x}, t) = \mathbf{u}_0(\mathbf{x}, t - \delta\tau) \qquad (2)$$

Eq. (2) can be viewed as a smooth approximation since it is a valid expression if the slowness perturbation δs varies smoothly within the medium. The reformulation of diffraction tomography (DT), as derived by Doornbos (1992), predicts a diffraction term as a perturbation to the time-shifted reference pulse (which is the smooth approximation of ST):

$$\mathbf{u}(\mathbf{x},t) = \mathbf{u}_0(\mathbf{x},t-\delta\tau) + \int_V \mathbf{B}\cdot\nabla\cdot\delta s\cdot dV \quad (3)$$

This reformulation alleviates some of the fundamental problems of both seismic and diffraction tomography. The velocity structure beneath the NORSAR array has been modeled down to a depth of 129 km using ST, Eq. (1), and using DT in the frequency domain with short-period (SP) subarray phase and amplitude residuals from 115 events, and long-period (LP) phase residuals from 31 events. Synthetic data can be computed after forward modeling using Eq. (1) (ray travel times) and Eq. (3) (synthetic wave recordings). Further details concerning these methods are given by Ødegaard and Doornbos (1992).

Correction tables

SP P-wave time correction tables have been constructed for the ST model, using Eq. (1) (ray travel time), and the DT model, after using Eq. (3) with a 1 Hz damped sine reference pulse and iterative correlation between the synthetic array beams and subarray beams for 1.5 s time windows. The two low-pass filtered time correction tables for subarray 01A are plotted in Figs. 7.4.1 and 7.4.2, for slowness values less than 0.08 s/km, corresponding to epicenter distances greater than 30^{o}. Figs. 7.4.3 and 7.4.4 display the predicted time residuals versus the observed time residuals for the two time correction tables and the 115 events. The ray travel time table constructed from the ST model predicts the observed time residuals slightly better than the DT correction table; the normalized squared error is 12% for the ST table and 19% for the DT table, and the correlation coefficient is 0.94 for the ST table and 0.91 for the DT model. For the purpose of constructing a time correction table, the ST model provides the best results. The ST model is given in Table 7.4.1. However, the DT model predicts the phase and amplitude spectra of the data significantly better than the ST model; the normalized squared error for the phase spectra is 20% for the ST model and 10% for the DT model, and the normalized squared error for the amplitude spectra is 75% for the ST model and 55% for the DT model (Ødegaard and Doornbos, 1992).

E. Ødegaard, Univ. of Oslo

References

Aki, K., A. Christoffersson and E.S. Husebye (1977): Determination of the three-dimensional structure of the lithosphere, *J. Geophys. Res.*, 82, 277-296.

Berteussen, K.-A. (1974): NORSAR location calibrations and time delay corrections. *Sci. Rep. 2-73/74*, NTNF/NORSAR, Kjeller, Norway.

Berteussen, K.-A. (1976): The origin of slowness and azimuth anomalies at large arrays, *Bull. Seism. Soc. Am.*, 66, 719-741.

Doornbos, D.J. (1992): Diffraction and seismic tomography, Geophys. J. Int., 108, 256-266.

Ødegaard, E. and D.J. Doornbos (1992): Seismic diffraction tomography of array data, *J. Geophys. Res.*, in press.

Layer 1 (0-15km) v_0 = **6.2 km/s**

=	=	=	=	=	=	=	=	=	=	=	=	=
=	=	=	=	=	=	=	=	=	=	=	=	=
=	=	=	=	=	0.8	-1.7	=	-0.4	=	=	=	=
=	=	=	=	0.5	-3.2	-0.9	=	-3.4	-0.2	=	=	=
=	=	0.4	-3.5	-4.5	=	3.5	0.1	0.9	1.1	0.2	=	=
=	=	-0.7	-4.9	-3.4	-1.5	-0.1	1.6	3.7	0.4	-1.5	=	=
=	=	=	-6.3	1.7	-1.0	1.8	0.9	0.6	-1.0	0.0	=	=
=	=	=	-3.2	2.3	4.1	4.7	3.0	1.9	-0.1	=	=	=
=	=	=	=	-3.9	0.7	3.6	1.5	-0.6	1.0	=	=	=
=	=	=	=	2.0	4.3	2.1	1.1	-0.1	-1.0	=	=	=
=	=	=	=	=	=	=	=	=	=	=	=	=
=	=	=	=	=	=	=	=	=	=	=	=	=
=	=	=	=	=	=	=	=	=	=	=	=	=

Layer 2 (15-34km) v_0 = **6.9 km/s**

=	=	=	=	=	=	=	=	=	=	=	=	=
=	=	=	=	=	0.1	-0.8	=	=	=	=	=	=
=	=	=	=	-0.9	-1.9	0.1	-1.9	1.0	-0.5	=	=	=
=	=	0.4	-1.2	-2.7	0.6	-0.2	2.8	0.7	3.0	0.8	=	=
=	=	-1.2	-3.3	-2.4	0.3	-0.1	1.0	1.1	-0.2	2.5	=	=
=	=	-4.8	-6.8	0.5	2.2	0.9	-0.8	-0.7	-1.8	0.2	-1.1	=
=	=	1.6	-1.7	0.0	0.5	1.0	0.3	-0.5	-1.5	4.0	=	=
=	=	1.0	-3.2	-3.3	-2.2	2.7	0.7	-0.2	3.7	=	=	=
=	=	=	0.2	2.5	0.2	1.0	2.7	-1.6	0.5	0.1	=	=
=	=	=	0.7	-0.4	-1.2	1.2	4.6	-0.3	1.8	0.2	=	=
=	=	=	=	0.1	-1.7	3.2	=	-0.4	1.3	=	=	=
=	=	=	=	=	=	=	=	=	=	=	=	=
=	=	=	=	=	=	=	=	=	=	=	=	=

Layer 3 (34-54km) v_0 = **8.1 km/s**

=	=	=	=	=	=	=	=	=	=	=	=	=
=	=	=	=	5.6	-0.5	-2.6	-2.1	0.5	-4.3	=	=	=
=	=	=	1.7	-1.2	-1.1	1.1	1.5	2.0	4.2	-2.8	=	=
=	=	1.0	-0.1	-4.8	-2.1	-2.0	-1.5	-0.8	2.9	-0.3	-2.5	=
=	0.1	0.4	-2.7	0.8	0.5	-2.9	-2.2	-2.5	1.5	-0.3	-3.9	=
=	4.4	-1.2	1.8	-0.3	-4.5	0.0	0.9	1.6	0.7	2.1	3.4	-1.3
=	-0.2	-0.1	0.8	-0.9	0.1	-2.1	1.2	0.7	4.5	-0.1	4.1	=
=	3.5	-0.4	0.4	-0.3	-1.8	-3.6	-1.1	0.8	0.6	-2.9	0.0	=
=	=	1.3	-2.9	-0.7	0.2	0.1	-1.7	1.8	4.5	-0.9	=	=
=	=	-0.1	-5.6	-0.7	1.9	0.5	1.2	3.3	2.9	4.5	=	=
=	=	=	0.2	-2.5	-3.3	-1.5	-1.0	2.6	5.6	2.2	=	=
=	=	=	=	=	0.4	1.6	0.3	=	=	0.4	=	=
=	=	=	=	=	=	=	=	=	=	=	=	=

Table 7.4.1. The ST model. The depth interval and initial P-wave velocity v_0 for each layer are given. Each value represents the velocity perturbation in %, relative to the initial value in a box with horizontal dimensions 15.4 x 15.4 km^2. "=" denotes no coverage. Subarray 01A is situated at the center of the grid. (Page 1 of 2)

Layer 4 (54-79km) $v_0 = 8.1$ km/s

=	=	=	=	-0.4	0.1	-1.2	-4.2	1.7	-3.6	-0.5	=	=
=	=	=	-0.5	1.6	0.8	-0.3	-1.4	-1.2	0.4	2.4	=	=
=	0.2	0.9	-0.9	1.3	1.4	-2.1	1.1	0.8	-1.4	-2.6	-1.6	-0.3
=	2.4	-1.0	-0.2	-2.3	-2.0	-0.2	0.5	0.0	1.4	-1.5	-2.3	-6.0
1.3	-2.0	0.4	-3.0	-3.4	0.6	-0.6	-1.7	-0.3	0.6	2.2	2.2	-3.3
3.9	-4.0	-1.0	-0.9	0.9	3.8	1.2	-0.1	-2.1	-0.4	3.0	5.1	-2.7
0.3	-1.7	-0.3	-1.3	0.0	1.2	0.3	-1.3	-0.5	0.4	0.2	5.2	2.1
2.0	-0.3	-1.3	-2.6	0.2	0.5	-1.5	-0.5	1.5	0.0	0.1	5.9	-0.4
2.0	1.8	-1.5	-3.2	-2.6	-2.2	0.7	3.3	1.5	1.8	-1.3	4.0	0.4
=	-2.0	1.9	-2.7	-5.2	-3.6	-2.0	1.3	5.4	3.4	-1.4	3.2	1.3
=	-0.3	-0.7	-4.0	-1.3	-2.4	-3.8	2.6	6.8	1.4	3.5	5.8	=
=	=	=	-0.2	0.7	1.2	2.5	-0.1	-2.3	2.2	4.6	0.7	=
=	=	=	=	=	0.5	=	2.2	=	=	1.1	=	=

Layer 5 (79-104km) $v_0 = 8.1$ km/s

=	=	0.0	-0.4	-1.1	-0.5	0.4	-0.1	-1.5	-1.4	-1.5	=	=
=	-0.3	-0.4	4.6	3.8	0.8	-1.7	-0.3	-1.9	-1.8	-1.8	-1.6	=
0.7	0.4	1.5	1.0	2.8	-1.6	0.2	-0.6	0.8	0.4	-1.1	-0.2	-1.5
=	2.2	-0.3	0.3	0.5	-2.4	-1.2	0.6	3.1	0.3	1.1	0.7	-3.4
1.2	1.2	-1.0	-1.5	-1.8	-2.4	-1.3	0.4	2.5	3.7	4.1	1.7	-1.2
2.2	-1.8	-3.1	-0.5	-3.3	-3.2	-2.9	-0.5	2.3	6.4	5.4	5.1	-1.1
-2.6	-2.2	-3.6	-2.3	0.6	-2.4	-2.8	-1.7	0.9	5.0	3.4	4.8	-0.2
-2.0	-6.7	-3.5	-2.5	-0.9	-2.5	-2.7	0.4	0.7	0.7	4.9	3.8	3.0
0.0	0.2	-3.3	-1.2	-1.7	-1.0	-2.3	-1.4	-0.1	2.0	3.6	3.4	8.2
0.9	-0.9	-0.5	0.2	1.2	-2.6	-1.5	-0.6	0.9	-3.3	1.9	3.6	7.7
-0.2	-3.2	-2.1	2.6	0.5	-0.2	0.5	0.0	-2.0	-2.1	-0.2	2.8	3.1
=	-1.3	0.3	-0.2	1.8	1.7	3.0	0.7	-4.2	-5.0	1.1	0.3	3.6
=	=	=	-1.3	0.1	2.5	-0.6	-0.6	1.1	-0.4	3.3	2.5	=

Layer 6 (104-129km) $v_0 = 8.1$ km/s

=	1.0	-0.6	2.6	0.0	0.5	0.3	-2.0	-0.7	-3.3	-0.4	0.1	-0.8
=	5.8	9.2	-1.1	1.8	3.3	1.7	0.3	-0.4	-1.6	-0.9	2.0	0.0
2.1	5.0	2.9	3.3	0.4	4.9	5.8	3.6	0.4	2.1	1.0	0.7	0.8
0.8	3.9	5.4	0.7	2.2	1.5	2.6	3.1	2.8	3.1	3.6	2.1	-0.1
1.0	0.7	-3.8	-3.5	-1.4	-1.6	-2.6	0.2	3.7	6.1	5.4	3.2	1.2
0.3	-2.4	-4.6	-4.7	-5.7	-3.7	-5.3	-3.0	3.0	6.1	6.0	4.7	-0.1
-0.8	-2.7	-5.1	-9.6	-8.3	-3.6	-7.4	-3.4	-0.6	4.9	6.3	4.5	3.2
-1.0	-3.7	-2.6	-6.2	-3.4	-4.1	-1.6	-3.2	-0.5	2.0	3.2	2.8	5.9
0.1	-0.8	0.1	-2.8	-3.0	-1.6	1.7	-1.1	-1.7	-2.5	1.2	3.7	5.4
-2.5	-1.6	-0.2	-0.6	0.7	5.5	3.8	-1.4	-3.9	-4.3	-0.9	2.6	4.4
-3.2	0.2	-1.1	2.4	2.7	6.8	2.6	-1.3	-4.4	-7.9	-2.5	2.7	3.3
-1.9	0.1	1.2	1.7	3.3	7.8	2.1	-3.3	-4.9	-5.2	-1.5	-0.1	4.1
=	0.0	0.2	0.5	4.4	1.4	3.7	-0.6	-2.6	-3.9	-2.0	0.0	1.8

Table 7.4.1 (cont.) (Page 2 of 2).

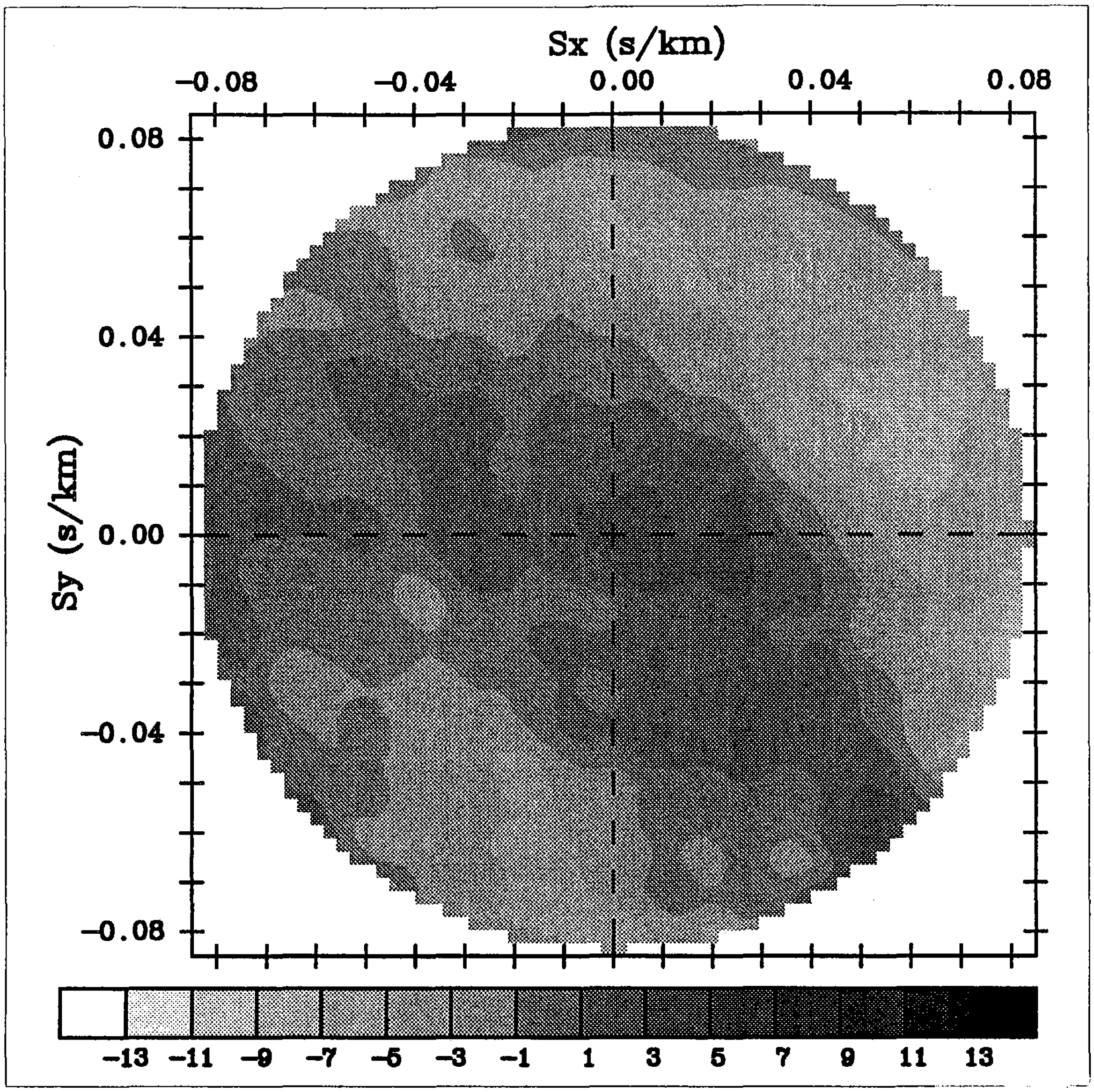

Fig. 7.4.1. The low-pass filtered SP P-wave ray travel time corrections at subarray 01A, for the ST model (given in Table 7.4.1) and for slowness values less than 0.08 s/km. The SP sampling rate is 20 Hz, and the time delay is given in units of 0.05 s.

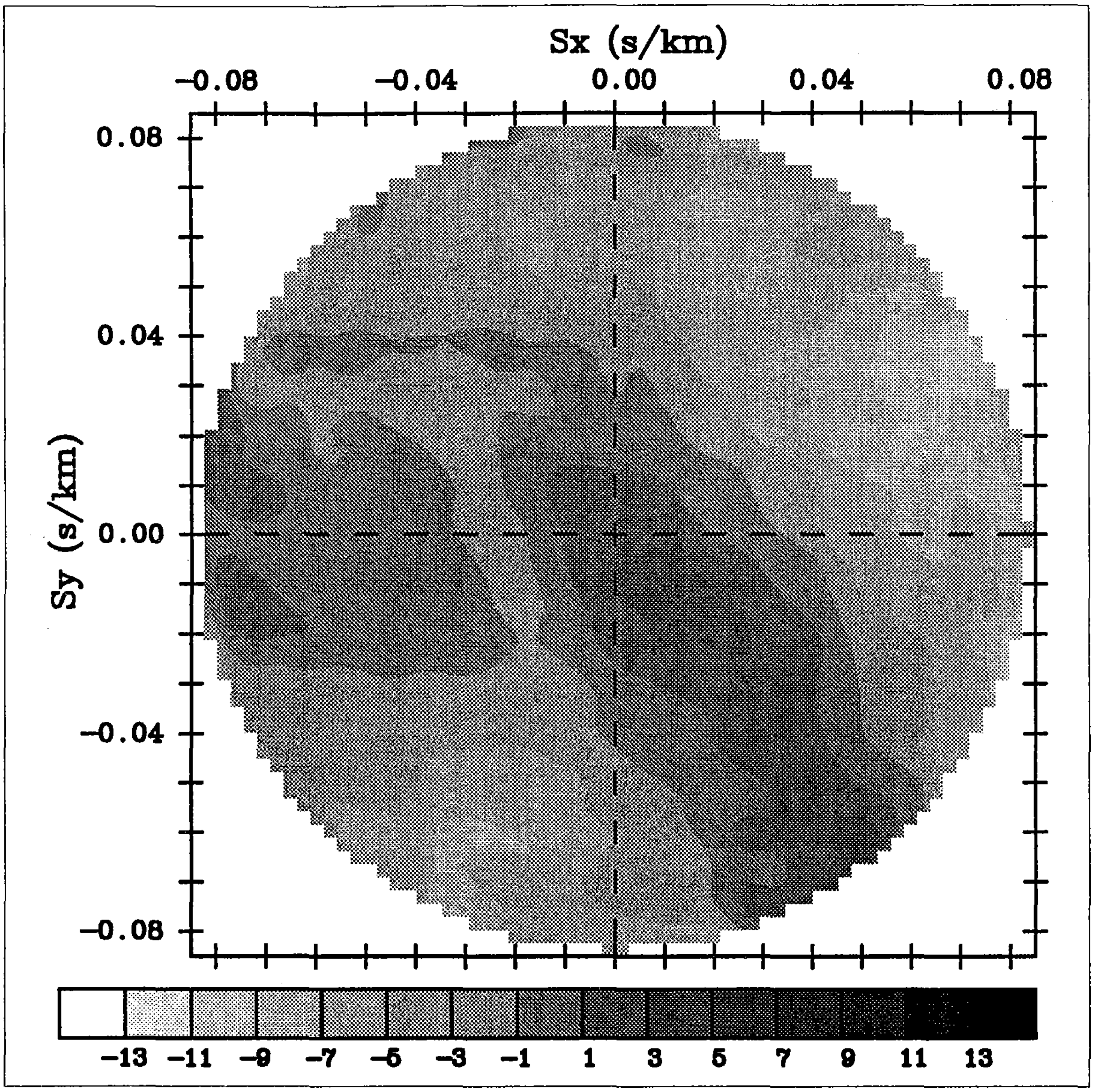

Fig. 7.4.2. The low-pass filtered SP P-wave time corrections at subarray 01A for the DT model and a 1 Hz damped sine reference pulse.

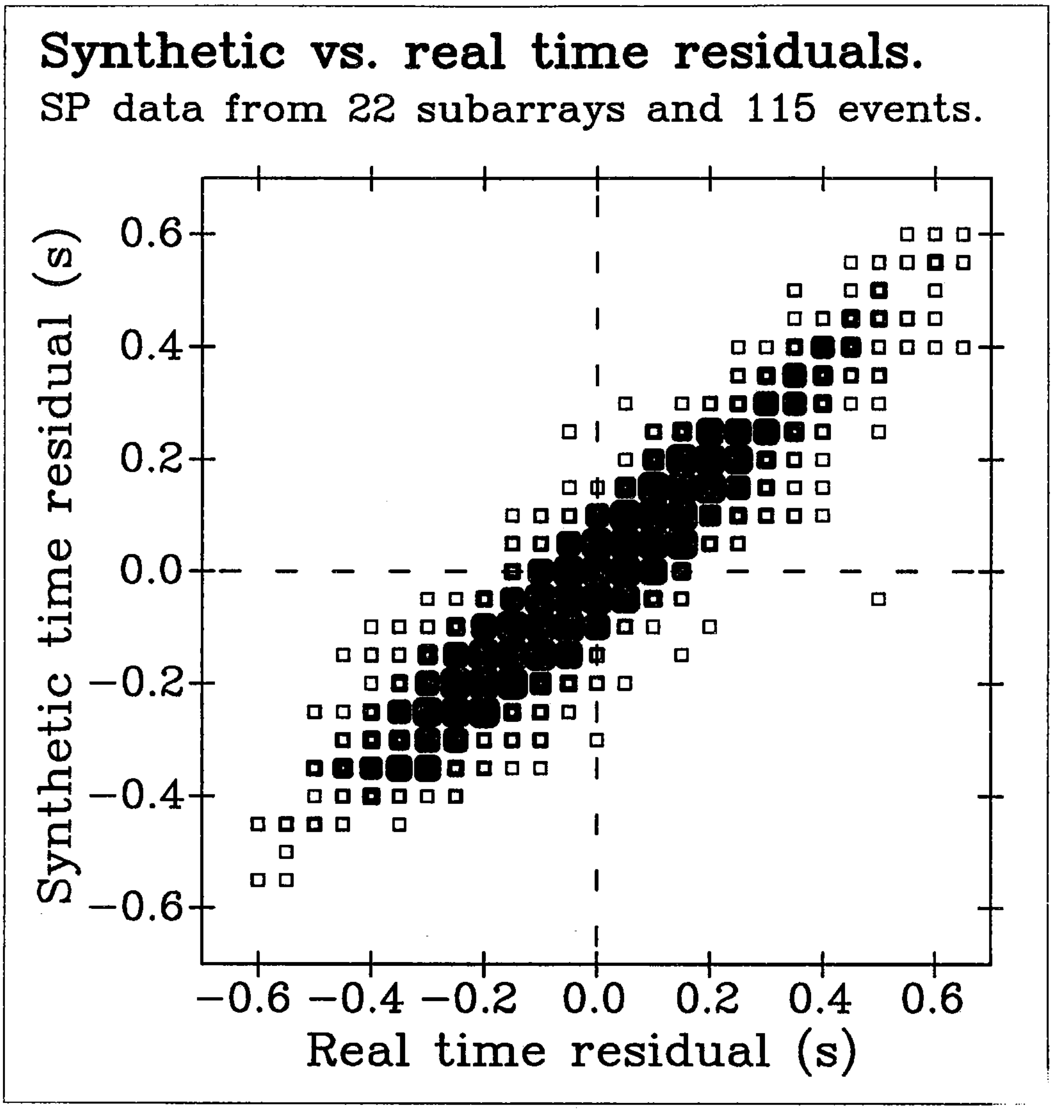

Fig. 7.4.3. Predicted SP P-wave ray travel time residuals versus observed time residuals for the ST model. Symbol size is proportional to number of data.

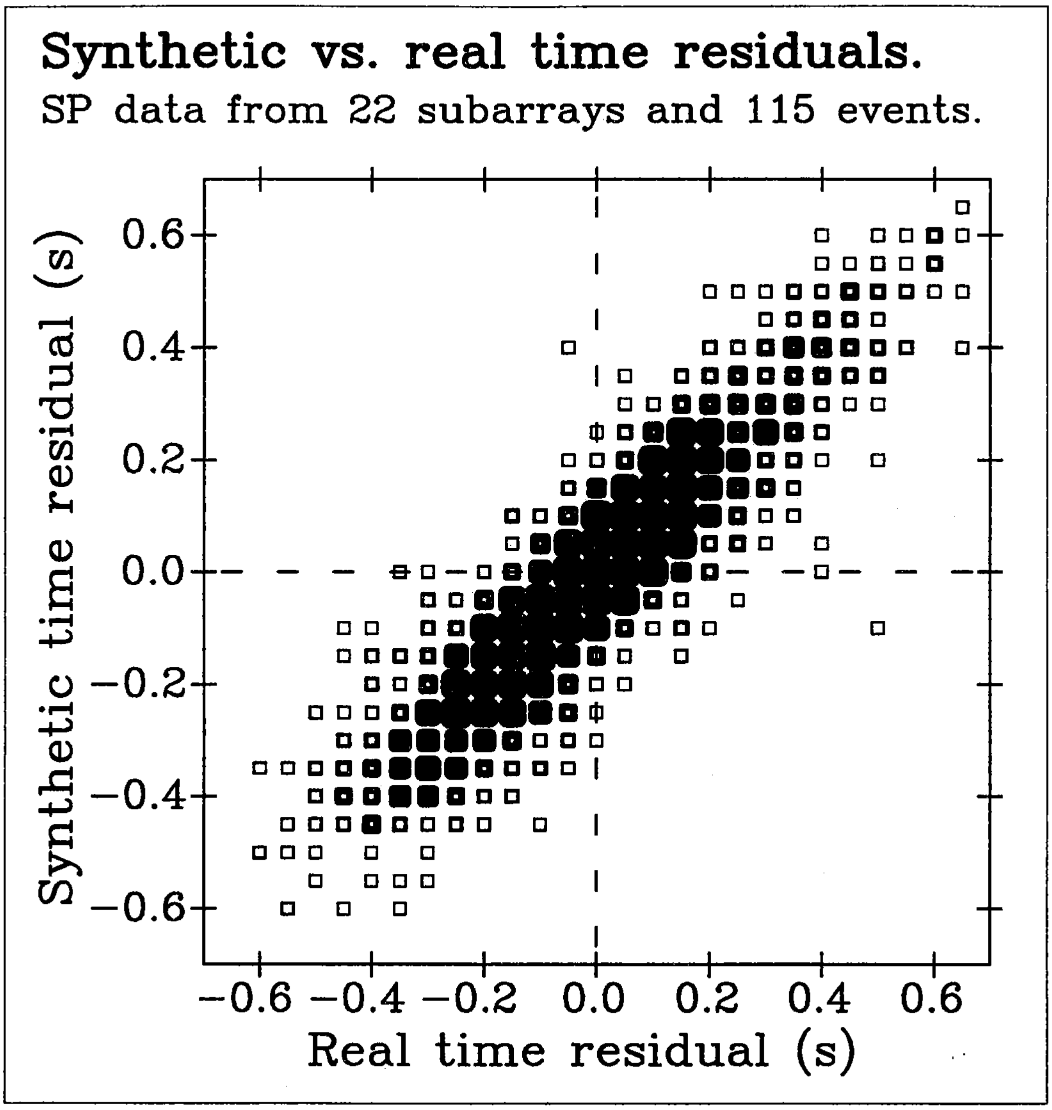

Fig. 7.4.4. Predicted SP P-wave time residuals versus observed time residuals for the DT model and a 1 Hz damped sine reference pulse.

7.5 Automatic phase association and event location using data from a network of seismic microarrays

Introduction

As the number of digital seismic stations around the world increases, it becomes more and more important to automate the data processing. Traditionally, the data processing has consisted of the following steps:

- Detection of phases at the individual stations.
- Extraction of parameters of the detected phases.
- Association of phases at the different stations to form events.
- Event location.

To be able to conduct automatic phase association and event location, initial identification and azimuth estimation of the detected phases are essential.

Using three-component data from NORESS and ARCESS, Suteau-Henson (1991) showed that P- and S-phases could be correctly classified from polarization attributes with a success rate of 82% for NORESS and 89% for ARCESS. P-wave azimuths at both stations were estimated with a standard deviation of 7-11^o. At ARCESS, the S-wave azimuths had a standard deviation of 18-19^o, although with a 180^o ambiguity, whereas the scatter in the S-wave azimuths at NORESS were signifcantly larger (a standard deviation of 25^o for L_g and 42^o for S_n).

Riviere-Barbier et al. (1992) conducted a similar study using three-component data from the IRIS/IDA stations in the former USSR. The results obtained from analysis of these 4 stations did not quite match the results obtained for NORESS and ARCESS, mainly due to more complex geology near the receivers. In both studies referenced above, the large differences in the wave propagation characteristics between the different regions required that the phase identification criteria be developed individually for each three-component station.

Despite the documented performance of different three-component processing schemes, there are to our knowledge no sparse three-component network where phase detection, phase association and event location are conducted in a completely automatic mode. It has, however, been demonstrated that the information provided by individual seismic arrays permits automatic phase association and event location using a network of array stations. The precise azimuth and apparent velocity estimates provided by f-k analysis of the array sensors constrain the use of the detected phases in the phase association procedure. Utilizing this information, the ESAL algorithm of the Intelligent Monitoring System (IMS) (Bache et al., 1990) produces routinely both regional and teleseismic event locations, using data from the 4 regional arrays in northern Europe (ARCESS, FINESA, GERESS and NORESS). Based on a somewhat different approach, the generalized beamforming method (GBF) (Ringdal and Kværna, 1989) produces automatically a regional bulletin using the same detection data.

A study of data recorded at the NORESS array (Kværna and Ringdal, 1992) showed that by supplementing a three-component station with a very small vertical sensor three-element array with a typical aperture of 300 meters, reliable phase identification could be obtained. The quite stable apparent velocity and azimuth estimates produced by f-k analysis of the 4 vertical sensors of this microarray, indicates that data from a network of such microarrays can be processed using existing phase associaton and event location algorithms.

In this contribution we will first evaluate the performance of microarrays at the ARCESS and FINESA sites. Although a separate study has been conducted at NORESS (Kværna and Ringdal, 1992), we will for comparison reevaluate the performance of a microarray at NORESS. Secondly, we will conduct network phase associaton and event location applying the GBF method to microarray data from ARCESS, FINESA and NORESS, see Fig. 7.5.1.

Microarrays

For all three microarrays we conducted automatic detection processing and post-detection analysis for a period of 12 days (9-20 April 1992). The detection processing was similar to that used in the study of Kværna and Ringdal (1992).

The post-detection processing included broadband f-k array analysis (Esmersoy et al., 1985; Kværna and Doornbos, 1986) of each detected signal using the 4 vertical-component sensors of the microarrays. For the f-k analysis, we used a 5 sec. long data interval starting 0.5 sec. before the estimated onset time, and a frequency band similar to the filter band of the detecting beam.

To obtain a data base against which to evaluate our results, we extracted all seismic phases detected by the three full arrays and associated with regional events for the 12-day period. Results from the generalized beamforming procedure (GBF) (Ringdal and Kværna, 1989) were used in order to validate these reference events. P-coda detections and multiple S-phases were ignored, so that each event provided a maximum of 3 phases (P, S and L_g). These phases were then matched to the detection lists produced by the microarrays, and the apparent velocity and azimuth estimates were compared.

The problem of false alarms is inevitably encountered when a detector is operated at a low detection threshold. In conducting automatic phase association and location it is critical to identify these false alarms. When processing the full arrays, phases with low apparent velocities (< 3.0 km/s) are generally discarded from further analysis. As the final step in the analysis of the individual microarrays, we evaluated their capability to identify phases with low apparent velocities. This was done by matching all detections of the microarray (both associated and unassociated phases) to the full array detection list, using the apparent velocitiy estimates of the full array as the reference.

ARCESS

The geometry of the ARCESS microarray is given in Fig. 7.5. 2. The center instrument A0 is three-component, whereas A1-A3 are vertical only. The aperture is about 300 meters.

Fig. 7.5.3 shows the apparent velocity estimates derived from vertical sensors of the microarray for *P* phases (circles) and *S* phases (asterisks) for the reference data set of phases associated with regional events. Of the 303 phases analyzed, 79.2% were correctly classified as *P* or *S* when an apparent velocity of 5.8 km/s was used to separate the two classes. These results are not as good as those earlier published for the NORESS site (Kværna and Ringdal, 1992), where a success rate exceeding 95% was found. It is particularly significant that for epicentral distances less than 600 km, several P-phases have S-type apparent velocities on the microarray. It is most likely that this phenomenon is due to the near-receiver structure, although no studies have been conducted to map the structure in any detail.

We have attempted to improve the initial phase identification by adding an additional constraint on the parameter data. We have observed that due to the preceding *P*-coda, the *S*-phases have seldom a high signal-to-noise ratio (SNR), whereas many of the *P* phases have high SNR. Based in these observations the following rule was introduced:

Phases with SNR > 10 and apparent velocity > 4.5 km/s are P-phases.

This improved the percentage of correctly classified phases to 84.8%.

In this study we have not attempted to include any three-component polarization attributes in the initial phase identification, but tried to evaluate what can be achieved using only f-k analysis of the 4 vertical sensors. As mentioned in the introduction, Suteau-Henson (1991) showed that by using three-component data from ARCESS, *P*- and *S*-phases could be correctly classified with a success rate of 89%. This indicates that if we combine the polarization attributes derived from the three-component instrument of the microarray with the attributes derived by f-k analysis of the 4 vertical sensors, there may be a significant improvement in the number of correctly classified phases.

Figs. 7.5.4 and 7.5.5 show a comparison between the azimuth estimates computed by f-k analysis of the microarray and the azimuth to the epicenters of the reference data set (computed by the GBF algorithm), for *P* and *S*-phases, respectively. For the *P*-phases of Fig. 7.5.4 the median error is 10.4^{o} and for the *S*-phases of Fig. 7.5.5 the median error is 6.8^{o}. These results show that azimuth constraints can be actively used in the phase association and event location procedure.

As the final step in the evaluation of the ARCESS microarray we estimated its capability to identify noise detections (false alarms). The reference data here were all detections of the full array where the f-k spectra showed typical signal behavior with a pronounced peak. The results are presented in Table 7.5.1a. From this table it is seen that 75.4% of the evaluated detections were correctly classified applying broadband f-k analysis to the microarray data.

For the 303 phases verified to be associated with regional events, a similar statistics is given in Table 7.5.1b. The important information in this table is that no associated phases are interpreted by the microarray as noise-detections (an apparent velocity of 3.2 km/s is used to determine the upper bound on the class of noise detections). From Tables 1a and 1b it can thus be concluded that for the data set considered, 36.3% of all microarray detections at ARCESS can be discarded from the automatic phase association and event location processing without classifying any verified regional phases as noise.

FINESA

The geometry of the FINESA microarray is given in Fig. 7.5.6. The sensors A1-A3 make an aperture of about 500 meters. The vertical component instrument A0 is not located at the center of the triangle, but is still the only candidate for a center instrument in the microarray. The three-component instrument is located at A1.

Fig. 7.5.7 shows the apparent velocity estimates derived from the four vertical sensors of the microarray or *P* phases (circles) and *S* phases (asterisks) for the reference data set of phases associated with regional events. Of the 355 phases analyzed, 78.6% were correctly classified as *P* or *S* when an apparent velocity of 5.8 km/s was used to separate the two classes. This is close to the success rate obtained for the ARCESS microarray. The majority of the events in the reference data base are found in the active mining areas in Estonia and western Russia, in a distance range between 150 and 250 km from the FINESA site. This is clearly seen on Fig. 7.5.7.

Another feature of Fig. 7.5.7 is the occurence of *P*-phases with very low apparent velocities in the same 150-250 km distance range. By comparing Figs. 7.5.6 and 7.5.2 we find that the aperture of the FINESA microarray is about 200 meters larger than the aperture of the ARCESS microarray. When processing local and regional phases with high dominant frequencies at the FINESA microarray, broad-band f-k analysis will suffer from spatial aliasing and the lack of coherency between the sensors, and some *P*-phases will therefore come out with low apparent velocities. We can overcome this problem by lowering the frequency band for f-k analysis or alternatively reduce the sensor spacing, but such steps have not been taken in this study. Note that for distances exceeding 400 km, the separation between *P* and *S*-phases are excellent.

Fig. 7.5.8 and Fig. 7.5.9 show a comparison between the azimuth estimates computed by f-k analysis of the microarray and the azimuth to the epicenters of the reference data set (computed by the GBF algorithm), for *P* and *S*-phases, respectively. For the *P*-phases of Fig. 7.5.8 the median error is 13.4^o and for the *S*-phases of Fig. 7.5.9 the median error is 8.5^o. This is more than observed at the ARCESS array. The apparent alignment of *P*-wave azimuth estimates at about 150^o (see Fig. 7.5.8) is also related to the problem with the lack of coherency and spatial aliasing at high frequencies. For such phases the f-k analysis often results in a low apparent velocity and an azimuth close to 150^o.

In Table 7.5.2a we present results from analysis of all detections at the FINESA microarray for the 12-day period. As for ARCESS we used the all full array detections where the f-k spectra showed typical signal behavior with a pronounced peak. 70.1% of the microarray detections were correctly classified, which is less than at ARCESS. For the 355 phases verified to be associated with regional events a statistics similar to that of Table 7.2.1b is given in Table 7.5.2b. Both Tables 7.5.2a and 7.5.2b show that a significant number of *P*- and *S*-phases obtain low apparent velocities from f-k analysis of the microarray. This implies that if we were to discard detections with low apparent velocities from further analysis, we would also miss some of the real *P*- and *S*-phases, and that the total benefit from discarding the low-velocity detections in the case of FINESA is very moderate.

NORESS

Although the performance of a microarray at NORESS has been evaluated in a separate study (Kværna and Ringdal, 1992), we will for comparison reevaluate its capability using the common 12-day data set. Fig. 7.5.10 shows the geometry of the NORESS microarray, which is similar to that of ARCESS.

Fig. 7.5.11 shows the apparent velocity estimates derived from the 4 vertical sensors of the microarray for *P* phases (circles) and *S* phases (asterisks) for the reference data set of phases associated with regional events. Of the 164 phases analyzed, 93.3 % were correctly classified as *P* or *S* when an apparent velocity of 6.0 km/s was used to separate the two classes. This confirms the results of the study of (Kværna and Ringdal, 1992).

Figs. 7.5.12 and 7.5.13 show a comparison between the azimuth estimates computed by f-k analysis of the microarray and the azimuth to the epicenters of the reference data set (computed by the GBF algorithm), for *P* and *S*-phases, respectively. For the *P*-phases of Fig. 7.5.12 the median error is 14.0^0 and for the *S*-phases of Fig. 7.5.13 the median error is 6.5^0.

Table 7.5.3a gives results from analysis of all detections at the NORESS microarray for the 12-day period. 77.0% of the microarray detections were correctly classified, which is somewhat less than the percentage obtained by Kværna and Ringdal (1992). 11.2% of the detections were classified as noise which is significantly less than the percentage obtained by Kværna and Ringdal (1992). This difference can be explained by a difference in the noise field, as there are time intervals at NORESS when the number of detections with low apparent velocity increases substantially due to increased water flow and industrial activity in the nearby regions (Kværna, 1990). As was done for the other two microarrays we alse computed a statistics for the phases verified to be associated with regional events. We find from Table 7.5.3b that only one of the associated phases is interpreted as noise when an apparent velocity of 3.2 km/s is used as the upper bound on the class of noise detections.

Summary

We have found that seismic microarrays at the ARCESS and FINESA sites do not match the NORESS microarray performance in separating *P*- and *S*-phases based on the apparent velocity estimates. The percentage of correctly classified regional phases were for ARCESS 79.2%, for FINESA 78.6% and for NORESS 93.3%. The success rate for ARCESS was increased to 84.8% when an additional constraint based on SNR and apparent velocity was placed on the definition of *P*-phases. No attempt has been made to include three-component data or context-sensitive information in the initial phase identification, although the potential for improvement is significant (Suteau-Henson, 1991, Riviere-Barbier et al., 1992).

A summary of the different success rates and median errors is given in Table 4. For direct comparison with the results of Riviere-Barbier et al. (1992), we have also included the percentage of phases with azimuth differences within 25°.

The simple procedure of using apparent velocity estimates to classify *P*- and *S*-phases is very different from the complex classification criteria used at three-component stations (Suteau-Henson, 1991, Riviere-Barbier et al., 1992). For the three microarrays analyzed, almost the same classification criterion could be applied to each site. The only difference was that at NORESS an apparent velocity of 6.0 km/s ws used to separate *P* and *S*, whereas at ARCESS and FINESA 5.8 km/s was used. This indicates that at microarrays, very little data and data analysis is required to make initial phase identification work properly. In the two studies of three-component data referenced above it was found that the polarization characteristics of seismic phases were strongly site dependent, and that consequently an extensive data set had to be collected at each station in order to find usable criteria for initial phase identification.

The topic for the next section is to test whether the results presented above are of sufficient merit to allow reliable, automatic phase association and event location using data from a network of microarrays.

Phase association and event location using microarray data

We will in this work apply the generalized beamforming (GBF) method (Ringdal and Kværna, 1989) for associating phases and locating regional events using the detections from the three microarrays. The method is currently in routine use at NORSAR for processing data from the 4 regional arrays in northern Europe (ARCESS. FINESA, GERESS and NORESS), and our attempt will be to process the microarray data without introducing major changes in the processing parameters of the now operational version of the GBF algorithm. For details on the method we refer to a documentation report now in progress. However, we will in the following briefly outline the basic principles.

The GBF algorithm

The basic idea behind the GBF method is to associate detected phases to form seismic events by counting the number of phases that match a hypothetical event at a given target (beam) location at a given origin time. In order to avoid interfering phases that do not belong to the event in question, we impose constraints as part of the phase matching process. The most important constraints of the current operational GBF method are the following:

- Constraint on phase type (*P*, *S* and *noise*) based on apparent velocity estimates.
- Constraint on azimuth to epicenter from actual phase azimuth estimates.

- Constraint on distance to epicenter inferred from values of apparent velocity and dominant frequency.
- Constraint on the allowable phase type based on the pattern of phase and coda detections for local and regional events.
- Constraint on distance to epicenter from the pattern of *P*- and *S*-phases for local and regional events.

When processing the microarrays with the GBF method, we only introduced one single modification to the current operational GBF parameters. This was by adding the possibility of redefining *S*-phases to *P*- phases at ARCESS (see section on the ARCESS microarray). We might as well have tuned the GBF parameters more specifically towards processing microarrays, but as one of our intentions was to check the robustness of the GBF algorithm, we initially avoided such fine tuning.

Reference events

The events declared by the GBF algorithm from processing of the full regional arrays ARCESS, FINESA and NORESS were used as a reference data base for the 12 day period (9-20 April 1992). The GBF output was manually checked for inconsistencies, and false events were removed. This resulted in 428 reference events, and those with magnitude above 1.5 are shown on the map of Fig. 7.5.14. Note the large number of mining explosions on the Kola peninsula and in Estonia. The magnitudes M_L were computed using the formula of Båth (1981), and in the cases where several arrays detected *S*-phases, the magnitudes were averaged.

The reference locations should be used with caution, as the event waveforms have not been interactively analyzed.

Event detectability

As a definition of a reference event found by GBF processing of the microarray network we have used the following criterion:

If the difference in event location is less than 400 km and the difference in origin time is less than 120 seconds, the event is declared as detected by the microarray network.

The motivation behind using such wide acceptance limits is that all of these events will be flagged as candidates for subsequent interactive analysis, such that errors in phase association and timing of the detected phases can be corrected by the analyst.

Fig. 7.5.15 illustrates the event detectability as a function of distance to the closest array. Detected events are marked as stars, whereas non-detected events are shown by circles. A total number of 261 events (61%) were found by the microarray network. It is seen that beyond 600 km, no event with magnitude less than 2.0 is detected, whereas just below this distance limit events close to magnitude 1.0 are detected. We will therefore in the following proceed with a detectability study for events within 600 km of the closest array. Having the the map of Fig. 7.5.14 in mind, this constitute a geographical region covering a triangle with the three microarrays in the corners extended by a circle sector of 600 km radius around each microarray. An area as defined above will also be the typical size of a region of interest for possible future microarrays.

A maximum likelihood estimation of event detectability (Ringdal, 1975) of the region defined above is presented in Fig. 7.5.16. From the number of detections/no detections at each magnitude, the 50% and 90% incremental detection thresholds are inferred. The 90% threshold is about $M_L = 1.8$, whereas the 50% threshold is found to be about $M_L = 0.8$. These numbers are further confirmed by comparing with the seismic bulletin of the University of Helsinki, Finland.

For an event to be defined by the GBF algoritm, a minimum of two defining phases are required. This might be, for example, a *P* and an *S* at one array or two *P*-phases at two arrays. In the previous section discussing the performance of each microarray, we found that a significant number of seismic phases were discarded from GBF processing due to erroneous estimates of apparent velocity and azimuth. In such cases where the azimuth or apparent velocity estimates fall outside the allowable range for GBF processing, it will often happen that a coda detection is used as a defining phase. This exploitation of redundant detections is one of the strong features of the GBF algorithm leading to the good event detectability of the microarray network, although the phase associations and the corresponding event location will not always be perfect.

Location differences

For 249 microarray events located within 600 km of the closest array, a histogram of the location difference between the microarray network and the full array network is given in Fig. 7.5.17. The median difference of the population is 47.4 km. The causes of the location differences can be divided into three types:

1. Differences in estimates of phase arrival times.
2. Use of coda phases as defining phases.
3. Occasionally, erroneous phase association.

Type 1 and 2 will in most cases result in minor to modest location differences, whereas type 3 often will cause large deviations.

By dividing the population into events with the same number of associated phases (microarray network), we obtain the distribution of Table 5. It is seen that the differences are generally reduced when the number of associated phases increase. This is due to the fact that the likelihood of erroneous phase association (type 3) is reduced when the number of associated phases increase.

False events

In practical operation of any phase association and event location algorithm, it is essential that the number of false events is kept at a moderate level. Our experience with the GBF algorithm applied to the full array network is that the number of false events is rather low.

A false alarm rate of 26% is found for the automatic GBF algorithm applied to the microarray network (see Table 7.5.6), which is a number that does not present a problem in an analyst review situation. No event with more than 3 associated phases (irrespective of number of arrays) were false (see Table 7.5.7), and the vast majority of the false events were one-array events with two defining phases (a *P* and an *S*-phase). From Table 7.5.8 it is clearly seen that most of the false 1-array events were found at the FINESA array. This is in accordance with our finding that the FINESA microarray had the lowest success rate in classifying *P* and *S*- phases from apparent velocity estimates.

Summary

It has been demonstrated that information derived from a sparse network of seismic microarrays (interstation distance ~ 1000 km) permits successful automatic phase association and regional event location using the GBF algorithm. The apparent velocity and azimuth estimates of the detected phases found by f-k analysis of the 4 vertical-component sensors of each microarray place strong constraints on the use of the detected phases. This enables subsequent GBF processing of the detection data to be performed with good event detectability combined with a low number of false events.

Although the initial phase identification based of the apparent velocity estimates from time to time resulted in mis-classification of the phases, the robustness of the GBF algorithm prevented events from being missed. The robustness was also accentuated by the fact that except for one change, the microarray network could be processed with the same parameter settings as the full array network.

For 249 events located within 600 km of the closest array, the median difference between automatic locations by the full array network and by the microarray network was only 47.4 km.

Information from the three-component sensors of the microarrays has not been used in this study, but the work of Suteau-Henson (1991) and Riviere-Barbier et al. (1992), indicate that further improvements in event detectability, correctness of phase association and consequently in event location can be achieved if this information is utilized.

Out of the 353 events formed after automatic GBF processing of the microarray network, only 92 (26%) were found to be false, a number that is easily handled in an analyst review situation. All events with 4 or more defining phases were real. The vast majority of the false events were associated with detections at the FINESA array.

In order to handle the large data volumes produced by modern digital seismic networks, a high degree of automated processing is essential. We have in this work shown that in Fennoscandia a sparse network of microarrays allows for such automated processing. Very little data collection and data analysis needs to be done to tune the parameters for the

algorithms for automatic phase association and event location. The Fennoscandian Shield constitutes a rather simple and homogeneous geological province, and it would therefore be if interest to investigate microarray performances in more complex geological environments.

T. Kværna

References

Bache, T., S. R. Bratt, J. Wang, R.M. Fung, C. Kobryn and J. W. Given (1990), The Intelligent Monitoring System, Bull. Seism. Soc. Am., 80, Part B, 1833-1851.

Båth, M. (1981): Local magnitude-recent research and current trends, Earth-Science Rev., 17, 315-398.

Esmersoy, L., V. F. Cormier and M. N. Toksöz (1985). Three component array processing, In The VELA Program, A. U. Kerr, Editor, Defence Advanced Research Projects Agency, Executive Graphics Services.

Kværna, T. (1990): Sources of short-term fluctuations in the seismic noise level at NORESS, Phys. Earth. Planet. Inter., 63, 269-276.

Kværna, T. and D.J. Doornbos (1986): An integrated approach to slowness analysis with arrays and three-component stations, Semiann. Tech. Summary, 1 October 1985-31 March 1986, NORSAR Sci. Rep. No 2- 85/86, Kjeller, Norway.

Kværna, T. and F. Ringdal (1992): Integrated array and three-component processing using a seismic microarray, Bull. Seism. Soc. Am., 82, 870-882.

Ringdal, F. and T. Kværna (1989): A multi-channel processing approach to real-time network detection, phase association, and threshold monitoring, Bull. Seism. Soc. Am., 79, 1927-1940.

Ringdal, F. (1975): On the estimation of seismic detection thresholds, Bull. Seism. Soc. Am., 65, 1631-1642.

Riviere-Barbier, F., A. Suteau-Henson, V.Z. Ryaboy and J.A. Carter (1992): Analysis of three-component data from IRIS/IDA stations in USSR, Bull. Seism. Soc. Am., 82, 192-220.

Suteau-Henson, A. (1991): Three-component analysis of regional phases at NORESS and ARCESS: Polarization and phase identification, Bull. Seism. Soc. Am., 81, 2419-2440.

	Classified as:		
Correct phase id (full array)	P (vel>5.8m/s)	S or Lg (3.2<vel≤5.8 km/s)	Noise (vel≤3.2 km/s)
P (vel>5.8)	343 (22.6%)	118 (7.8%)	58 (3.8%)
S or Lg (3.0<vel≤5.8 km/s)	109 (7.2%)	365 (24.0%)	55 (3.6%)
Noise (vel≤3.0 km/s)	6 (0.4%)	28 (1.8%)	439 (28.9%)

Total number of microarray detections evaluated: 1521

Total number of phases correctly classified: 1147 (75.4%)

Table 7.5.1a. All detections of the ARCESS microarray have been used as the basis for this statistics. The detections are classified based on estimated apparent velocities applying broadband f-k analysis to the vertical components of the microarray and "correct" phase identification is based on f-k results from the full ARCESS array.

	Classified as:		
Correct phase id	P (vel>5.8m/s)	S or Lg (3.2<vel≤5.8 km/s)	Noise (vel≤3.2 km/s)
P (from GBF)	86 (28.4%)	47 (15.5%)	0 (0.0%)
S or Lg (from GBF)	16 (5.3%)	154 (50.8%)	0 (0.0%)
Noise (none)	0 (0.0%)	0 (0.0%)	0 (0.0%)

Total number of phases evaluated: 303

Total number of phases correctly classified: 240 (79.2%)

Table 7.5.1b. In this table we have used the phases (*P*, *S* or L_g) verified to be associated with regional events as the "correct" phase identification, and the phases were classified based on estimated apparent velocities applying broadband f-k analysis to the vertical components of the ARCESS microarray.

	Classified as:		
Correct phase id (full array)	P (vel>5.8m/s)	S or Lg (3.2<vel≤5.8 km/s)	Noise (vel≤3.2 km/s)
P (vel>5.8)	385 (31.4%)	70 (5.7%)	42 (3.4%)
S or Lg (3.0<vel≤5.8 km/s)	42 (3.4%)	370 (30.2%)	172 (14.0%)
Noise (vel≤3.0 km/s)	5 (0.4%)	35 (2.9%)	104 (8.5%)

Total number of microarray detections evaluated: 1225
Total number of phases correctly classified: 920 (70.1%)

Table 7.5.2a. All detections of the FINESA microarray have been used as the basis for this statistics. The detections are classified based on estimated apparent velocities applying broadband f-k analysis to the vertical components of the microarray and "correct" phase identification is based on f-k results from the full FINESA array.

	Classified as:		
Correct phase id	P (vel>5.8m/s)	S or Lg (3.2<vel≤5.8 km/s)	Noise (vel≤3.2 km/s)
P (from GBF)	121 (34.1%)	16 (4.5%)	23 (6.5%)
S or Lg (from GBF)	12 (3.4%)	158 (44.5%)	25 (7.0%)
Noise (none)	0 (0.0%)	0 (0.0%)	0 (0.0%)

Total number of phases evaluated: 355
Total number of phases correctly classified: 279 (78.6%)

Table 7.5.2b. In this table we have used the phases (*P*, *S* or L_g) verified to be associated with regional events as the "correct" phase identification, and the phases were classified based on estimated apparent velocities applying broadband f-k analysis to the vertical components of the FINESA microarray.

	Classified as:		
Correct phase id (full array)	P (vel>6.0m/s)	S or Lg (3.2<vel≤6.0 km/s)	Noise (vel≤3.2 km/s)
P (vel>6.0)	260 (39.9%)	13 (2.0%)	9 (1.4%)
S or Lg (3.0<vel≤6.0 km/s)	51 (7.8%)	185 (28.4%)	7 (1.1%)
Noise (vel≤3.0 km/s)	12 (1.8%)	58 (8.9%)	57 (8.7%)

Total number of microarray detections evaluated: 652
Total number of phases correctly classified: 502 (77.0%)

Table 7.5.3a. All detections of the NORESS microarray have been used as the basis for this statistics. The detections are classified based on estimated apparent velocities applying broadband f-k analysis to the vertical components of the microarray and "correct" phase identification is based on f-k results from the full NORESS array.

	Classified as:		
Correct phase id	P (vel>6.0m/s)	S or Lg (3.2<vel≤6.0 km/s)	Noise (vel≤3.2 km/s)
P (from GBF)	70 (42.7%)	2 (1.2%)	0 (6.5%)
S or Lg (from GBF)	8 (4.9%)	83 (50.6%)	1 (0.6%)
Noise (none)	0 (0.0%)	0 (0.0%)	0 (0.0%)

Total number of phases evaluated: 164
Total number of phases correctly classified: 153 (93.3%)

Table 7.5.3b. In this table we have used the phases (*P*, *S* or L_g) verified to be associated with regional events as the "correct" phase identification, and the phases were classified based on estimated apparent velocities applying broadband f-k analysis to the vertical components of the NORESS microarray.

	ARCESS	FINESA	NORESS
Percentage of correctly classified phases	79.2% (84.8%)	78.6%	93.3%
Median azimuth error for P-phases	10.4°	13.4°	14.0°
Percentage of P-phases within 25°	78.5%	73.0%	86.1%
Median azimuth error for S-phases	6.8°	8.5°	6.5°
Percentage of S-phases within 25°	98.2%	88.0%	94.6%
Percentage of all detections classified as noise	36.3%	26.0%	11.2%
Percentage of verified phases classified as noise	0.0%	13.5%	0.6%

Table 7.5.4. This table contain a summary of the success rates for initial phase identification and the median errors in the azimuth estimates of the three microarrays considered. We have also included the percentage of P and S-phases with azimuth differences within 25° of the reference azimuth. Note that f-k analysis of the 4 vertical sensors of the microarrays is the only method being used to obtain these results.

	Number of defining phases (microarray network)						
	2	3	4	5	6	7	8
Number of events	144	53	23	14	9	3	3
Median location difference (km)	55.3	47.4	47.3	33.7	45.3	37.6	0.0
Median magnitude M_L	1.17	1.47	2.10	2.33	2.26	2.53	2.50

Table 7.5.5. After dividing the events into classes based on the number of defining phases, we give for each class the number of events, median location difference to the full network location and the median magnitude. Note that the location differences are generally reduced when the number of associated phases increase.

Declared events	Real events	False events
353	261 (74.0%)	92 (26.0%)

Table 7.5.6. Distribution of real and false events for the 353 events declared after GBF processing of the microarray network.

	1 array	2 arrays	3 arrays
2 associated phases	62	18	-
3 associated phases	3	7	2

Table 7.5.7. Distribution of detecting arrays and the number of associated phases for the false events. No events with more than three defining phases were false.

ARCESS	FINESA	NORESS
12	45	8

Table 7.5.8. Distribution of detecting arrays for false one-array events.

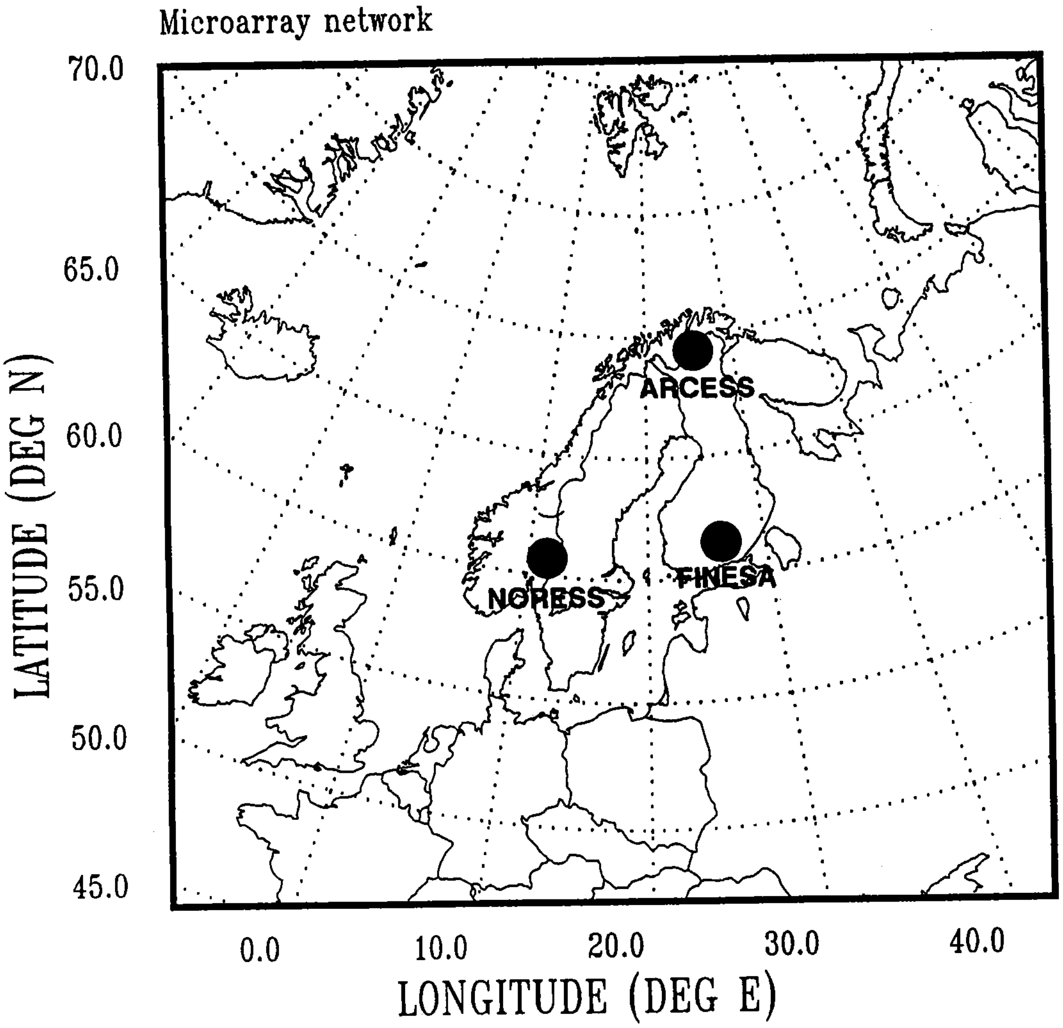

Fig. 7.5.1. Map showing the location of the three Fennoscandian arrays (ARCESS, FINESA and NORESS). The microarray configurations analyzed in this paper are subsets of these arrays.

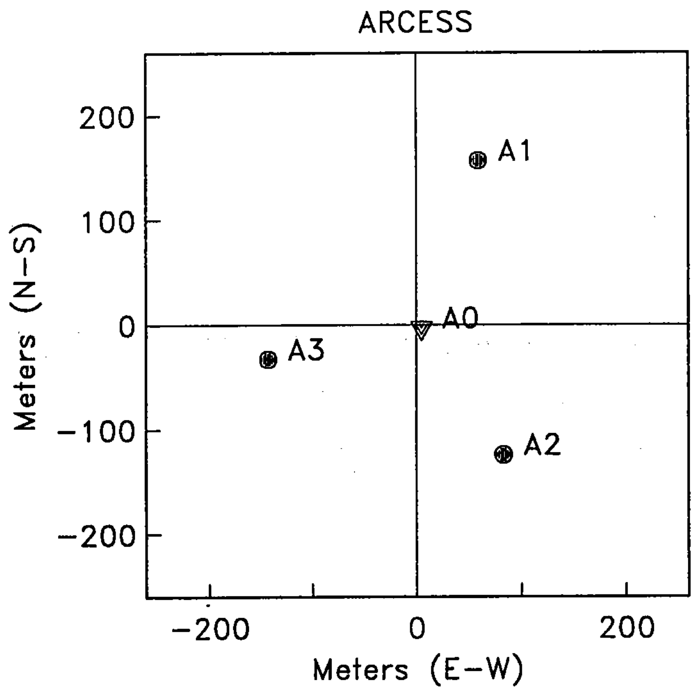

Fig. 7.5.2. This figure gives the locations of the sensors of the ARCESS microarray. The vertical-component sensors are indicated by filled circles, whereas the filled delta symbol represent the 3-component sensor.

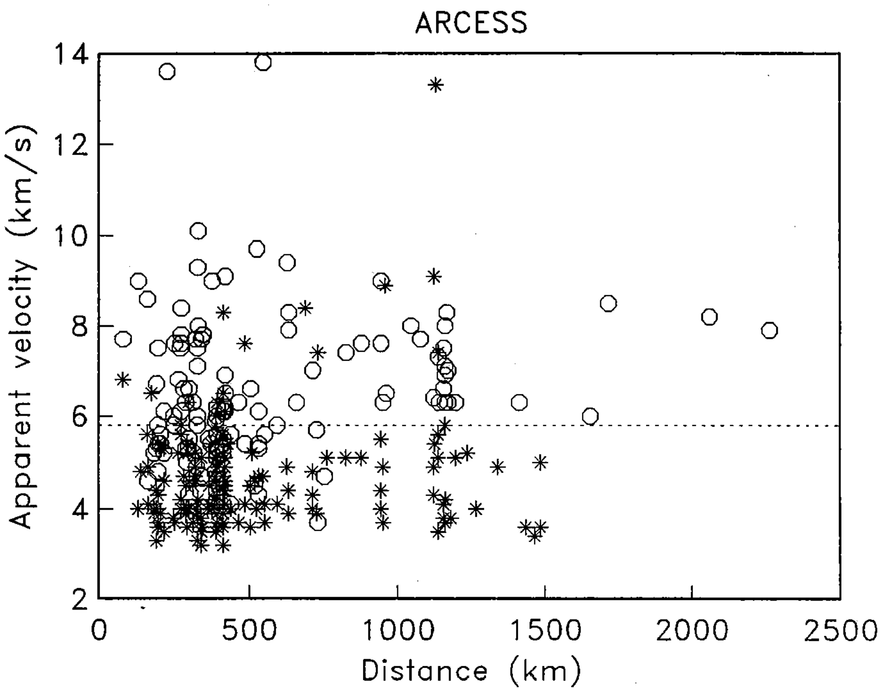

Fig. 7.5.3. Estimated apparent velocities from applying broadband f-k analysis to the vertical components of the ARCESS microarray for *P* phases (circles) and *S* phases (asterisks). An apparent velocity of 5.8 km/s (dashed line) has been used to classify the phases as *P* or *S*. The success rate is 79.2%.

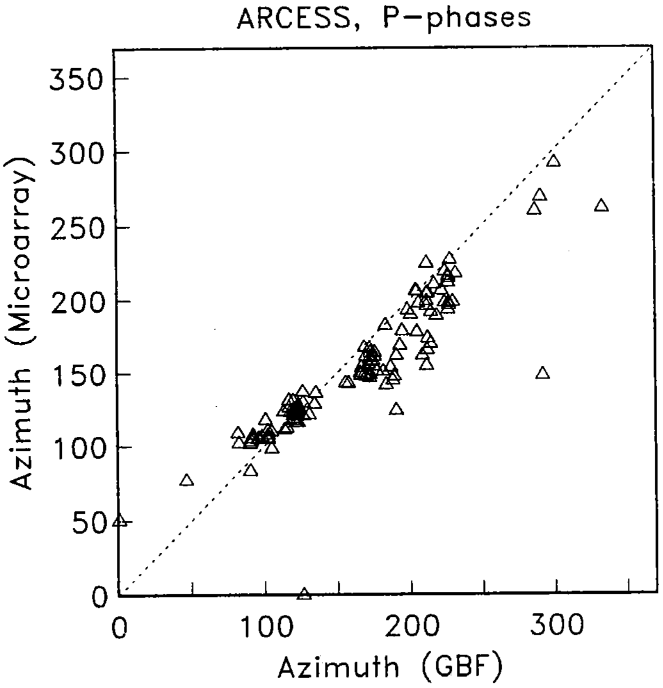

Fig. 7.5.4. Comparison of estimated azimuths of *P* phases using the full ARCESS array and the four vertical components of the ARCESS microarray. The median difference is 10.4°.

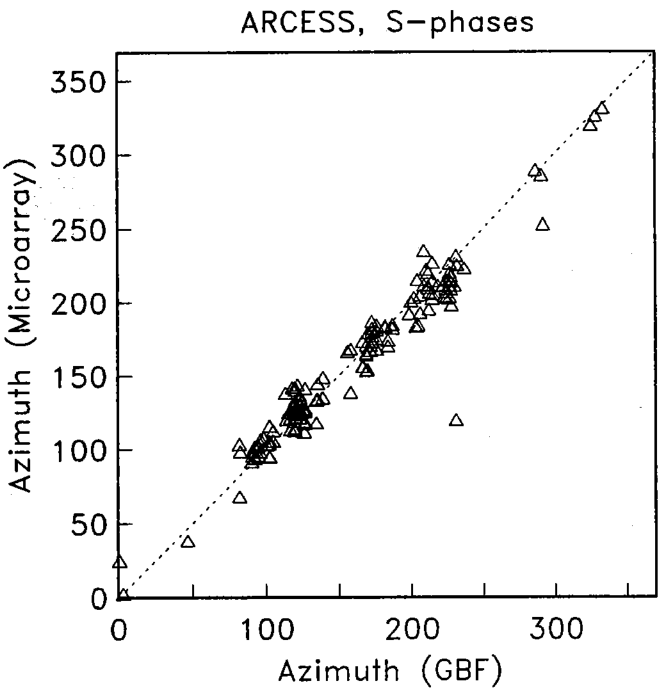

Fig. 7.5.5. Comparison of estimated azimuths of *S* phases using the full ARCESS array and the four vertical components of the ARCESS microarray. The median difference is 6.8°.

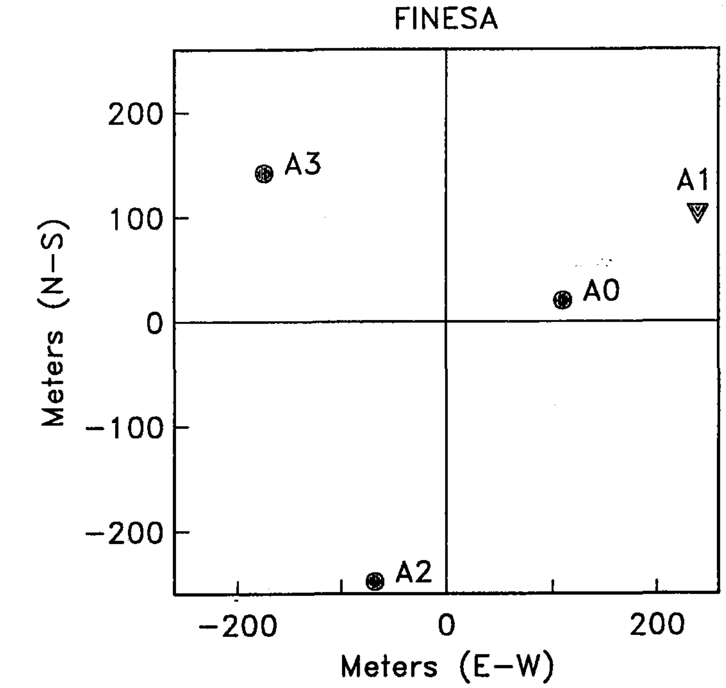

Fig. 7.5.6. This figure gives the locations of the sensors of the FINESA microarray. The vertical-component sensors are indicated by filled circles, whereas the filled delta symbol represent the 3-component sensor.

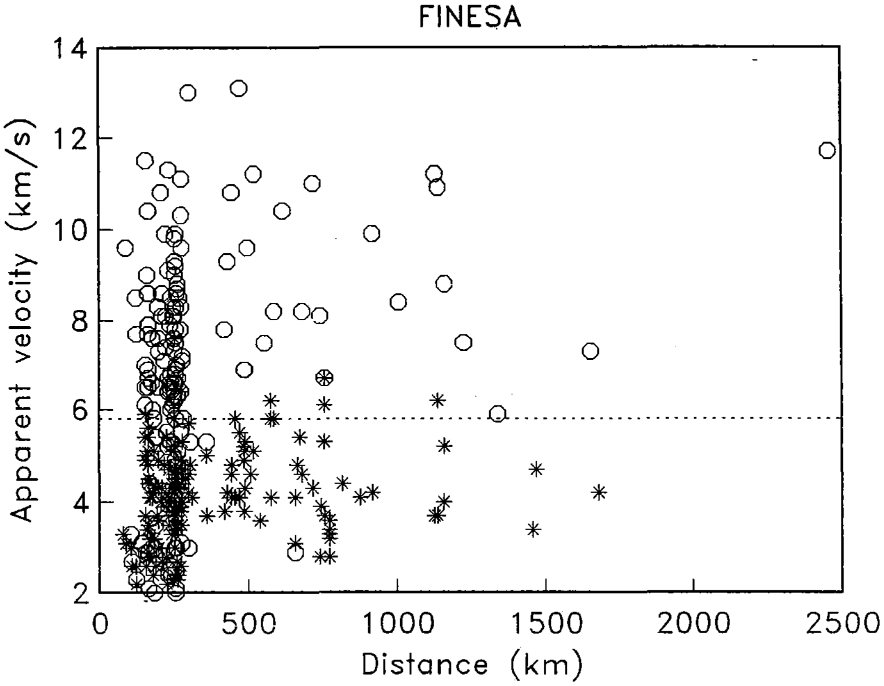

Fig. 7.5.7. Estimated apparent velocities from applying broadband f-k analysis to the vertical components of the FINESA microarray for *P* phases (circles) and *S* phases (asterisks). An apparent velocity of 5.8 km/s (dashed line) has been used to classify the phases as *P* or *S*. The success rate is 78.6%.

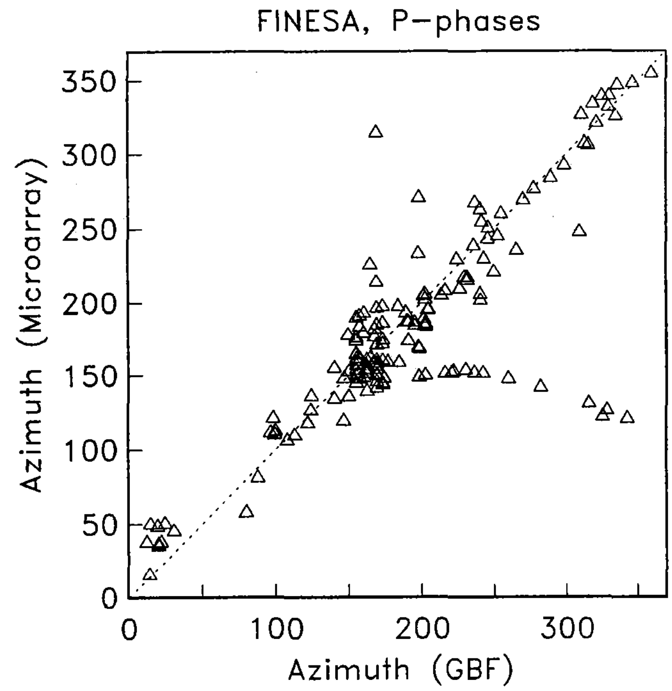

Fig. 7.5.8. Comparison of estimated azimuths of *P* phases using the full FINESA array and the four vertical components of the FINESA microarray. The median difference is 13.4°. Due to the large aperture of the FINESA microarray in comparison with the ARCESS microarray (see Figs. 7.5.2 and 7.5.6) there were some problems with lack of coherency and spatial aliasing at high frequencies. This is the reason for the apparent alignment of *P*-wave azimuth estimates at about 150°.

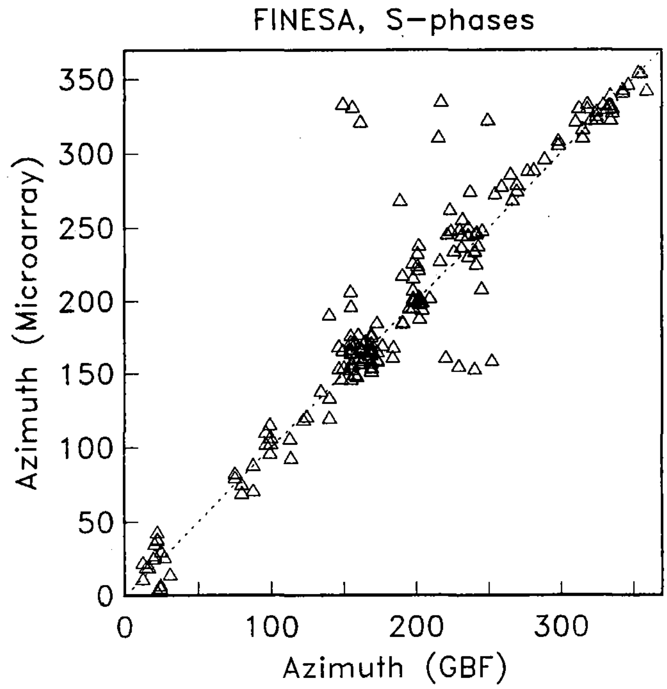

Fig. 7.5.9. Comparison of estimated azimuths of *S* phases using the full FINESA array and the four vertical components of the FINESA microarray. The median difference is 8.5°.

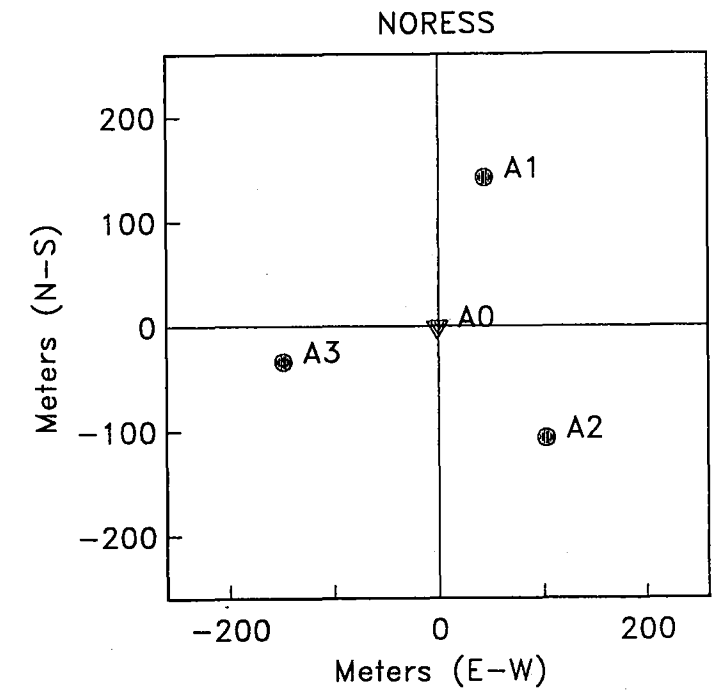

Fig. 7.5.10. This figure gives the locations of the sensors of the NORESS microarray. The vertical-component sensors are indicated by filled circles, whereas the filled delta symbol represent the 3-component sensor.

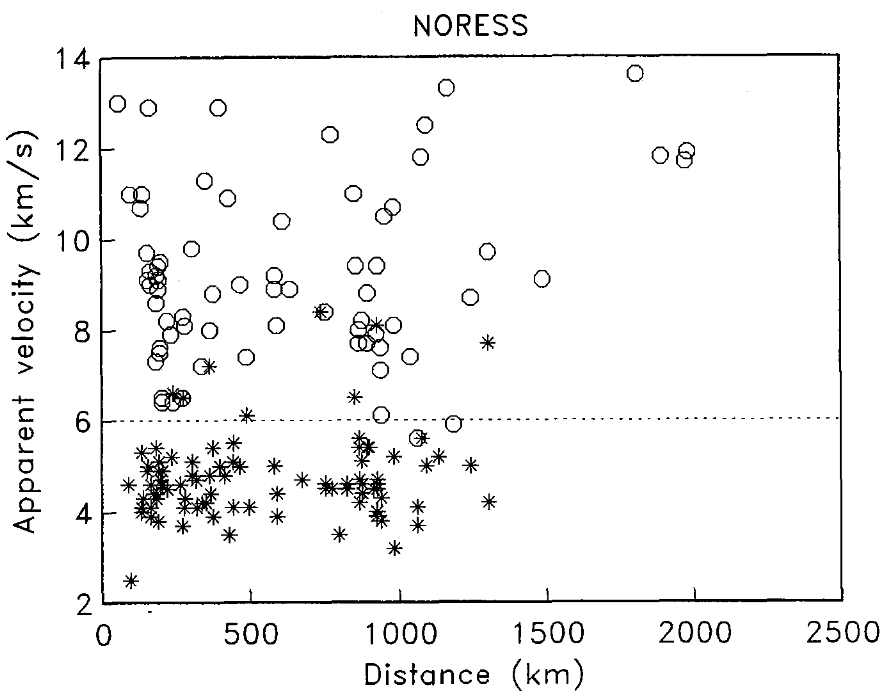

Fig. 7.5.11. Estimated apparent velocities from applying broadband f-k analysis to the vertical components of the NORESS microarray for *P* phases (circles) and *S* phases (asterisks). An apparent velocity of 5.8 km/s (dashed line) has been used to classify the phases as *P* or *S*. The success rate is 93.3%.

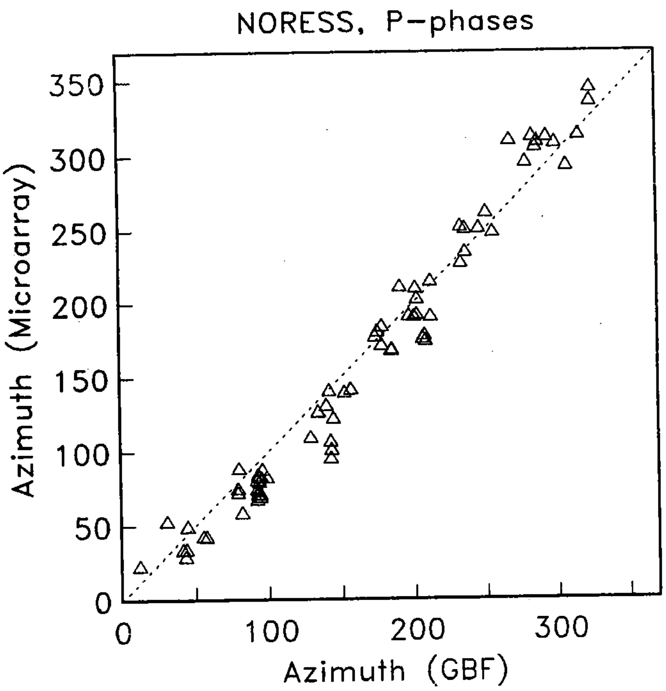

Fig. 7.5.12. Comparison of estimated azimuths of *P* phases using the full NORESS array and the four vertical components of the NORESS microarray. The median difference is 14.0°.

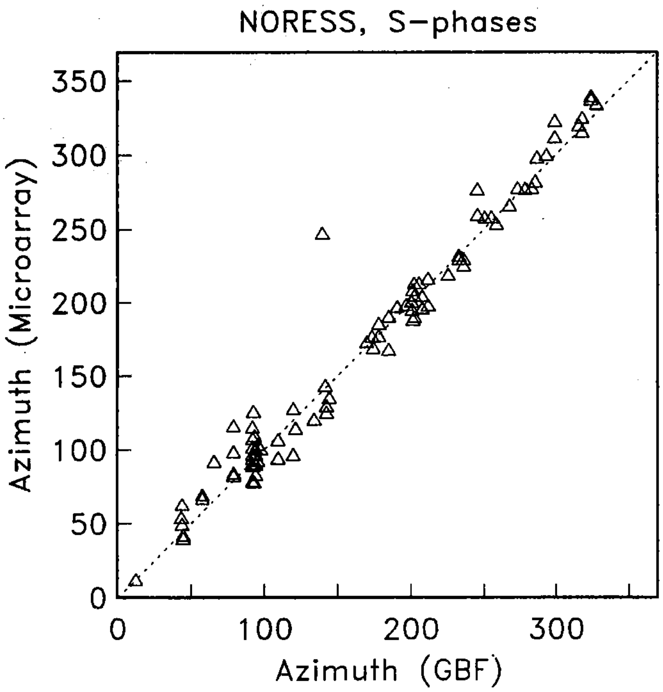

Fig. 7.5.13. Comparison of estimated azimuths of phases using the full NORESS array and the four vertical components of the NORESS microarray. The median difference is 6.5°.

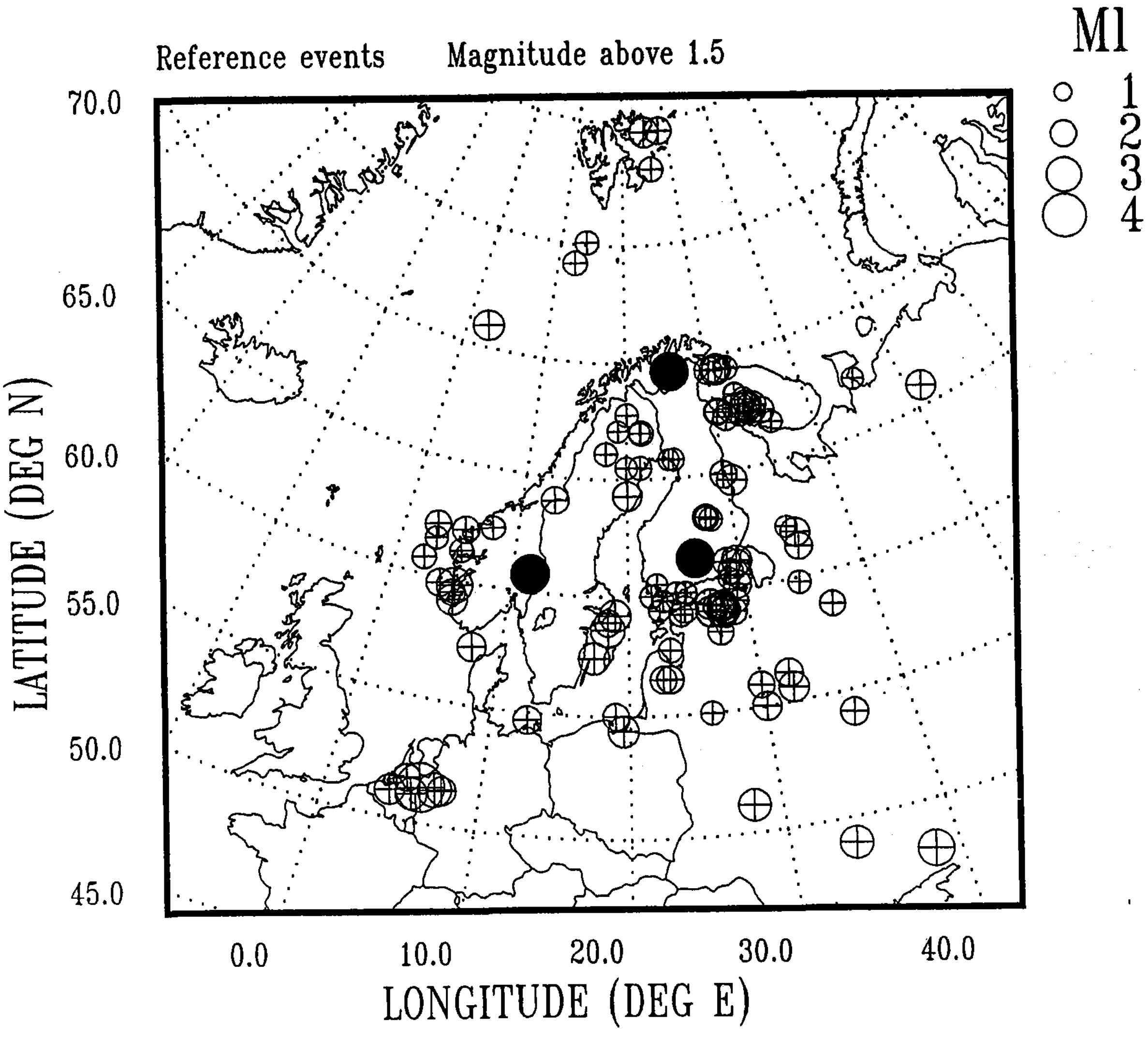

Fig. 7.5.14. Map with reference events with magnitude above 1.5. Note the large number of events (mining explosions) on the Kola peninsula and in Estonia.

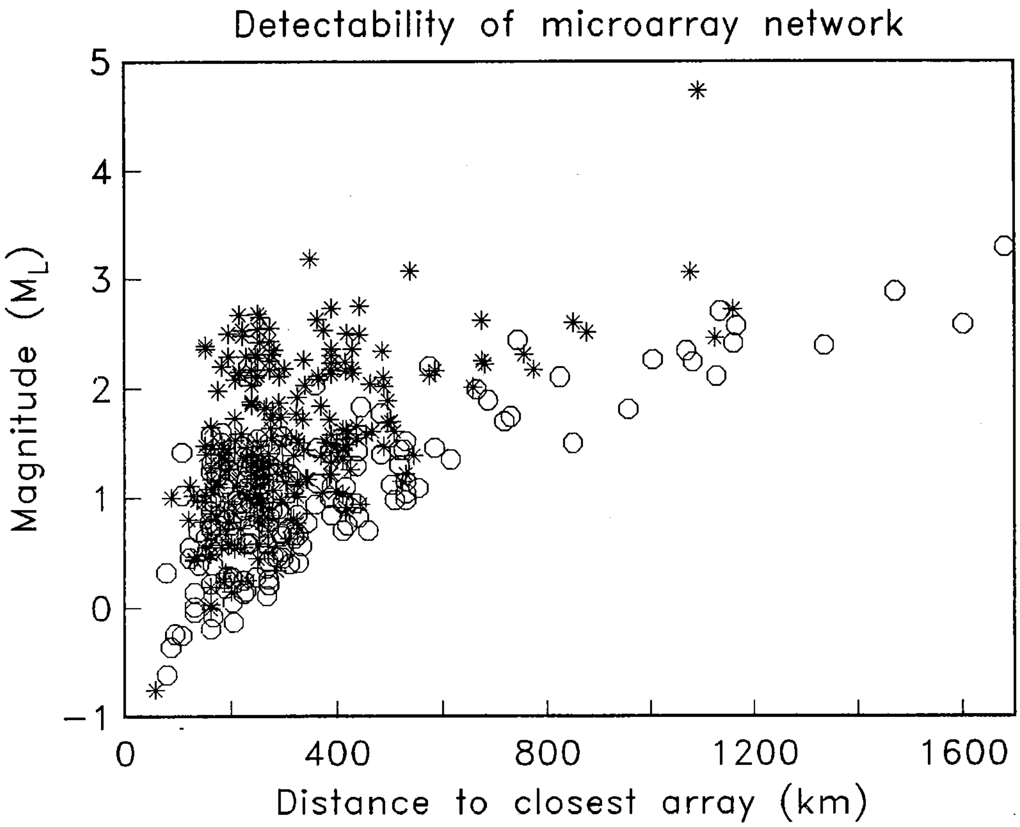

Fig. 7.5.15. Magnitude of reference events versus distance to the closest array. Events found after GBF processing of the microarray network are marked by stars, whereas missed events are marked by circles.

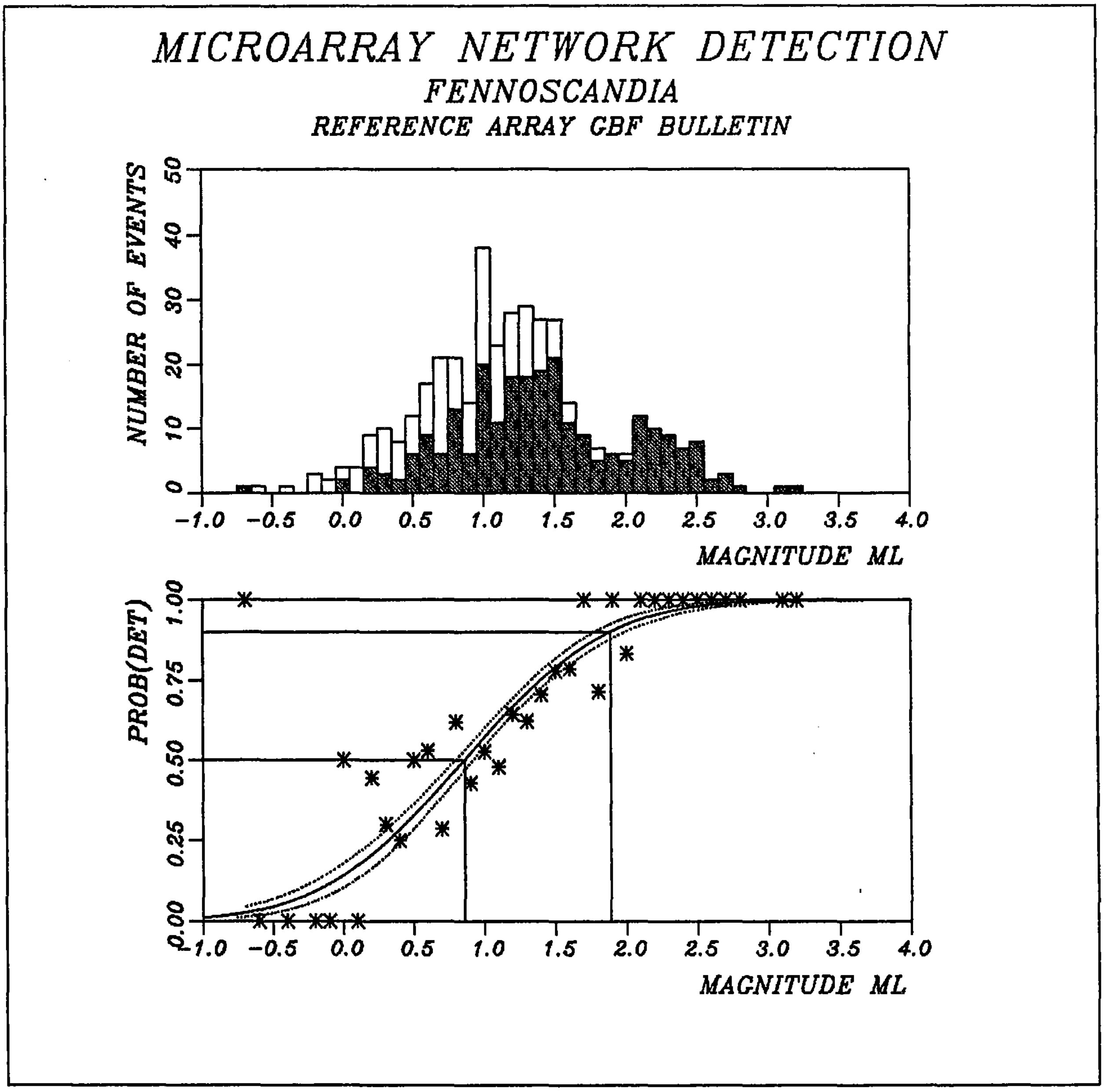

Fig. 7.5.16. Maximum likelihood detectability estimation of the microarray network for Fennoscandia-NW Russia using the GBF bulletin as a reference. The upper half shows the reference set and the number of events found by the microarray network for each magnitude. The lower half shows the maximum likelihood detectability curve and its confidence limits. The actual percentage of detected events at each magnitude is also shown.

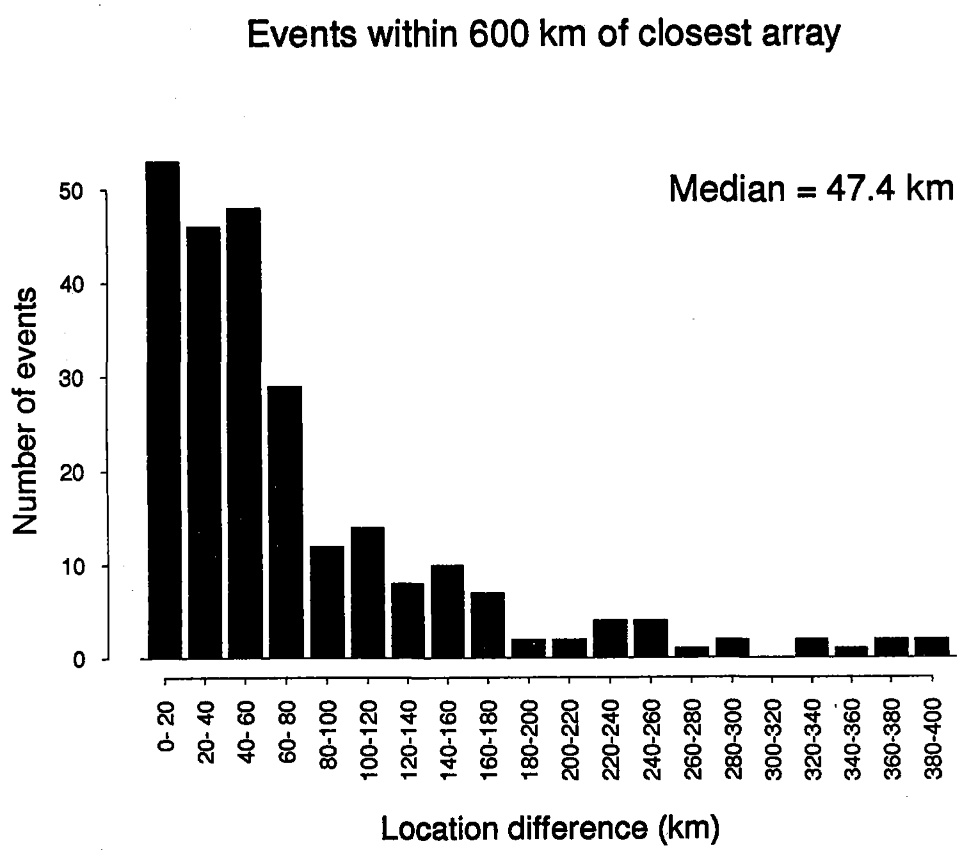

Fig. 7.5.17. This histogram shows the location difference between the microarray network and the full array network for the 249 events located within 600 km of the closest array. The median difference of the population is 47.4 km.

7.6 Distribution in slowness space of regional array detections

One of the main features of advanced regional arrays is their ability to reliably determine the slowness vector of incoming signal energy. This is important for seismic phase identification, and can be used to characterize detected phases as teleseismic P or PKP, regional P, S, Lg or Rg (Mykkeltveit et al. 1990). As shown, e.g., by Kvaerna (1990), this ability can also be used to identify the origin of various seismic noise sources, many of which show very consistent azimuth, frequency and velocity characteristics.

This report summarizes statistics on the number of detections versus apparent slowness vector for the four regional arrays NORESS, ARCESS, GERESS and FINESA. In a series of 3-D plots, we display all of the detections reported by each individual array for the six-month period October 91 - March 92. We also show a figure with the slowness distribution for those detections that have been associated to an event in the IMS analysis.

Figs. 7.6.1 - 7.6.4 show number of detections versus slowness for each of the arrays. The slowness space corresponds to the same grid of 51 by 51 points used in the on-line broadband fk-analysis. The slownesses range from -0.4 to 0.4 s/km. This corresponds to apparent velocities ranging from 1.78 km/s to infinity.

The X-axis (left-right) corresponds to eastward direction. The Y-axis (front-back) correspond to northward direction. Each figure is separated into two parts. The upper part shows detections with estimated signal frequency below 6.0 Hz. The lower part shows detections with estimated signal frequency above 6.0 Hz.

Fig. 7.6.1 shows NORESS detections. There are dominant peaks in the center for high velocities and a ridge towards east-north for velocities around 3.0 km/s. The 3.0 km/s peaks have been documented as seismic Rayleigh waves from an industrial area and from the large river Glomma running north-south about 20 km east of NORESS (Kvaerna, 1990).

Fig. 7.6.2 shows ARCESS detections. Dominant peaks are found corresponding to P and S velocities from the Kola mines (azimuth 100-130 degrees). A large number of detections with direction from north and velocities around 6.0 km/sec have not been identified. The high frequency detections towards west may be noise from a main road passing the west side of the array.

Note that when the source is very close, or within the array, the slowness estimate may be wrong. See also section 7.9 for a report on correlation between number of detections and temperature fall (ice cracks) in the ARCESS array.

Fig. 7.6.3 shows FINESA detections. Dominant peaks are found corresponding to P, Lg and Rg velocities from the mines in Estonia. In addition, there is a large number of very low velocity detections from the north. The origin of these detections is unknown.

Fig. 7.6.4 shows GERESS detections. Here, the low frequency detections are concentrated to relatively high apparent velocities. The high frequency detections are spread well out in slowness space, but a typical ring of Pn velocities can be identified.

When evaluating the statistics given above, it must be taken into account that the f-k analysis can fail to give the correct estimate in some cases. From our experience, this can happen in particular if the signal frequency is high, or if the noise source is located within or very close to an array. Data spikes or segments of bad data quality may of course also produce erroneous results.

In sections 3.5 and 3.6 of this Semiannual report, we noted that the percentage of detections associated to events by either the Intelligent Monitoring System (IMS) or the Generalized Beamforming process (GBF) was in the range 11 to 20%. These low figures are obviously due to the fact that most of the detections have slowness estimates outside the range permitting the detections to be attributed to seismic phases such as Pn or Lg. A natural question is whether these phases actually belong to seismic events, and this may be answered by investigating the results of analyst review of the regional array bulletins.

Fig. 7.6.5 shows the number of detections versus slowness for phases automatically associated to events by IMS (upper part) and estimated slowness for phases accepted or associated by analyst (lower part). (Note that vertical scale is now 500 as opposed to 1000 for Figs. 7.6.1-7.6.4). These figures include detections for all of the four arrays. Detections should normally correspond to certain "seismic" slownesses, since the slowness parameter is used for event association rules. But in the lower figure, the analyst has all detections available regardless of slowness. A seismic phase may be associated and slowness overruled to include the arrival time as a defining parameter for the event solution.

We note from the lower figure that the number of very slow phases is about the same as in the upper figure. This indicates that the estimated slowness parameter is mostly consistent with the solution as accepted by the analyst.

J. Fyen

References

Kvaerna, T. (1990): Sources of short-term fluctuations in the seismic noise level at NORESS), *Phys. Earth Planet. Int.*, 63, 269-276,

Mykkeltveit, S., F. Ringdal, T. Kværna & R.W. Alewine (1990): Application of regional arrays in seismic verification, *Bull. Seism. Soc. Am.*, special issue, 80, 1777-1800.

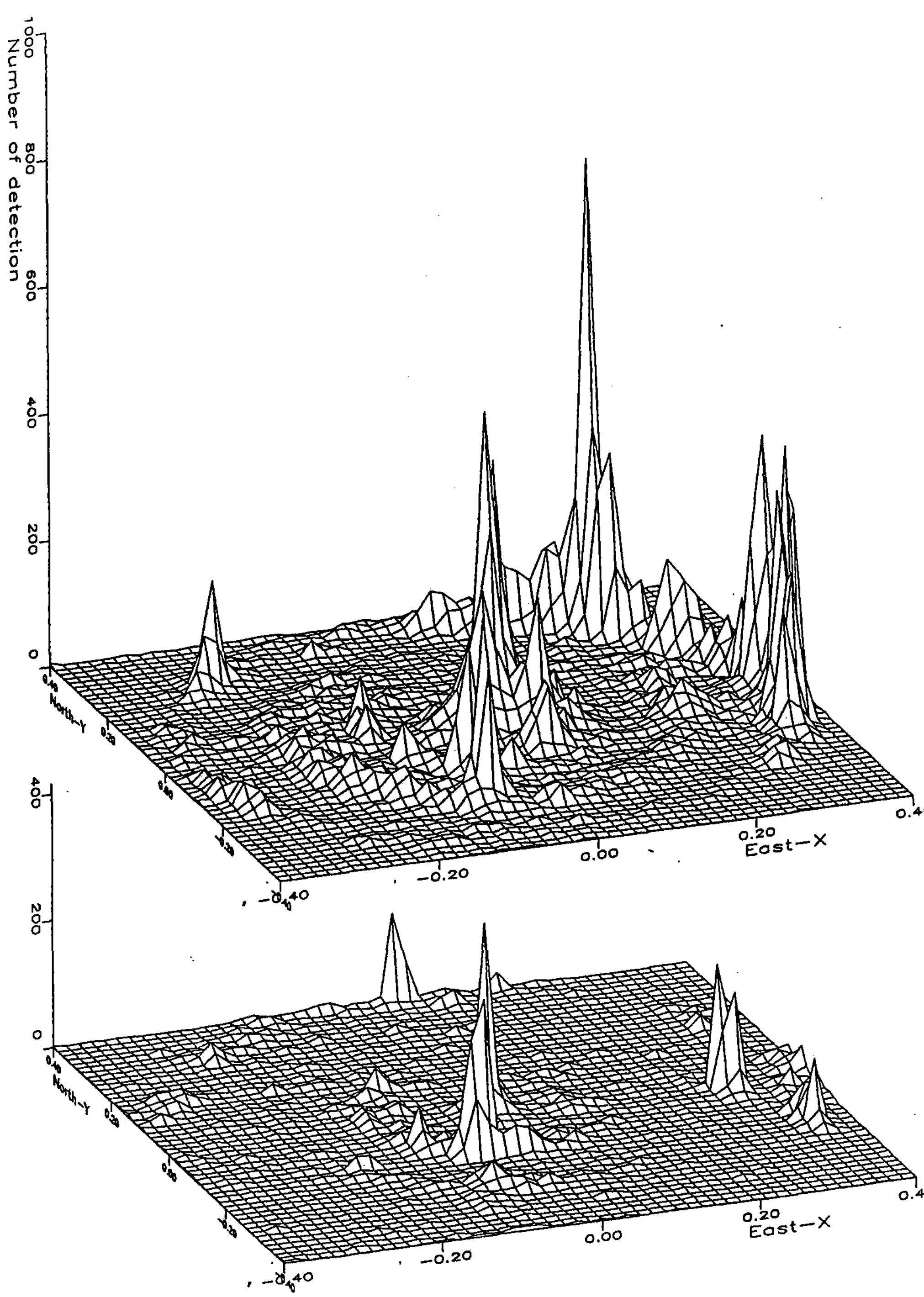

Fig. 7.6.1. Number of NORESS detections versus apparent slowness vector for the 6-month period October 1991 - March 1992. The X-axis (left-right) corresponds to eastward direction with 51 slowness points ranging from -0.4 to 0.4 sec/km. The Y-axis (front-back) correspond to northward direction with 51 slowness points ranging from -0.4 to 0.4 sec/km. The upper part shows detections with estimated signal frequency below 6.0 hz. The lower part shows detections with estimated signal frequency above 6.0 hz.

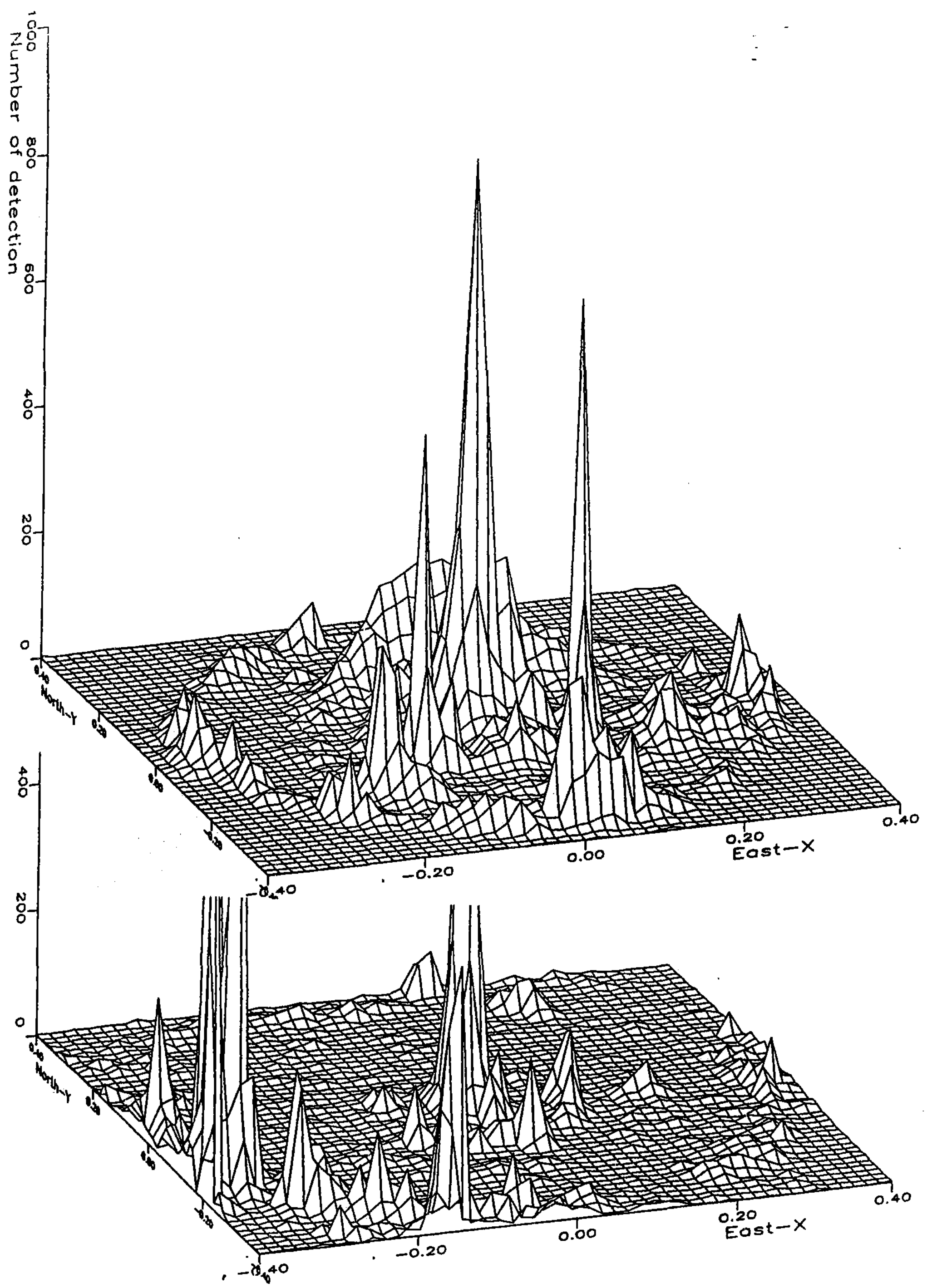

Fig. 7.6.2. Number of ARCESS detections versus apparent slowness vector for the 6-month period October 1991 - March 1992. The X-axis (left-right) corresponds to eastward direction with 51 slowness points ranging from -0.4 to 0.4 sec/km. The Y-axis (front-back) correspond to northward direction with 51 slowness points ranging from -0.4 to 0.4 sec/km. The upper part shows detections with estimated signal frequency below 6.0 hz. The lower part shows detections with estimated signal frequency above 6.0 hz. The lower figure has been clipped.

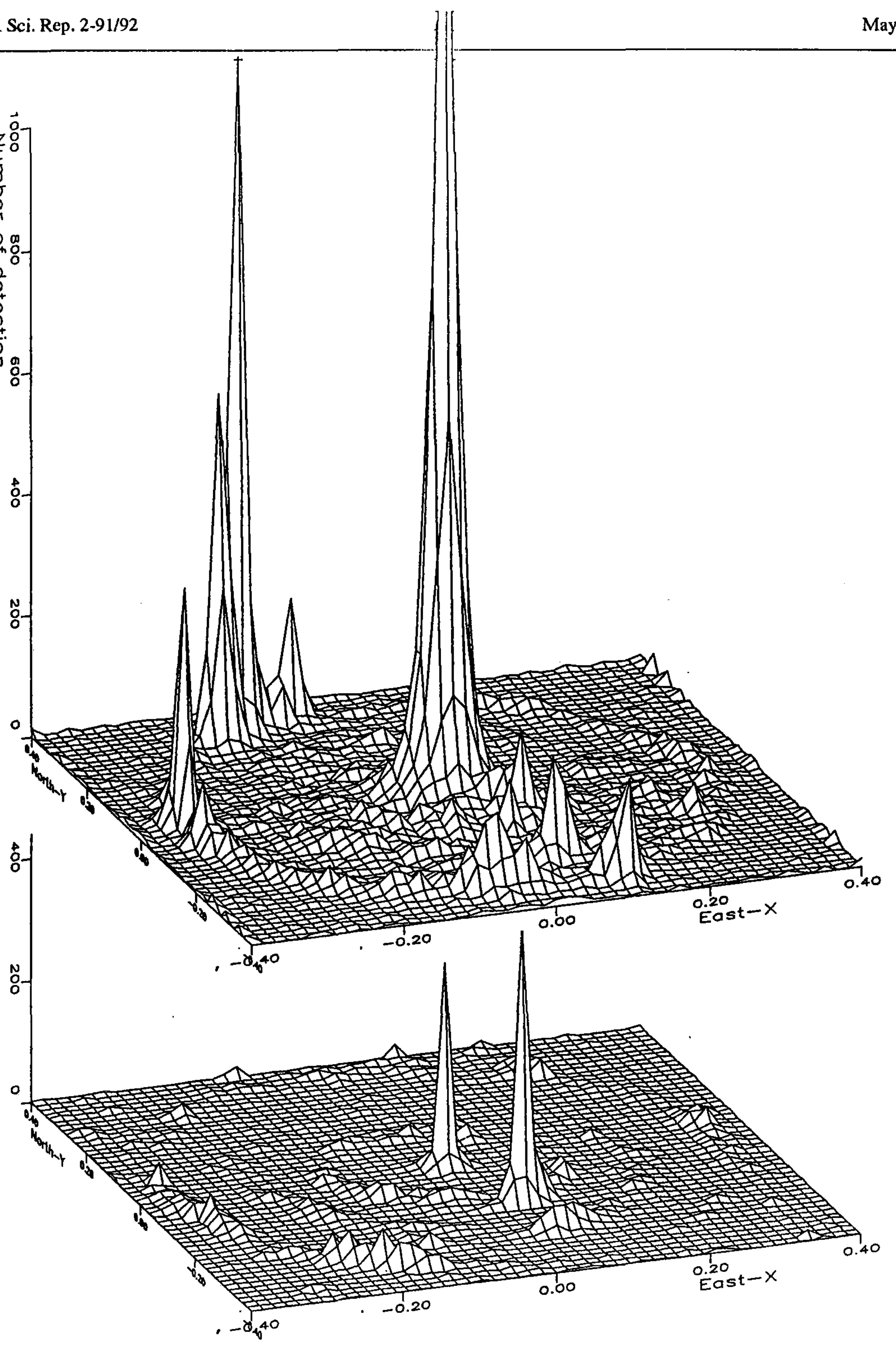

Fig. 7.6.3. Number of FINESA detections versus apparent slowness vector for the 6-month period October 1991 - March 1992. The X-axis (left-right) corresponds to eastward direction with 51 slowness points ranging from -0.4 to 0.4 sec/km. The Y-axis (front-back) correspond to northward direction with 51 slowness points ranging from -0.4 to 0.4 sec/km. The upper part shows detections with estimated signal frequency below 6.0 hz. The lower part shows detections with estimated signal frequency above 6.0 hz.

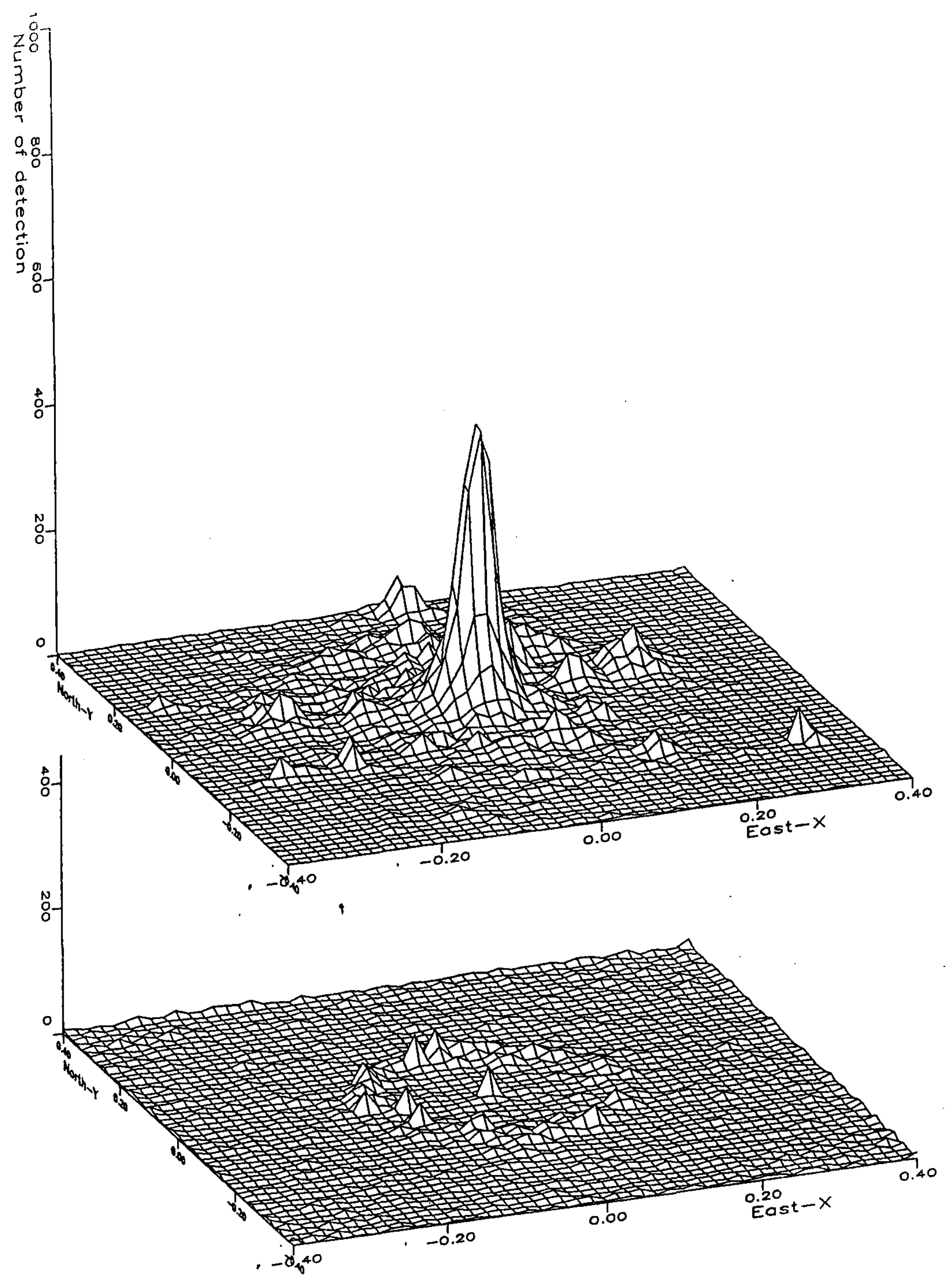

Fig. 7.6.4. Number of GERESS detections versus apparent slowness vector for the 6-month period October 1991 - March 1992. The X-axis (left-right) corresponds to eastward direction with 51 slowness points ranging from -0.4 to 0.4 sec/km. The Y-axis (front-back) correspond to northward direction with 51 slowness points ranging from -0.4 to 0.4 sec/km. The upper part shows detections with estimated signal frequency below 6.0 hz. The lower part shows detections with estimated signal frequency above 6.0 hz.

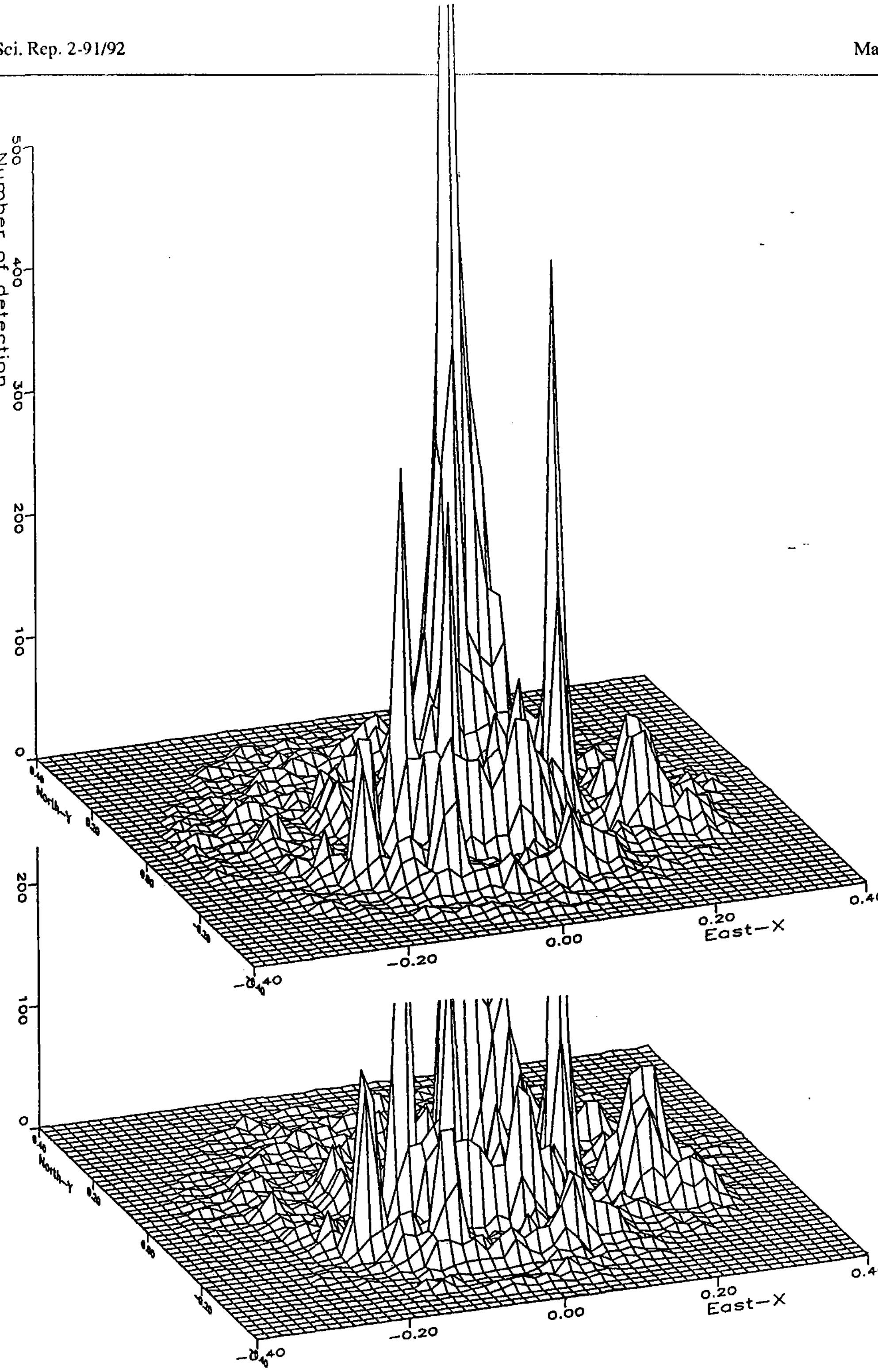

Fig. 7.6.5. The upper part shows number of detections versus apparent slowness vector for the 6-month period October 1991 - March 1992, for detections automatically associated to events by IMS. (All arrays). The X-axis (left-right) corresponds to eastward direction with 51 slowness points ranging from -0.4 to 0.4 sec/km. The Y-axis (front-back) correspond to northward direction with 51 slowness points ranging from -0.4 to 0.4 sec/km. The lower part shows number of detections associated to events that was accepted by analyst review.

7.7 NORAC: A new array controller

Introduction

NORSAR personnel have long experience in operating and maintaining arrays and other types of seismic stations, and have over the years also actively participated in array installation work jointly with other organizations. A typical such deployment comprises co-located sensors and digitizers, transmission of data to a central site within the array, and an array controller that performs synchronization, time tagging and transfer of data to a remote data processing facility. Work at NORSAR has traditionally concentrated on development of software for acquisition and processing of data, rather than development of equipment for the field installation. An exception here is the array controller at the FINESA array site, which was largely designed and developed by NORSAR personnel.

We embarked during the spring of 1991 on a new in-house development project aimed at designing a general-purpose array controller that would accept data from various vendors of digitizers, and prototyping of such a unit, named NORAC (NORsar ARray Controller), started during the summer of 1991. The main design idea has been to develop a simple unit that can handle input data from many digitizers. Data processing options and graphics displays would not be part of the array controller design, as these functions can more easily be performed by a Unix workstation on site or at a remote data center. A prototype unit was installed in December 1991 at the NORESS array site and acquired data from one instrument for a period of two months, with real time data transmission to Kjeller. The synchronization and time tagging functions of NORAC have also been tested successfully.

Our current plan is to consider the NORAC unit for use in three different projects now underway, namely, the new high-frequency arrays in Apatity, Russia, and on Spitsbergen, and the NORSAR refurbishment. The exact configuration for these three systems will be different, and the flexibility of NORAC in allowing for different types of communication and also different systems for reception of timing signals is essential.

The following paragraphs offer descriptions of NORAC design requirements, NORAC hardware configuration, NORAC software configuration and a description of how NORAC interfaces to Sun workstations.

NORAC design requirements

At the outset of this development project, the following design requirements were specified for the NORAC unit:

- drivers to different manufacturers of digitizers
- timing of data in the field and support for different clocks such as GPS, Omega and radio clocks
- synchronization of several digitizers from external clock source
- standardized hardware from a vendor represented in several countries
- integration with local or remotely located Unix-based computers

- flexible configurations ranging from 3-component stations to arrays
- option for local recording and archiving of data
- configurable in the field
- communication with remote computer using either asynchronous communication, synchronized communication (SDLC) or Ethernet (TCP protocol and sockets)
- watchdog for automatic restart
- all programs in EPROM/PROM
- should be capable of handling data from up to 32 digitizers

These requirements were largely based on our experience with array controllers at NORSAR, NORESS, ARCESS, FINESA and GERESS.

NORAC hardware configuration

The NORAC unit is based on Motorola VME boards. All boards are standard boards that may be acquired from any Motorola distributor. This subsection describes the different boards and their function in the NORAC unit. The NORAC unit is composed of the following boards:

- Collection board
- Communication board
- Digitizer interface board
- Clock interface board

A system may comprise 1 to 4 boards, depending on the configuration.

<u>Collection board</u>

This board is the main board of the NORAC system. The collection board hosts all programs in EPROM/PROM and typically has 4Mb of memory on board. The configuration of NORAC is stored in BBRAM (Battery Backup RAM) on the collection board. The following functions may be performed by this board:

- time stamp data from digitizers
- synchronize data from different digitizers
- collect statistics
- record data on locally attached disk
- transmit data to a computer using asynchronous protocol
- transmit data to a computer using Ethernet and socket communication
- archive data on tape and disk
- input of timing information using the asynchronous port

A minimum configuration can run on the collection board only. This configuration will contain 1 or 2 digitizers, external time received on the RS232 port and asynchronous communication or Ethernet communication to a local or remote host.

Digitizer interface board

The digitizer interface board has 8 ports for digitizers, its own buffer and CPU. Each port is asynchronous and can run at a speed of 38.4 Kbits/s at the maximum. A NORAC unit may contain as many as 4 digitizer interface boards, thus allowing up to 32 digitizers total.

Communication board

This board is used for performing the SDLC communication. The transmission speed is controlled by the external modem. The board has been tested at speeds from 2.4 to 64 Kbits/s. Data can optionally be compressed.

Clock interface board

We have implemented several options for timing of the data stream. Time information can be retrieved through a special board or from an asynchronous port. The following are the different timing options:

- an ASCII-coded data stream received once a second
- a BCD-formatted word received on a parallel interface
- timing information received directly from the VME bus

There are several different types of clocks (e.g., GPS, Omega and radio based) that deliver time information in one of the three different ways mentioned above.

A system based on an ASCII-coded data stream does not need a special clock board. This time information is read from the collection board as mentioned above.

The BCD-formatted stream on a parallel interface requires a digital input board in the NORAC unit. There are drivers for both Data Translation DT1417 and Acromag avme9460.

We have developed a driver for a VME clock board from Bancom. This board is based on the GPS system.

NORAC software configuration

The NORAC software is designed as a modular system where each task has a dedicated function. All programs are written in C and use functions from SVIDlib. SVIDlib is available through the VMEexec development environment offered by Motorola. All programming (including compiling and loading) is done on a Unix computer running Unix System V. The final system is burned into EPROMs. The following is a list of tasks running on NORAC:

- collect
- todisk
- tosdlc
- toasync
- toether
- fromport
- status

Collect task

Collect is the main task in NORAC. This task synchronizes all other tasks and formats one-second data blocks from all digitizers. Collect updates several statistics and creates all queues used in the system. Tasks such as todisk, tosdlc, toasync and toether retrieve data from a structure in the collect task. Tasks that need statistical information retrieve this from a structure in the collect task.

Todisk task

Todisk writes data onto a local disk loop using the FFS (Fast File System). Todisk can also write data directly on a Unix file system if a Unix CPU is configured into the same system.

Tosdlc task

Tosdlc transmits data on a synchronous communication port using the SDLC protocol. Tosdlc has an option for data compression.

Toasync task

This task uses an asynchronous port for transmitting data. The maximum speed on the asynchronous port is 38.4 Kbits/s. Data can optionally be compressed.

Toether task

This task uses the Ethernet as the communication medium. Sockets are used for establishing a connection between the toether task in NORAC and a task in another computer on the network. The protocol used is TCP/IP for which most Unix computers have support.

Fromport task

Fromport is the controlling task for all ports connected to external digitizers. Fromport has one subroutine for each type of digitizer connected to the system. The following are the digitizers currently supported:

- RD3 from Nanometrics
- RDAS-300P from Teledyne Geotech

- 72A series from Refraction Technology, Inc.

Fromport creates one task for each port with a digitizer connected. Each task is responsible for one digitizer at one specific port. Each task time stamps data from that digitizer as soon as data are received, and transmits data to the collection task which synchronizes data from all ports together in a one-second block.

Other digitizers can easily be interfaced to the system. The only work that needs to be done is writing a subroutine specific for that digitizer in the fromport program. Collect knows from the parameter area in BBRAM what type of digitizer is connected to each port.

Status task

The main function for status is to display statistics, transmit commands to digitizers and configure NORAC. There are also some diagnostic commands available in status. Status is operated from the asynchronous console port on the collect board.

Interfacing to Sun workstations

We have developed all necessary software for interfacing data from the NORAC unit. Data may be received in three ways:

- as an asynchronous data stream. This is not recommended for systems with more than 4 channels
- as a synchronized data stream using the SDLC protocol. An SBUS SDLC board is used as the hardware interface in the Sun workstation.
- as packets on the Ethernet. The Sun workstation is on the same LAN/WAN.

We have developed drivers to all data streams mentioned above. Data are written onto a circular disk loop and archived on Exabyte cassettes. Both the acquisition software and the archiving software are the same as NORSAR is using today for recording and archiving of all existing array data.

R. Paulsen

7.8 Continuous seismic threshold monitoring of the northern Novaya Zemlya test site; long-term operational characteristics

Introduction

This paper is a summary of a comprehensive report (Kværna, 1992) giving a detailed analysis of the performance of the continuous threshold monitoring technique applied to the northern Novaya Zemlya test site for a full one-month period.

The theoretical background for and applications of the continuous seismic threshold monitoring metod (CSTM) have been described in several articles. The approach was introduced by Ringdal and Kværna (1989), who showed that by continuously monitoring the seismic amplitude level at several seismic stations or arrays, one can at any time obtain an instant network-based magnitude threshold for a given target region. The magnitude threshold can be interpreted as the maximum magnitude of a possible clandestine explosion, given a predefined level of confidence. In the context of a comprehensive or threshold test ban treaty, the continuous assessment of the magnitude thresholds makes it possible to focus attention upon those specific time intervals when realistic evasion opportunities exist, while retaining confidence that no treaty violation has occurred at other times.

Kværna and Ringdal (1990) presented results from a one-week experiment of continuously monitoring the northern Novaya Zemlya test site. Data from the Fennoscandian regional array network (ARCESS, FINESA, and NORESS), see Fig. 7.8.1, were used to calculate the magnitude thresholds. It was found that the test site could be consistently monitored at a very low magnitude level (typically $m_b = 2.5$). In fact, every occurrence of the threshold exceeding $m_b = 2.5$ could be explained as resulting from an identified interfering event signal either at teleseismic or regional distance.

The excellent capability of the Fennoscandian regional array network to monitor the northern Novaya Zemlya test site was further confirmed by an experiment where recordings of the Novaya Zemlya nuclear test of October 24, 1990 were downscaled to $m_b = 2.6$ and superimposed on different noise intervals (Kværna, 1991).

In the context of using CSTM as a tool in routine monitoring, it is important to determine how the method will work under different conditions. Variability in the seismic noise level, occurrences of large earthquakes and aftershock sequences, station downtimes and data quality problems are all factors that will influence the performance of CSTM. Again focusing on the northern Novaya Zemlya test site, using data from the Fennoscandian regional array network, we have analyzed one month of magnitude threshold data (February, 1992) for the purpose of evaluating the long-term operational characteristics of CSTM.

Analysis of network threshold peaks

Our monitoring experiment was conducted in the same way and with the same parameter settings as used by Kværna and Ringdal (1990). In Kværna (1992) the monitoring results were presented in terms of plots covering one data day each. In Figs. A-1 to A-29 of the Appendix of that report, each covering one day of February, 1992, all time periods where the network magnitude thresholds at the 90% confidence level exceeded $m_b = 2.6$ have been identified.

For the remainder of this paper, the term magnitude threshold implies the magnitude threshold at the 90% confidence level.

From investigation of the distribution of all network CSTM data (totally 696 hours for February, 1992), we found that the network magnitude threshold exceeded $m_b = 2.6$ for about 50 minutes, see Fig. 7.8.2. This is only 0.12% of the total time, and we found $m_b = 2.6$ to be a suitable magnitude limit, in the sense that we were able to identify all interfering event signals causing the threshold to exceed this limit. One might of course argue that we should instead attempt to explain all peaks exceeding $m_b = 2.5$, but with reference to the actual CSTM data, we found that there were several intervals with m_b between 2.5 and 2.6, which we were not able to account for by signals from identified events. These intervals were all characterized either by a high background noise level at ARCESS, or with gaps in the ARCESS recordings.

Figs. 7.8.3 and 7.8.4 show two typical examples of a one-day plot (February 1 and 21). The upper three traces of each figure represent the magnitude thresholds obtained from the three indivitual arrays, whereas the bottom trace illustrates the network threshold. Typically, the individual array traces have a number of significant peaks for each 24-hour period, due to signals from interfering events (regional or teleseismic). On the network trace, the number and sizes of these peaks are significantly reduced, because an interfering event usually will not provide matching signals at all stations. From probabilistic considerations, it can in such cases be inferred that the actual network threshold is lower than these individual peaks might indicate.

The arrows on the one-day threshold plots indicate peaks with network magnitude threshold exceeding $m_b = 2.6$. A **T** at the arrow indicates that the peak is caused by signals from a teleseismic event, whereas an **R** indicates signals from a regional or local event. On three different occasions during February the threshold slightly exceeded 2.6 due to gap in the ARCESS recordings. These peaks were indicated by a **G** at the arrows.

A summary of the threshold peaks and the events causing the peaks is given in Table 7.8.1 covering the entire month of February 1992. Following the definition of the CSTM peaks (i.e., date, time, magnitude threshold, and number of seconds with the threshold exceeding $m_b = 2.6$), there is a bulletin of the events causing the peaks in the magnitude threshold traces. From Table 7.8.1 it can be seen that in some cases more than one event is contributing to the same peak in the threshold trace.

During the first half of February, there were several large teleseismic events causing increases in the network threshold (see events reported by the Quick Epicenter Determinations (QED) of the USGS), whereas during the second half of February, almost all CSTM peaks were caused by regional events. The regional events were all processed and located by the Intelligent Monitoring System (IMS) (Bache et al., 1990). The epicenters of the regional events of Table 1 are plotted on the map of Fig. 7.8.5. Except for one felt earthquake in southern Norway (M_L = 3.26), the events are most likely mining explosions, as their epicenters coincide with known mining sites. Within the context of practical monitoring, it is interesting that for a 5-day period (February 23 through 27) there were no threshold peaks exceeding m_b = 2.6.

Continuous thresholds during noise conditions

For the purpose of analyzing the long-term fluctuations of the magnitude thresholds, we have for every 4-hour interval computed the median thresholds. The robust median estimator has been chosen to ensure that we are minimizing the influence of the short-term event peaks. These statistics have been computed for the network and for each array separately. The thresholds are all derived from filtered array beams, and thereby reflect the noise fluctuations within the applied frequency bands. The frequency filters used for ARCESS, FINESA and NORESS are 3.0-5.0 Hz, 2.0-4.0 Hz and 1.5-3.5 Hz, respectively.

Fig. 7.8.6a illustrates the results for each array for the month of February. It is clearly seen that ARCESS (the lower dashed line) has the best average capability for monitoring the northern Novaya Zemlya test site. Except for a few short time intevals, ARCESS has on the average lower magnitude thresholds than any of the other two arrays (NORESS - solid line, FINESA - upper dashed line). The ARCESS threshold curve has five pronounced peaks during the month, and shows internal variations of more than 0.5 m_b units. During quiet noise conditions, the median magnitude thresholds fluctuate around m_b = 2.0, but during the high-noise periods the thresholds approaches m_b = 2.5. Two of the peaks have been verified to correlate with severe wind and weather conditions in the ARCESS region, and it is also likely that the other three peaks are weather generated.

Compared to ARCESS, the NORESS magnitude thresholds show rather small variations, and fluctuate between m_b 2.4 and 2.5 during the entire period, see Fig. 7.8.6a. The small diurnal variations (of the order of 0.1 m_b units), are consistent with the findings of Fyen (1990). He found that for frequencies below 2 Hz, there was little difference between daytime and nighttime noise levels, whereas at higher frequencies, the diurnal variations are more significant (0.2-0.3 m_b units). It is only for a short time interval on February 6 that NORESS on the average has the best monitoring capability of the three arrays, but it has to be emphasized that this is not necessarily representative for time periods when seismic signals are present.

The median magnitude thresholds of FINESA, given by the top dashed line of Fig. 7.8.6a, exhibit strong weekly and diurnal variations. The diurnal variations are particularly significant on workdays. One peak for each of the five workdays are followed by a quiet weekend, reflecting the relative behavior of the background noise field in the frequency band of the P-beam steered towards Novaya Zemlya (2.0-4.0 Hz). The median thresholds during the weekends are approaching that of NORESS, whereas the workday levels are 0.2 to 0.4 m_b units higher. From Fig. 7.8.6a it can thus be inferred that FINESA on the average is contributing less than the other two arrays to the network monitoring capability of the northern Novaya Zemlya test site, but again, this may not be representative for time periods when seismic signals are present.

In Fig. 7.8.6b, we compare the median network performance (solid line) and the median ARCESS performance (dashed line) for monitoring the northern Novaya Zemlya test site. It is seen that when the ARCESS thresholds are low, the two curves almost coincide, implying that ARCESS alone determines the average network monitoring performance. However, during the ARCESS peak periods, the network curve is lower. This shows that even during background noise conditions, the other two arrays (FINESA and NORESS) contribute to lowering the magnitude thresholds.

We have in this section discussed the average properties of the CSTM performance of the Fennoscandian array network for monitoring the northern Novaya Zemlya test site. We have concluded that for most of the time, ARCESS is the array with the best capability, but that the other two arrays also play an important role, particularly when the ARCESS noise level is high.

Continuous thresholds during intervals with interfering signals

The dramatic improvement in the practical monitoring capability when using a network of arrays instead of a single array is illustrated in Fig. 7.8.7. We have for the month analyzed counted the number of threshold peaks exceeding a given magnitude, both for the network and for the best array (ARCESS). The barplots of Fig. 7.8.7 show that at a threshold of 2.6, the number of network threshold peaks are reduced by a factor of five in comparison to the threshold peaks at ARCESS alone (i.e., from 293 to 56). At a threshold of 3.0 the improvement is better than a factor of ten (i.e., from 41 to 3).

Conclusions

This work has documented the practical capability of the Continuous Seismic Threshold Monitoring method to monitor a specific nuclear test site at a very low threshold over an extended time period.

Specifically, we have used the Fennoscandian array network (NORESS, ARCESS and FINESA) to monitor the northern Novaya Zemlya test site for one full month (February 1992). We have shown that the magnitude threshold stays below $m_b = 2.50$, 99.72% of the total time. We have further "explained" all of the peaks exceeding $m_b = 2.6$ as resulting from one of the following three conditions: 1) a "large" identified teleseismic event, 2) a "large" identified regional event and 3) a short outage of the most important array (ARCESS).

The natural question is then as follows: Do these results imply that at the given confidence level there has been no seismic event of mb ≥ 2.6 at the test site during February 1992?

The answer is in practice "yes", since such an event only could have occurred during one of the time intervals when the network threshold trace exceeds 2.6. We have noted that the combined time span of such exceedances was only 50 minutes, or 0.12% of the total time. Since all the peaks were explained as resulting from known causes, it seems extremely unlikely that an event of mb 2.6 actually occurred during one of these short event intervals.

In theory, in a hypothetical monitoring situation for a comprehensive test ban treaty, there might be an "evasion" possibility if any of such high threshold periods could be predicted. But we do not consider this to be a realistic scenario. First, such predictions require exact knowledge of the configuration and the performance of the monitoring network, and second, there are a lot of practical problems involved in carrying out such a clandestine explosion so that the probability of getting detected is very high.

We have studied the relative contributions of the three arrays and found that ARCESS is clearly the most important, followed by NORESS and FINESA. During time periods when the ARCESS noise level is high, or when there are interfering events, the relative contributions of NORESS and FINESA increase significantly. The redundancy created by using several arrays is also essential during outages of one or more of the arrays.

The average magnitude thresholds at FINESA exhibit strong weekly and diurnal variations. The latter are particularly significant on workdays. The average NORESS thresholds show rather small variations, whereas at ARCESS, internal differences of more than 0.5 m_b units are observed. The peak periods at ARCESS are most likely caused by severe wind and weather conditions.

In the near future, additional array stations are planned for installation in the Arctic region. These stations would contribute to further improving the CSTM capability, both for Novaya Zemlya and on a general regional basis. This will be the subject for additional studies in the future.

T. Kværna

References

Bache, T., S. R. Bratt, J. Wang, R.M. Fung, C. Kobryn and J. W. Given (1990), The Intelligent Monitoring System, *Bull. Seism. Soc. Am.*, 80, Part B, 1833-1851.

Fyen, J. (1990): Diurnal and seasonal variations in the microseismic noise level observed at the NORESS array, *Phys. Earth Planet. Inter.*, 63, 252-268.

Kværna, T. (1992): Continuous seismic threshold monitoring of the northern Novaya Zemlya test site; long-term operational characteristics, AFGL Sci. Rep. No. 12, NORSAR, Kjeller.

Kværna, T. and F. Ringdal (1990): Continuous threshold monitoring of the Novaya Zemlya test site, *Semiannual Tech. Summary, 1 Apr - 30 Sep 1990*, NORSAR Sci. Rep. 1-90/91, NORSAR, Kjeller, Norway.

Kværna, T (1991): Threshold monitoring of Novaya Zemlya: A scaling experiment, *Semiannual Tech. Summary, 1 Oct 1990 - 31 Mar 1991*, NORSAR Sci. Rep. 2-90/91, NORSAR, Kjeller, Norway.

Ringdal, F. and T. Kværna (1989): A multi-channel processing approach to real-time network detection, phase association, and threshold monitoring, *Bull. Seism. Soc. Am.*, 79, 1927-1940.

Date	TM peak	Mag	Sec	Ev	Or. time	Lat	Lon	Dep	Mag	Bull	Region
02/01	11.46.11	2.66	20	R	11.46.08.8	67.592	30.300	0F	2.46	IMS	European Russia
02/01	19.12.08	2.99	88	T	19.04.05.3	35.164	139.702	107	5.6	QED	S.coast of Honshu
02/02	05.04.20	2.63	12	R	05.05.01.4	67.659	33.417	0F	2.41	IMS	European Russia
02/02	17.51.03	2.65	9	T	05.05.01.4	67.659	33.417	33F	5.5	QED	Kuril Islands
02/03	13.55.17	2.69	15	R	13.54.44.6	60.836	29.220	0F	2.41	IMS	European Russia
02/05	05.40.43	2.72	15	T	05.33.11.4	45.021	150.972	33F	5.6	QED	Kuril Islands
02/05	10.56.54	2.64	2	T	10.54.38.0	44.600	150.500	33F	4.3	NORSAR	Kuril Islands
02/05	13.21.09	2.90	69	T	13.13.42.5	52.163	-170.130	48	5.4	QED	Fox Islands
02/05	23.14.43	2.65	8	T	23.10.50.9	31.407	66.825	33F	5.1	QED	Afghanistan
02/06	01.23.52	2.95	181	T	01.12.41.2	-5.609	103.271	55	6.0	QED	Southern Sumatra
02/06	03.42.24	2.71	77	T	03.35.17.2	29.511	95.635	33F	5.6	QED	Xijang-India border
02/06	04.05.32	2.63	4	T	03.54.43.7	-5.374	103.197	72	5.5	QED	Southern Sumatra
02/06	05.13.26	2.63	3	T	04.57.28.0	-33.400	-175.200	33F	3.8	NORSAR	Kermadec Islands
02/06	09.19.03	2.78	39	R	09.18.47.9	61.243	29.875	0F	2.07	IMS	Finland-Russia border
				R	09.19.55.1	68.147	32.846	0F	1.90	IMS	European Russia
02/06	12.19.03	2.61	3	R	12.21.00.0	69.344	30.570	0F	2.14	IMS	Norway-Russia border
02/06	16.27.43	2.66	9	R	16.28.20.4	67.176	20.792	0F	1.83	IMS	Sweden
02/07	00.13.59	2.88	49	T	00.06.28.6	43.140	146.611	54	5.4	QED	Kuril Islands
02/07	06.42.13	2.67	20	T	06.35.26.0	52.925	159.555	49	5.3	QED	Off east coast of Kamchatka
02/07	08.38.36	2.66	15	R	08.41.05.1	67.633	33.715	0F	2.41	IMS	European Russia
02/07	09.20.39	2.61	1	R	09.21.16.4	68.190	32.875	0F	1.98	IMS	European Russia
				R	09.23.00.4	67.969	32.870	0F	1.92	IMS	European Russia
				R	09.25.08.3	59.298	26.399	0F	1.06	IMS	European Russia
02/07	09.54.59	2.65	15	T	09.48.38.7	55.795	160.753	138	5.0	QED	Kamchatka
02/07	09.59.36	2.64	5	R	10.00.44.9	64.692	30.728	0F	2.11	IMS	Finland-Russia border
02/07	12.18.59	2.80	21	R	12.20.52.2	69.329	30.842	0F	2.40	IMS	Norway-Russia border
02/08	11.44.28	2.69	29	R	11.44.41.2	67.648	30.594	0F	2.24	IMS	European Russia
02/09	04.09.14	2.63	5	R	04.09.41.1	67.574	33.741	0F	2.35	IMS	European Russia
02/09	07.56.42	2.57	-	T	07.49.21.5	51.497	-178.364	66	5.1	QED	Andreanof Islands
02/09	22.08.59	2.84	47	T	22.01.58.4	47.982	152.979	123	5.6	QED	Kuril Islands
02/12	01.09.22	2.82	42	T	01.02.01.9	51.299	177.926	33F	5.2	QED	Rat Islands
02/13	01.45.47	2.77	70	T	01.29.17.1	-15.923	166.215	33F	6.1	QED	Vanuatu Islands
02/13	02.45.31	2.82	54	T	02.38.18.4	53.576	-165.706	44	5.5	QED	Fox Islands
02/13	23.34.08	2.72	33	R	23.35.20.5	67.720	21.067	0F	1.84	IMS	Sweden
02/14	08.23.25	2.99	136	T	08.18.27.7	53.576	-165.706	33F	5.3	QED	Lake Baykal Region
02/14	08.48.02	2.61	1	R	08.48.20.2	67.391	32.939	0F	2.31	IMS	European Russia
02/14	12.19.23	2.96	115	R	12.21.00.9	69.322	30.727	0F	2.50	IMS	Norway-Russia border
02/15	11.47.38	2.62	1	R	11.49.21.2	67.656	30.374	0F	1.87	IMS	European Russia
02/15	12.57.21	2.76	61	T	12.52.55.0	42.846	46.588	33F	4.7	QED	Eastern Caucasus
02/16	08.49.11	2.70	27	R	08.49.50.5	67.636	33.547	0F	2.54	IMS	European Russia
02/16	21.55.47	2.53	-	R	21.54.36.6	67.667	20.841	0F	1.03	IMS	Sweden
02/17	00.04.52	3.13	136	T	00.01.56.7	79.190	124.625	10	5.8	QED	East of Severnaya Zemlya
02/17	08.13.48	2.65	27	G							Gap in ARCESS recording
02/17	14.23.57	2.71	33	R	14.25.24.0	69.638	30.430	0F	1.95	IMS	Norway-Russia border
02/17	15.45.13	2.63	4	G							Gap in ARCESS recording
02/18	12.42.04	2.68	8	R	12.42.01.9	59.337	27.065	0F	2.61	IMS	European Russia
02/19	06.40.25	2.91	226	R	06.39.32.9	59.240	10.886	0F	3.26	IMS	Southern Norway
02/19	12.26.49	3.25	302	R	12.25.03.0	69.257	30.575	0F	2.09	IMS	Norway-Russia border
				R	12.26.30.0	64.722	30.553	0F	2.78	IMS	Finland-Russia border
02/19	12.42.45	2.88	33	R	12.43.59.4	67.595	33.647	0F	2.46	IMS	European Russia
02/20	20.52.21	2.55	-	T	20.35.24.3	-33.498	-179.673	48	5.9	QED	South of Kermadec Islands
02/20	21.16.05	2.79	60	R	21.16.27.7	67.647	33.555	0F	1.98	IMS	European Russia
				R	21.16.50.5	67.918	33.951	0F	2.39	IMS	European Russia
02/21	08.59.39	2.74	103	R	08.59.25.1	67.657	33.791	0F	2.63	IMS	European Russia
02/21	11.01.46	3.14	173	R	11.01.53.5	64.672	30.801	0F	2.72	IMS	Finland-Russia border
02/21	12.49.06	2.99	135	R	12.50.11.2	69.341	30.688	0F	2.16	IMS	Norway-Russia border
				R	12.51.02.8	69.380	30.683	0F	2.46	IMS	Norway-Russia border
02/21	16.32.43	2.80	42	R	16.32.43.4	67.117	21.049	0F	2.02	IMS	Sweden
02/22	11.45.00	2.72	44	R	11.46.12.7	67.485	29.529	0F	1.87	IMS	Finland-Russia border
				R	11.46.59.0	67.558	30.328	0F	2.24	IMS	European Russia
02/22	11.59.31	2.70	35	R	12.00.18.7	67.599	33.659	0F	2.50	IMS	European Russia
02/28	08.58.22	2.75	36	R	08.58.59.1	67.617	33.769	0F	2.50	IMS	European Russia
02/28	12.07.37	2.63	2	R	12.09.56.9	59.170	27.332	0F	1.80	IMS	European Russia
02/28	12.19.10	2.69	37	G							Gap in ARCESS recording
02/28	12.43.14	2.92	243	R	12.45.11.0	69.365	30.647	0F	2.52	IMS	Norway-Russia border
02/28	14.30.16	2.68	17	R	14.30.29.5	67.709	33.695	0F	2.16	IMS	European Russia
				R	14.31.39.7	67.522	33.677	0F	2.31	IMS	European Russia

Table 7.8.1. List of peaks in the network threshold traces and the events causing the peaks. Following the definition of the CSTM peaks (i.e., date, time, maximum magnitude threshold, and number of seconds with the threshold exceeding $m_b = 2.6$), there is a bulletin of the events causing the peaks in the magnitude threshold traces. It can be seen that in some cases more than one event is contributing to the same peak in the threshold trace.

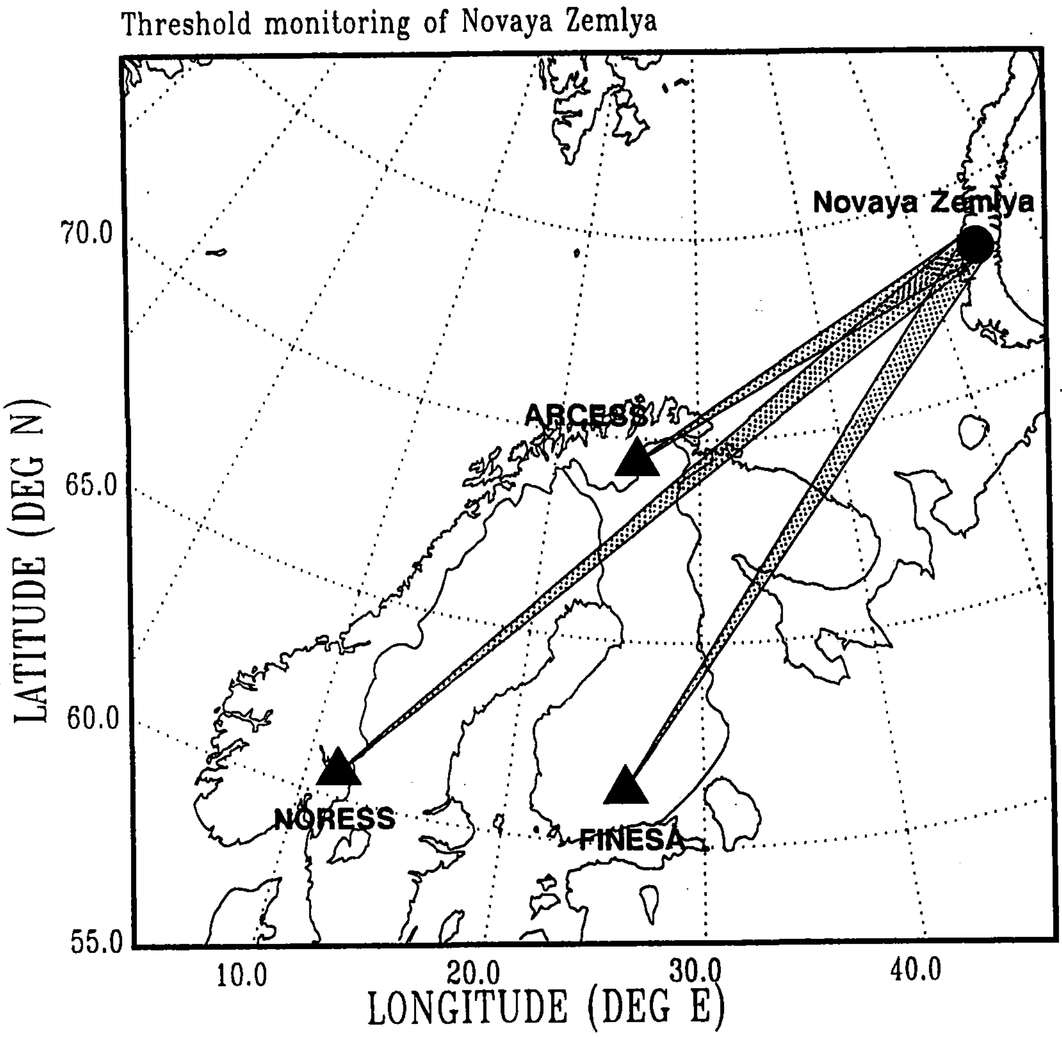

Fig. 7.8.1. Map showing the location of the northern Novaya Zemlya test site and the Fennoscandian array network. The distances of the three arrays from the test site are for NORESS 2280 km, for ARCESS 1100 km and for FINESA 1780 km.

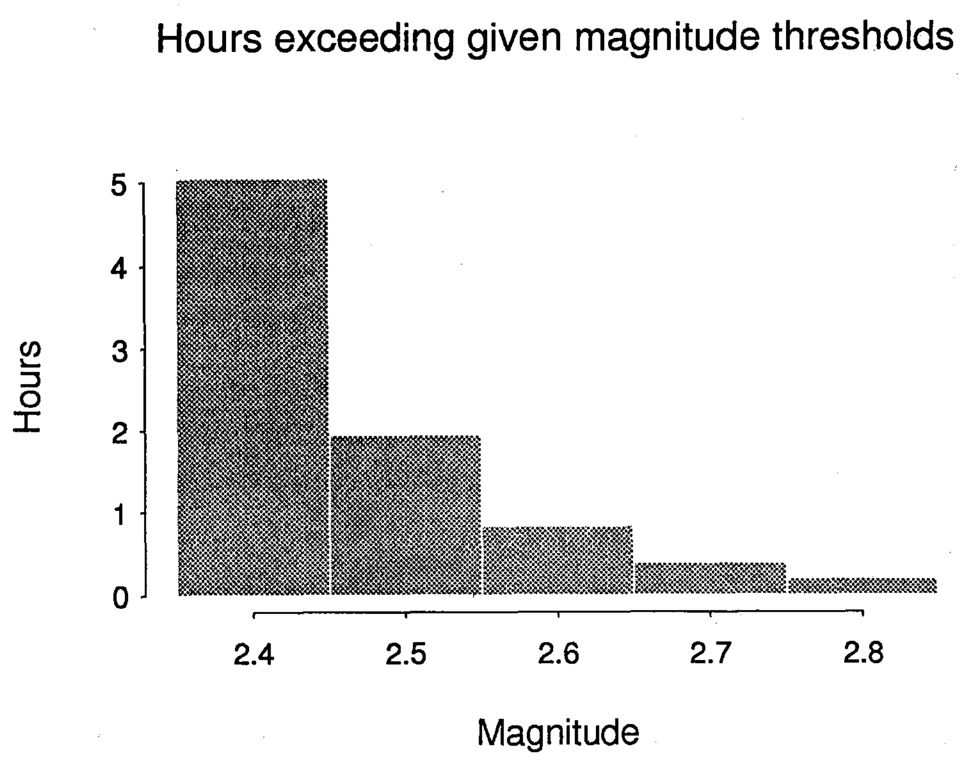

Fig. 7.8.2. Barplot showing the number of hours where the 90% network magnitude threshold exceeds a given magnitude, for the month of February, 1992.

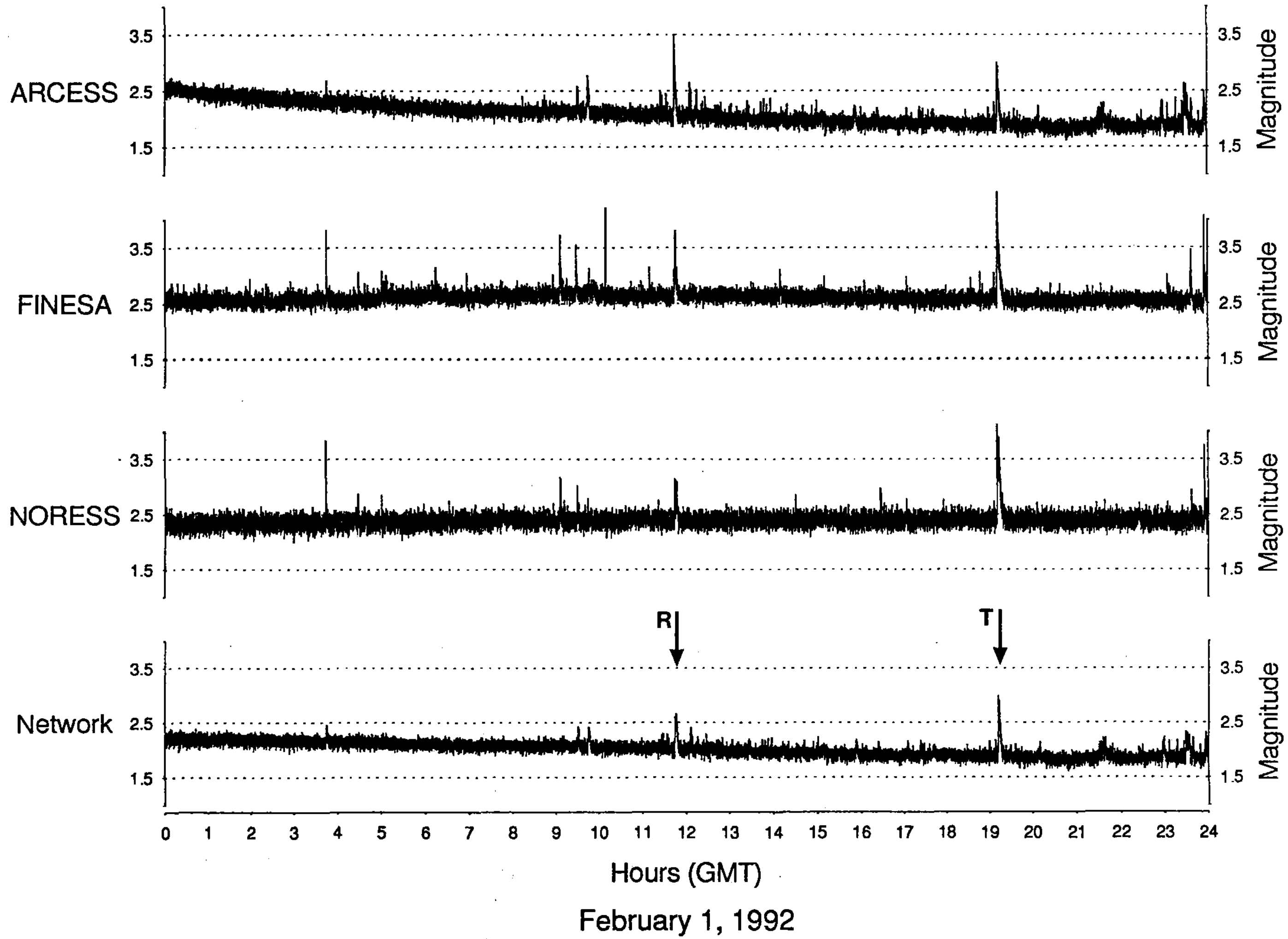

Fig. 7.8.3. The upper three traces represent the 90% magnitude thresholds obtained from the individual arrays, whereas the bottom trace illustrates the network threshold. The arrows indicate peaks with network magnitude threshold exceeding $m_b = 2.6$. A **T** at the arrow indicates that the peak is caused by signals from a teleseismic event, whereas an **R** indicates signals from a local or regional event.

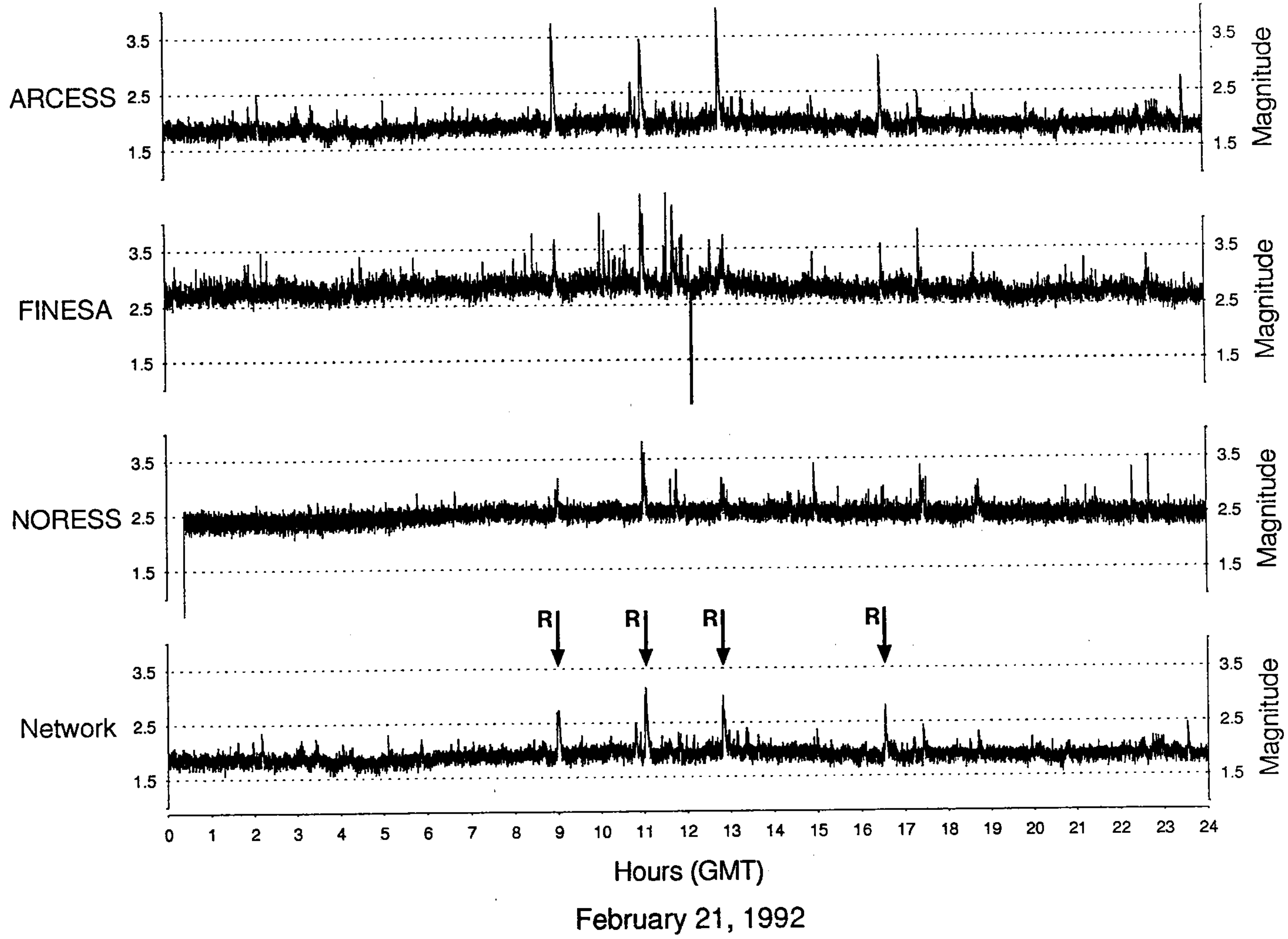

Fig. 7.8.4. The upper three traces represent the 90% magnitude thresholds obtained from the individual arrays, whereas the bottom trace illustrates the network threshold. The arrows indicate peaks with network magnitude threshold exceeding $m_b = 2.6$. A **T** at the arrow indicates that the peak is caused by signals from a teleseismic event, whereas an **R** indicates signals from a local or regional event.

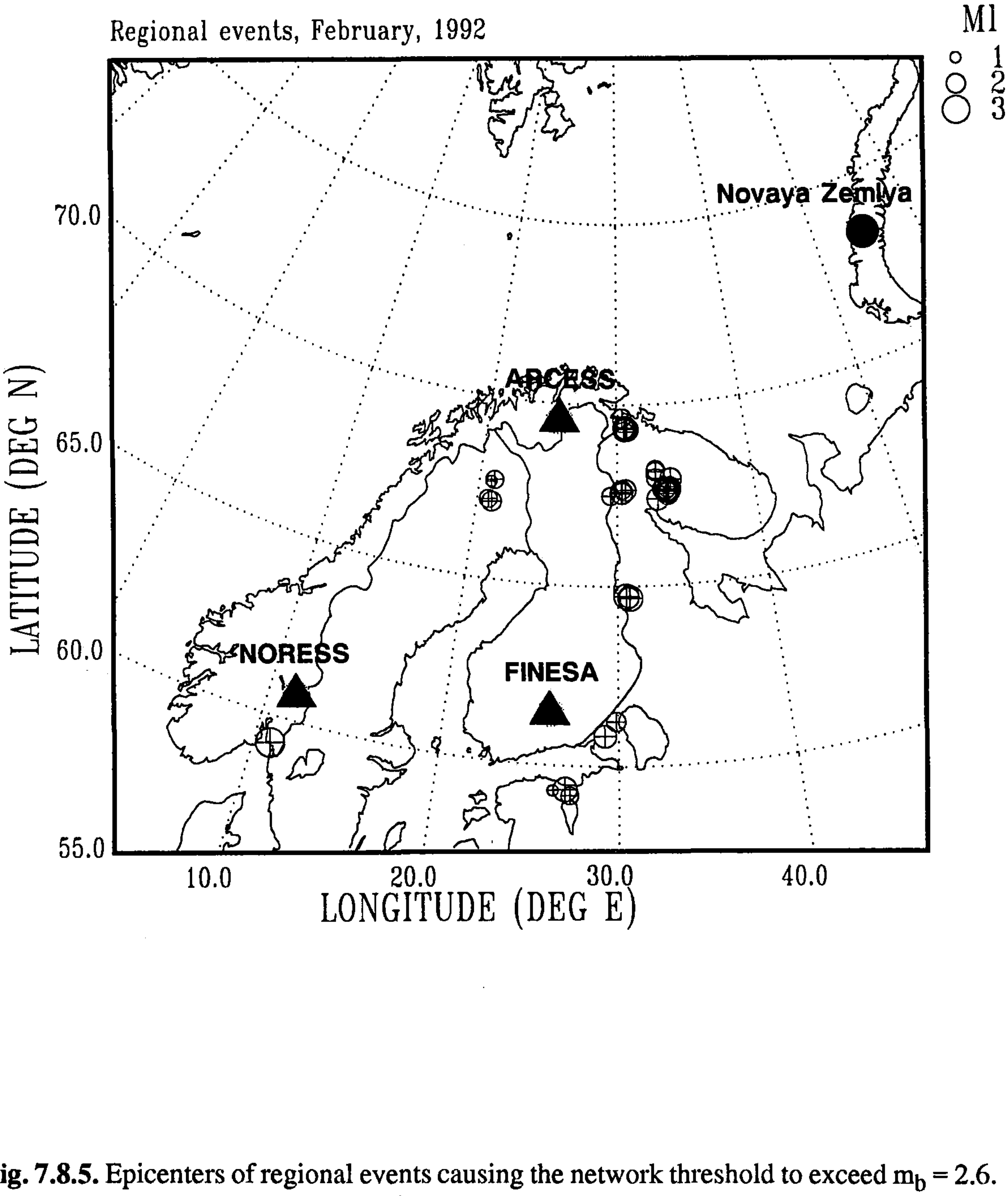

Fig. 7.8.5. Epicenters of regional events causing the network threshold to exceed $m_b = 2.6$. All events, except one felt earthquake in southern Norway, are probable mining explosions. Note the large number of events on the Kola peninsula.

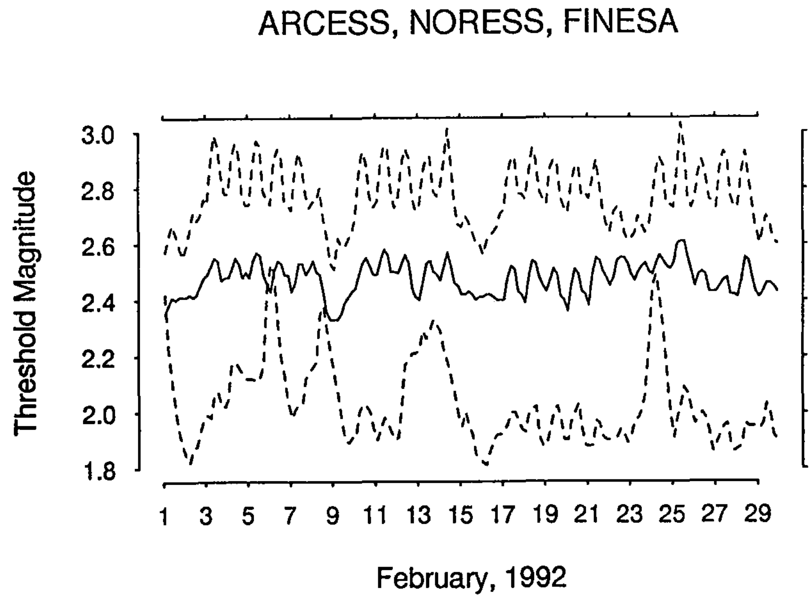

Fig. 7.8.6a. Four-hour medians of the magnitude thresholds for each array for the month of February 1992.

Lower dashed line: ARCESS
Middle solid line: NORESS
Upper dashed line: FINESA

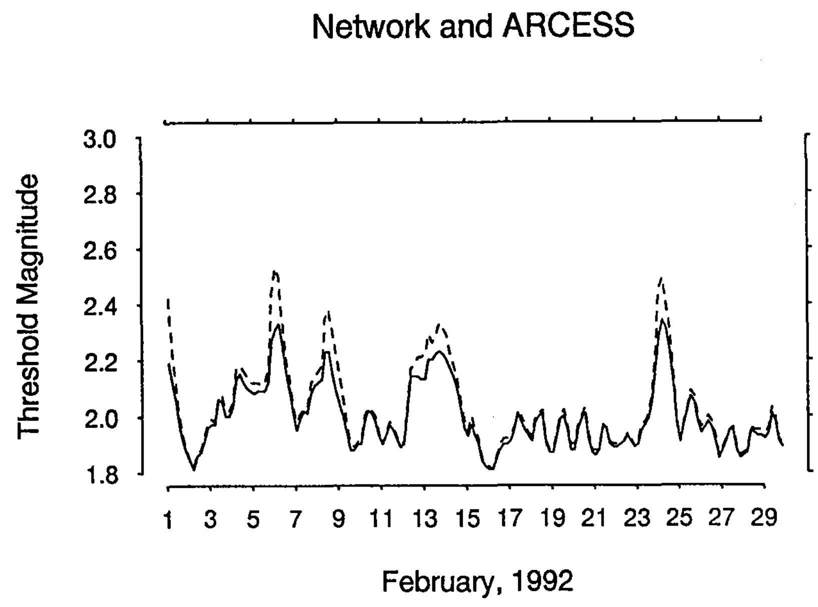

Fig. 7.8.6b. Four-hour medians of the magnitude thresholds for ARCESS and for the network for the month of February 1992.

Solid line: Network
Dashed line: ARCESS

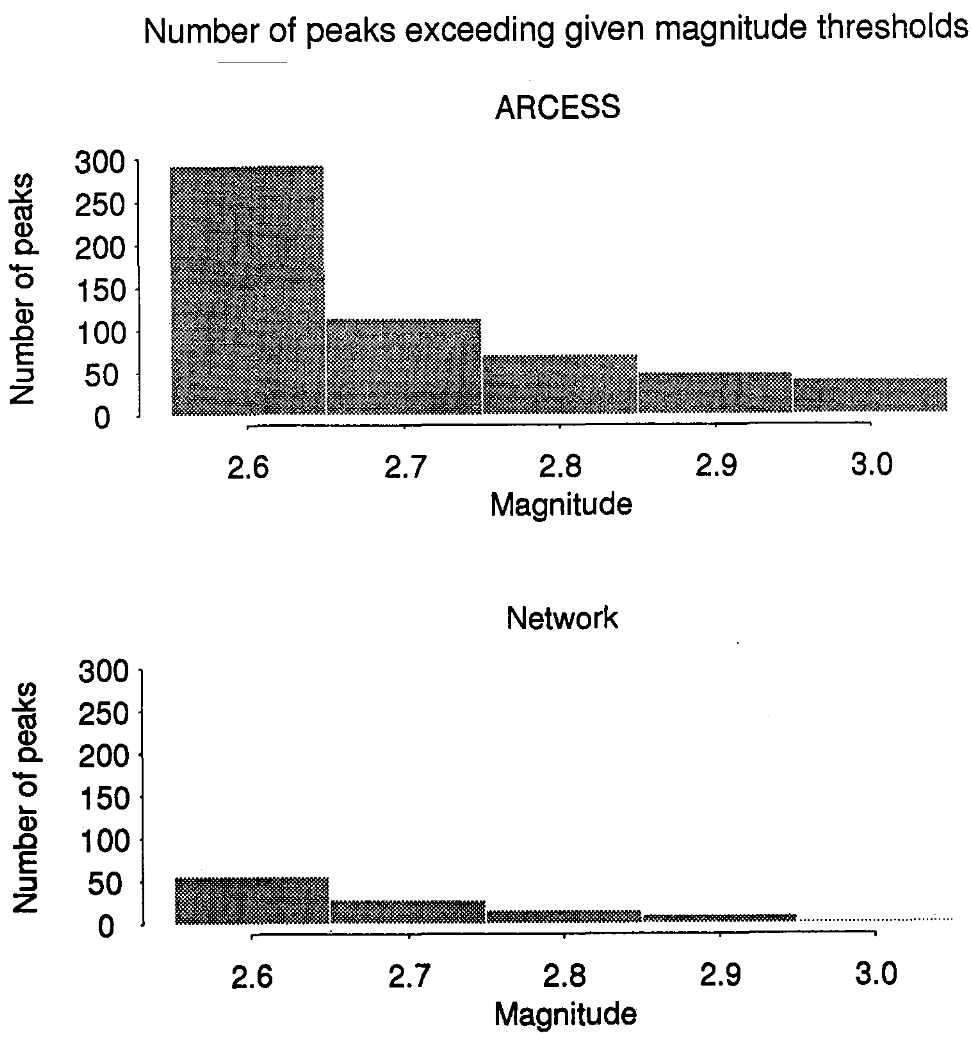

Fig. 7.8.7. Number of peaks exceeding given magnitude thresholds.

Upper part: ARCESS
Lower part: Network

7.9 Correlation between temperature and number of detections

When operating an automatic detector such as the STA/LTA detector in effect at the regional arrays in northern Europe, the number of false detections as a function of STA/LTA threshold, frequency and slowness is an important consideration. As discussed in Section 7.6, the f-k analysis is an effective tool at these arrays to separate such false alarms from real seismic detections, by using the calculated phase velocity. In addition, the estimated azimuths and signal frequency can be used to obtain some indications about the origins of these noise detections.

A number of sources contribute to such detections. Some are of cultural origin, others are environmentally determined. In some cases there are significant noise detection effects only during certain times of the year, or during certain environmental conditions.

Luosto and Saastamoinen (1964) have demonstrated a clear correlation between large temperature variations and ice-shocks in a lake. Ice-shocks were observed during the freezing period in early winter, and then a strong correlation between number of ice-shocks and temperature decline was found in March/April. During this latter spring period, the temperature goes above the freezing point during the day, and falls to 10-20 degrees Celsius below freezing point during the night.

In a study of NORESS noise detections, Kværna (1990) found a strong correlation between the water flow in the nearby river Glomma and the number of low-velocity phase detections. Fyen (1990) showed that the noise level is also strongly correlated with the water flow. The noise at certain frequencies is furthermore very strongly affected by various sources of industrial activity.

Many of such noise 'events' are very strong. For the ARCESS array, they are often located within, or very close to the array.

Figs. 7.9.1 and 7.9.2 show the number of detections and termperature at ARCESS and NORESS, respectively, each for a two-week period. We notice a clear correlation between temperature and detection rate. During nighttime, the detection rate is considerably higher than during daytime.

In Fig. 7.9.3, we report a longer period for ARCESS, and we see a very typical increase in the number of detections during the first freezing night in the autumn, but thereafter the connection between freezing temperature and number of detections is not as clear during the mid-winter. However, when the spring comes, we again see a clear correlation between large temperature variations and peaks in the number of detections.

Although these examples are clear enough, we find other periods when the number of detections increases dramatically, without any obvious correlation with temperature changes. One other potential source of such increase in the number of detections is the increase of waterflow in the nearby rivers (Kværna, 1990).

Fig. 7.9.4 illustrates the intensity of these events. The STA/LTA detector classifies this correctly as an "event", but the subsequent fk-analysis classifies it as a "false alarm", which is also correct with respect to what we are looking for.

J. Fyen
K. Hansvold

References

Luosto, U. and P. Saastamoinen (1964): , Observations about ice-shocks on lake Saaksjarvi, Geophysica, Vol. 9, No.1, University of Helsinki.

Kværna, T. (1990): Sources of short-term fluctuations in the seismic noise level at NORESS, PEPI, 63, 269-276.

Fyen, J. (1990): Diurnal and seasonal variations in the microseismic noise level observed at the NORESS array, *Phys. Earth Planet. Int.*, 63, 252-268.

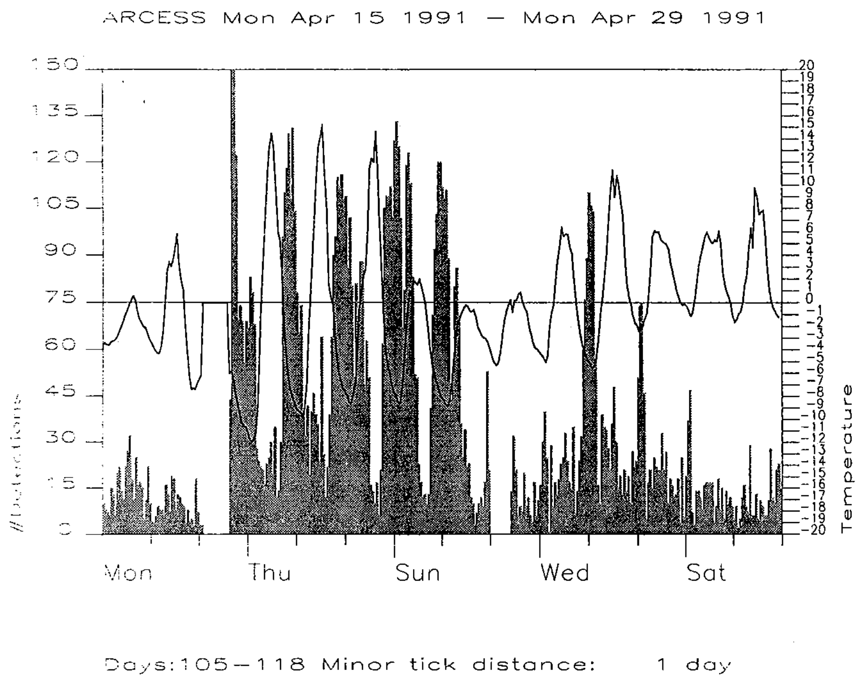

Fig. 7.9.1. Number of detections (shaded) and temperature for ARCESS during the period April 15 through April 28, 1991.

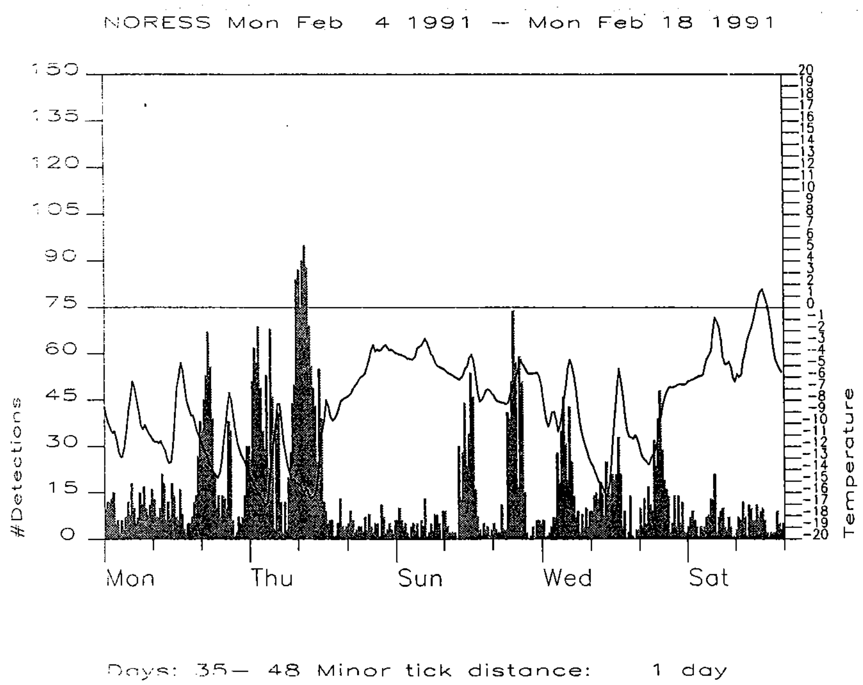

Fig. 7.9.2. Number of detections (shaded) and temperature for NORESS during the period February 4 through February 17, 1992)

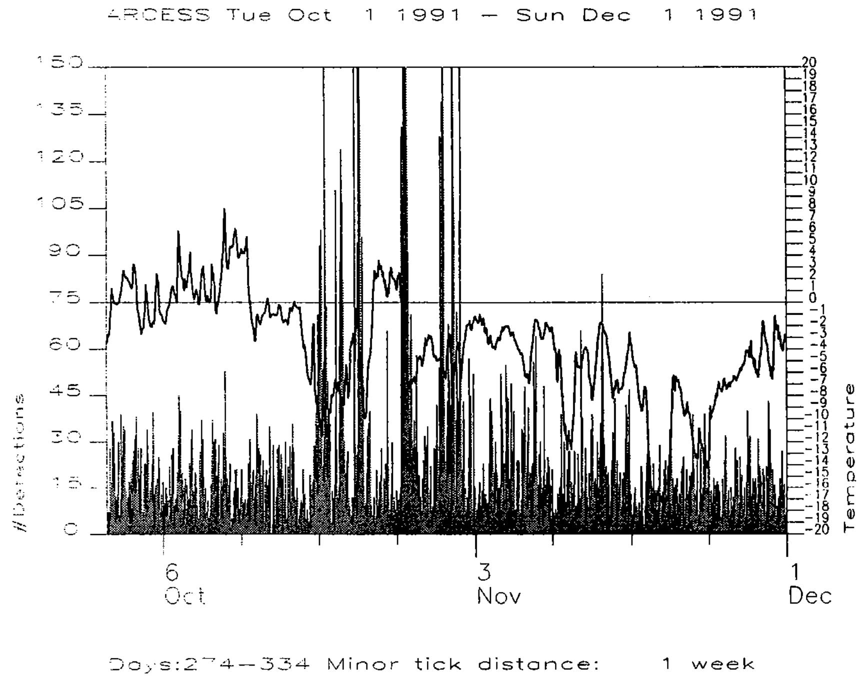

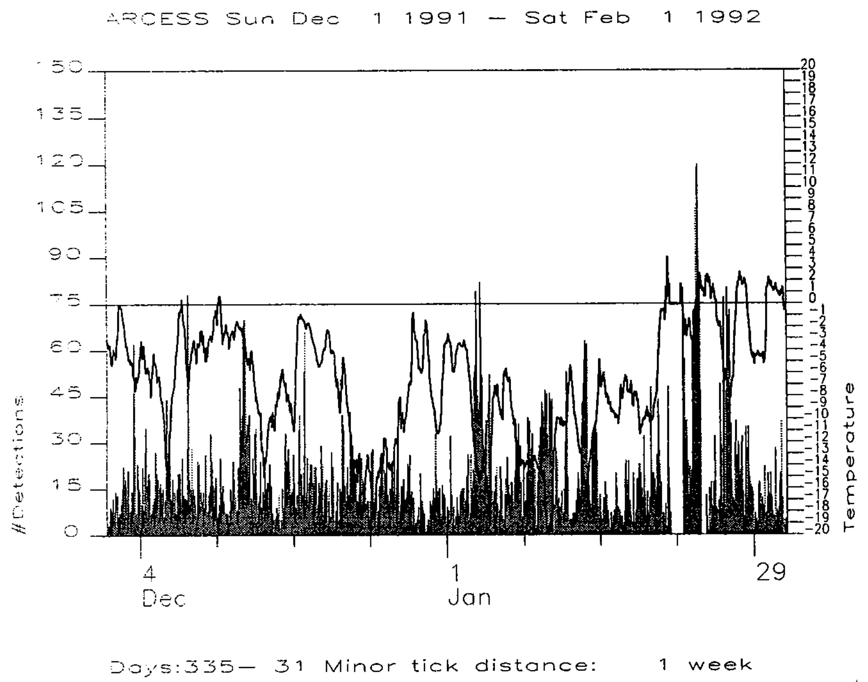

Fig. 7.9.3. Number of detections and temperature (bold line) for ARCESS during the period October 1 to December 1, 1991 (upper) and December 1, 1991, to February 1, 1992 (lower)..

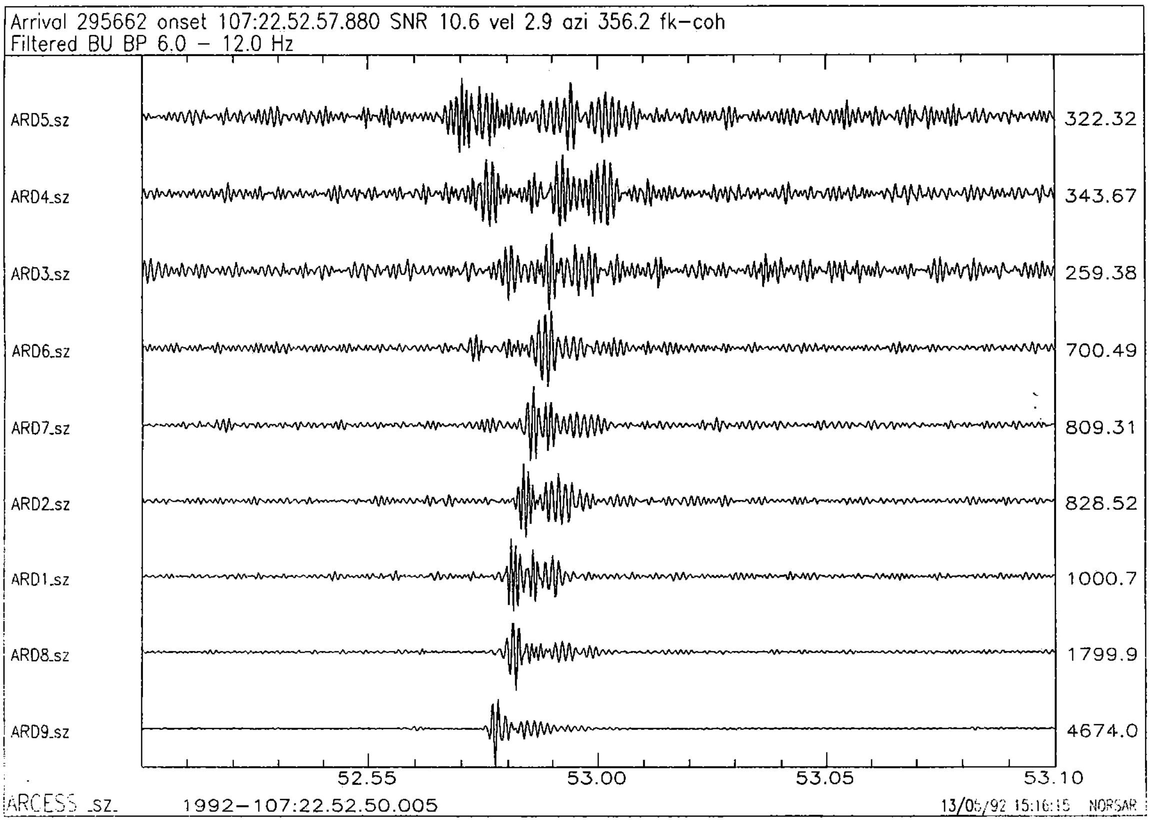

Fig. 7.9.4. Example of a "false alarm". This event originated very close to the array, and is interpreted as an "ice-shock". The fk-analysis classified this event as "noise", by reporting apparent velocity 2.9.